INVESTIGATION OF COMPONENTS OF THE mRNA METHYLATION COMPLEX IN ARABIDOPSIS

BY DOHA ABDULLAH ALBALAWI, MSc

Thesis submitted to the University of Nottingham for the degree of Doctor of Philosophy

September 2019

ABSTRACT

N^6-methyl-adenosine (m^{6}A) is the most abundant internal mRNA modification and is critical to the development of many eukaryotic organisms, being involved in many different biological processes. The formation of this modification is catalysed by the methyltransferase (MTase) "writer" complex. A core set of mRNA m^{6}A writer proteins in *Arabidopsis* thaliana includes MTA (METTL3), MTB (METTL14), FIP37 (WTAP), VIRILIZER (VIRMA) and the E3 ubiquitin ligase HAKAI. In this study, we aim to elucidate the role and regulation of MTB in mRNA methylation in *Arabidopsis* through mutant characterization, complementation and promoter studies. Different approaches were adopted in order to establish stable lines with reduced MTB expression, thus allowing the functional role of MTB during *Arabidopsis* development to be investigated. Firstly, we identified two heterozygous T-DNA insertion mutants of MTB. Plants containing either of these T-DNA insertions could only be isolated as heterozygous, the homozygous knockout in MTB resulted in embryo lethality and the seeds had an embryo lethal phenotype. In order to rescue the homozygous embryo lethal mutation phenotype, the transgenic plants that contained the T-DNA insertion (SALK-056904) were crossed with plants containing MTB transgene under the control of a seed-specific promoter. The homozygous plants obtained using this approach showed developmental defect phenotypes similar to but more severe than either *MTA*, *FIP37* or *Virilizer* knockdowns (which have a reduction of m^{6}A level by more than 80% compared with that in WT). In a further approach to investigate the function of the MTB protein, versions of *MTB* in which the S-adenosylmethionine (SAM) binding domain (methyl donor) has been mutated were generated (MTBΔSAM) for use in overexpression and complementation studies and then compared with previous similar MTAΔSAM results. The Northern blotting analyses confirmed the overexpression of

both MTBΔSAM and MTAΔSAM, but only those plants expressing the MTAΔSAM construct gave rise to a dominant negative phenotype with reduced m^6A, whereas *MTB* mutants more closely resembled WT. Moreover, this project also sought to investigate the interaction between MTB and two arginine methylases via yeast two-hybrid (Y2H). In a previous study, the PRMT4a and PRMT4b (a pair of Arginine methyltransferases in *Arabidopsis*) were found to interact with MTB methylase in Y2H assay, and from proteomics data 4 methylated arginine sites were found in MTB. A construct of MTB-lysine in which the four known sites of arginine methylation are replaced with lysine was generated and used in Y2H. We confirmed the weak interaction between MTB and PRMT4a and PRMT4b via Yeast two-hybrid analysis. Further mutant crosses with, and m^6A measurements in, the *prmt4a/b* double mutant sought to investigate the importance of MTB arginine methylation in m^6A writing. Collectively, our findings suggest that MTB is required for embryogenesis, development and normal growth patterns in plants, apical dominance, is involved in regulating trichome morphology and is necessary for full m^6A mRNA methylation and our results could pave the way to start studying the interaction between RNA methylation and Arginine methylation in plants and other organisms.

ACKNOWLEDGMENT

I would like to thank God for giving me the power, ability and opportunity to finish this research project. This challenging journey would not have been possible without the support of a number of valued people who assisted and supported me. I owe my deepest gratitude and thanks to all of them.

First, I would like to express my special appreciation and thanks to my supervisor Professor Rupert G. Fray for giving me the opportunity to do the project and be a member of his group. I greatly appreciate his kindness, guidance, patience and valuable suggestions. I have been extremely lucky to have his support and continuous encouragement throughout my PhD study.

I would also like to thank Dr. Zsuzsanna Bodi, Prof. Graham Seymour my co-supervisor and Prof. Zoe Wilson my assessor for the valuable suggestions and help provided me during my PhD study.

A heartfelt thanks to my loving husband, Marwan, who stood beside me and has been immensely supportive over the years. His love, support and continuous help have encouraged me to reach this stage. To my little angels, my lovely children, Hoor and Yousef, who are the impetus for me to complete the study, I am really thankful to all three for their patience, understanding and support during this journey.

I am especially grateful to my loving family, my parents, brothers and sisters, for supporting and encouraging me, and for given me all the sincere prayers throughout my studies and in all aspects of my life over the years. I always knew that you believed in me and wanted the best for me.

My special thanks goes to all past and present members of the Rupert's group who made such a supportive and enjoyable atmosphere in the lab especially Fatima

Alzahrani , Mi Zhang, Enas, Eleanor, Alex, Cameron and all others, I am greatly indebted for their helps, support, and many good suggestions providing me during my PhD study. It was a pleasure working with them.

Many thanks to all my friends: Fatima, Khulud, Abeer, Noura, Asma, Dalia, Shiah and many others, for providing me support and sincere prayers throughout my study. Last, I also thank the Saudi Ministry of Education in particular, Tabuk University for the financial support providing me during my PhD study.

TABLE OF CONTENTS

TABLE OF FIGURES

LIST OF TABLES

ABBREVIATIONS

ABI3	ABSCISIC ACID INSENSITIVE3
Am	2'-*O*-dimethyladenosine
APA	alternative polyadenylation
bp	Base pair
cDNA	Complementary DNA
Col-0	Columbia-0
CRISPR-Cas9	clustered regularly interspaced short palindromic repeat CRISPR associated 9
DTT	Dithiothreitol
dNTPs	Deoxyribonucleotide triphosphate
eIF3	eukaryotic initiation factor 3
EDTA	Disodium ethylene diamine tetraacetate
ESCs	embryonic stem cells
E. coli	*Escherichia coli*
FIP37	FKBP12 INTERACTING PROTEIN 37
FTO	fat mass and obesity-associated protein
Fl(2)d	Female lethal 2
GFP	Green Fluorescence Protein
hm5C	5-hydroxymethylcytidine
Ime4	inducer of meiosis 4
IP	Immunoprecipitation
Kan	Kanamycin
LB	Left Border Primer
LP	Forward Primer
LR	Lateral root
mRNA	Messenger Ribonucleic Acid
m^1A	N1-methyladenosine
m^5C	5-methyl- cytidine
m^6Am	N6, 2´-*O*-dimethyladenosine
m^6A	N6-methyl-adenine
METTL3	methyltrans-ferase-like 3
METTL14	methyltrans-ferase-like 14
MeRIP-seq	methylated RNA immunoprecipitation sequencing
miRNA	microRNA
MTase	methyltransferase
Mum2	muddled meiosis 2
MS	Murashige-Skoog salt
NAA	1-naphthalene acetic acid
NPA	N-1-naphthylphthalamic acid
nt	Nucleotide
PMSF	phenylmethanesulfonyl fluoride
PCR	polymerase chain reaction
PRMT	Protein arginine methyltransferase
RBM15	RNA binding motif protein 15
RP	Reverse Primer
RNA	Ribonucleic acid
SAM	S-adenyl-methionine
Sxl	Sex-lethal
TLC	Thin layer chromatography
T-DNA	Transfer DNA
UV	Ultraviolet

UTR	untranslated region
WTAP	Wilms' tumour 1-associating protein
WT	Wild type
Y2H	Yeast two-hybrid
3-AT	3-Amino-1,2,3-triazole
Ψ	Pseudouridine
°C	Degree Celsius
µl	Microlitre

CHAPTER 1 INTRODUCTION

1.1 General Introduction

Both DNA and histone proteins are known to undergo diverse chemical modifications to regulate gene expression (Strahl and Allis 2000; Suzuki and Bird 2008), and their modifications have been well studied. On the other hand, it is known that post-transcriptional modifications occur to RNAs, but their effects on the regulation of gene expression have only recently been investigated (He 2010). So far, over 150 diverse chemical RNA modifications have been discovered in different types of eukaryotic RNAs, including transfer RNA (tRNA), ribosomal RNA (rRNA), messenger RNA (mRNA), and small nuclear RNA (snRNA) (Cantara et al., 2010; Machnicka et al. 2013; Boccaletto et al., 2017). However, the enzymes catalysing the formation of each modification and the biological roles of these modifications are mostly unknown. The recent few years have witnessed significant developments in our understanding of regulation of gene expression by post-transcriptional RNA-modifications, leading to the emerging field of "Epitranscriptomics" (Li et al.,2017; Saletore et al.,2012).

1.2 Background to post – transcriptional processing

Messenger ribonucleic acid (mRNA) is transcribed from a DNA template by RNA polymerase II (Pol II) to produce a pre-mRNA that after processing conveys genetic information from DNA to the ribosome where the encoded protein is synthesised. In eukaryotes, to produce a mature RNA, pre-mRNA undergoes several post-transcriptional modifications and processing events in the cell nucleus before the mRNA is exported and translated in the cytoplasm. These processes are important for the effective export of the mRNA from the nucleus to cytoplasm, proper translation by the ribosomes, and they also may play important role in the gene expression

regulation at the post-transcriptional level. (He 2010, Yi and Pan, 2011). These RNA processes including mRNA capping at the 5' end, splicing, polyadenylation at the 3' end, and methylation of internal bases in the mRNA molecule, are generally well characterised with the exception of adenine methylation in mRNA (m^6A). Although this methylation was first reported several decades ago, understanding of the methylation complex and its regulation remained limited. Understanding the pathway and the role of these modifications could help researchers to find new layers of gene regulation at the RNA level.

1.2.1 The Major Internal mRNA Modifications of the Eukaryotic Cell Transcriptome.

In addition to the 5′ cap and 3′ polyadenylation, several modifications that can affect the metabolism and function of eukaryotic mRNAs have been reported including 5-methylcytidine (m^5C), *N6*-methyladenosine (m^6A), inosine (I), 5-hydroxylmethylcytidine (hm^5C), pseudouridine (Ψ) and *N1*-methyladenosine (m^1A) (Figure 1.1).

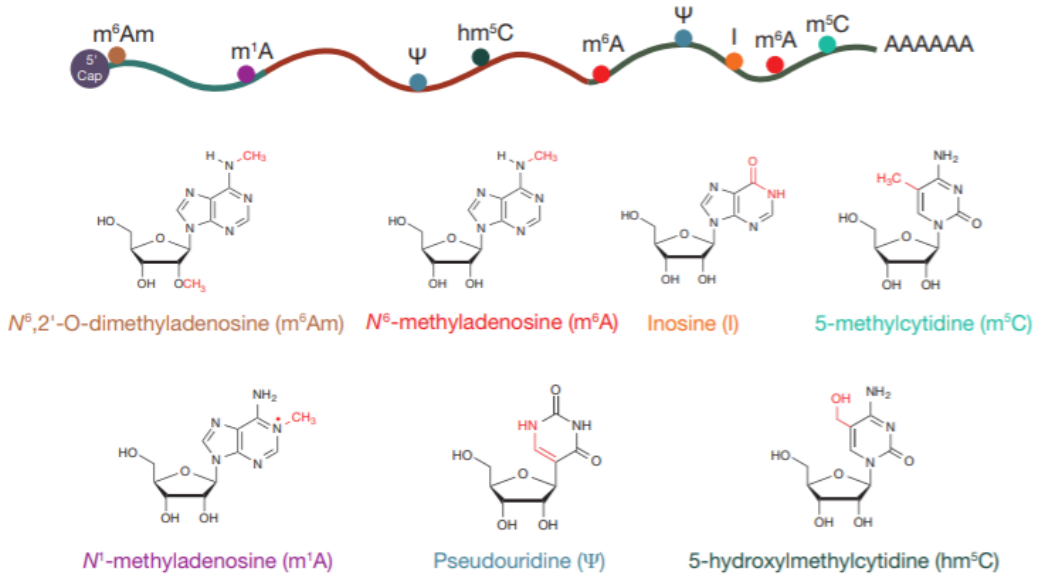

Figure 1.1: Diverse mRNA modifications in Eukaryotic cells (Li et al., 2017). Schematic diagram represents the common chemical modifications that found in internally in eukaryotic mRNA transcripts. N6-methyladenosine (m6A), is the most abundant mRNA modification.

1.2.1.1 Adenosine Methylations

Among diverse modifications found in mRNAs, *N6*-methyladenosine (m^6A) is the most abundant of these internal modifications in eukaryotes (Bokar, 2005; Desrosiers et al., 1974; Rottman et al.,1974). Although it was discovered over 40 years ago, its role was unclear until recently. Recent advances in the study of m^6A have revealed its important role in post-transcriptional regulation of mRNA and noncoding RNA (ncRNA). This modification within mRNAs has an impact on various aspects of the metabolism of RNA for instance: splicing, RNA export from the nucleus to the cytoplasm, alternative polyadenylation, and translation (Haussmann et al., 2016; Xiao et al., 2016; Zheng et al., 2013; Meyer et al., 2015; Wang et al., 2015).

m^6A modification occurs in plants (Nichols 1979), animals (Wei et al., 1976), flies (Levis and Penman, 1978), yeast (Clancy et al., 2002) and viruses that replicate within the nucleus, such as the influenza virus and Rous sarcoma virus (RSV) (Krug et al., 1976; Kane and Beemon, 1985). Additional to mRNA, m^6A has also been found in rRNA (Iwanami and Brown ,1968), tRNA (Saneyoshi et al.,1969), and snRNA (Bringmann and Luhrmann,1987), but in different consensus motifs. In addition, m^6A has been discovered in introns, and this proved that this modification occurred before mRNA splicing (Carroll et al., 1990). The abundance of m^6A had been estimated to be about 0.1–0.4% of the total adenosine residues in cellular mRNA which is ~3–5 m^6A sites per mRNA in mammals (Wei et al., 1975). A number of early studies revealed that the m^6A modification occurs in a conserved methylation sequence identified as RACs (R: G or A) (Schibler et al. 1977; Wei and Moss 1977). Further studies in Rous sarcoma virus RNA established RRACH as a larger consensus site for m^6A (Kane and Beemon,1987). Recently, transcriptome-wide m^6A maps reconfirmed this consensus sequence of m^6A modification in different eukaryotic organisms (Dominissini et al., 2012; Meyer et al., 2012; Schwartz et al., 2013; Lence et al., 2016).

Compared to m^6A, m^1A is less abundant in both human and mouse tissues and, if double-stranded, occurs on the Watson-Crick interface (Roundtree et al.,2017). This modification carries a positive charge which can affect RNA structures or protein-RNA interactions (Roundtree et al.,2017). Furthermore, m^1A can be demethylated by ALKBH3, and transcriptome-wide mapping recently showed that the m^1A is enriched around the translation start site and first splice site and a role in mRNA translation has been suggested (Dominissini et al., 2016; Li et al., 2017).

In addition to internal base modifications m^6A and m^1A in mRNA of higher eukaryotes, a terminal modification at the mRNA cap can occur at the 2’ OH on the

first and second nucleotides after the 7-methylguanosine cap (Schibler and Perry, 1977). When a 2′-O-methyladenosine residue occurs in the 5′ end of mRNA, it can be further methylated at the N6 position forming m^6Am (Wei et al.,1975; Keith et al.,1978). This modification was discovered in 1975 in virus and animal cell mRNAs (Wei et al.,1975). Recently, a transcriptome-wide map of m^6Am showed that transcripts which start with m^6Am are more stable than those that start with other nucleotides. This is likely because the m^6Am makes transcripts resistant to the mRNA-decapping enzyme DCP2 and thereby, less susceptible to mRNA degradation (Mauer et al., 2016). Furthermore, the same study showed that fat mass and obesity-associated protein (FTO) can demethylate m^6Am, suggesting that m^6Am is a dynamic and reversible modification in mRNA. Additional modifications of adenosine have been identified in eukaryotic RNA termed as (m^6,^{6}A) but have yet to be detected within coding transcripts (Machnicka et al., 2013). The cap adjacent m^6Am and 2'OH methylations are not found in plant or yeast mRNAs and the enzymes required for their formation are not present within their genomes.

1.2.1.2 Cytosine Modifications

m^5C modification is a common epigenetic marker in DNA and has been well studied (Li et al.,2017). Similar to m^6A, m^5C modification in mRNA was discovered more than 40 years ago (Dubin and Taylor, 1975), however, understanding of its regulatory role in mRNA metabolism is still very limited. Furthermore, m^5C is also present in noncoding RNAs such as; tRNA and rRNA (Machnicka et al.,2013). Mapping of m^5C sites in human mRNAs showed its enrichment in untranslated regions and near Argonaute binding regions (Squires et al., 2012). The formation of m^5C in higher eukaryotes is carried out by two RNA methyltransferases NSUN2 and DNMT2

(Squires et al., 2012). Moreover, m^5C modification can be read by the mRNA export adaptor protein ALY/REF, suggesting a role in regulating mRNA export (Yang et al., 2017). Similar to oxidation of 5-methylcytosine in DNA, the ten-eleven translocation (Tet) family of enzymes can oxidize m^5C in RNA, forming (hm^5C) (Fu et al., 2014). hMeRIP-seq analysis of hm^5C in *Drosophila melanogaster* revealed the distribution of this modification in coding sequences (Delatte et al., 2016).

1.2.1.3 Other modifications in mRNA

Pseudouridine (Ψ, 5-ribosyluracil), is the most prevalent modification in rRNA and tRNA (Cohn, 1960). Recently, Ψ was also identified in mRNA, and the ratio of Ψ/U estimated to be ∼0.2%–0.7% in mammalian cells (Li et al., 2015). Despite its abundance in mammalian mRNA, the biological function of this modification in mRNA remains unclear (Li et al., 2015). In the other types of RNA, Ψ has important roles in controlling their function. For example, Ψ is needed to fold rRNA properly and for ribosome translation efficiency and it stabilizes structure in tRNA (Li et al.,2017). Adenosine to inosine editing (A-to-I), are also found in mRNAs of most higher eukaryotes and involves the conversion of adenosine to inosine residues. This post-transcriptional modification can be catalysed by adenosine deaminases acting on RNA (ADARs) (Nishikura 2010). A-to-I editing plays various roles in the regulation of gene expression for instance: altering alternative splicing, recoding codons, and playing a role in the regulation of miRNA biogenesis pathway (Wulff et al., 2011). A to I editing has not been reported in plants or yeast.

Collectively, great advances have been made in the field of RNA modification or "Epitranscriptomics" over the past decade, unravelling transcriptome-wide maps of diverse modifications on different types of RNA and their dynamic occurrence.

However, we are still "scratching the surface" of the field and further studies are required to understand these modification's mechanisms and biological roles.

1.3 Techniques for detecting m^6A residue locations and its distribution in various eukaryotic mRNA

Precise and reliable mapping of specific m^6A modification sites in RNA is still a highly challenging task in the Epitranscriptomics field. Unlike other forms of post-transcriptional modification which cause a sequence change following reverse transcription, for instance; A-to-I conversions, m^6A is recognized as adenosine and is therefore not detected by cDNA sequencing (Bodi et al.,2012). Two-dimensional thin layer chromatography (TLC) is one of the most robust, relatively simple and sensitive approaches used to measure m^6A levels (Keith, 1995; Zhong et al., 2008; Bodi and Fray, 2017). In this method, poly(A) RNA is digested by ribonuclease T1 (RNase T1) to cut after every guanosine residue and then the short polynucleotides are labelled with [γ-^{32}P] ATP at 5' ends. Afterwards, the labelled polynucleotides digested by using nuclease P1 to produce mononucleotides, then separated by TLC (Zhong et al., 2008) (Figure1.2). One limitation of using this method is that it does not cover all A sites due to specificity of T1 ribonuclease that is used (Zhong et al., 2008; Wang and Zhao, 2016).

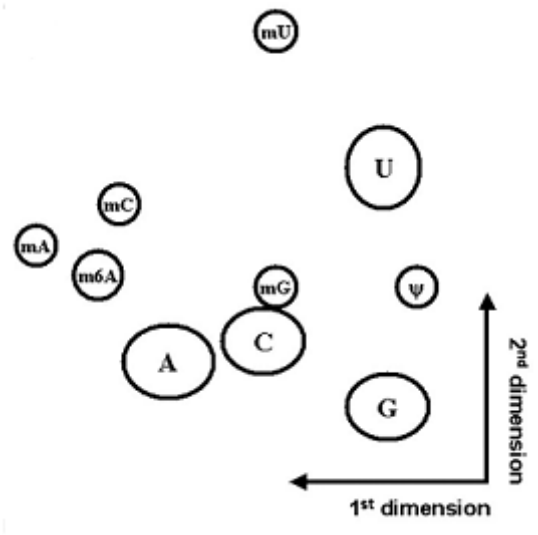

Figure 1.2: Schematic diagram of the relative positions of nucleotide spots on two-dimensional thin layer chromatography (Zhong et al., 2008). The TLC detection method was used in vitro to give quantitative values for m6A relative to A. The mRNA is digested by T1 ribonuclease to cut after every guanosine residue followed by T4 PNK radiolabeling and P1 digestion to produce nucleotide 5′ monophosphates then separated by TLC. A: adenosine; C: cytosine; U: uridine; G: guanosine; m6A: N6 methyladenosine; mA: 2'-O-methyladenosine; mC: 2'O-methylcytosine; mU: 2'-O-methyluridine; mG: 2'-O-methylguanosine and ψ is pseudouridine.

In addition to traditional detection and quantification strategies, two independent reports in 2012 profiled the transcriptome-wide distribution of m^6A in mammalian cells. These studies used an m^6A RNA immunoprecipitation approach followed by high-throughput sequencing known as (MeRIP–seq) or (m^6A-seq) (Dominissini et al., 2012; Meyer et al., 2012). This new approach has facilitated the identification of RNA modification locations and uncovered the distinct distribution patterns of these modifications throughout the transcriptome. In this technique, the extracted mRNA is fragmented to 100-150 nucleotides, followed by immunoprecipitation using a specific antibody against m^6A, then cDNA libraries are generated from immunoprecipitated and input control fragments. The enriched m^6A-containing RNA pool and the RNA input control are subjected to high-throughput sequencing in the final step (Dominissini et al., 2012) (Figure 1.3). More than 7000 mammalian mRNA transcripts were identified in these studies, in addition to 300 non-coding RNA (ncRNA), which

demonstrates that m^{6}A modification is spread widely (Dominissini et al., 2012; Meyer et al., 2012; Fu et al., 2014).

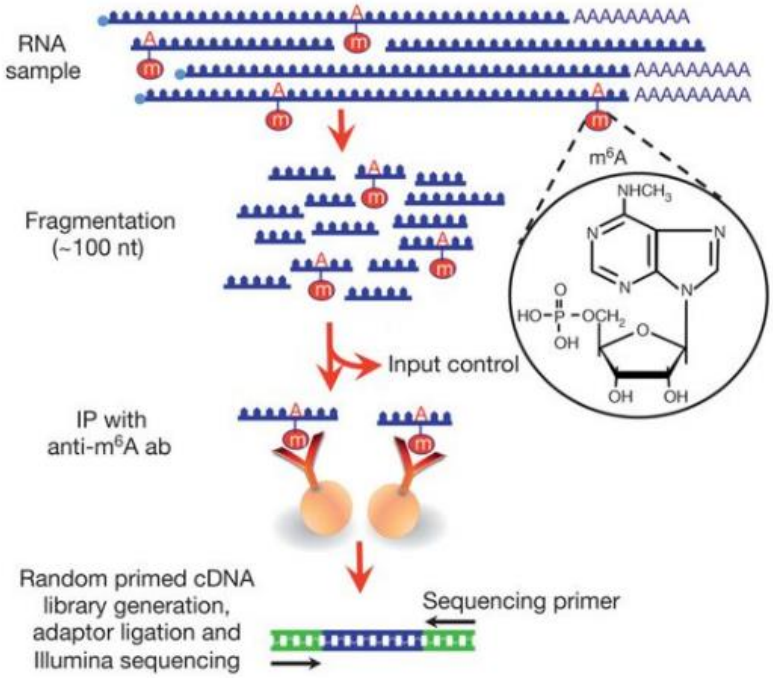

Figure 1.3: Schematic diagram of m^{6}A-seq approach (Dominissini et al., 2012). In this method purified RNA is chemically fragmented into ~100- nucleotides and subjected to immunoprecipitation using a specific antibody against m6A. Both immunoprecipitated and input control fragments are converted to cDNA using random hexamer primers then subjected to adapter ligation and Illumina sequencing in the final step. nt= nucleotide, IP= immunoprecipitation, ab= antibody.

However, it was not possible to provide information at single-nucleotide resolution within an immunoprecipitated RNA fragment due to the difficulty in distinguishing an unmodified adenine from m^{6}A in the last part of the MeRIP technique (sequencing step) (Maity and Das,2015). In addition, the part of the target mRNA that is modified at a specific site cannot be determined by using antibody-based m^{6}A profiling method (Maity and Das, 2015). To overcome these problems, a recent robust method termed site-specific cleavage and radioactive labelling followed by ligation-assisted

extraction and thin layer chromatography (SCARLET) has been developed to determine the location of m^6A site at a particular site with single-nucleotide resolution (Liu et al., 2013). This procedure uses RNase H and a sequence-specific 2′-OMe/2′-H chimeric oligonucleotide to direct a targeted cleavage 5′ of the candidate site. This is followed by radiolabelling of this site using ^{32}P. Subsequently, by using DNA ligase, the labelled RNA fragment is splint-ligated to DNA oligonucleotides. This product is then digested with RNases T1/A, but ^{32}P-labeled sites remain protected from digestion. Finally, thin-layer chromatography (TLC) is then used to analyse the mixture of adenine and methyladenine (Liu et al., 2013; Maity and Das, 2015).

Recently, two types of UV-induced RNA-antibody crosslinking techniques have been developed, allowing m^6A mapping at base resolution based on m^6A-seq/MeRIP-seq (Li et al.,2017). One of them is photo-crosslinking-assisted m^6A-sequencing (PA-m^6A-seq). In this method, 4-thiouridine (4SU) is added into the growth medium, resulting in its incorporation into RNA. This is followed by m^6A immunoprecipitation step. Subsequently, and by using 365-nm UV light, m^6A-containing RNA is crosslinked to the anti-m^6A antibody. Afterwards, using RNase T1, the crosslinked RNA is digested to about 30 nt and then subjected to sequencing. Because 4SU leads to a T-to-C mutation at the crosslinking site, single consensus methylation sequences can be identified within about 23 nt by this method. However, if the distance between m^6A modifications and 4SU incorporation is too large, this technique may fail to detect m^6A locations (Chen et al.,2015; Li et al., 2017; Zhang et al.,2019). Another UV crosslinking technique is known as m^6A-CLIP/IP and miCLIP (m^6A individual-nucleotide-resolution crosslinking and immunoprecipitation) (Ke et al.,2015; Linder et al.,2015). Anti-m^6A antibodies are crosslinked to RNA under 254-nm UV light in this approach to generate crosslinks between antibodies and RNA. Subsequently, the

crosslinked RNA is then reverse transcribed, thereby mutations or truncations are generated in the cDNA. These mutational signatures are then profiled throughout the transcriptome to detect m^6A sites at single-nucleotide resolution.

The m^6A distribution along the length of transcripts is non-random and asymmetric. Bodi et al. (2012) showed that m^6A methylation is predominantly located within a particular 100-150 nucleotide region before the poly(A) tail of *Arabidopsis* mRNAs by using chemical fragmentation and TLC analysis methods. In addition, subsequent MeRIP-Seq transcriptome-wide mapping studies in mammals also revealed m^6A methylation is highly enriched near the stop codon, 3' UTR and atypically long internal exons (Dominissini et al., 2012; Meyer et al., 2012). Moreover, analyses in yeast cells also revealed m^6A are 3′ biased and tightly correlated with the stop codon (Schwartz et al., 2013). Contrary to earlier studies, Ke et al. (2015) demonstrated a precise enrichment of m^6A at the beginning of the last exon but not around stop codons using site-specific localization of m^6A by m^6A cross-linking immunoprecipitation (m^6A-CLIP) analyses.

1.4 Proteins involved in m^6A methylation event

m^6A occurs as a one-step reaction during processing of the nascent pre-mRNA. The methyl group is transferred from the S-adenosyl-L-methionine (AdoMet or SAM) which acts as methyl group donor to the N6 position of the adenine substrate (Scavetta, 2000) (Figure 1.4). Three groups of factors orchestrate the formation and consequences of the m^6A RNA methylome in the eukaryotic cell: m^6A methyltransferases (writers), m^6A, demethylases (erasers), and m^6A binding proteins (readers), according to their function in m^6A catalysis, removal and recognition, respectively.

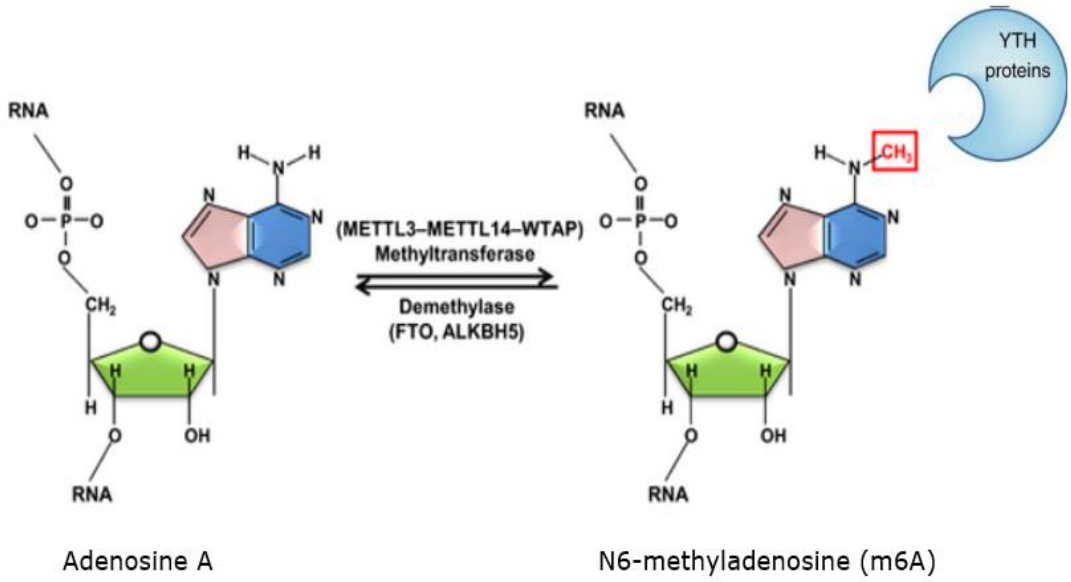

Figure 1.4: Formation of *N6*-methyladenosine (m^6A) from Adenosine A. This reaction is catalysed by m^6A methyltransferase with the presence of SAM (methyl donor) and can be reversibly removed by m^6A demethylases (FTO, ALKAB5). The m^6A mark also can be recognized by various "readers", (YTH) domain family1.The methyl group is shown in red (adapted from Maity and Das,2015).

1.4.1 m^6A writers- adenosine methyltransferases

1.4.1.1 METTL3

Transferring the methyl group from the S-adenosyl-L-methionine (AdoMet or SAM) to the N6 position of the adenine substrate is catalysed by a multicomponent complex (known as m^6A writers). Bokar et al. (1997) identified the first component of a methyltransferase complex in mammalian cells known as MT-A70 as a part of a ~200-kDa MT complex extracted from mammalian cell nuclear extract , and later was assigned as methyltransferase-like 3 (METTL3) by the Human Genome Organization (HUGO) Gene Nomenclature Committee (Gray et al., 2015). Subsequent bioinformatics analysis identified a conserved family of three methyltransferases in eukaryotes, these are A, B and C lineages as well as a more distantly related D lineage associated with some bacteria (Bujnicki et al., 2002, Zhong et al., 2008). METTL3 has a SAM-binding domain and a DPPW motif (Asp-Pro-Pro-Trp) and is highly conserved

in eukaryotes from yeast to humans and its enriched subcellular localization is found in nuclear speckles (Liu et al.,2014). In all the organisms that have been tested to date, the knockout of *METTL3* or its homologs results in apoptosis in mammals, inhibit oogenesis in *Drosophila*, embryonic lethality in *Arabidopsis*, severe sporulation defects in Yeast and increased apoptosis in Zebrafish (Bokar et al., 2005;Hongay and Orr-Weaver, 2011; Zhong et al 2008; Clancy et al., 2002; Ping et al.,2014).

1.4.1.2 METTL14

In 2014, another component of MTase complex and a homolog of METTL3 was identified, known as methyltransferse-Like 14 (METTL14) (Liu et al.,2014; Wang et al.,2014; Ping et al.,2014; Schwartz et al.,2014). METTL14 is highly conserved in mammals and interacts with METTL3 to form a stable heterodimer complex, which deposits m^6A on mRNAs (Liu et al.,2014). The METTL3–METTL14 complex has a much higher methyltransferase catalytic activity *in vitro*, whereas they exhibited a weak activity individually (Liu et al.,2014; Wang et al.,2016; Huang and Yin, 2018). Based on crystal structure studies of the METTL3-METTL14 methyltransferase domain (MTD) complex it was proposed that METTL3 is the catalytically active subunit, while METTL14 is dispensable for activity and plays a structural role for substrate RNA binding (Wang X et al., 2016a; Wang P et al., 2016b; Sledz and Jinek, 2016). Despite no catalytic activity found in METTL14, it still plays an important role in the activity of the writer complex and is involved in vital roles in various biological processes. *METTL14* knockout lead to embryonic developmental defects, inhibits differentiation and stem cell self-renewal, and impaired gametogenesis in other organisms (reviewed by Yang et al.,2018).

1.4.1.3 Other m^{6}A writer proteins

Other regulatory proteins, such as Wilms' tumor 1-associating protein (WTAP) , vir-like m^{6}A methyltransferase associated protein, (KIAA1429 or VIRMA) , and RNA binding motif protein 15/15B (RBM15/RBM15B), are also involved in the m^{6}A writers complex, and shown to be required for m^{6}A methylation. Disruption of these components influences m^{6}A levels in mammals, yeast, and plants (Huang and Yin, 2018). WTAP was found to regulate m^{6}A level of RNA transcripts by interacting with METTL3 and METTL14 (Ping et al., 2014; Zhong et al., 2008; Liu et al., 2014). In 2008, the plant homologue of WTAP was identified as a regulatory component of the RNA N6-methyladenosine methyltransferase complex, Zhong et al, (2008) studied the MTA (the METTL3 m^{6}A methyltransferase homologue in *Arabidopsis*) and found the orthologue of WTAP in *Arabidopsis*, FKBP12 INTERACTING PROTEIN 37(FIP37) interacted with MTA. Later, and consistent with this result, WTAP was found also to interact with METTL3 and METTL14 in mammals (Liu et al.,2014; Ping et al.,2014). Although it does not have methyltransferase domains and displays no catalytic activity of m^{6}A methylation or influences on the activity of the METTL3-METTL14 complex *in vitro*, WTAP co-localised with METTL3-METTL14 complex in nuclear speckles (Liu et al.,2014; Ping et al.,2014; Yang et al.,2018). WTAP is needed for progression of the cell cycle and early mammalian embryonic development (Fu et al., 2014), probably due to its role in the writer complex. Furthermore, knockdown of *WTAP* significantly decreases endogenous m^{6}A levels in human cell lines (Liu et al., 2014; Ping et al.,2014) and in *Arabidopsis* plants (Růžička et al., 2017)

In 2013, KIAA1429 and RBM15 were identified as a part of a WTAP complex, which was believed to be involved in alternative splicing (Horiuchi et al., 2013). Further

studies showed that these proteins are also involved in m^{6}A formation as a part of the MTase complex (Patil et al.,2016; Schwartz et al.,2014). KIAA1429 is required for the full methylation program in mammals, and depletion of *KIAA1429* by siRNA in human A549 cells leads to substantial reduction in m^{6}A levels, suggesting a crucial role of KIAA1429 in the methyltransferase complex (Schwartz et al., 2014). In recent studies, RBM15 and its paralog, RBM15B, were reported to be involved in the methyltransferase complex (Patil et al.,2016). Knockdown of *RBM15* and *RBM15B* causes a decrease of m^{6}A levels in human embryonic kidney 293T (HEK293T) cells (Patil et al.,2016).

More recently, Zc3h13 is a newly discovered component of mammalian m^{6}A methyltransferase complex and regulates m^{6}A methylation. Zc3h13 was shown to be required for the Zc3h13-WTAP-Virilizer-Hakai complex localization and plays a significant role in the self-renewal of mouse embryonic stem cells (ESC) via facilitating m^{6}A methylation (Wen et al.,2018). In addition, Zc3h13 acts as an adapter between RBM15 and WTAP, connecting RBM15 to the m^{6}A machinery to enhance m^{6}A deposition on mRNAs in mouse cells (Knuckles et al.,2018).

1.4.1.4 m^{6}A writer proteins in other organisms

In *Arabidopsis thaliana*, a core set of mRNA m^{6}A writer proteins includes MTA (METTL3), MTB (METTL14), FIP37 (WTAP), VIRILIZER (VIRMA) and the E3 ubiquitin ligase HAKAI. The knockout of any of these protein except *Hakai* are embryo lethal, indicating an essential function for this modification in plant development (Zhong et al 2008;Bodi et al.,2012; Růžička et al., 2017). This will be discussed extensively in section (1.7).

In the yeast *Saccharomyces cerevisiae,* m^6A has a fundamental role in the initiation of meiosis and can only be detected in mRNA during meiosis. The ratio of m^6A to A in a GA context is estimated to be 1.0% in the poly(A) RNA extracted from cells growing for 3h in a sporulation medium (Bodi et al., 2010). Inducer of Meiosis 4 (Ime4) is the yeast homologue of mammalian METTL3 and *Arabidopsis* MTA and functions as an inducer of meiosis during sporulation (Bodi et al., 2010; Clancy et al., 2002; Shah and Clancy, 1992). Mutations of the putative active site in the methyltransferase motif of Ime4 led to the loss of m^6A in the mRNA and severe sporulation defects (Clancy et al., 2002). In addition, another component in *S. cerevisiae* known as Karyogamy protein 4 (KAR4, a homologue of METTL14 and *Arabidopsis* MTB) has been reported to have a physical association with Ime4, however, no characteristic S-adenosyl methionine binding domain has been found in yeast KAR4 which suggests it may be playing a different role to mammalian METTL14 (Ito et al., 2001; Bujnicki et al., 2002; Lahav et al., 2007; Růžička et al.,2017). Two other components have been identified as Ime4 interacting partners in the methylation complex, Mum2 and sporulation specific with a leucine zipper motif protein 1 (Slz1) and these were found to be required for m^6A formation (Agarwala et al., 2012). Mum2 is homologous to *Arabidopsis* FIP37 and human WTAP, while no homologous to Slz1 was found in humans. Moreover, a previous study showed that when the yeast cells enter meiosis in a nutrient-poor liquid medium, the level of m^6A increases, whereas it declines rapidly when nutrients are returned, and cells begin foraging and subject to pseudohyphal growth. These findings suggest the role of m^6A methylation in controlling cell fate and the initiation of meiosis in yeast (Jia et al., 2013).

Likewise, *Drosophila* mRNA also contains m^6A, and has dIme4 and dKAR4 (Inducer of meiosis 4 and Karyogamy protein 4), and Female-lethal (2)d (Fl(2)d) and Virilizer

(Vir), which corresponding to the homologues of mammalian methyltransferase proteins METTL3, METTL14, WTAP and KIAA1429 respectively (Niessen et al., 2001; Horiuchi et al., 2013; Bokar et al., 1997; Penalva et al., 2000; Liu et al., 2014; Haussmann et al., 2016). dIme4 has been shown to have an important role in Notch signalling regulation during oogenesis in *Drosophila* (Hongay and Orr-Weaver, 2011). Contrary to the full knockouts of mammals (*METTL3*) and plant (*MTA*), null mutants of *dIme4* remain viable though flightless, and display a sex bias to maleness (Haussmann et al.,2016). Moreover, Fl(2)d and Vir in *Drosophila* are important to regulate sex-dependent alternative splicing of the sex determination factor Sex lethal (Sxl) (Schütt and Nöthiger, 2000; Haussmann et al., 2016). In zebrafish, knockdown targeting of *WTAP* or *METTL3* results in multiple developmental defects and increased apoptosis (Ping et al.,2014). The findings of m^6A in these other organisms indicate that this modification is significantly involved in different roles of mRNA metabolism.

1.4.2 m^6A erasers- demethylases

Although over 40 years from the discovery of METTL3 as m^6A writer, the identification of m^6A demethylases remained a mystery until 2011. Jia et al, (2011) discovered the first mRNA demethylase known as FTO (fat mass and obesity-associated), which belongs to a family of enzymes that activate oxidation reactions. A more recent study identified another m^6A demethylase, α-ketoglutarate-dependent dioxygenase alkB homolog 5 (ALKBH5) (Zheng et al., 2013). These discoveries of m^6A demethylase indicate that m^6A is a reversible and dynamic post-transcriptional modification in mRNAs. Depletion of both *FTO* and *ALKBH5* lead to significant increases in total m^6A levels of polyadenylated RNAs (Zheng et al., 2013; Jia et al., 2011). Although these two proteins display similar activity when they are

demethylating m^6A on single-stranded RNA (ssRNA), their pathways are distinct (Huang and Yin,2018). While ALKBH5 converts m^6A to adenosine in the direct way (Huang and Yin,2018), FTO demethylates m^6A via two intermediates, N6-hydroxymethyladenosine (hm^6A) and N6-formyladenosine (fm^6A) (Chen et al., 2015; Huang and Yin, 2018), Additionally, recent research showed that FTO also exhibits demethylase activity in ssRNA towards m^6Am (Mauer et al., 2017).

1.4.3 m^6A readers-binding proteins

While methyltransferase complex proteins act as the "writer" and demethylases (FTO and ALKBH5) serve as the "eraser" of m^6A on mRNA, the "reader" of the m^6A modification maybe represented by m^6A-selective-binding proteins, which also could play an important role in regulatory functions through selective recognition of methylated RNA (Luo et al., 2018). The best characterized of these proteins have a characteristic protein domain termed a YTH domain. The YTH domain family in eukaryotes is widespread. In the human genome, there are five YTH domain-containing proteins categorised into three groups: YTHDC1 (DC1 family), YTHDC2 (DC2 family), and YTHDF1–3 (DF family) (Liao et al., 2018). YTHDC1 is the only nuclear member of YTH family proteins and is involved in pre-mRNA splicing (Xiao et al., 2016; Zhao et al., 2017), whereas the other four members regulate m^6A responses in the cytoplasm. Among them, YTHDF1, YTHDF3, and YTHDC2, together or alone, are involved in promoting mRNA translation efficiency (Dominissini et al., 2012; Hsu et al., 2017; Li et al., 2017;Wang et al., 2014; Huang and Ping, 2018), whereas YTHDF2 decreases mRNA stability and regulates mRNA degradation by interacting with the CCR4-NOT deadenylase complex (Wang et al., 2014; Du et al., 2016; Huang and Ping, 2018) . Besides the YTH family proteins, eukaryotic initiation factor 3 (eIF3) , HNRNPA2B1, and embryonic lethal, abnormal

vision-like protein 1 (ELAVL1) have also been reported as an m^6A readers (Liao et al.,2018).

1.5 Consequences of m^6A modifications in mRNA metabolism

Recent cumulative studies showed the role of m^6A methylation in almost every stage of mRNA metabolism, from nucleus (pre-mRNA processing) to cytoplasm (translation and mRNA decay) (Roundtree et al.,2017; Zhao et al.,2017; Nachtergaele and He, 2017; Yang et al.,2015).

1.5.1 The role of m^6A methylation in splicing

Based on the findings that showed methylation to occur in the nucleus and that many m^6A sites are detected in introns of pre-mRNAs, m^6A methylation was suggested to function as a regulator of splicing (Stoltzfus and Dane, 1982; Carroll et al.,1990). m^6A writers and erasers including; METTL3, METTL14, WTAP, FTO, ALKBH5, KIAA1429 and YTHDC1 (m^6A reader) are all predominantly located in nuclear speckles, where the mRNA splicing and storage of splicing factors take place (Ping et al.,2014; Jia et al.,2011; Zheng et al.,2013; Xu et al.,2014). Recently, the data from PAR-CLIP (photoactivatable-ribonucleoside-enhanced crosslinking and immunoprecipitation) analysis illustrated that many METTL3-binding sites are located in introns (Ping et al.,2014), and in mouse embryonic stem cells, depletion of *METTL3* usually favours exon skipping and intron retention (Geula et al.,2015). Moreover, immunofluorescence microscopy studies showed that endogenous METTL14 colocalizes with the pre-mRNA splicing factor SC35 (serine/arginine-rich splicing factor 2) in nuclear speckles (Ping et al., 2014). In addition, nuclear speckle staining of FTO and ALKBH5 also suggests a close relation between mRNA demethylation and mRNA splicing. FTO protein partially colocalizes with SART1 (U4/U6.U5 tri-snRNP-associated protein 1) and SC35 (serine/arginine-rich splicing

factor 2), and RNA polymerase II phosphorylated at Ser2 (Pol II-S2P) splicing or splicing-related speckle factors (Jia et al., 2011). Furthermore, ALKBH5 was found to be co-localised in nuclear speckles with splicing factors SC35, SM (Smith antigen) and ASF/SF2 (alternative splicing factor/splicing factor 2) (Zheng et al., 2013). Further studies also strongly support the functional role of m^6A modification in splicing. For instance, knockdown of either *METTL3*, *WTAP*, or *ALKBH5* caused abnormal mRNA splicing, distortion of splice isoform ratios, and nuclear speckles alteration (Dominissini et al.,2012; Ping et al., 2014; Jia et al., 2011; Zheng et al., 2013; Maity and Das, 2015). FTO also affects splicing; a previous study showed that an *FTO* knockdown in mouse pre-adipocytes enhances the RNA binding ability of SRSF2 (serine- and arginine-rich splicing factor 2), which may promote inclusion of target exons (Zhao et al., 2014). m^6A readers also affect splicing for example; YTHDC1 regulates exon-inclusion by promoting pre-mRNA splicing factor (SRSF3) but blocking binding by SRSF10 (Xiao et al.,2016). In addition, The RNA-binding protein HNRNPA2B1 also appears to act in a similar manner to METTL3 in alternative splicing regulation (Alarcon et al.,2015). In *Drosophila*, female-specific Sxl splicing is regulated by m^6A writers and YT521-B, a *Drosophila* m^6A reader (Haussmann et al.,2016; Lence et al., 2016; Kan et al., 2017). Taken together, these findings suggest a regulatory role of m^6A methylation in pre-mRNA splicing.

1.5.2 m^6A methylation and Alternative polyadenylation

Alternative polyadenylation (APA) has also been reported to be associated with m^6A (Ke et al., 2015; Molinie et al., 2016).The presence of two-thirds of m^6A sites at the 3′ UTR of the last exon, where APA sites exist and the changes in APA due to knockdown of m^6A writers complex, suggests a possible role of m^6A in alternative polyadenylation (APA) (Ke et al.,2015).

1.5.3 m^{6}A enhances mRNA nuclear export

The process responsible to connect transcription in the nucleus to translation in the cytoplasm is known as mRNA nuclear export, which plays a crucial role in the eukaryotic gene expression regulation (Wickramasinghe and Laskey, 2015). Depletion of *METTL3* affects circadian clock gene mRNA (e.g. Per2 and Arntl), thus delaying their export from the nucleus to the cytoplasm (Fustin et al., 2013). Furthermore, another report showed that ALKBH5, m^{6}A demethylase affects mRNA export, and the knockdown of *ALKBH5* results in accelerating mRNA export to the cytoplasm (Zheng et al., 2013). YTHDC1 is a nuclear m^{6}A-binding protein that also affects nuclear export of methylated mRNAs by interacting with the nuclear export adaptor protein SRSF3 and nuclear RNA export factor 1(NXF1) (Roundtree et al.,2017). A more recent paper demonstrated that the m^{6}A-methylase complex is involved in mRNA export regulation by recruiting TREX to m^{6}A modified mRNAs (Lesbirel et al.,2018).

1.5.4 The role of m^{6}A methylation in translation

A recent study has shown a key functional role of mRNA methylation in enhancing mRNA translation (Wang et al.,2015). This study applied photoactivatable ribonucleoside crosslinking and immunoprecipitation (PAR-CLIP) approach and showed that m^{6}A on RNA transcripts can be recognized by YTHDF1 inside mammalian cells. Additionally, high-throughput sequencing methods revealed a positive correlation on the target mRNAs between the ribosome loading of YTHDF1-targeted mRNAs and the number of YTHDF1-binding sites. The same study further showed YTHDF1, the m^{6}A reader protein, interacts with initiation factors e.g., eukaryotic initiation factor3 (eIF3) and directly promotes mRNA translation in an m^{6}A-dependent manner (Wang et al.,2015). Moreover, another study showed that the

m^{6}A reader protein YTHDF3 also promotes translation via interacting with ribosomal 40S/60S subunits (Li et al.,2017). In addition, RNA methyltransferase (METTL3) was recently reported to enhance mRNA translation during translation initiation directly by recruiting eIF3. This activity was independent of METTL3 methyltransferase domain activity or the presence of other m^{6}A writer complex and m^{6}A reader proteins (Lin et al., 2016). Two other papers demonstrated that m^{6}A methylation in the 5′ UTR of mRNAs can enhance cap-independent translation (Meyer et al., 2015, Zhou et al., 2015). Collectively, these findings provide evidence for the involvement of the m^{6}A modification in translation via several mechanisms.

1.6 Regulatory roles of m^{6}A methylation in cellular processes in eukaryotes

1.6.1 The role of m^{6}A in cell differentiation.

Unlike DNA and protein epigenetic modifications, the involvement of mRNA modification (m^{6}A) in controlling stem cell differentiation is beginning to emerge only recently (Noack and Calegari, 2018). Recent studies proposed that m^{6}A modification also impacts the maintenance and differentiation of embryonic stem cells (mESCs) (Batista et al., 2014; Wang Y et al., 2014; Aguilo et al., 2015; Chen et al., 2015; Geula et al., 2015). Conflicting results have been produced by several researchers investigating the role of m^{6}A in mouse and human embryonic stem cells (ESCs) (Zhao and He, 2015). Wang et al., 2014) demonstrated that the knockdown of either *Mettl3* or *Mettl14* caused deficiency of RNA m^{6}A methylation and led to reduced self-renewal capability of mouse ES cells and hence defective cell regeneration. This indicated an important contribution of the modification of m^{6}A in the maintenance of the mESC ground state and the induction of differentiation (Wang et al.,2014; Maity and Das, 2015; Zhao and He, 2015). By contrast, Batista et al, (2014) found that complete knockout of *Mettl3* by CRISPR–Cas9 in mESCs gave rise to improved self-

renewal, thereby preventing differentiation efficiency (Batista et al., 2014; Zhao and He, 2015). A more recent study demonstrated that the role of m^6A methylation in the differentiation of mESCs relied on the state of the cells; naïve or primed pluripotency states (Geula et al., 2015).The cell differentiation in the naïve pluripotent state was blocked by the knockout of *METTL3*, hence leading to hyper-naïve state which failed to produce mature neurons or transit into a primed state (Geula et al., 2015). On the other hand, the depletion of *METTL3* in the primed pluripotent state resulted in minimal self-renewal and fast differentiation, hence disrupting the primed state stability and causing cell death (Geula et al., 2015). Moreover, another recent study showed that the m^6A modification is required for regulating cell reprogramming in mouse embryonic fibroblasts (MEFs). Increased m^6A abundance promotes the reprogramming efficiency of (MEFs), while *METTL3* knockdown, hence inhibition of m^6A formation, caused hindrance of reprogramming (Chen et al., 2015). Aguilo et al., (2015) reported that chromatin-associated zinc finger protein 217 (ZFP217) interacts with METTL3 and restrains m^6A RNA modification. The depletion of *ZFP217* results in a global increase of m^6A methylation level in the pluripotency factors of ESCs, thereby affecting their stability and leading to faster degradation, thus, causing ESC differentiation (Aguilo et al., 2015). In addition, knockout of *Mettl14* in embryonic mouse brains delays cortical neurogenesis and is associated with prolonged cell-cycle progression (Yoon et al.,2017). Similarly, deletion of m^6A reader protein *Ythdf2* delays mouse cortical neurogenesis. (Li et al.,2018). Together, these results suggest a critical role of m^6A modification in embryo development and stem cell function.

1.6.2 Other roles of m^6A

Controlling the mammalian circadian rhythm was one of the earliest proposed influences of m^6A on cell function. Fustin and colleagues demonstrated that several

clock genes bear m^6A modification sites on their transcripts. Knockdown of *METTL3* leading to m^6A methylation inhibition of clock genes, results in elongation of circadian period (Fustin et al., 2013). m^6A also has been shown to be important for viability and developmental processes in eukaryotes. The disruption of *METTL3* led to apoptosis of human Hela cells (Bokar, 2005). Similar to *METTL3*, the knockdown of either *METTL14* or *WTAP* also caused cell death in Hela cells (Liu et al.,2014). Moreover, mutation in orthologues of the METTL3 in yeast (*Ime4*) causes several sporulation defects (Clancy et al., 2002; Bodi et al., 2010). In *Arabidopsis thaliana*, disruption of the *Arabidopsis* m^6A writer complex, including *MTA*, *MTB*, *FIP37* and *Virilizer*, led to embryo lethality, while the deficiency of *MTA* rather than full knockout influences *Arabidopsis* development and growth (Zhong et al.,2008; Bodi et al., 2012; Vespa et al., 2004; Růžička et al., 2017). Furthermore, knockdown of *WTAP* or *METTL3* in zebrafish, caused early development defects and increased apoptosis (Ping et al.,2014). These observations suggest that in eukaryotes, m^6A has crucial functions in viability and development.

1.6.3 m^6A and human diseases

The participation of m^6A methylation in many important cellular functions suggests its affiliation with a range of human diseases. A nucleotide polymorphism within the first intron of the m^6A demethylase gene FTO is implicated in human obesity and energy metabolism. This SNP is linked with body mass index in various human populations (Frayling et al.,2007; Loos and Yeo, 2013). Knockdown of *FTO* led to decreased body weight and fat mass in mouse cells (Fischer et al.,2009; Church et al.,2009; McMurray et al.,2013; Gao et al.,2010), whereas overexpression of *FTO* resulted in raised body weight and fat mass (Church et al.,2010). In addition, a mutation in the (*R316Q*), a catalytic domain of FTO in humans results in a severe

phenotype of growth retardation accompanied by several malformations (Boissel et al., 2009). Furthermore, a recent report has shown that FTO has a direct impact in obesity by affecting the adipogenic differentiation of primary adipocytes (Zhao et al.,2014). Taken together, these studies indicate a role of cellular m^6A methylation status, in particular FTO in the regulation of fat mass and obesity.

Hess et al (2013) demonstrated that FTO was also involved in midbrain dopamine (DA) regulation, which in turn is linked to ageing-related neurodegenerative disorders, for example; the disease of Parkinson's. In addition, the RNA m^6A demethylase FTO also affects neurogenesis, and is crucial for learning and memory, thus m^6A modification is considered to be linked to Alzheimer's disease (Li et al., 2017; Tang et al.,2019). Another study showed that the ALKBH5, (RNA m^6A demethylase) associates to the major depressive disorder (MDD) in Chinese populations (Du et al., 2015). Furthermore, it has long been known that the cellular components of m^6A methylation are intimately related to cancer (Maity and Das,2015), such as, WTAP is associated antigen in leukemia (Casalegno-Garduño et al.,2010). In addition, colorectal cancer and carcinoma cell cultures, endometrial carcinomas, and stomach cancer have been linked to a mutation of *FTO* (Linnebacher et al.,2010). Moreover, phosphorylation of METTL3 has been found to associate with cellular DNA damage (Matsuoka et al.,2007) and tumorigenesis, suggesting a possible function of this m^6A modification in the onset and progression of cancer (Maity and Das, 2015). The growth of some types of cancer such as breast cancer, liver cancer, and colon cancer have been shown to be inhibited by increasing levels of SAM, the methyl group donor of m^6A methylation formation (Pakneshan et al., 2004; Pascale et al., 2002; Ramani et al., 2009;Guruswamy et al., 2008; Maity and Das, 2015). Recent studies revealed that the knockdown of *METTL3* or *METTL14* led to reduced m^6A formation and changed

mRNA expression of genes e.g. (ADAM19), thus dramatically promoting human glioblastoma stem cell (GSC) growth and self-renewal, while the overexpression of *METTL3* inhibits GSC growth and self-renewal (Cui et al., 2017). Collectively, these findings strongly suggest a relation between m^6A methylation and cancer progression. Despite the increasing interests in the methylation of mRNA (m^6A) and its possible regulatory role in different human diseases, the study of m^6A modification under the context of diseases has been limited.

1.7 m^6A modification in plants

1.7.1 m^6A is abundant and conserved in *Arabidopsis thaliana* mRNA

m^6A modification has been found in the mRNA of different types of plants, such as; maize, wheat and oats (Kennedy and Lane, 1979; Nichols 1979; Haugland and Cline, 1980). In the mRNA of the model organism *Arabidopsis thaliana*, the presence of m^6A was first reported in 2008 and was shown to be dependent upon the activity of mRNA adenosine methylase (MTA) [homolog of human METTL3], the catalytic component of *Arabidopsis* m^6A methyltransferase complex (Zhong et al.,2008). The ratio of m^6A to A in *Arabidopsis* was found to be similar to recorded values in mammalian cells and was estimated to be 1.5% of the As in a GA context, although this varied with plant organ type (Zhong et al.,2008). In *Arabidopsis* mRNA transcripts, m^6A predominantly locates at the 3' end (within 150 nt of the poly(A) tail) (Bodi et al.,2012) with an RRACH consensus motif. In addition, recent *Arabidopsis* MeRIP-Seq data demonstrated that the m^6A is enriched also around the start codon of some transcripts (Luo et al.,2014).

1.7.2 m^6A writer, eraser, and reader proteins in Arabidopsis.

A potential methyltransferase complex responsible for m^6A modification in *Arabidopsis* has been identified. To date this includes MTA (METTL3), MTB

(METTL14), FKBP12 interacting protein 37FIP37 (WTAP), VIRILIZER (VIRMA), and the E3 ubiquitin ligase HAKAI (Zhong et al.,2008; Bodi et al.,2012; Shen et al., 2016; Ruzicka etal., 2017) (Figure 1.5). An orthologue of the animal RNA binding motif protein 15/15B (RBM15/RBM15B) not been shown for plants yet.

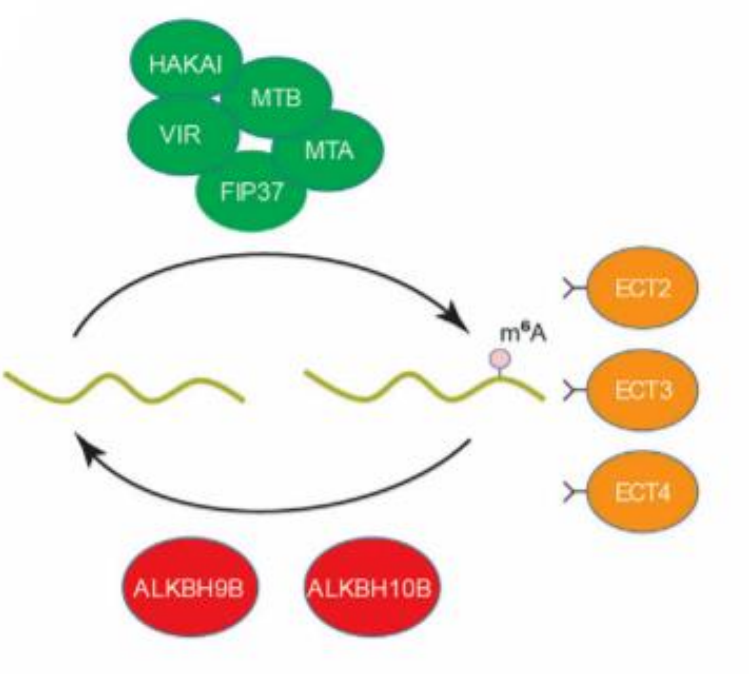

Figure 1.5: m^{6}A modification in *Arabidopsis* is catalysed by methyltransferase complex (writers) include (MTA, MTB, FIP37, VIR, and HAKAI) and removed by demethylases ALKBH9B and ALKBH10B (eraser), and recognized by ECT2, ECT3, and ECT4 (reader) (Liang et al.,2018).

MTA is the *Arabidopsis* m^{6}A methyltransferase METTL3 homologue and is encoded by At4g10760. Inactivation of *MTA* causes an embryo-lethal phenotype and prevents the progression of the developing embryo from passing the globular stage (Zhong et al., 2008) (Figure 1.6 A-D). Plants engineered for a reduction in *MTA* levels rather than a full knockout lead to decreased m^{6}A level by more than 90% and caused developmental defects including; reduced apical dominance, increased trichome

branching and organ abnormality (Figure 1.6 E) (Bodi et al.,2012). These data demonstrate the important role of m^6A in plant development.

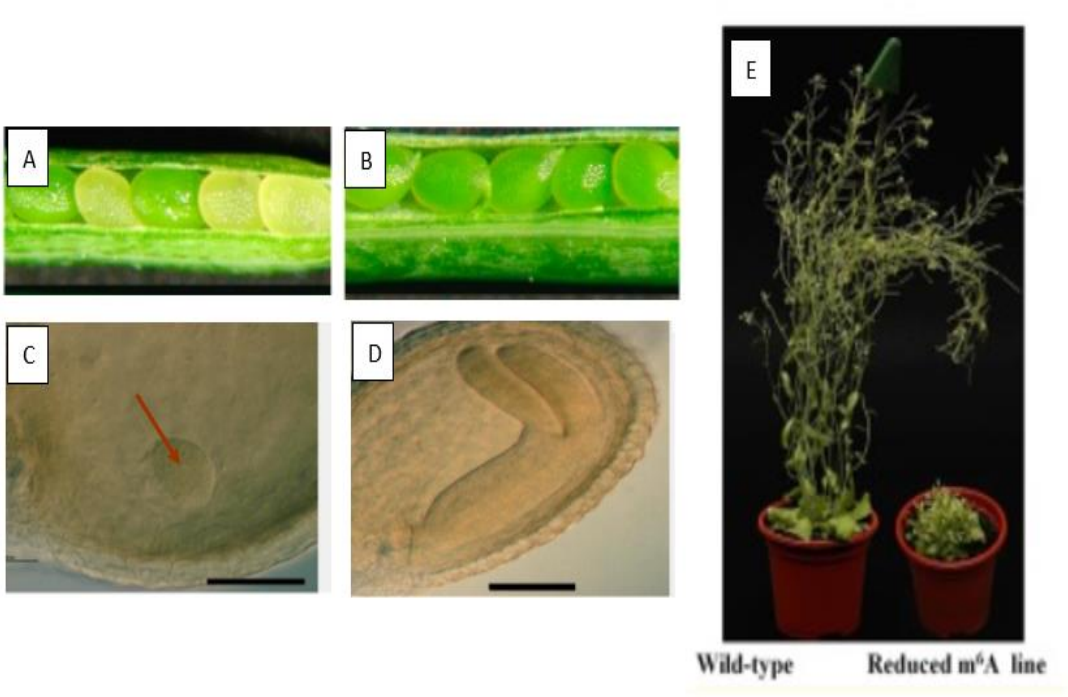

Figure 1.6: The phenotypic characteristics of *MTA* mutant compared to the wild type. A) Silique from *mta* mutant line carrying embryo lethal seeds (white seeds). B) - Control plant (Wild type). C) - The arrested embryo at a globular stage compared to the normal one in D (taken from Zhong et al. 2008). E)- Complementation of homozygous line for the SALK_074069 insertion in MTA with (ABI3-MTA cDNA) shows the different developmental defects (taken from Bodi et al., 2012).

FKBP12 INTERACTING PROTEIN 37 (FIP37, AT3G54170) interacts with MTA and is the *Arabidopsis* ortholog of mammalian WTAP, *Drosophila* protein FEMALE LETHAL2D, and *S. cerevisiae* MUM2 (Muddled Meiosis 2) (Zhong et al.,2008; Shen et al., 2016; Růžička et al., 2017). The full knockout of *FIP37* also leads to embryonic lethality and partial knockdown caused massive over-proliferation of shoot meristems which confirms an indispensable role of FIP37 in the m^6A mRNA modification pattern in *Arabidopsis* (Vespa et al., 2004, Zhong et al., 2008; Shen et al., 2016).

MTB (encoded by AT4G09980) is the homolog of human METTL14 and yeast KAR4, which has also been identified to be associated with m^6A methyltransferase

complex and to form heterodimers with MTA, but its role in mRNA methylation has yet to be clarified (Růžička et al., 2017). Disruption of *MTB* also results in embryo lethality (Bodi et al.,2012). MTB was found to interact with Hakai (the recently discovered factor of m^6A methyltransferase complex) (Růžička et al., 2017). Knockdown of *MTB* by RNA interference (RNAi) led to a decrease in the m^6A levels by 50% (Růžička et al., 2017). Furthermore, additional proteins VIRLIZER (VIR, AT3G05680) and HAKAI (AT5G01160) have also been shown to be required for N6-adenosine methylation of mRNA in *Arabidopsis*, but they have not yet been associated with any specific function within the m^6A methylation complex (Růžička et al., 2017). Null mutation of *VIR* is also embryo lethal, meaning it is essential for embryo development. Hypomorphic lines of *VIR* also lead to severe developmental defects in *Arabidopsis*. The null mutants of *Hakai* are viable and the *Hakai* knockdown gives a 40% reduction in m^6A but the morphological phenotype resembles wild type (Růžička et al., 2017).

The modification of m^6A is reversible and can be removed by the m^6A demethylases in *Arabidopsis*. In the *Arabidopsis* genome, thirteen proteins of the AlkB family proteins have been identified (Mielecki et al.,2012; Fray and Simpson,2015). Two of them, ALKBH9B and ALKBH10B, have been shown to be active m^6A demethylases in plant systems (Duan et al., 2017; Martínez-Pérez et al., 2017; Bhat et al., 2018). ALKBH9B was the first m^6A demethylase in *Arabidopsis* shown to positively affect viral abundance in plant cells (Martínez-Pérez et al., 2017). Duan et al., (2017) demonstrated that ALKBH10B is involved in the regulation of the floral transition in *Arabidopsis*. They showed that the knockdown of *ALKBH10B* led to an increase in the level of m^6A in poly(A) RNA and thus caused delayed floral transition, whereas,

ALKBH10B overexpression reduces the total m^6A level, which led to early flowering phenotype in the resulting plants.

Furthermore, *Arabidopsis thaliana* has 13 genes encoding YTH domain containing proteins, but their functions are yet to be demonstrated (Li et al., 2014a, Fray and Simpson, 2015). Out of those, 11 have been characterized as EVOLUTIONARILY CONSERVED C-TERMINAL REGION1-11 (ECT1-11). Ok et al., (2005), showed that the ECT1 and ECT2 associated with CIPK1 (CBL-INTERACTING PROTEIN KINASE1); therefore, suggested to be involved in the CIPK1 signalling pathway. Recently, (ECT2/3 and 4) were shown to be important for normal leaf morphology including trichome branching, and mutation in these genes result in developmental defects (abnormal leaf shape and abnormal trichome shape with increased numbers of branches) in *Arabidopsis* which closely resemble those of previously described knockdown lines in the m^6A writer complex (Arribas-Hernández et al.,2018; Bodi et al.,2012).

1.7.3 Physiological Roles of m^6A in plants

Although the m^6A methylation field in plants is still evolving, it is obvious that this modification plays a critical role in plant development. The fact that the deficiency of any of m^6A methyltransferase complex proteins is lethal for plants confirms the important role of this modification. The analysis of gene expression showed the possible association between m^6A methylation with numerous stress and/or stimuli responses in *Arabidopsis* (Bodi et al.,2012; Luo et al., 2014). According to m^6A-IP data, m^6A peaks have been identified in the transcripts of photosynthesis related genes, for instance *SERINE/THREONINE PROTEIN KINASE (STN8)*, suggesting a possible role of m^6A in this vital process (Luo et al., 2014). Zhong et al. (2008) demonstrated that the MTA expression is highly correlated to dividing tissues, especially

reproductive organs, shoot meristems, and emerging lateral roots. In addition, TLC analysis showed that the m^6A content in *Arabidopsis* mRNA varied across tissues, indicating some role of m^6A in organ development, and the highest levels of m^6A/A was detected in flower buds (Zhong et al.,2008). Furthermore, the unique distribution of m^6A modifications has also been linked with plant-specific molecular pathways, including those involving chloroplasts (Luo et al., 2014). Recently, the role of m^6A methylation has been investigated in other plants such as; tobacco and rice (Li et al.,2014; Bhat et al., 2018). Transcriptome-wide m^6A profiles of rice callus and leaves showed m^6A patterns in transcripts similar to those previously observed in *Arabidopsis*. In addition, Pearson correlation analysis showed a negative correlation between m^6A methylation enrichment and gene expression (Li et al., 2014).

1.8 Project aims and objectives.

This project aims to understand the role of MTB in mRNA methylation in *Arabidopsis thaliana* through mutant characterization, complementation and promoter studies. Furthermore, we sought to investigate the possible role of post-translational modification of MTB by arginine methylation.

CHAPTER 2 GENERAL MATERIALS AND METHODS

2.1 Chemical materials

All chemicals used in this study were obtained from Sigma-Aldrich Co. Ltd. (Poole, Dorset, UK), Fisher Scientific Ltd. (Loughborough, UK), and VWR International Ltd. (Lutterworth, UK) unless otherwise stated. Q5® high-fidelity DNA polymerase, Taq DNA Polymerases, restriction endonucleases and T4 DNA ligase enzymes were purchased from Promega (Southampton, UK), and New England Biolabs (Hitchin, UK). Oligonucleotide primers used in PCR reactions were purchased from Eurofins MWG Operon (Ebersberg, Germany) and Sigma-Aldrich Co. Ltd. (Poole, Dorset, UK). [α-^{32}P] rCTP radiolabelled nucleotides were purchased from Perkin-Elmer (Waltham, MA, USA).

2.2 Bacterial Strains

The *E. coli* strains DH5α and TOP10 (Invitrogen™, Life Technologies, Carlsbad, CA, USA) were used for all routine cloning work as a plasmid host. *Agrobacterium tumefaciens* C58 strain was used for *Arabidopsis* transformation.

2.3 Plant Materials

Arabidopsis thaliana seeds used in this study are listed in Table (2.1).

Table 2.1: Arabidopsis thaliana mutant lines.

Gene ID	Line name	Source	Description
At4g09980	SALK_056904	NASC	T-DNA inserted in exon 3 of MTB genomic DNA
At4g09980	GK_332G03	Bielefeld University, Germany	T-DNA inserted in intron 4 of MTB genomic DNA
At4g09980	MTB-GFP	Rupert Fray's group	MTB genomic DNA under its own promoter in *mtb* mutant background, with GFP tag downstream.
At4g09980	ABI3:MTB	Rupert Fray's group	MTB genomic DNA driven by ABI3 promoter (ABI3:MTB)
At4g10760	MTAΔSAM	Rupert Fray's group	Generated by mutating the Sadenosylmethionine (SAM) binding domain (DPPW) in MTA gene.
At4g09980	MTBΔSAM	Rupert Fray's group (Generated in this study)	Generated by mutating the Sadenosylmethionine (SAM) binding domain (DPPW) in MTB gene.

2.4 Seeds sterilization and growth conditions

In a laminar flow hood , the seeds were sterilized in 1 ml of 70 % ethanol for 30 sec, and then washed with 1 ml of sterile water. The seeds were then soaked in 5% (v/v) NaClO for 4 min with mixing. The bleach was discarded, and the seeds were washed 5 times with sterile water. The seeds were then poured onto a sterile filter paper and allowed to dry. After drying, the seeds were sprinkled on MS or ½ MS plates with appropriate antibiotic. The plates then were kept at 4^{o}C, in the dark for two days and

then transferred to the tissue culture room at (16 h light/ 8 h dark, 22°C) to allow them germinate and grow. After germination, seedlings were transferred to compost in a 9 cm pots and kept in the phytotron (16 h light/8 h dark, 22°C day/18°C night). Seeds were harvested from dry plants and then stored at room temperature.

2.5 DNA extraction using Edward's buffer

Genomic DNA was extracted following the method developed by Edwards et al., (1991). 20 mg of fresh Plant tissue (leaf) was flash-frozen in liquid nitrogen and ground to a fine powder with pestle under liquid nitrogen. 700 ml of extraction buffer (200 mM Tris-HCl pH 7.5, 250mM NaCl, 25 mM EDTA, 0.5% SDS) was added to the tube. The mixture was then spun down for 5-10 min. The supernatant was transferred to a new Eppendorf® tube. An equal volume of isopropanol was added, then vortexed and precipitated at -20 °C overnight. Next day, the tube was centrifuged at 13,000 rpm for 10 min, then the supernatant was discarded. The pellet was washed with 70%(v/v) ethanol, centrifuged, and dried by vacuum before being resuspended in 50 µl of sterile water and stored at store at -20 °C; 1:30 dilution of this extract was used for PCR reactions.

2.6 Plasmid extraction

Plasmid DNA was isolated according to the manufacturer's recommendation (GeneJET Plasmid Miniprep Kit, Thermo Scientific). RNase A was added to the resuspension buffer before using. 10 ml of overnight culture was centrifuged at 14,000 rpm. 250 µl of the resuspension solution was added to the pellet and mixed until it was homogeneous. Then 250 µl of lysis solution was added to the tube and the tubes were gently inverted 4-6 times until the solution appeared viscous. Then 350 µl of neutralization solution was added and again the tubes were inverted 4-6 times. The mixture was then centrifuged for 5 min at maximum speed. The supernatant was

transferred to the supplied GeneJET spin column by pipetting and was centrifuged for 1 min, and the flow-through was discarded. 500 µl of wash solution was added and centrifuged at maximum speed for 1 min, again discarding the flow-through. This step was repeated twice. Then the spin column was centrifuged 1 min to remove residual wash buffer. The GeneJET spin column was transferred into a sterile /clean 1.5 ml microcentrifuge tube. Then 50 µl of distilled water was added to the centre of column to elute the plasmid DNA. The tube was incubated at room temperature for 2 mins then centrifuged for 2 mins at 14000 rpm. The column was discarded, and the purified plasmid was sent for sequencing to confirm the insertion and the remaining DNA was stored at -20°C to be used in other experiments.

2.7 General PCR amplification of DNA using Q5® high-fidelity DNA polymerase and Programmes.

Specific oligonucleotide primers (Appendix I) were designed from sequences of the MTB gene. PCR reactions were generally performed in a 25 µl reaction volume containing 5 µl of Q5® reaction buffer, 0.5 µl of dNTP (10 mM), 1.25 µl of the forward primer (10 µM), 1.25 µl of the reverse primer (10 µM), 1 µl of DNA template (50–100 ng/µl), 15.75 µl of SDW, and 0.25 µl of Q5® high-fidelity DNA polymerase. The conditions of PCRs programme were selected according to the annealing temperature of the primers and the size of the fragment being amplified. However, the general conditions were as follows: Initial denaturing: 94°C 5 min; denaturing: 94°C 30 s; annealing: 30 s, temperature depends on primer's Tm, extension: 72°C, time depends on the size of PCR fragment, 25-35 cycles; final extension: 72°C 5 min.

2.8 Genotyping PCR

Genotyping PCR was used to screen *Arabidopsis* mutant lines with T-DNA insertions and crossing progenies of these lines. A primer on the T-DNA sequence (Left border primer on the inserted TDNA, LB) was used with two flanking the inserted T-DNA on the genomic DNA sequence (Left primer, LP and right primer, RP). Because the MTB is lethal gene only heterozygous lines were obtained with (LB-TDNA +LP left primer). Primers details used in this study are listed in (Appendix I).

2.9 Colony PCR

Colonies were picked by using sterile pipette tips from LB agar plates then were put in Eppendorf® tube containing 50 µl of distilled water. The tube was incubated in boiling water for 2 min then centrifuged at 13,000 rpm for 2 min. 1µl then was used for PCR reaction.

2.10 Gel electrophoresis

Agarose gels (1%, w/v) were commonly prepared using 1xTBE buffer. 5 µl of 10 mg/ml Ethidium bromide (EtBr) was added to the flask to visualize the DNA under ultraviolet (UV) light then were allowed to solidify. Gels were run in 1x TBE at 100 V for 35-45 min and then were exposed to UV light and photographed.

2.11 Restriction enzyme digestion

Normal DNA digestion reactions were generally performed in a 50 µl reaction volume by mixing 5µl of specific buffer for each enzyme, 1µg of DNA, 2 µl of restriction enzyme and up to final reaction (50 µl) by distilled water. The digested reaction was then incubated at 37 ºC for 1-2 h or according to the recommended temperature and time for the enzyme used. Then 5 µl of loading dye was added before running on 1% (w/v) agarose gel.

2.12 DNA extraction from agarose gel:

For quick and simple purification of DNA from agarose gels, a spin column was prepared by placing a 0.5 ml tube inside a 1.5 ml Eppendorf tube and made a hole at the bottom of the 0.5 ml tube with a needle. Inside the 0.5 ml tube a small piece of wet filter paper was placed. Subsequently, under UV light, the fragment of desired DNA band was extracted from agarose gel and then transferred into the 0.5 ml tube and frozen in liquid nitrogen. The tube was then centrifuged at 13,000 rpm for 5 min. The flow-through liquid was collected into a new tube and this step repeated twice. The DNA precipitated by the addition of 5 µl of Dextran and 3 volumes of 100% ethanol with mixing, and then kept at -20°C overnight. The next day the tube was centrifuged for 10 min. Then the supernatant was discarded and pellet washed with 70% (v/v) ethanol, the pellet was dried by vacuum and dissolved in sterile water and stored at -20°C to be used in the subsequent cloning experiments.

2.13 Cloning

2.13.1 Gateway™ cloning

One method of cloning the DNA sequence of the gene of interest into a plasmid was using the Gateway cloning system (Life Technologies). Amplified PCR products were cloned to Gateway entry vectors to generate constructs needed. PCR with fusion polymerase that have "proofreading" function normally produces greater than 95% blunt - end fragments. These fragments can be tailed with A overhanging using Taq DNA Polymerase before any ligation into entry vector with T-overhung ends. 15 µl of gel purified product was added, 2 µl of dNTPs, 5µl of 5X Taq Reaction Buffer, 0.5 µl of Taq polymerase and Nuclease-free water to a final volume of 25µl. This reaction was incubated at 73 ºC for 30 min. The PCR product was then precipitated overnight by adding 2 µl of 3 M sodium acetate (pH 5.2) and 60 µl of absolute ethanol. Next

day, the DNA pellet was dissolved in 10 µl of sterile water. The following TOPO cloning reaction was prepared by mixing 4 µl of fresh PCR product +1 µl of salt solution + 1µl of water and 1µl of TOPO® vector. The mixture then was incubated at room temperature for 2 or 3 h then used for transformation to *E.coli* DH5a competent cells (section 2.15).. The transformed cells were plated on LB agar plates containing Spectinomycin for colony selection. The plates were incubated in a 37 °C incubator overnight. The positive clones were confirmed using transgene-specific primers and PCR. Each plasmid was extracted, named, and sequenced to confirm its predicted sequence. The correct plasmid was used for the following LR reaction using Gateway® LR Clonase™ II Enzyme Mix (Invitrogen).

The LR reaction was set to a volume of 8 µl containing: entry clone (50-150 ng), destination vector (150 ng/µl), 2µl of LR clonase (enzyme) and completed the volume to 8µl by distilled water. The reaction mixture was incubated for 1 h at 25°C. Then 1 µl of the Proteinase K solution was added to the mixture to terminate the reaction and incubated at 37°C for 10 minutes. The mixture was then used for *E. coli* transformation (section 2.15). After growth, a colony PCR was set up to check and confirm the insertion into the vector. Then plasmid DNA was extracted, sent for sequencing and transferred to *Agrobacterium tumefaciens* by electroporation (section 2.16) and used for plant transformation using the floral dip method (section 2.17).

2.13.2 pJET1.2/blunt Cloning Vector

The mixture consists of 10 µL of 2x Reaction buffer +1µl of purified PCR product +1µl of pJET1.2/blunt Cloning Vector (50 ng/µl) + 7µl of water +1µl of T4 DNA ligase. The mixture was vortexed and incubated at room temperature for 1 h then transformed to *E.coli* (DH5a competent cells).

2.14 T4 DNA Ligation:

To prepare 20 µl ligation reaction, mix 50 ng of vector, an appropriate amount of DNA (3:1 insert to vector molar ratio), 2 µl of T4 DNA Ligase Buffer (10X), 1µl of T4 DNA ligase and complete the volume to 20 with distilled water. The mixture was mixed and incubated overnight in the cold room (4^{o}C), then used for *E. coli* transformation (section 2.15).

2.15 Heat shock transformation:

The DH5α *E. coli* competent cells were taken out of -80°C and thawed on ice for approximately 10 min. 5 µl of the DNA was added to the cells. Subsequently, the mixture of competent cell/DNA was placed on ice for 30 min.The mixture tube was heat shocked in a 42°C water bath for 45 sec, and immediately was put back on ice for 3-5 min. 500 µl of LB medium was then added to the cells. Tubes were placed in a 37°C shaking incubator for 1 hour and 30 min. Some of the transformation mixture was plated onto LB agar plates containing the appropriate antibiotic and incubated at 37°C. After growth a colony PCR was carried out to confirm the transformation.

2.16 Transformation of *Agrobacterium* via electroporation method

Transferring genes into bacteria in order to transform them into the target plant can be achieved by electroporation. It is based on the use of the short electrical pulses of high field strength. *Agrobacterium tumefaciens* strain C58 and 3µl of DNA were mixed and transferred to a cold electroporation cuvette. The cold cuvette then was placed in the Gene Pulser apparatus and electroporated by pushing buttons until a beep sound. Then immediately 1 ml of LB media was added to the cuvette. The mixture then was transferred from the cuvette to 1.5 ml tube and incubated on a shaker at 28 ºC for 2-3

hours before spreading on the LB plates containing appropriate antibiotic. After growth a colony PCR was carried out to confirm the transformation.

2.17 *Agrobacterium* –mediated floral dip transformation of Arabidopsis:

When the *Arabidopsis* plants started flowering, the floral dip method was used to transform *Arabidopsis* using *Agrobacterium tumefaciens*. The *Agrobacterium tumefaciens* strain carrying the gene of interest on a binary vector was prepared and grown in 200 ml of LB with appropriate antibiotic for the plasmid and placed in a 28^{o}C shaking incubator for 2-3 days to OD_{600}=0.8. The culture was then spun down (12000 rpm for 10 mins) and resuspended in 200 ml of 5% (w/v) Sucrose solution. Prior to dipping, Silwet L-77 was added to a concentration of 0.05% (v/v) along with 100 µM final concentration of acetosyringone and mixed well. The upper parts of plants (flowers) were dipped in *Agrobacterium* solution for 30 seconds. These plants then were covered with a plastic bag for 24 h to maintain humidity. The plants were grown and watered normally for 3-4 weeks until seeds became matured. The mature seeds of the transformed plants were harvested and screened on ½ MS media containing the appropriate antibiotics.

2.18 Confocal Microscopy

Arabidopsis seeds were grown on ½ MS media in sterile 100 × 100 mm square plates. The plates were put in the cold room 4 ^{o}C , in the dark for 2 days, and then were transferred to the cultural growth room for 5 days. Roots were then used for localisation analysis by using confocal microscopy (Leica TCS SP5).

2.19 Total RNA extraction following phenol-chloroform method

RNA was extracted following the method developed by Schmitt et al., (1990). Plant tissues were ground into a fine powder using a chilled mortar and pestle under liquid

nitrogen., 400 µl of AE buffer (50 mM sodium acetate pH 5.2, 10 mM ethylenediaminetetraacetic acid), 40 µl of 10% (w/v) sodium dodecyl sulfate SDS and 400 µl of AE saturated phenol were added and vortexed. The samples were incubated at 65°C for 4 min. The samples were again flash-frozen by submerging them in liquid nitrogen for a few seconds each time. This was repeated 4-5 times until phenol crystals appeared. The samples were centrifuged at 14,000 rpm for 5 min and the supernatant was then transferred to a new Eppendorf® tube and phenol:chloroform solution (1:1, v/v) was added and mixed by vortexing. then centrifuged for 5 min. The aqueous phase of each sample was again transferred to a new Eppendorf® tube and precipitated by adding 1/10th volume of 3 M sodium acetate and 3 volumes of absolute ethanol, and the tubes were then vortexed and kept at −20 °C overnight. Next day, to precipitate the RNA, the tubes were centrifuged at 14,000 rpm for 10 min and the supernatant was discarded. The RNA pellets were washed with 80% (v/v) ethanol, centrifuged for 5 min, and dried. the RNA pellet was resuspended in 15 µl sterile water. The total RNA was then checked by NanoDropTM 1000 spectrophotometer and run on 1% (w/v) agrose gel.

2.20 Poly (A) RNA Purification

Before starting, two solutions were prepared: (NEBNext RNA binding buffer and NEBNext wash buffer) as described in Appendix II. Total RNAs were prepared following the protocol described in section (2.19). Two hot blocks were heated one to 80°C and the other to 65°C, and two Eppendorf's containing 100µl of sterile water were put in the 80°C hot block to heat. (1) Prepare the RNA sample: 1-5µg of total RNA was diluted with RNase free water to a final volume of 50µl. (2) Prepare oligo d(T) beads: in a sterile Eppendorf tube, 20µl of oligo d(T) beads was used, then the tube was placed on a magnetic stand and after 2 minutes the supernatant was discarded.

Afterwards, the beads were washed with 100 µl of RNA binding buffer and gently pipetting up and down, then put it back on the magnetic rack and the supernatant was removed. The wash step was repeated once more. (3) The magnetic beads were resuspended in 50µl of RNA binding buffer and the 50 µl of RNA was added. (4) After that, the tubes containing RNA and magnetic beads was placed on the 65°C heat block for 5 minutes then put it on ice. (5) The beads were then mixed gently up and down by pipetting for 6 times to mix thoroughly and incubated at RT for 5 minutes. (6) The step 5 was repeated three more times. (7) The tube was placed on magnetic rack for 2 minutes and the supernatant was removed. (8) The beads were washed twice in 200 µl wash buffer. (9) 50 µl of preheated water was added to the tube of beads and incubated at 80°C for 2 minutes, then was cooled at RT. (10) 50µl of RNA binding buffer was added and pipetted up and down for 6 times then incubated at RT for 5 minutes. (11) The step 10 was repeated twice. (12) The tubes were placed on the magnetic rack and the supernatant was discarded. (13) The beads were washed with 200µl of wash buffer, then the buffer was removed. (14) RNA was eluted with 10µl of prewarmed water, then incubated at 80°C for 2 minutes. (15) The supernatant Poly (A) RNA was collected in new tube and stored at -80 C until use.

2.21 m^6A Measurement

m^6A levels were measured as described in (Zhong et al., 2008) by two-dimensional TLC analysis. T1 digestion mixture was prepared as follows: 25 ng of the poly-A RNA +1µl of polynucleotide kinase (PNK) buffer + 1 µl of RNase T1 (1,000 U·ml-1; Fermentas) + 4.5µl sterile water. The reaction mixture was incubated for 30 minutes at 37°C. Afterwards, the digested RNA was labelled with 0.5 µl of [γ-32P] ATP (6,000 Ci·mmol-1; PerkinElmer) and 1µl of T4 PNK was added and incubated for 1 hr at 37°C. then was precipitated by 1/10 volume of 3 M sodium acetate (pH 5.2) and 3

volumes of absolute ethanol at -20°C overnight. Next day, the labelled RNA was centrifuged for 20 minutes at 13,000 RPM. The supernatant was removed, and the pellet was dried for 5 minutes in the 37°C hot block, then resuspended in nuclease P1 (Sigma-Aldrich) reaction mixture (1µl 10x p1 buffer,1 µl of nuclease P1, 8.5 µl sterile water). The reaction mixture was incubated at 37°C for 2 h. 1 µl of the digested sample was loaded onto the cellulose TLC plate (20 × 20 cm; Merck) and developed in a solvent system, with first dimension buffer: isobutyric acid:0.5 M NH4OH (5:3, v/v) and isopropanol:HCl:water (70:15:15, v/v/v) as the second dimension buffer. The plates were taken out from the tank and kept to drying then were sealed. The identification and Quantification of the labelled nucleotides were carried out by using a storage phosphor screen (Fuji-Screen) and Bio-Rad Molecular Imager FX system with Quantity One software.

CHAPTER 3 GENERATING MTB HYPOMORPHIC LINES

3.1 Overview

One of the most effective ways of identifying the function of genes is creating knockout or reduced expression of the gene of interest, then analysing the resulting phenotype. *Agrobacterium* mediated T-DNA insertion has been used in both monocotyledonous and dicotyledonous plants as a method of implementing reverse genetics. This can be achieved through the introduction of RNAi constructs that target the gene of interest, introduction of genes encoding dominant-negative versions of the protein or through insertional disruption of the target gene. In this latter method, a population of plants containing random T-DNA insertions have been generated and screened by sequencing the genomic sequences flanking the T-DNA borders to identify the insertion sites. From such a population, plants can be selected with mutagenic insertion(s) in a specific gene. A PCR genotyping strategy can then be used to detect the presence of a T-DNA insertion within the gene of interest by using one gene-specific primer and one T-DNA specific primer. The goal of this technique is the determination of a phenotype that is produced by mutation of a particular gene. However, for some essential genes homozygous insertion lines cannot be obtained due to lethality. Such mutants can be only maintained as heterozygous plants and any phenotypes that might result from reduced rather than blocked expression will not be apparent. In the current study, we investigate the role of MTB in mRNA methylation in *Arabidopsis* plants. Therefore, different T-DNA insertion mutants in MTB were characterised and genotyped. Plants containing this insertion could only be isolated as heterozygotes, the homozygous knockout in *MTB* resulted in embryo lethality and the seeds had an embryo lethal phenotype. In order to rescue the homozygous embryo

lethal mutant phenotype, the transgenic plants that contain a T-DNA insertion (SALK_056904) were crossed with plants containing an MTB transgene under the control of a seed-specific promoter (ABI3). The ABI3 promoter was used to direct the MTB gene expression in homozygous seeds during embryogenesis and limit the MTB production during vegetative growth. Therefore, the impact of the absence (or decrease) of MTB protein in homozygous seedlings was examined at germination. The homozygous plants obtained using this approach (mtb ABI3prom:MTB) show more severe developmental defects than either *MTA*, *FIP37* or *Virilizer* knockdowns.

3.2 Aims and objectives of this chapter

The work in this chapter is focused on characterising two T-DNA insertion mutants in MTB and using these to create MTB hypomorphic lines using complementation with an MTB transgene driven by weak promoter. These hypomorphic lines were then assayed for altered m^6A methylation levels and phenotypic consequences of this such as altered trichome branching.

3.3 Results

3.3.1 Characterization of T-DNA insertion lines in MTB and genotyping analysis

To investigate the functional role of MTB (At4g09980) during *Arabidopsis* development, different T-DNA insertion lines were characterized. SALK_056904 and GK_332G03 contain a T-DNA insertion in the third exon and fourth intron, respectively (Figure 3.1, A). The seeds were screened on ½ MS medium then were transferred to compost following germinating. The identification of seedlings containing the T-DNA insertion in MTB was determined by isolation of the genomic DNA from these plants and amplification by PCR. The PCR strategy for analysis of the T-DNA insertion in MTB mutant lines is depicted in (Figure 3.1 B & C). Primers LP (named intron 1), the gene's specific forward oligo, and primer LB-SALK a T-DNA, left border reverse primer were designed to amplify a 700 bp band of the MTB T-DNA (SALK_056904) from heterozygous (or homozygous) plants (Figure 3.1, B). In addition, a left T-DNA border primer named GK.TDNA and the gene-specific forward primer (MTB-GK-FW) were used to distinguish heterozygous plants for MTB T-DNA insertion line GK_332G03 (Figure 3.1, C).

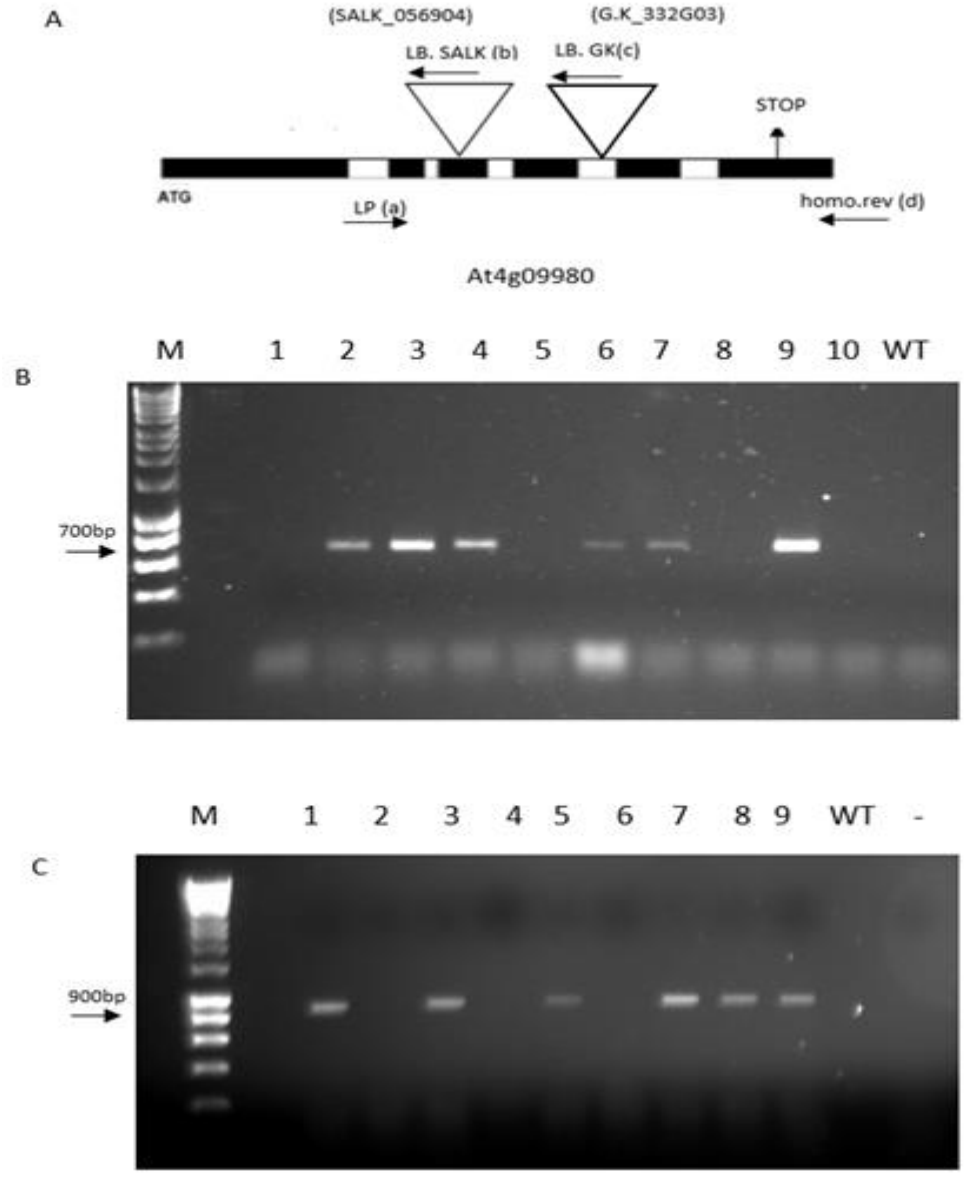

Figure 3.1: Screening MTB T-DNA insertion mutants. (A) At4g09980 map showing the location of T-DNA insertion lines (SALK-056904), (GK_332G03) and oligonucleotides that were used. LP(a)= left primer in first intron of MTB, LB.SALK (b)=left border primer on the (SALK_O56904) inserted T-DNA, LB.GK (c)= left border primer in the T-DNA insertion (GK_332G03), and homo.rev (d)=reverse primer used later for homozygous plants. (B) Genotyping PCR analysis for MTB T-DNA insertion (SALK-056904) line. Primers (a+b) were designed and used to amplify T-DNA insertion (heterozygous plants) and the product size=700bp. (Lanes 2,3,4,6,7,9), showing the heterozygous plants, and the rest showing Wild type. (C) Genotyping PCR analysis for MTB T-DNA insertion (GK_332G03) line. Primers (a+c) were designed and used to amplify T-DNA insertion (heterozygous plants only) and the product size = 900 bp. (Lanes 1,3,5,7,8,9), showing the heterozygous plants in (GK_332G03) T-DNA insertion line. The rest showed Wild type bands. PCR products were run on 1 %(w/v) agarose gel, and HyperLadder 1Kb (Bioline) was used as a marker. Genotyping was conducted on wild type to confirm the predicted genotyping bands (data not shown).

Plants containing either of these two T-DNA insertion mutant lines in MTB could only be isolated as heterozygotes, and a quarter of their seeds showed an embryo lethal

phenotype indicated by small brown shriveled up seeds in (Figure 3.2). This result for the *MTB* insertion mutants was similar to that found for *MTA* methylase knockout and suggests that the homozygous knockout in *MTB* is embryonic lethal (Zhong et al.,2008).

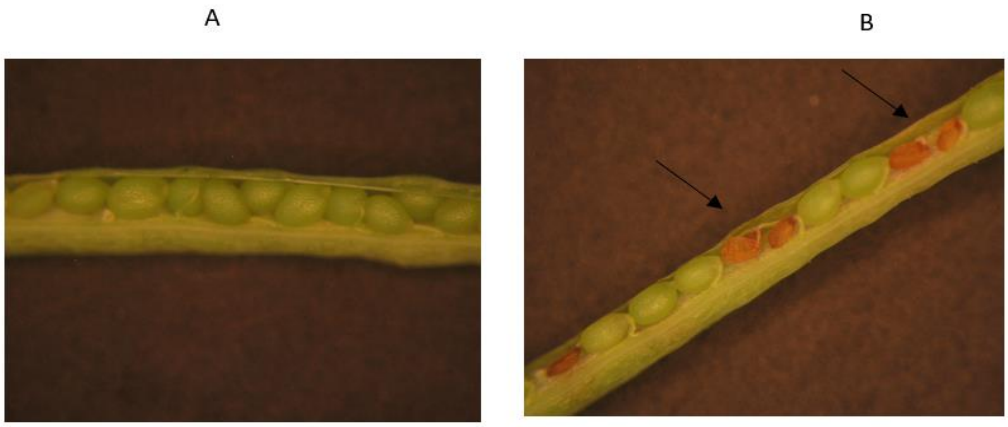

Figure 3.2: The embryo lethal phenotype of the homozygous (GK-332G03) T-DNA insertion. (A) WT control with all green seed. (B) The self-pollinated heterozygous GK-332G03 line gives ~25% dead seeds (indicated by small brown seeds) due to the embryo lethal nature of the mutation.

3.3.2 Crossing MTB (SALK_056904) line with the MTB gDNA under the control of the ABI3 promoter

The homozygous T-DNA insertion embryos in *MTB* did not complete the full developmental process and gave rise to inviable seeds. In order to bypass the embryo lethal defect of the MTB T-DNA insertion lines, we have employed an already successful technique applied to rescue of *MTA* embryo lethal phenotype (Bodi et al., 2012). We crossed the heterozygous plant of MTB T-DNA insertion (SALK_056904) line with a plant harbouring MTB under the control of the ABI3 promoter. The ABI3 promoter gives good expression during embryonal development, but very weak expression in vegetative organs compared with MTB gene's endogenous promoter (Figures 3.3 & 3.4). The construct of genomic MTB with ABI3 promoter was generated during a previous study in our group (Figure 3.5).

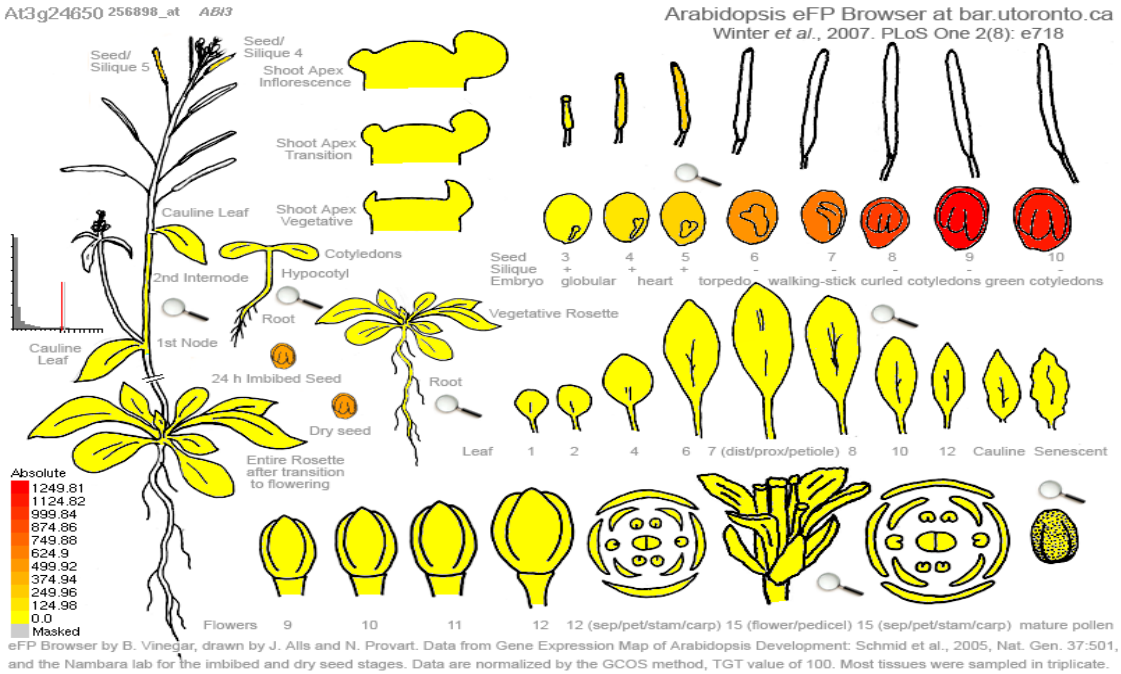

Figure 3.3: "Default" eFP Browser in *Arabidopsis thaliana* showed the expression levels of ABI3 (At3g24650). Stronger expression is illustrated by a darker red color. http://bar.utoronto.ca/ExpressionAngler/.

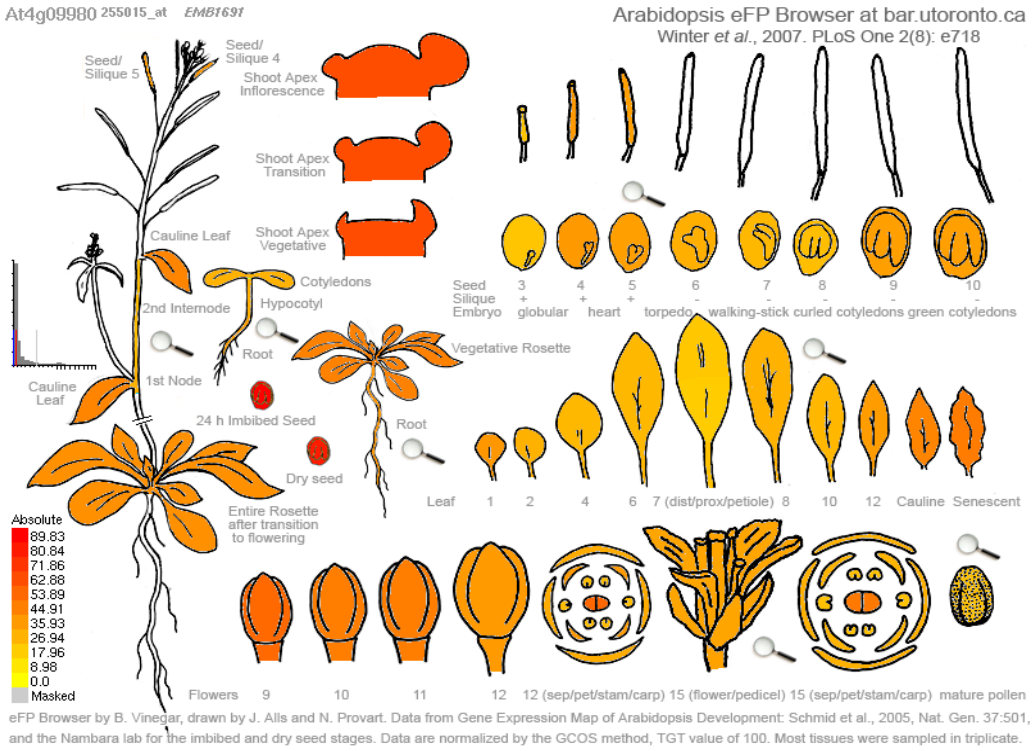

Figure 3.4: MTB (At4g09980) expression pattern, http://bar.utoronto.ca/ExpressionAngler/.

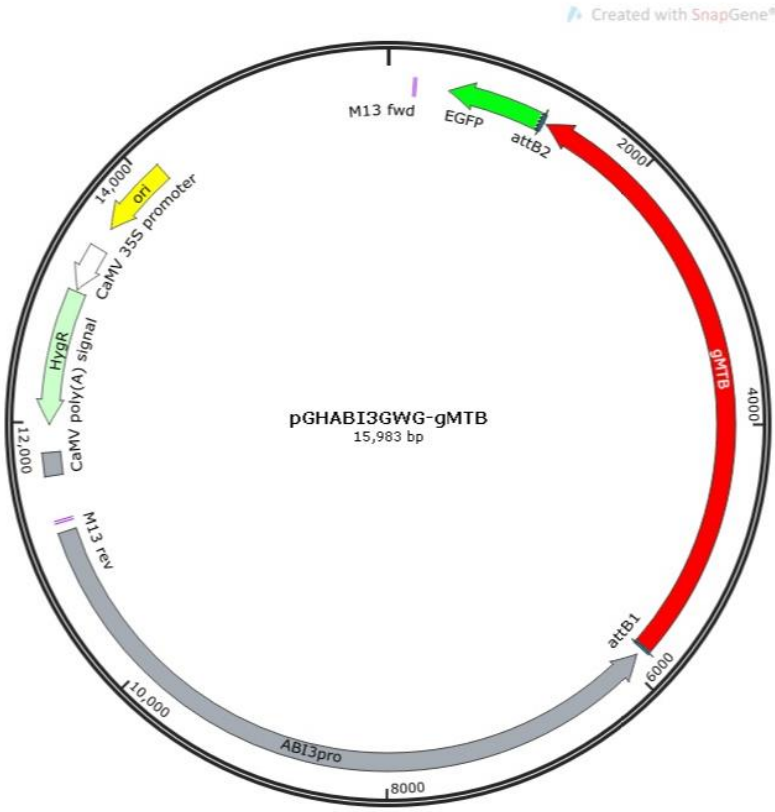

Figure 3.5: Schematic of recombinant ABI3:gMTB construct generated by Snap Gene Software. Expression was driven by the ABI3 promoter and the MTB was fused at its C-terminus to GFP. Hyg: Hygromycin resistance for plants.

Transgenic seedlings of the crossed line were selected on Hygromycin, and in the F1 generation, progeny heterozygous for MTB T-DNA insertion (SALK_056904) and with the presence of the ABI3:MTB construct were identified by PCR. Primer pairs used for PCRs were forward primer (intron1) on the MTB genomic DNA and the reverse primer on the inserted T-DNA (LB.SALK) to distinguish the heterozygous plants for MTB T-DNA insertion (SALK_056904) (Figure 3.6 A), whereas the presence of the ABI3:MTB construct was verified by using the forward primer in MTB and reverse one in GFP (MTB.FW.1 + GFP REV); a band of 900 bp should be amplified (Figure 3.6 B).

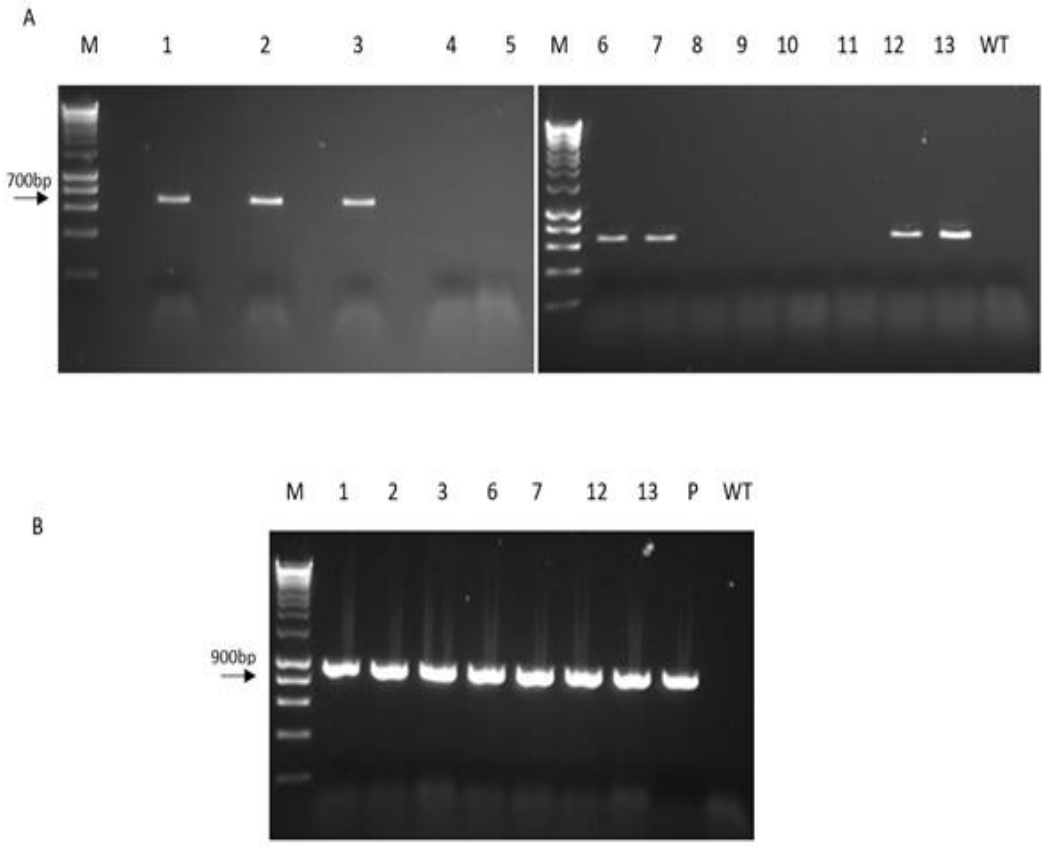

Figure 3.6: Screening F1 progenies of *mtb* insertion mutants (SALK_056904) crossed with ABI3:MTB. (A) Genotyping PCR to check *mtb* (SALK_056904) T-DNA insertion in F1. Lines (1, 2, 3, 6, 7, 12, and 13) represent 7 heterozygous individual F1 plants. (B) PCR to check the presence of ABI3:MTB construct in plant (1, 2, 3, 6, 7, 12, and 13). P=positive control using MTB-GFP positive line and WT = wild type used as negative control.

In the F2 generation, progenies showing phenotypes were further confirmed to be homozygous for (SALK_056904) T-DNA with the presence of ABI3:MTB by genotyping PCRs. The homozygosity of the MTB T-DNA insertion (SALK_056904) was verified by the absence of the 2500 bp wild type band in lanes (1, 2, 3 and 4) with primers (a+d), and the amplified band (700 bp) obtained with primers (a+b) confirmed the presence of the (SALK_074069) T-DNA insertion (Figure 3.7 A). Moreover, all observed homozygous plants also contained the ABI3:MTB construct and were confirmed by PCR using the forward primer in MTB and reverse primer in GFP

(MTB.FW.2 + GFP REV) (Figure 3.7 B). These lines were named *mtb ABI3prom:MTB*. All primers were shown previously in (Figure 3.1 A). These homozygous lines had some developmental defects including serrated leaves and very short flower stems (Figure 3.8), which were similar to but more severe than the previously published *MTA*, *FIP37* and *VIRILIZER* mutant plants (Bodi et al., 2012). Unfortunately, these homozygous plants died before flowering and so we could not continue to subsequent generations.

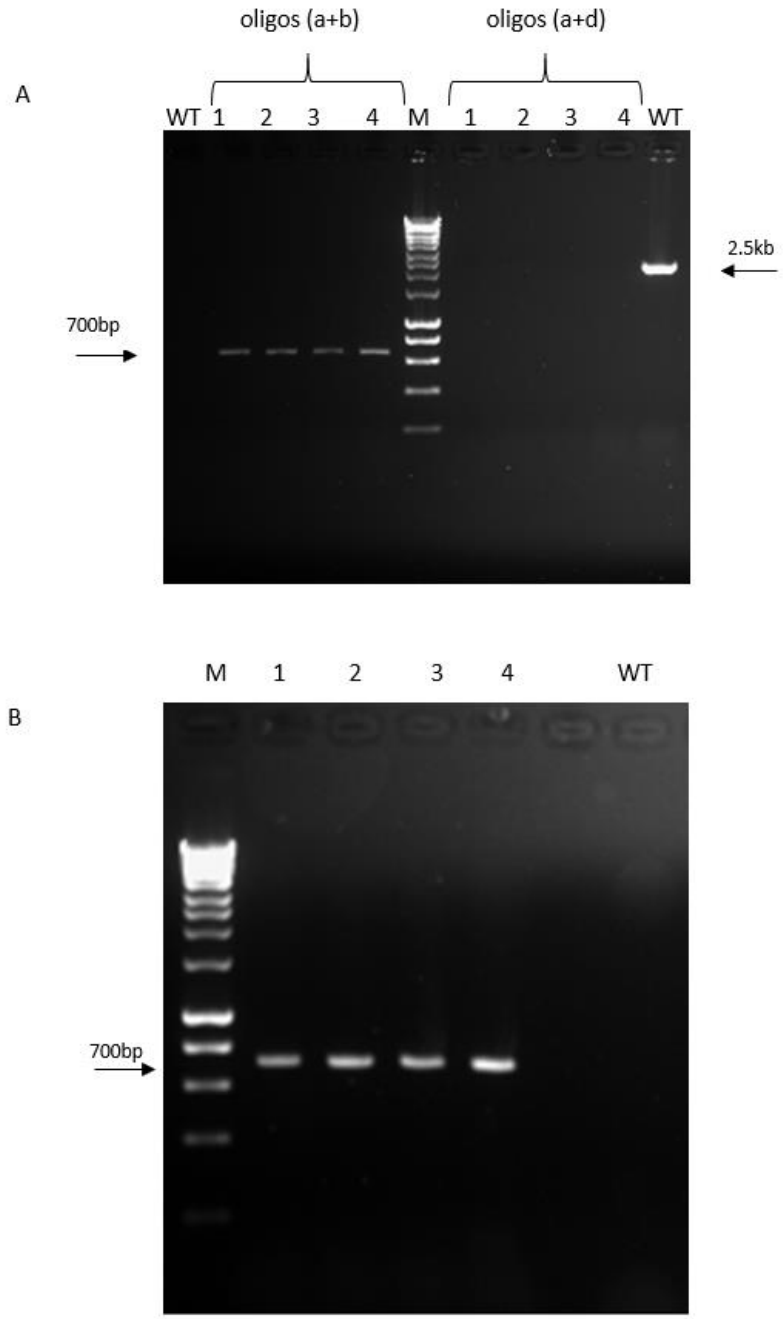

Figure 3.7: Genotyping PCR to confirm F2 lines homozygous for *mtb* (SALK_056904) T-DNA insertion. (A)- The presence of the SALK_056904 insertion was confirmed by the presence of a band of 700 bp with oligonucleotides Intron1 (a) and LB.SALK (b) (lanes 1–4, left). The homozygosity of the SALK insertion was confirmed by the lack of the 2500 bp wild type band in lanes (1-4, right) by using oligonucleotides intron1(a) and homo-rev(d). B) - PCR to confirm the presence of the ABI3: MTB construct in plants (1-4) WT=Wild type.

Figure 3.8: Phenotypic characterisation of F2 generation of 3 week old homozygous plants of hypomorphic line *mtb* ABI3prom:MTB. All observed plants had very short flowering stems, stunted growth and serrated leaves compared with WT. Top panel is all enlargement of the bottom row. Scale bar= 1 cm.

3.3.3 m^6A level of Hypomorphic line of MTB.

As shown in Figure 3.8, the embryo lethal phenotype of *mtb* can be complemented by using ABI3:MTB, and it was hypothesised that in the homozygous complementing lines where expression is driven by the ABI3 promoter, the level of m^6A should be reduced. To confirm this the m^6A level of MTB in ABI3 promoter driven transgenic plants was measured by two-dimensional TLC analysis as described in section (2.21) (Figure 3.9). As expected, the m^6A to A ratio in the homozygous plants was significantly less than the ratio in the wild-type *Arabidopsis*, with more than 80 % reduction compared to wild type (Figure 3.10).

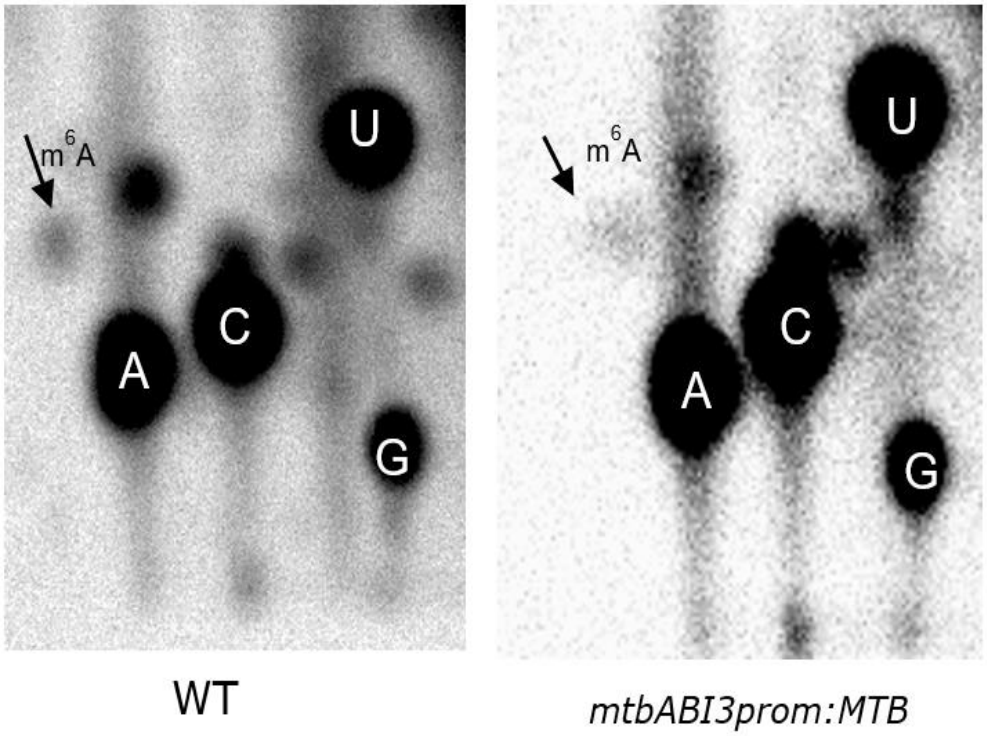

Figure 3.9: Two-dimensional TLC analysis of poly(A) RNA from 3-week old *Arabidopsis* seedlings (mtbABI3prom:MTB) line relative to WT. Spots representing m^6A are indicated by black arrows. The m^6A spots were measured by Quantity One software.

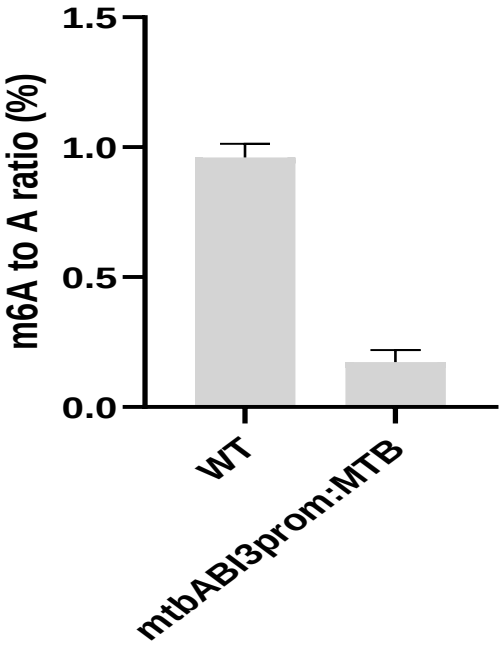

Figure 3.10: m^6A levels of (mtbABI3prom:MTB) transgenic lines checked by the TLC method. Levels of m^6A in homozygous plants is reduced by more than 80% compared to WT. Bars represent SD of three replicates.

3.3.4 Reduction in the expression of MTB affects Trichome Branching in *Arabidopsis*.

Previous studies have shown that the reducing MTA expression led to increased trichome branching in *Arabidopsis* (Bodi et al., 2012). Moreover, overexpression of *AtFIP3*, also increases trichome branching in *Arabidopsis* (Vespa et al., 2004), as does knock out of the m^6A YTH reader protein *ECT2* (Wei et al., 2018). Interestingly, in this study we obtained a similar phenotype for the reduced m^6A plants. The transgenic lines for mtbABI3prom:MTB exhibited numerous and highly branched trichomes on the adaxial leaf epidermis compared to WT (Figure 3.11 A). The proportion of four or more branched trichomes are increased from 17.69% to 64.84 % in the homozygous plants of (mtbABI3prom:MTB) (Figure 3.11 B).

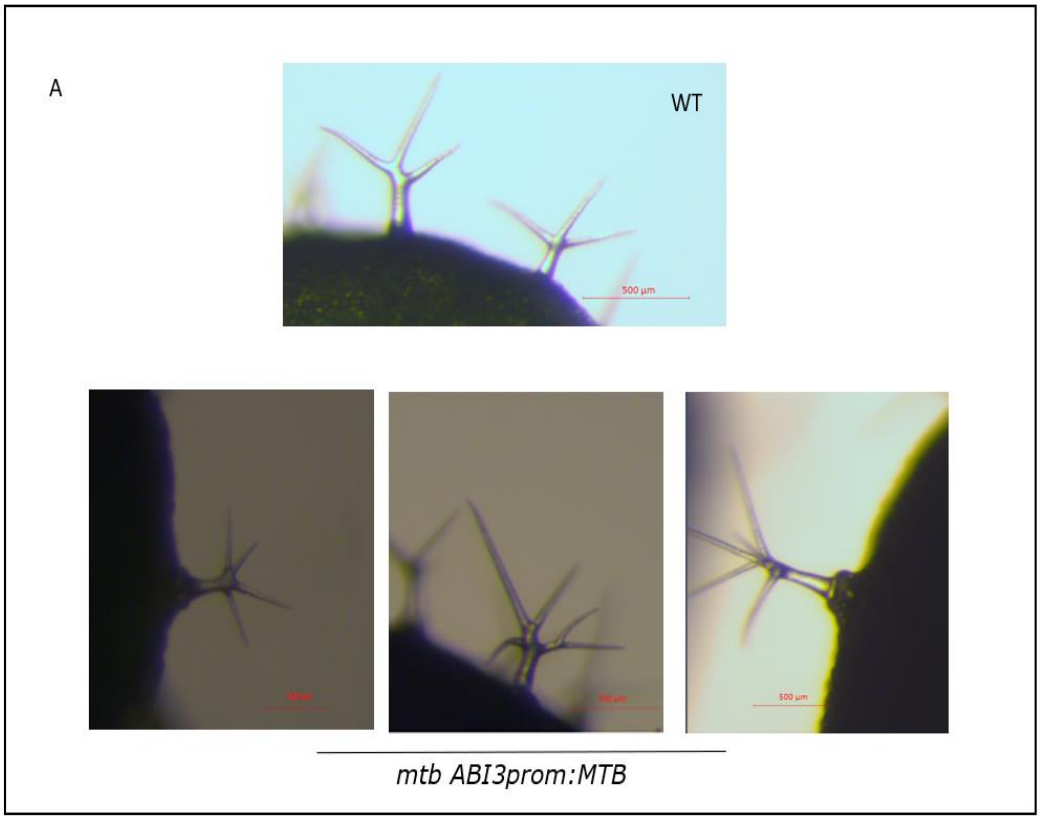

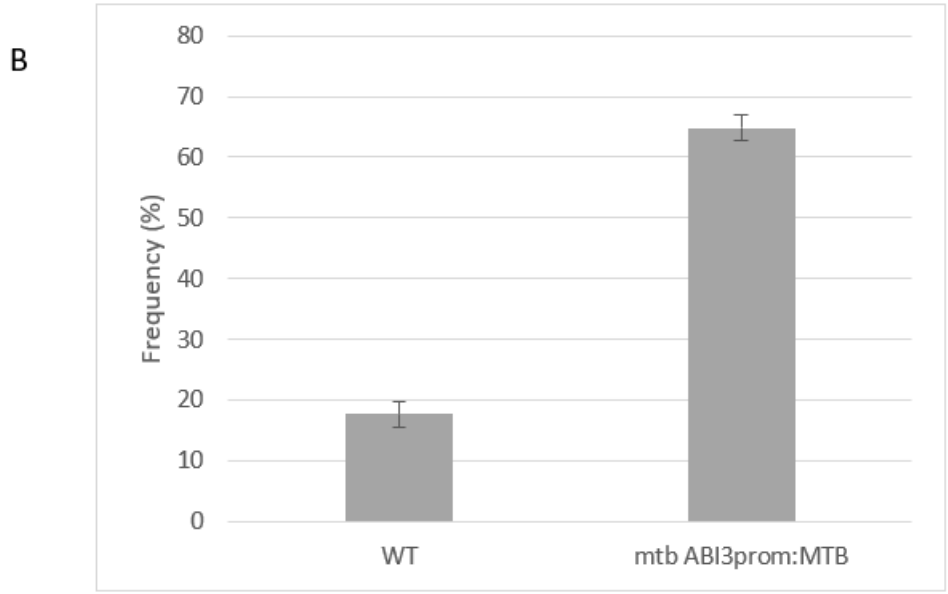

Figure 3.11: Altered number of trichomes branching in the 3-week-old seedlings of mtbABI3prom:MTB lines. (A) Illustration of the increase in trichome branching number for leaves in homozygous plants relative to WT. (B) 64.84% of trichomes from low methylation plants (mtbABI3prom:MTB) had four or more branches, whereas just 17.69% in wild type. Error bars represent SD of the replicates. Scale bar=500 µm

3.4 Discussion

In 2008, Zhong et al investigated the role of MTA during *Arabidopsis* development by characterizing a T-DNA insertion mutant in MTA (At4g10760) and they demonstrated that the null mutation in MTA T-DNA insertion SALK_074069 results in embryo lethality and embryo arrest at the globular stage. Therefore, the mutants can only be maintained as heterozygotes. In 2012, Bodi et al., generated an m^6A reduction mutant of *A. thaliana,* rather than full knockout, by rescuing the homozygous embryo lethal phenotype in *MTA* by complementation of SALK_074069 with the MTA cDNA under the control of the embryo-specific ABI3 promoter. This allowed the role of MTA in seedlings and mature plants to be studied (Bodi et al., 2012; Rohde et al.,1999; Despres et al., 2001). Thus, the ABI3 promoter can be used to complement embryo lethal phenotypes in order to determine the phenotype associated with a reduction in expression of a gene of interest in adult tissues, conferring very low basal expression in post-germination plant organs (Bodi et al 2012, supplemental Figure A1). The expression of *ABI3* has previously been extensively characterized and the promoter has been used to rescue other embryo-lethal mutations in order to study vegetative gene function (Rhode et al., 1999; Despres et al., 2001). The observed plants of ABI3:MTA had multiple developmental defects, including reduced inflorescence internode lengths, leaf crinkling, reduced apical dominance and were bushy compared to the WT (Bodi et al., 2012) (Figure 1.6 E).

The current study focused on MTB (AT4G09980), which is a member of the MT-A70 family sub-lineage B (Bujnicki et al.,2002) and is a homolog of METTL14 and KAR4 in mammals and yeast respectively. Homozygous knockout of this methylase in *Arabidopsis* also leads to embryo lethality, indicating an essential role of MTB during

embryogenesis development (Bodi et al., 2012). One-quarter of the seeds from heterozygous immature siliques of the T-DNA insertion lines in *MTB* had an abnormal brown colour that were randomly distributed along the silique relative to the wild-type with all green seeds. Because the lethality phenotype of mutant *MTB* did not allow us to identify the precise function of MTB in adult tissues, and in order to study the MTB role after germination, we have employed the same technique used to rescue the *MTA* embryo lethal phenotype (Bodi et al., 2012). We crossed the *MTB* T-DNA insertion (SALK_056904) with a plant harbouring MTB under the control of *ABI3* promoter to allow us to recover mature plants homozygous for the knockout *MTB* gene. As a result, we obtained more than 80 % decrease in m^6A levels from 3-week-old *Arabidopsis* seedlings of *MTB* hypomorphic lines. These *mtbABI3prom:MTB* plants had various developmental defects which were similar to but more severe than the previously published *MTA* and *FIP37* mutant plants (Bodi et al., 2012) . These phenotypic changes including crinkled leaves and shorter inflorescence internode lengths suggest problems with organ definition. Furthermore, consistent with previous results of increasing trichome branching in *Arabidopsis* for reduced *MTA* methylation (Bodi et al., 2012), overexpression of *FIP37* (Vespa et al.,2004), and knock out of the m^6A YTH reader protein *ECT2* (Wei et al.,2018), we also observed significant alterations in trichome branching. Trichome cells are regularly distributed on the epidermal layer on the leaves of *Arabidopsis* plants and ''have been used as a model for cell shape and polarity control in plants, and the degree of branching may also be an indication of changed endoreduplication'' (Bodi et al., 2012; Hülskamp et al., 1994). The transgenic mtbABI3prom:MTB lines have numerous branched trichomes on the adaxial leaf epidermis compared to WT. In addition, homozygous lines showed a bleaching phenotype in the leaves and these results show that the white or yellow leaves

production are correlated with the mutation on the *MTB* which may lead to the cell death, and the plants died before setting seed. Currently, we can get homozygous seedlings, but these are more severe than the other hypomorphic lines and die before flowering and so still have to be maintained as heterozygotes. Levels of MTA or MTB protein from transgene construct will depend upon transcription rate, mRNA half-life, translation rate, and protein half-life. Previously, ABI3-MTA allowed sufficient complementation to allow growth to seed set, whereas ABI3-MTB complemented lines die at the seedling stage and this could be due to mRNA half-life. The half-life of MTA is (1.98h) whereas the MTB half-life is (0.6 h) and this is very low compared to the average of mRNA half-life in *Arabidopsis* which is 3.8 h (Narsai et al., 2007). In addition, a previous study showed that approximately 100 of unstable transcripts in *Arabidopsis thaliana* were described as being quickly degraded with half-lives of < 60 min (Gutierraz et al., 2002).

CHAPTER 4 ENGINEERING OF MTA AND MTB TO CREATE DOMINANT-NEGATIVE m^{6}A WRITER MUTANTS

4.1 Overview

Dominant-negative mutations can be defined as those causing mutant polypeptides that disrupt the function of the wild-type gene when over-expressed (Herskowitz, 1987). Where available, such mutants can be useful for studying gene function in plants. Methylation inhibitors were used in early investigations into m^{6}A function in mRNA. Such studies used competitive inhibitors of S-adenosylmethionine such as cycloleucine to prevent the formation of m^{6}A, and from these experiments m^{6}A was proposed to have a function in RNA splicing events and/or the transport of mRNA from nucleus to the cytoplasm (Camper et al., 1984; Stoltzfus and Dane, 1982; Finkel and Groner, 1983). However, such inhibitors often had pleiotropic effects, making firm conclusions difficult. In this study, an alternative approach to investigate the function of the MTB gene was undertaken. Both MTA and MTB contain motifs characteristic of S-adenosylmethionine (SAM) (methyl donor) binding domains. At the core of this SAM binding domain are the four amino acids DPPW (Bujnicki et al.,2002; Bokar et al.,1997). In previous work from the Fray group (unpublished and presented below), it had been found that constitutively over-expressing an *MTA* cDNA in which the DPPW SAM binding site had been mutated, gave rise to *Arabidopsis* plants similar in appearance to the low m^{6}A *ABI3MTA* lines. Thus, the *MTA* transgene with the mutated SAM binding domain appeared to function as a dominant negative mutant when over-expressed. The plant MTB peptide harbours a similar DPPW (predicted SAM binding) domain, so the objective was to create a mutant *MTB* protein lacking this domain, for introduction into wild-type *Arabidopsis* plants. The mutations

selected were D482A, where Aspartic acid was replaced by Alanine (GAC → GCC), and W485G, where Tryptophan was replaced with Glycine (TGG → GGG). This DPPW to APPG mutation was similar to that previously shown to be effective in *MTA*. The target sites were altered by oligonucleotide-directed mutagenesis. Two constructs containing this mutation were generated using the Gateway cloning system as described in section (2.13.1) and pGKPGWG as destination vector and these were named (35S:MTBΔSAM-nostop) and (35S:MTBΔSAM-stop). The resulting mutant *MTB* constructs were transformed to *Arabidopsis* (WT) through the *Agrobacterium*-mediated method and subsequently also crossed with mutant *MTB* (GK_332G03) T-DNA insertion line.

4.2 The aim of this chapter

The work described in this chapter sought to investigate the role of MTB by creating a mutant *MTB* protein lacking the SAM binding domain (MTBΔSAM) and to compare this with a similarly mutated *MTA* protein. The work in this chapter is focused on preparation and characterisation of MTBΔSAM overexpressing plants and a comparison of these with similar MTAΔSAM lines.

4.3 Methods

4.3.1 Generation of *MTB* Dominant-negative Lines.

Gateway cloning was used to generate recombinant constructs containing (MTBΔSAM) transgene as described in section (2.13.1).

4.3.2 Screening of (MTBΔSAM) transgenic Lines

Seeds harvested from floral-dipped *Arabidopsis* plants (T0) were sterilized as described in section (2.4) and screened by planting them on ½ MS medium with 50mg/ml Kan to screen positive T1 plants. Therefore, positive T1 plants were further confirmed by PCR using the forward primer on MTB sequence and the reverse one on GFP. In the following generations, homozygous (MTBΔSAM) lines were checked by screening seeds on ½ MS medium with 50 mg/ml Kan. Positive plants were transferred to compost and checked by PCR. The positive plants were used for subsequent analysis.

4.3.3 Checking Transcriptional Levels of (MTBΔSAM) by Northern Blotting.

4.3.3.1 Northern blot Solutions

0.5 M EDTA (pH 8.0): Dissolve 18.61 g $Na_2EDTA{\cdot}2H_2O$ in 100 ml of deionised water by adding 1.8-2 g of NaOH pellets to completely dissolve $Na_2EDTA{\cdot}2H_2O$ and adjust the pH to 8.0. Autoclave and store at room temperature.

5 M NaCl: Dissolve 29.22 g NaCl in 100 ml of deionised water. Autoclave and store at room temperature.

20 × saline-sodium citrate (SSC) (1 L): Dissolve 175.3 g sodium chloride and 88.2 g sodium citrate in 1L of deionised water. Autoclaving and store at room temperature.

10 (W/V) % Sodium Dodecyl Sulfate (SDS) (400ml): Dissolve 40 g SDS in 400 ml of deionised water

1 M Sodium phosphate buffer (pH 6.5): Mix 64.8 mL of 1 M sodium dihydrogen phosphate (NaH_2PO_4) and 35.2 mL of 1 M disodium hydrogen phosphate (Na_2HPO_4) stock solutions to a total volume of 100 ml.

Ethidium bromide buffer: 1ml of deionised formamide, 550 µl of sterile distilled water, 330 µl of formaldehyde (37%), 40 µl of 0.5 EDTA (pH 8.0),40 µl of 1 M sodium phosphate buffer (pH 6.5) and 40 µl of 10 mg·ml-1 ethidium bromide.

5× Bromophenol blue loading dye: 0.25% (w/v) bromophenol blue, 0.25% (w/v) xylenecynol FF, 40% (w/v) sucrose in sterile distilled water.

4.3.3.2 Electrophoresis of RNA

Total RNA was prepared using the phenol-chloroform method as described in section (2.19). The gel tray, comb and electrophoresis tank were soaked using 1% (w/v) SDS for 30 min and then rinsed with sterile water. The northern agarose gel (1.2% [w/v]) gel was prepared with 90 ml of sterile water, 2 ml of 1 M sodium phosphate buffer (pH 6.5) and 1.2 g of agarose. When the gel cooled to about 60°C, 8 ml of formaldehyde (37%, pH 7.0) was added. RNA samples were prepared by mixing 8 µg of total RNA with an equal volume of ethidium bromide buffer in a 1.5 ml Eppendorf® tube and the mixture was denatured at 65°C for 5 min, then cooled on ice for 1 min. Then, 4 µl of bromophenol blue loading dye was added to the mixture. Simultaneously, 8 µl of the ssRNA ladder (NEB) was prepared in the same way. Samples were loaded into wells and the gels were run at 90 V in running buffer (593.5

ml SDW, 50 ml formaldehyde pH 7.0, and 13 ml of sodium phosphate buffer) for 1-2 h. Gels were then photographed under UV light.

4.3.3.3 Transfer of RNA to membrane (blotting)

The nylon membrane (PerkinElmer) and two sheets of Whatman paper were cut to the same size as the gel. In addition, the corner of the gel near the loading site of the RNA ladder was cut as an indication of the position of the samples. 500 ml of 10× SSC (blotting buffer) and 200 ml of 2× SSC (for soaking the membrane and two sheets of Whatman paper) were also prepared. The gel was inverted and stacked on top of Whatman® filter paper on a bridge suspended over a container containing 10× SSC buffer with filter paper hanging into the solution. Nylon hybridisation transfer membrane (Perkin-Elmer) was placed on top of the gel and any air bubbles between the membrane and the gel removed. Two sheets of Whatman® filter papers were then placed on top of the gels and the corners were covered with Parafilm® to ensure that the RNA was transferred only to the membrane. Additionally, Parafilm® was used to cover the container to prevent evaporation of the 10× SSC buffer. Stacks of hand towels and a 500 mg weight was placed on the top of the Parafilm® cover to secure it in place. After overnight blotting, the membrane was rinsed with 2× SSC and then UV crosslinked.

4.3.3.4 Prehybridisation

The crosslinked membrane was placed in a glass cylinder, RNA side towards the inside, filled with 20 ml of prehybridisation buffer (4 ml of 5 M NaCl, 3 ml of sterile water, 10 ml of formamide, 2 g of Dextran sulphate, 1 ml of heat denatured salmon

sperm DNA [10 mg·ml-1] and 2 ml of 10% [w/v] SDS) and incubated at 55°C with rotation for 2 h.

4.3.3.5 Radiolabelling of probes

The transcription template for the RNA probe was generated by PCR using primers in which one was flanked by a T7 promotor sequence. The amplified fragment was then purified by agarose gel electrophoresis. RNA was labelled with [α-^{32}P] rCTP and the transcription reagents were prepared *in vitro* using the Riboprobe® system T7 according to the manufacturer's instructions (Promega). The mixture was incubated for 1 h at 37 °C and then 2 U RQ1 RNase-Free DNase was added. Afterwards, the mixture was incubated at 37 °C for another 15 min. The labelled RNA was then purified via Bio-Spin® 30 column (Bio-Rad) as recommended by the manufacturer's instructions. Subsequently, the RNA probe was fragmented using a carbonate/bicarbonate buffer system (Bodi et al., 2012). The volume of the RNA probe was brought to 80 µl using sterile water and then 10 µl of 400 mM $NaHCO_3$ and 10 µl of 600 mM Na_2CO_3 (both freshly prepared using sterile water) was added. The fragmentation was carried out at 60°C. The fragmentation time was calculated using the following formula: t = (L0-Lt)/(kL0Lt), where L0 = initial length of transcript (in kb), Lt = desired RNA fragment length (in kb, normally 0.05-0.06 kb), k = constant = 0.11 kb·min-1, t = time (min).

4.3.3.6 Hybridisation

The labelled RNA probes were added to the pre-hybridisation buffer and incubated overnight for 20 h at 65 °C in a rotating oven.

4.3.3.7 Washing Membrane

The pre-hybridisation buffer containing the probe was decanted and the membrane was washed several times with different concentrations of SSC buffers containing 0.1% (w/v) SDS, starting with 2× SSC at room temperature for 5 min, followed by 2× SSC, 1× SSC, 0.2× SSC and 0.1× SSC at 65°C for 15 min each time to remove any unhybridised probes. The membrane was then sealed and put down under a phosphor screen (Fuji-Screen) for two days and scanned using a Molecular Imager FX™ imaging device in combination with Quantity One® software (Bio-Rad).

4.3.4 Crossing of plants

To further study the role of MTB in the MTase complex, crossing was made between (MTBΔSAM) transgenic plants and MTB (GK_332G03) T-DNA insertion line.

4.4 Results

4.4.1 Generation of *MTB* dominant negative (MTBΔSAM) and comparing with similar (MTAΔSAM) lines

In attempting to introduce a dominant negative mutation in MTB, the SAM binding domain present in plant METTL14 homologues was selected for mutation. This region contains the conserved DPPW amino acid motif. MTA also contains this motif, and previous work (Fray's Group unpublished and presented below) indicated that overexpressing a version of *MTA* in which this was mutated could lead to a mutant phenotype similar to a low m^{6}A plants. The sequence corresponding to the mutated loci is shown with the D482A Aspartic acid to Alanine (GAC → GCC) and the W485G Tryptophan to Glycine (TGG → GGG) mutations (Figure 4.1). These sites were altered by oligonucleotide-directed mutagenesis (Table 4.1).

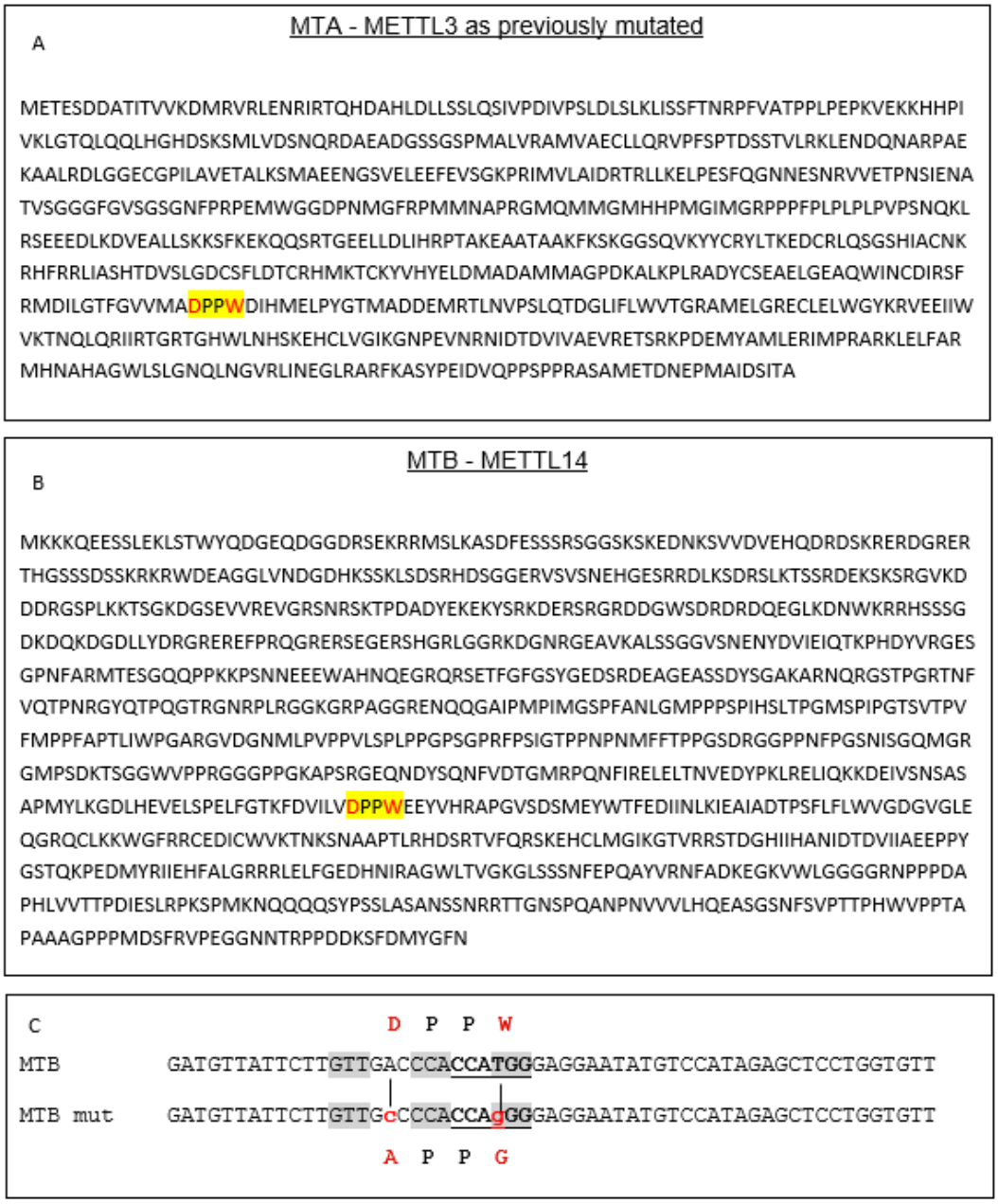

Figure 4.1: Generation of a mutant *MTB* (MTBΔSAM) and comparison to similar (MTAΔSAM) lines. A: showing the amino acid sequence for MTA gene, the shaded region is SAM binding domain where the mutation was generated by Silin Zhong (Fray group). B: showing the amino acid sequence for MTB gene, the shaded region is SAM binding domain where the mutation was made in this study. C: Sequence corresponding to the mutated loci are shown with the D482A (GAC → GCC) and the W485G (TGG → GGG) mutations.

Five oligonucleotides were designed for this experiment; two of them contained changed nucleotides (A→C) and (T→G) with created restriction sites of BamHI and XmaI. These primers were used for three PCR amplifications named: A, B and C to divide the MTB gene into two parts to create the mutation by changing 2 nucleotides,

then ligated them together by using a DNA T4 ligase. The reverse primer of the fragment A (shown in Table 4.1, primer No.2) contained the modified nucleotides and the XmaI and BamHI restriction sites at the end. The forward primer for both fragments B and C (Table 4.1, primer No.3) contained the modified nucleotides and XmaI restriction site whereas the reverse primers of them (Table 4.1, primers No. 4 and 5) contained the BamHI restriction site. This allowed the ligation of fragment A with B and A with C, creating two mutant *MTB* gene entry vectors, one of them without the stop codon (A+B ligated fragments) and the other with the stop codon (A+C). The PCR samples were run on 1% agarose gel and the bands appeared at the correct sizes. PCR products from each amplification were extracted and purified, (Figure 4.2).

Table 4.1: The altered primers which used to direct the mutagenesis. These primers were used for MTBmut construction. Primers No.2 (MTBmutBamRev) and No.3 (MTBmutFor) contained changed nucleotides (A→C) and (T→G) with created restriction sites of BamHI and XmaI. Primers No.4 (MTBnoStopBam) and No.5 (MTBStopBam) were engineered with BamHI. Restriction enzyme sites are underlined. BamHI= GGATCC, XmaI= CCCGGG.

Primer name	Sequence (5' to 3')
1-MTBForKoz	aaaCaATGAAGAAGAAACAAGAAGAGAG
2-MTBmutBamRev	ggaTCCCcgGGTGGGgCAACAAGAATAACATCAAAC
3-MTBmutFor	CCACCcgGGGAGGAATATGTCCATAGAG
4-MTBnoStopBam	ggatccATTAAAGCCGTACATGTCAAAAC
5-MTBstopBam	ggatccTCAATTAAAGCCGTACATGTC

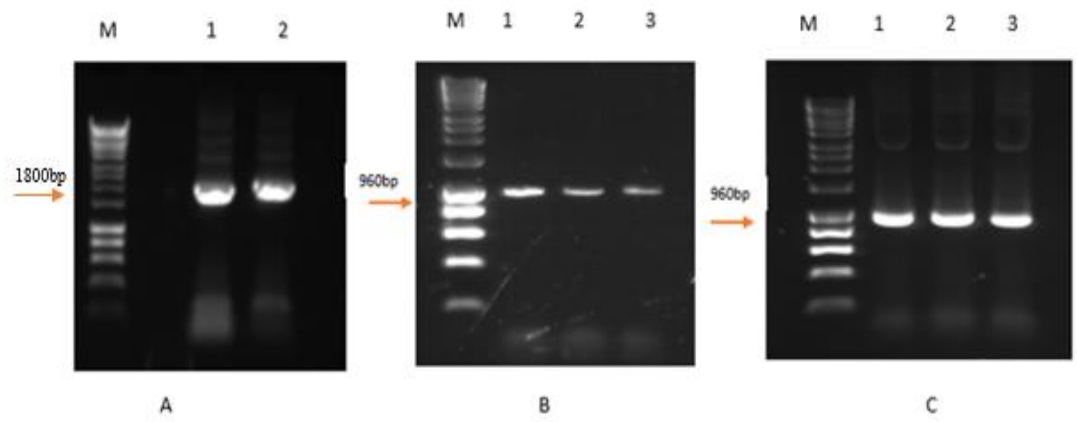

Figure 4.2: Preparation of the MTBΔSAM with and without stop codon constructs using MTB cDNA as the template. A: PCR amplification of MTB cDNA with the (MTBForKoz+MTBmutBamRev) primers. B: PCR amplification of MTB cDNA with the primers (MTBmutFor+ MTBnoStopBam). C: PCR amplification of MTB cDNA with the primers (MTBmutFor+MTBstopBam). The size of the expected band is indicated by an arrow in each figure panel: 1800bp, 960bp, and 960bp respectively. PCR product were run on 1 %(w/v) agarose gel, and HyperLadder 1Kb (bioline) was used as a marker.

PCR product A was cloned into pCR™8/GW/TOPO® vector, whereas PCR B and PCR C were cloned into pJET1.2/blunt vector as described sections 2.13.1 and 2.13.2. Afterwards, the mixtures were transformed into *E. coli DH5a* competent cells as described in section 2.15, with appropriate antibiotic selection, Spectinomycin for PCR A and Ampicillin for PCR B and C. Some colonies for each mixture were chosen and checked by colony PCR using forward primer (B-sequence-FW) and reverse primer (MTBnostop) for PCR A and using the forward primer (MTBmutFor) and reverse primer (MTBnoStopBam) for PCR B and C, (Figure 4.3) to confirm the presence of the insert. All primers used are shown in Appendix I. The positive colonies (lanes 1A, 2B, and 2C) were chosen for plasmid extraction and verified by sequencing (Figure 4.4).

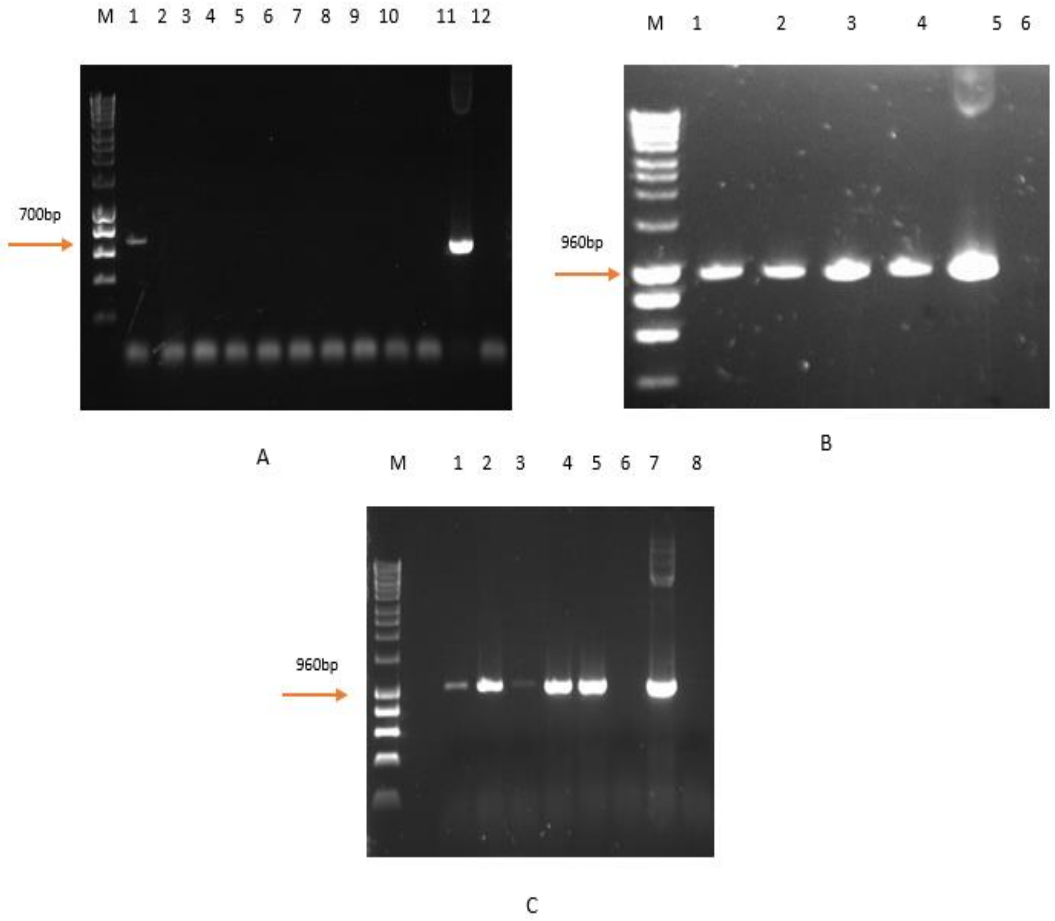

Figure 4.3: Colony PCR for *E.coli DH5α* transformed with (pCR8 containing PCR A) and (pJET with PCR B and pJET with PCR C). A: Results of PCR A ligated to pCR™8/GW/TOPO® vector, the positive colony only in the lane 1. B) Results of PCR B ligated to pJET1.2/blunt vector, the positive colonies appeared in the lanes 1, 2, 3 and 4. C: Results of PCR C ligated to pJET1.2/blunt vector, the positive colonies appeared in the lanes 1, 2, 3, 4 and 5. The arrows indicate the expected size of the bands 700bp, 960bp, 960bp respectively. Positive control located in lanes (11A, 5B, 7C) using (MTBcDNA) as a template, while negative control in (12A, 6B, 8C) using water as a template. PCR products were run on a 1 %(w/v) agarose gel and HyperLadder 1Kb (Bioline) was used as a marker.

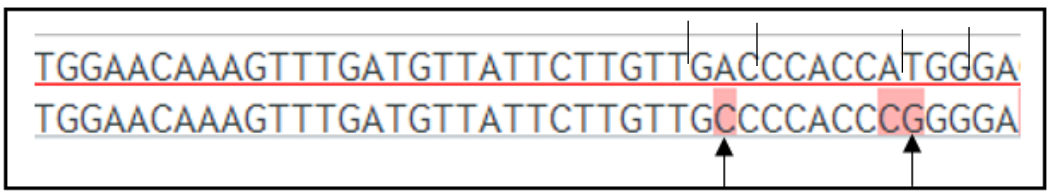

Figure 4.4: Sequencing profile showing the mutated target sites in MTB indicated by black arrows D482A (GAC → GCC) and the W485G (TGG → GGG) mutations. The additional mutation A → C is Xma I site (CCCGGG).

Recombinant plasmids were digested with XmaI and BamHI and after 1 h plasmid A was treated with the calf-intestinal alkaline phosphatase (CIP) to prevent the plasmid from self-ligating in subsequent cloning. Digested products were electrophoresed through a 1% agarose gel (Figure 4.5) (the appearance of the bands that were similar to the uncut plasmid is evidence that these digestions were not 100% efficient; using old enzymes could have caused this problem).

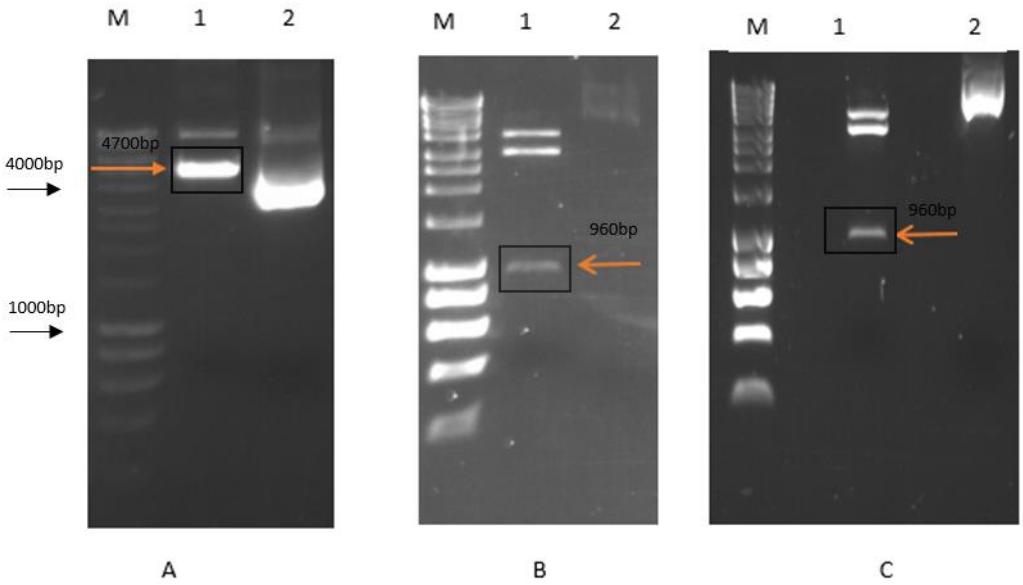

Figure 4.5: Restriction digestion of all plasmids with BamHI and XmaI. A: Plasmid containing PCR A digested with BamHI and XmaI, lane 1 shows the target band at 4700bp, lane 2: uncut plasmid. B: Plasmid containing PCR B digested with BamHI and XmaI, lane 1 shows multiple bands, the target band at 960bp, and the second band at 2900bp for the pJET vector. Lane 2: the uncut fragment. C: Plasmid containing PCR C digested with BamHI and XmaI, lane 1 shows the target band at 960bp, and the second band at 2900bp for the pJET vector. Lane 2: uncut fragment. Arrows indicate target bands of correct size. PCR product were run on a 1 %(w/v) agarose gel, and HyperLadder 1Kb (Bioline) was used as a marker.

The target bands for A, B, and C, located at 4700bp, 960bp, and 960bp respectively, were excised from the gel and purified. Two ligations were performed using T4 DNA ligase. Firstly, the fragment B was ligated into fragment A and named (PCR8:MTBΔSAM-nostop). The second one was fragment C which was ligated into fragment A and named (PCR8:MTBΔSAM-stop). These were then transformed to

E.coli DH5α competent cell, and the resulting colonies checked by PCR using (MTBmutFor + MTBnoStopBam) primers (Figure 4.6).

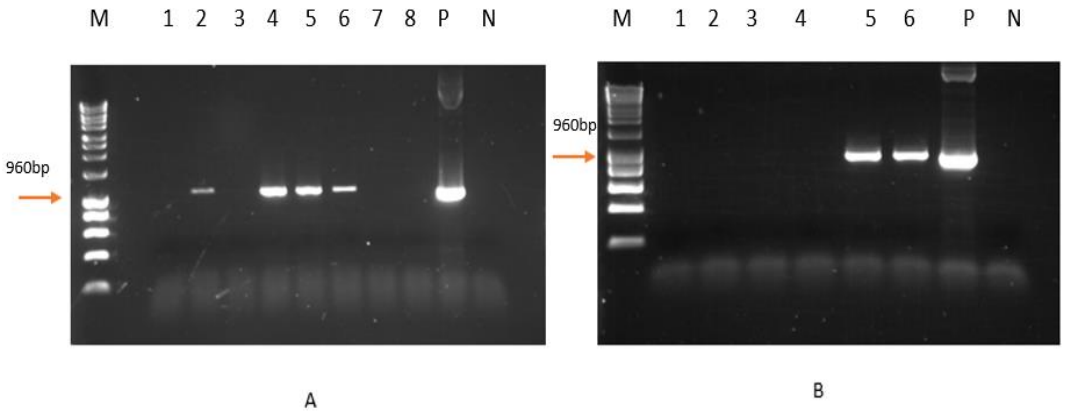

Figure 4.6: Colony PCR for *E.coli DH5α* transformed with entry vectors (PCR8:MTBΔSAM-nostop) and (PCR8:MTBΔSAM-stop). A: the entry vector of PCR8:MTBΔSAM-nostop, lanes (2,4,5, and 6) shows positive colonies. B: the entry vector of PCR8:MTBΔSAM-stop lanes (5 and 6) show positive colonies. P: positive control using (MTBcDNA) as a template and N: negative control using water as a template. Arrows indicate the expected size of the bands at 960bp. PCR product were run on a 1 % (w/v) agarose gel and HyperLadder 1Kb (Bioline) was used as a marker.

All bands in Figure 4.6 appeared at the expected size of about 960 bp. The colonies in lane 4A and lane 5B were chosen for plasmid preparation, and sequence analysis which further confirmed the insertion of the desired sequence. Thereafter, these two entry vectors (PCR8:MTBΔSAM-nostop) and (PCR8:MTBΔSAM-stop) were cloned into the plant binary vector pGKPGWG containing the CaMV35s promoter via an LR clonase (Invitrogen) reaction as described in section 2.13.1. The constructs were named, (35S:MTBΔSAM-nostop) and (35S:MTBΔSAM-stop) (Figure 4.7).

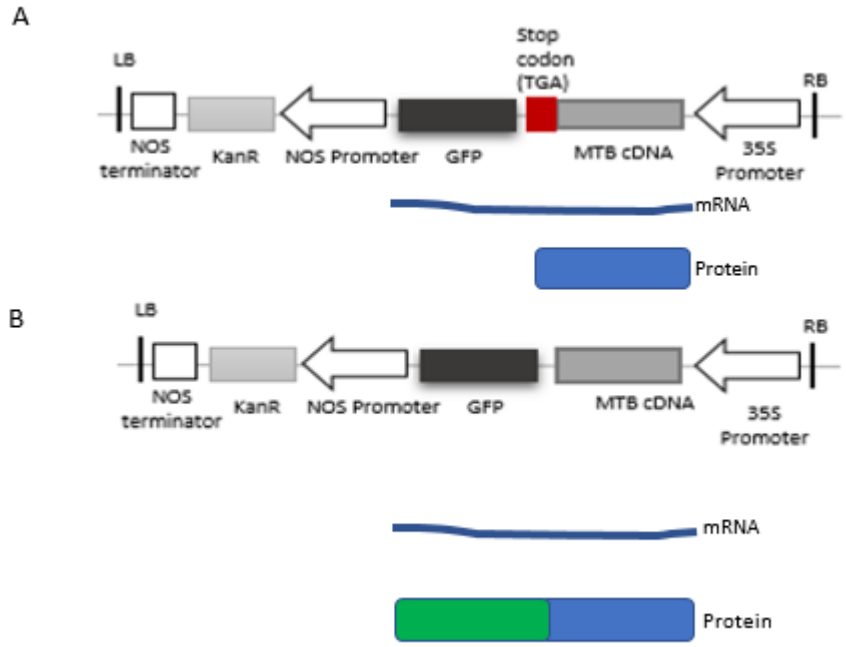

Figure 4.7:The schematic of recombinant MTBΔSAM constructs. (A) 35S: MTBΔSAM-stop. (B) 35S: MTBΔSAM-no stop. KanR: kanamycin resistance marker for plant transgene selection.

These constructs were transferred to *E.coli DH5α* competent cell with Kanamycin resistance then the colonies were checked by colony PCR using (MTBmutFor + MTBnoStopBam) primers (Figures 4.8 and 4.9).

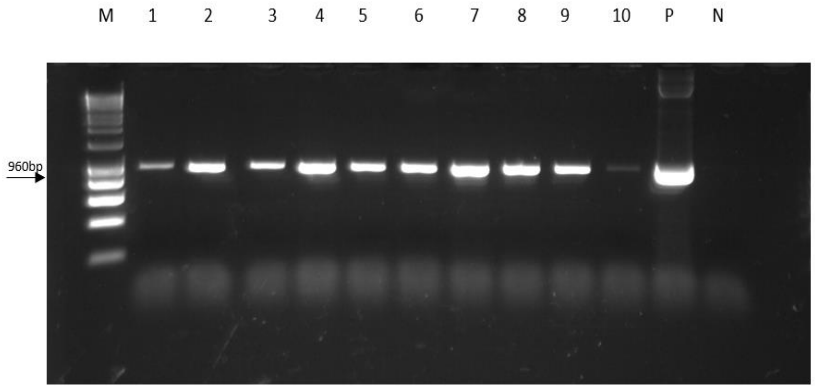

Figure 4.8: Colony PCR for *E.coli* transformed with ((35S:MTBΔSAM-nostop) and (35S:MTBΔSAM-stop) using (MTBmutFor + MTBnoStopBam) primers. Lanes 1-5 show the positive colonies that contain the construct (35S:MTBΔSAM-nostop), whereas lanes 6–10 show the positive colonies of the construct (35S:MTBΔSAM-stop). P: positive control using (MTBcDNA) as a template and N: negative control using water as a template. Arrow indicates to the expected size of the bands at 960bp. PCR product were run on a 1 % (w/v) agarose gel, and HyperLadder 1Kb (Bioline) was used as a marker.

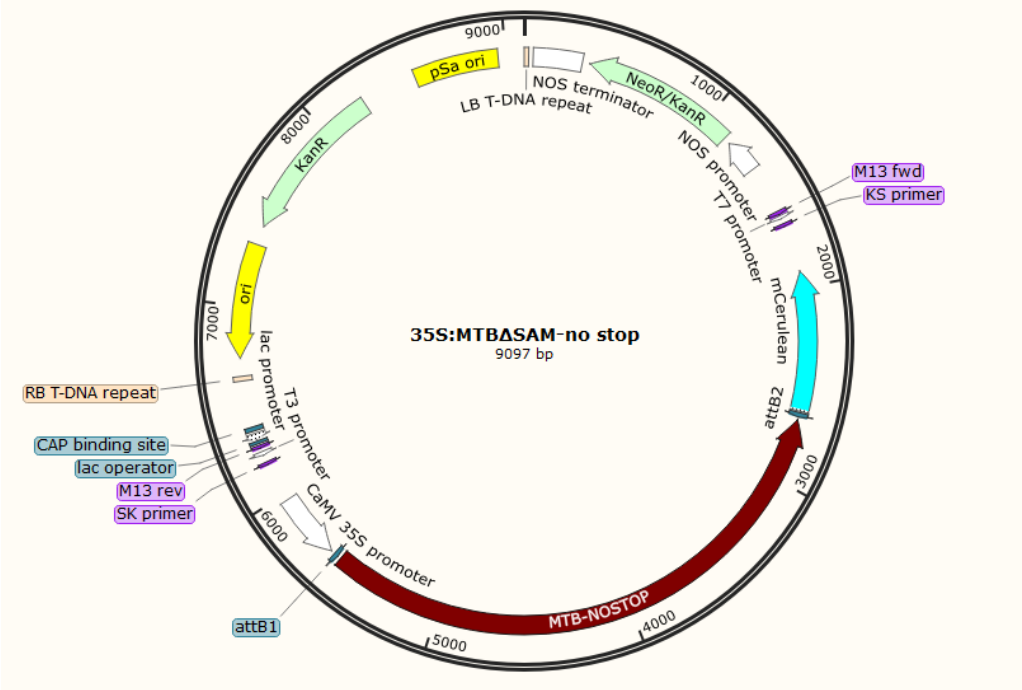

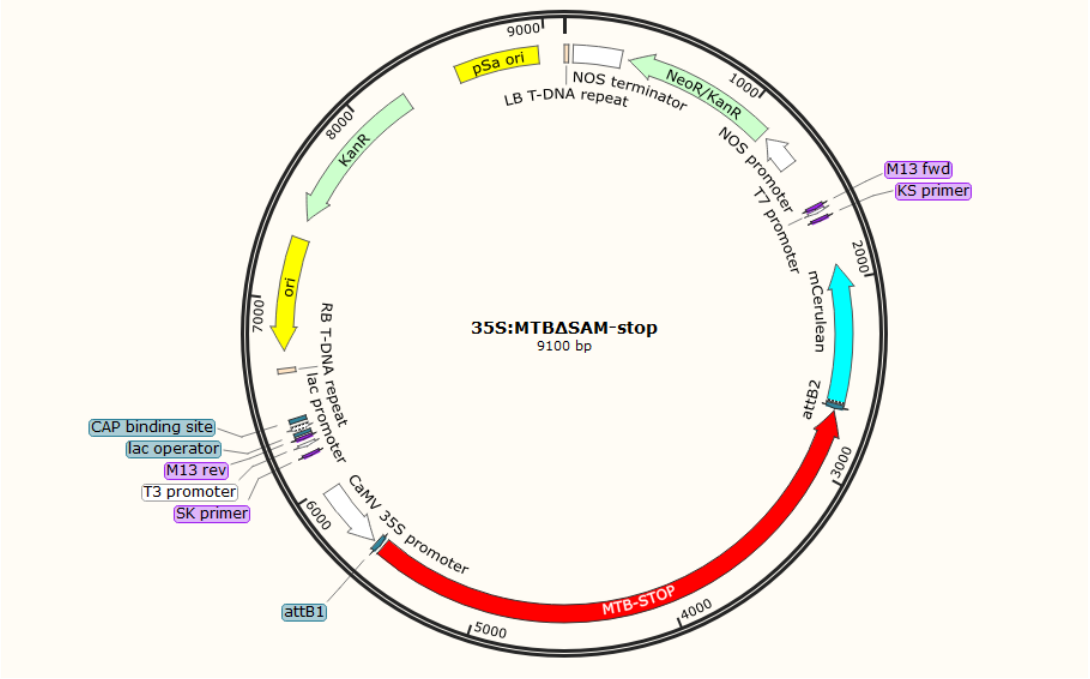

Figure 4.9: Plasmid maps of MTBΔSAM constructs with CaMV35s (generated by Snap Gene Software). Expression was driven by the constitutive CaMV 35S promoter and the MTB was fused at its C-terminus to GFP. KanR: Kanamycin resistance gene.

One positive colony from each construct was chosen for plasmid extraction and verified by sequencing. The two constructs were then transferred to the *Agrobacterium* strain C58 by electroporation (section 2.16). The presence of the construct was confirmed using the MTBmutFor and MTBnoStopBam primers, giving an amplified fragment of 960 bp (Figure 4.10). Transgenic *Agrobacterium* were transformed then into *Arabidopsis* wild type plant, Col-0, by floral dip transformation (section 2.17).

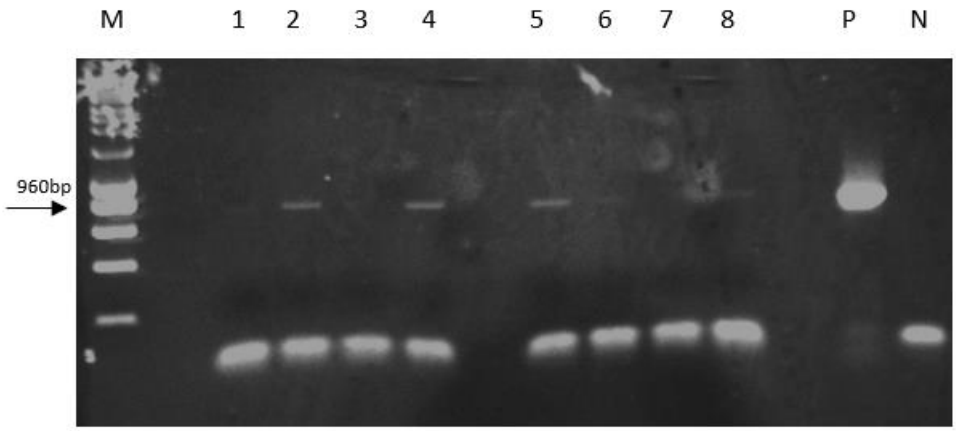

Figure 4.10: Colony PCR of *Agrobacterium* strain C58 transformed with MTBΔSAM constructs. (35S: MTBΔSAM-no stop) lanes 1-4 and (35S: MTBΔSAM-stop) lanes 5-8 using (MTBmutFor + MTBnoStopBam) primers. P: positive control using (MTBcDNA) as a template and N: negative control using water as a template. PCR products were resolved on a 1% (w/v) agarose gel using HyperLadder 1-kb (Bioline) as a marker.

Beside the SAM deleted constructs 35S: MTBΔSAM-no stop and 35S: MTBΔSAM-stop, another construct containing MTBcDNA (WT) instead of MTBΔSAM was generated as a control by cloning it into the plant binary vector pGKPGWG containing the CaMV35S promoter via an LR clonase (Invitrogen) reaction. All cloning figures and maps are shown in the Supplementary Data 5.6.2.

4.4.2 Analysis of the *MTB* Dominant Negative Transgenics.

Following floral dip transformation to the *Arabidopsis* wild-type, positive T1 plants for both constructs were screened on ½ MS medium supplemented with 50 mg/ml kanamycin. Green seedlings obtained by the screening were transferred to soil and

allowed to grow and then confirmed by PCR using the forward primer on MTB genomic sequence and the reverse one on GFP (Figure 4.11).

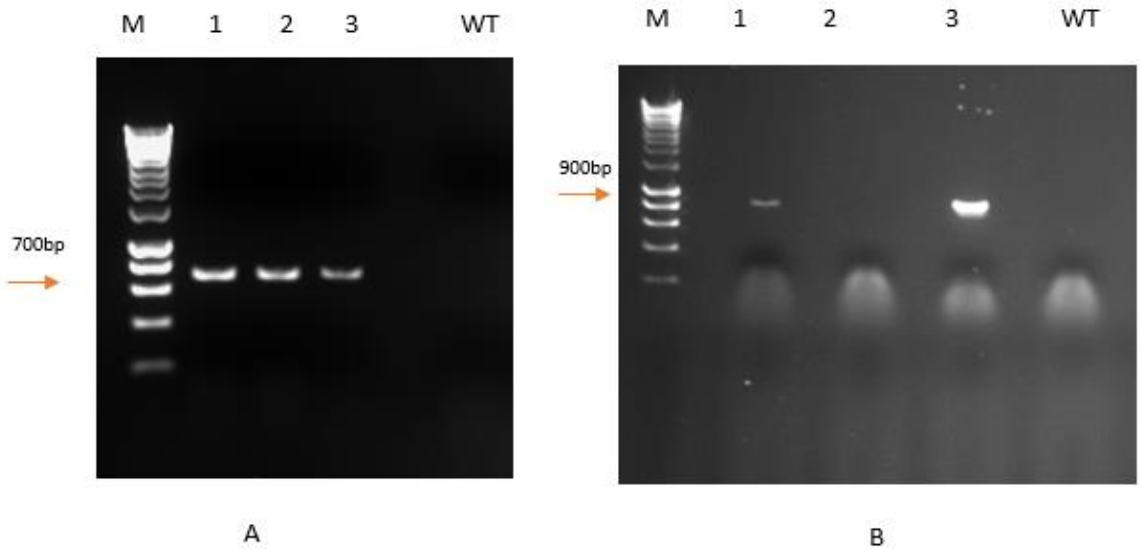

Figure 4.11: PCR analysis for checking positive MTBΔSAM T1 plants. A: 35S:MTBΔSAM-nostop plants using MTB.FW2 +GFP rev primers. Samples 1 to 3 represent three individual T1 plants. B: 35S:MTBΔSAM-stop plants using MTB.FW1 +GFP rev primers. Samples 1 and 3 represent two individual T1 plants.

T2 generation from Line 1 (35S:MTBΔSAM-nostop) and Line 3 (35S:MTBΔSAM-stop) were germinated on ½ MS medium supplemented with 50 mg/ml kanamycin to screen for homozygous lines. Green seedlings obtained by the screening were transferred to soil and allowed to grow for 2 weeks then confirmed by PCR using the forward primer on MTB genomic sequence and the reverse one on GFP (Figures 4.12). Also planted were those with GFP (35S:MTBΔSAM-nostop) on vertical plates containing ½ MS medium to check for *MTB* mutant protein localization. One homozygous line of MTBΔSAM-nostop and two homozygous lines of MTBΔSAM-stop were discovered (Figure 4.13). These lines were termed MTBΔSAM no stop-10, MTBΔSAM stop-5 and MTBΔSAM stop-6. Confocal microscopy analysis of GFP signal showed that mutant *MTB* (MTBΔSAM) was primarily localised in the nuclei of

root tips (Figure 4.14). In addition, the line of *MTB* mutant with stop codon (MTBΔSAM) was also chosen for subsequent analysis because the equivalent MTAΔSAM plants had previously given a strong phenotype.

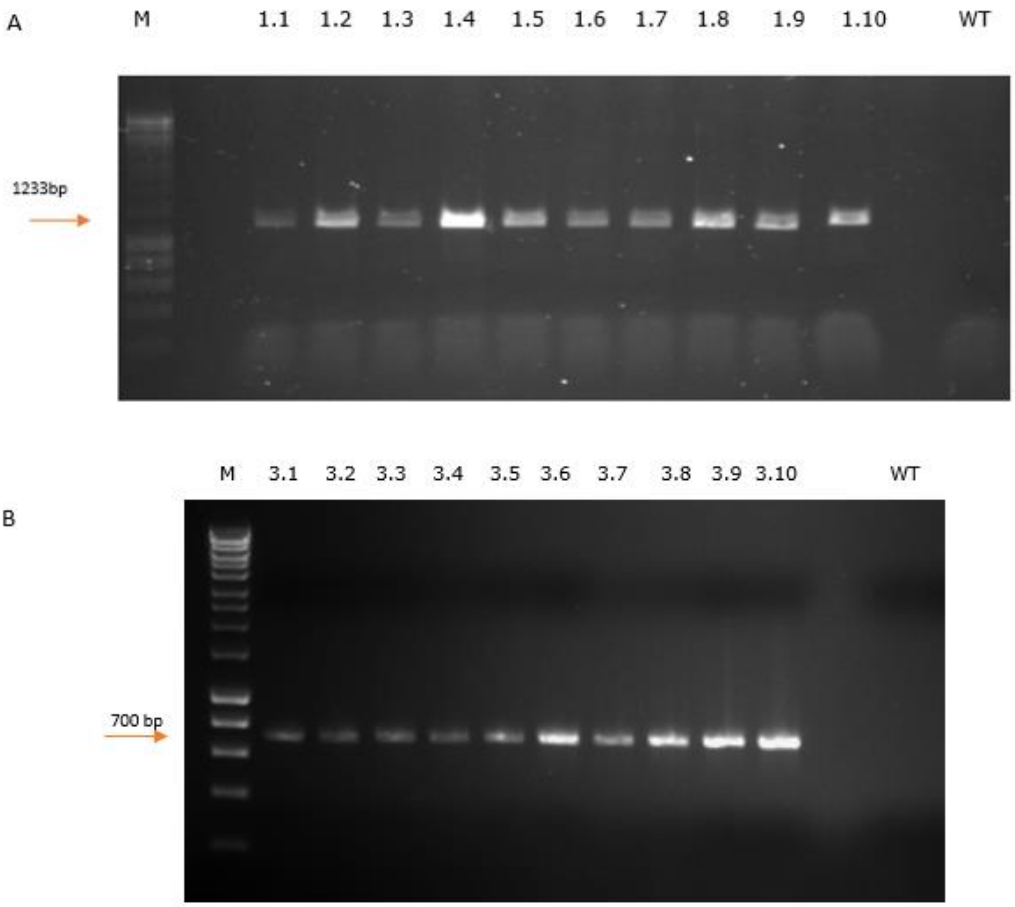

Figure 4.12: PCR analysis for checking positive mutant *MTB* (MTBΔSAM) T2 plants selected by Kan. A: 35S:MTBΔSAM-nostop plants using MTBmutFor +GFP rev primers. B: 35S:MTBΔSAM-stop plants using MTB.FW2 +GFP rev primers. All plants showed PCR products of the expected size.

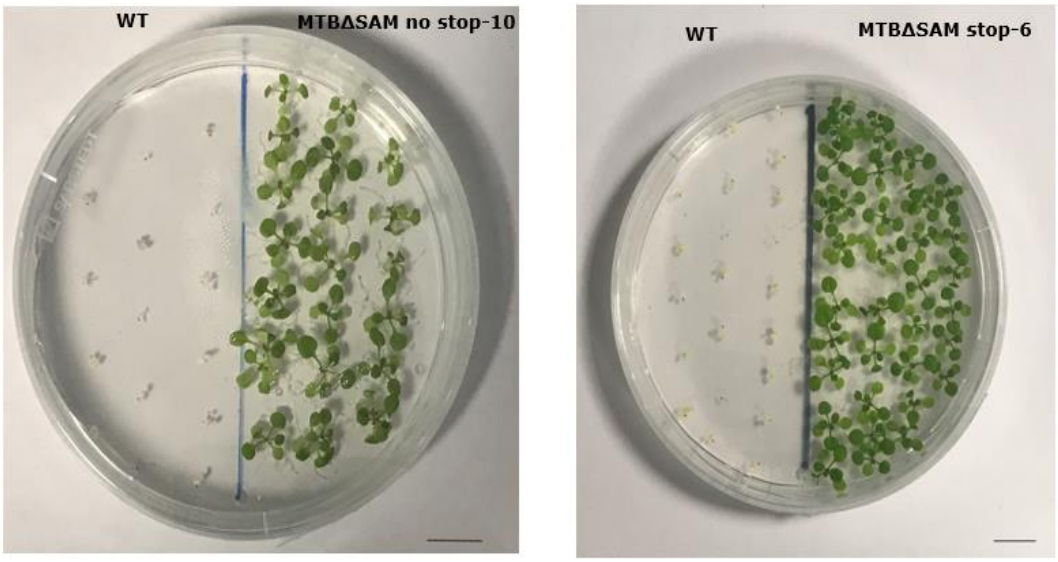

Figure 4.13: 12-d old homozygous MTBΔSAM plants for both constructs with and without stop codon lines on ½ MS medium with Kan. MTBΔSAM no stop-10 represents homozygous line of MTBΔSAM-nostop. whereas, MTBΔSAM stop-6 represents homozygous line of MTBΔSAM-stop. Scale bar = 1 cm

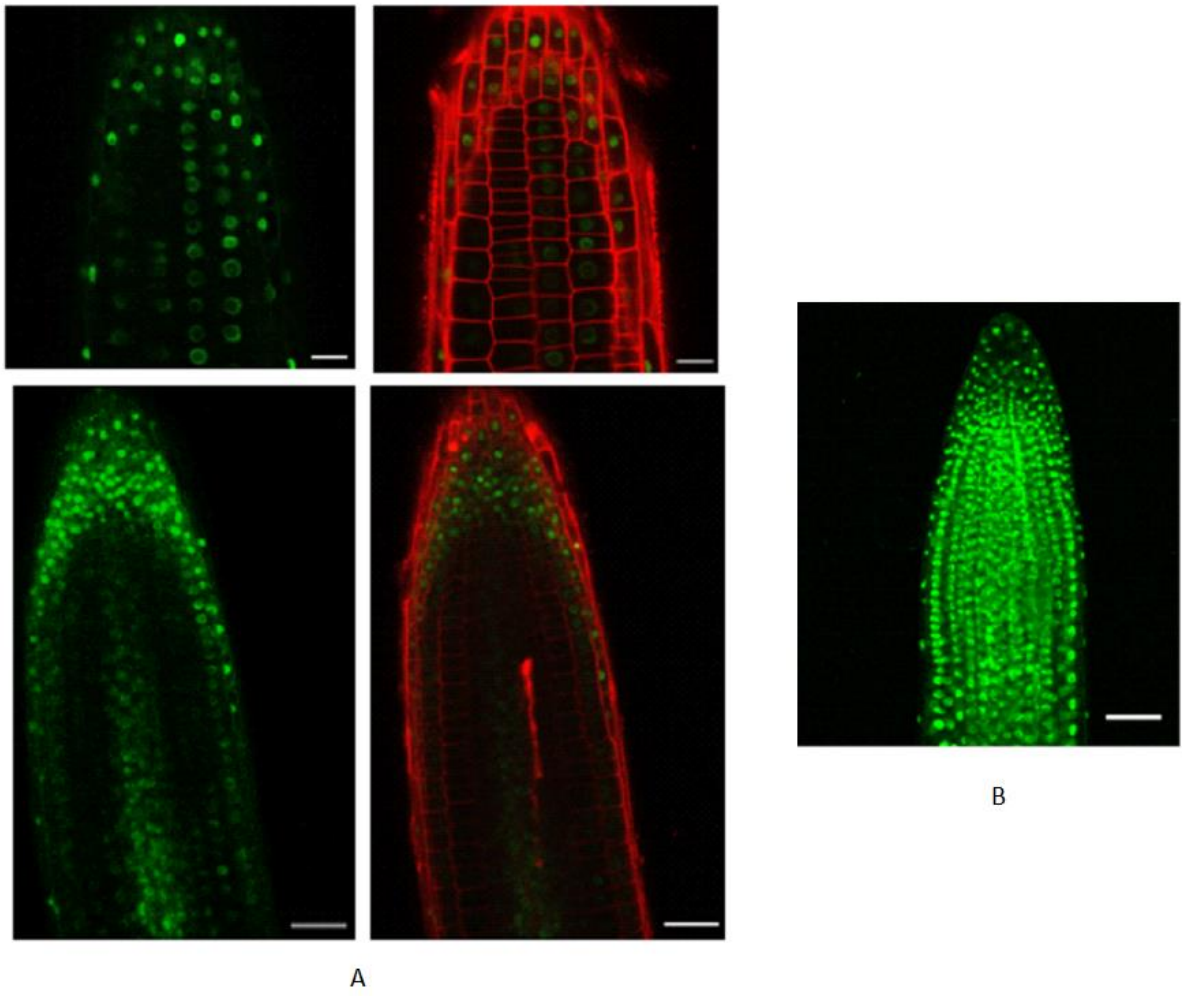

Figure 4.14: Confocal microscopy analysis of MTBΔSAM. A- Confocal images showing GFP localisation in the nucleus in the root tips of 5-d old seedlings of MTBΔSAM over-expression mutant, Scale bar = 100 µm. B) The MTB-GFP expression control is also expressed in the nuclei of cells in the primary root tip, Scale bar = 50 µm.

4.4.3 Characterisation of MTBΔSAM overexpressing plants and a comparison of these with similar MTAΔSAM lines.

Northern blot assays were carried out to confirm the over-expression of the full-length MTB mRNA in the total RNA extracted from the leaves of MTBΔSAM and MTAΔSAM T2 transgenic lines. The MTB cDNA probe used for membrane hybridisation was generated by PCR amplification using the primers MTBnor-fw and MTBnor-rev, and the MTA cDNA probe was generated in the same way using the primers A6fwd1 and T7A6revNEW1 (Figure 4.15). The results confirmed that all of the three transgenic plants identified overexpressed both *MTB* and *MTA* mRNA transcripts of the expected sizes and the relative abundance of the transcript of *MTB* and *MTA* was higher in dominant negative transgenics (MTA) than that in Col-0 wild type plants (Figure 4.16). These over-expressed plants in *MTA* show delayed development, reduced apical dominance and crinkled leaves, whereas *MTB* mutants more closely resembled WT (Figure 4.17).

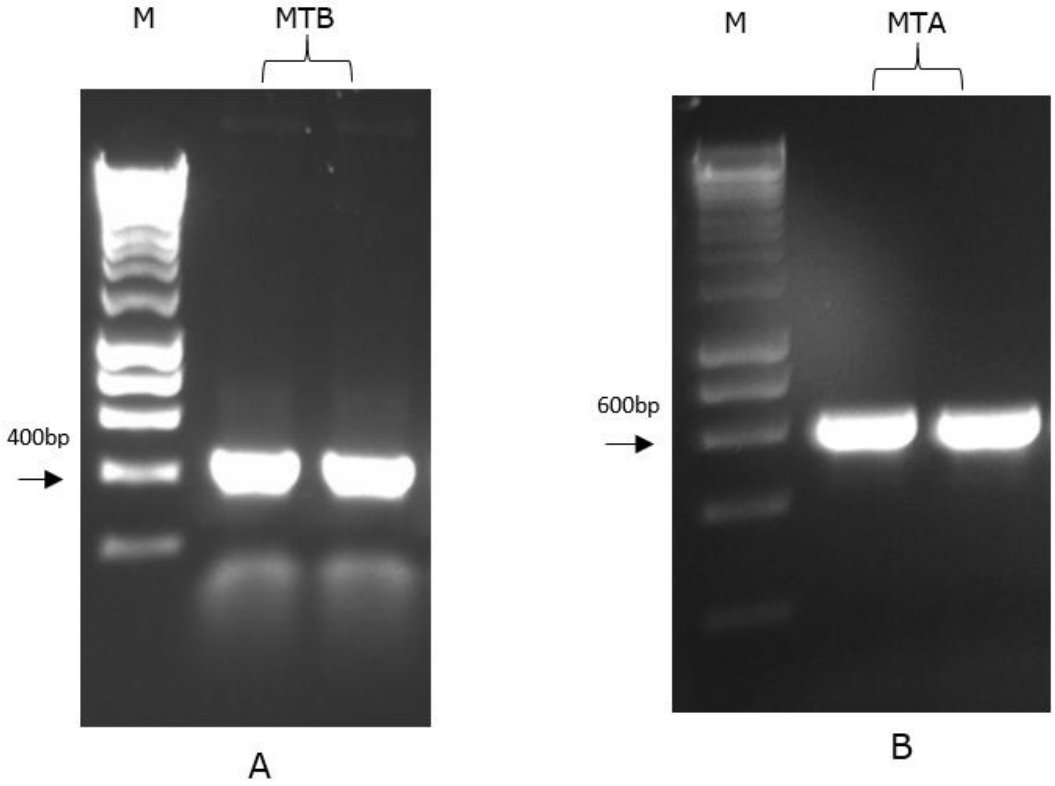

Figure 4.15: A- Probe used for northern blot membrane hybridisation for MTBΔSAM. B- Probe used for MTAΔSAM.

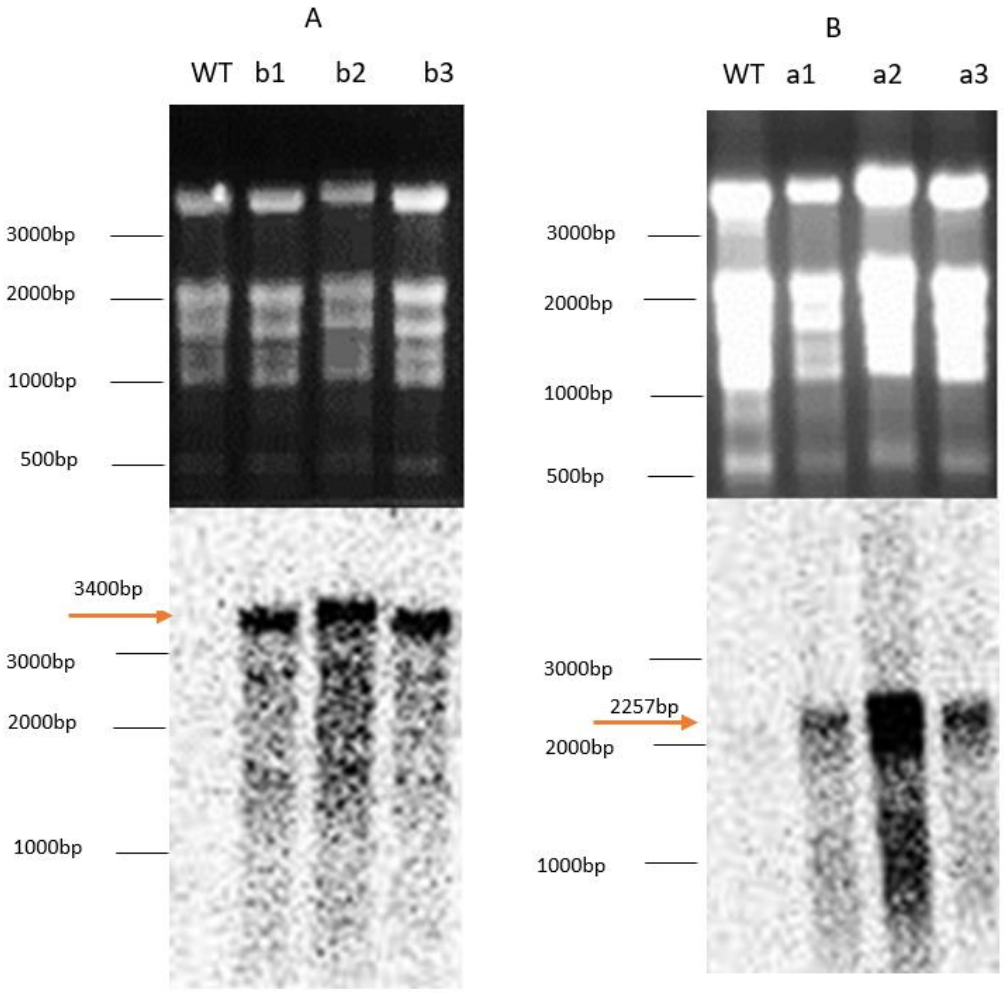

Figure 4.16: A- Northern blot analysis of (MTBΔSAM) WT: wild type. Lanes 1, 2, and 3 shows transgenic plants for MTBΔSAM. B- Northern blot analysis of (MTAΔSAM). The top panel shows denatured RNA a formaldehyde northern gel while the bottom panel shows the hybridised radiolabelled probes. Arrows indicate to the expected size of MTB and MTA transcripts in the mutants.

Figure 4.17: 5-week- old mutant *MTB* (MTBΔSAM) compared with the similar MTA. Inset image is an enlargement of the severe MTAΔSAM line. MTBΔSAM more closely resembled WT, while MTAΔSAM show delayed development, reduced apical dominance and crinkled leaves. Scale bar = 1 cm

The m^{6}A to A ratio in the *MTA* dominant negative transgenic plants was measured by two-dimensional TLC analysis and showed a significant decrease in mutant plants with more than 70 % reduction compared to the WT (Figures 4.18 & 4.19) (Fray's group unpublished). The m^{6}A measurement for MTBΔSAM expressing lines was not performed due to time constraints.

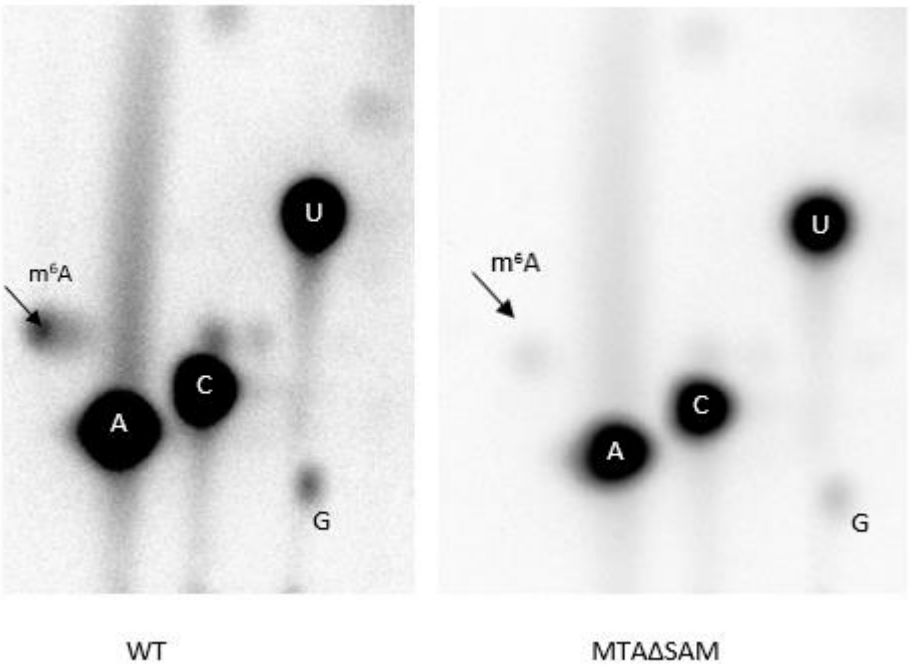

Figure 4.18: Two-dimensional TLC analysis of m^{6}A level from 3-week old plants of MTAΔSAM. Arrows indicated to m^{6}A spots (Mi Zhang).

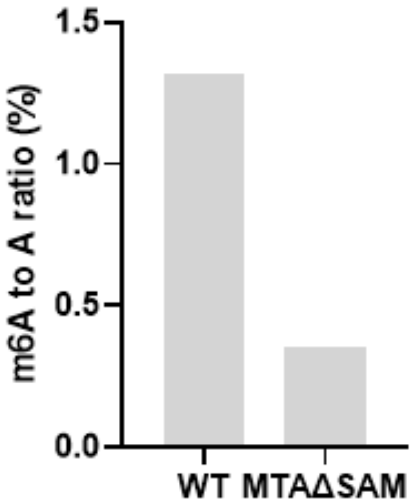

Figure 4.19: m^{6}A levels of MTAΔSAM checked by the TLC method. Level of m^{6}A in MTAΔSAM is reduced by 73% compared to WT (Mi Zhang).

4.4.4 Generation of MTBΔSAM in mutant background

Unlike the over-expressing MTAΔSAM plants, no altered phenotype was observed for MTBΔSAM. This difference could be explained if the SAM binding domain is dispensable for MTB function but not for MTA. To test this the MTBΔSAM transgenic line was crossed with MTB G.K line to generate MTBΔSAM in the insertion mutant background. If MTB had a function independent of any SAM binding ability, for example by providing a structural role to support the assembly of the larger methylation complex, then the MTBΔSAM transgene might be able to complement the GK insertion mutant. In the F1 generation, progeny heterozygous for *MTB* (GK_332G03) T-DNA insertion line and with the presence of the MTBΔSAM construct were identified by PCR. To distinguish the heterozygous plants for MTB T-DNA insertion *(*GK_332G03), the forward primer MTB-GK-REV on the MTB genomic DNA and the reverse one on the inserted T-DNA (GK-TDNA) were used (Figure 4.20 A), whereas the presence of the MTBΔSAM construct was verified by using the primers MTB.FW2 + GFP rev, for which a band of 700 bp should be amplified (Figure 4.20 B).

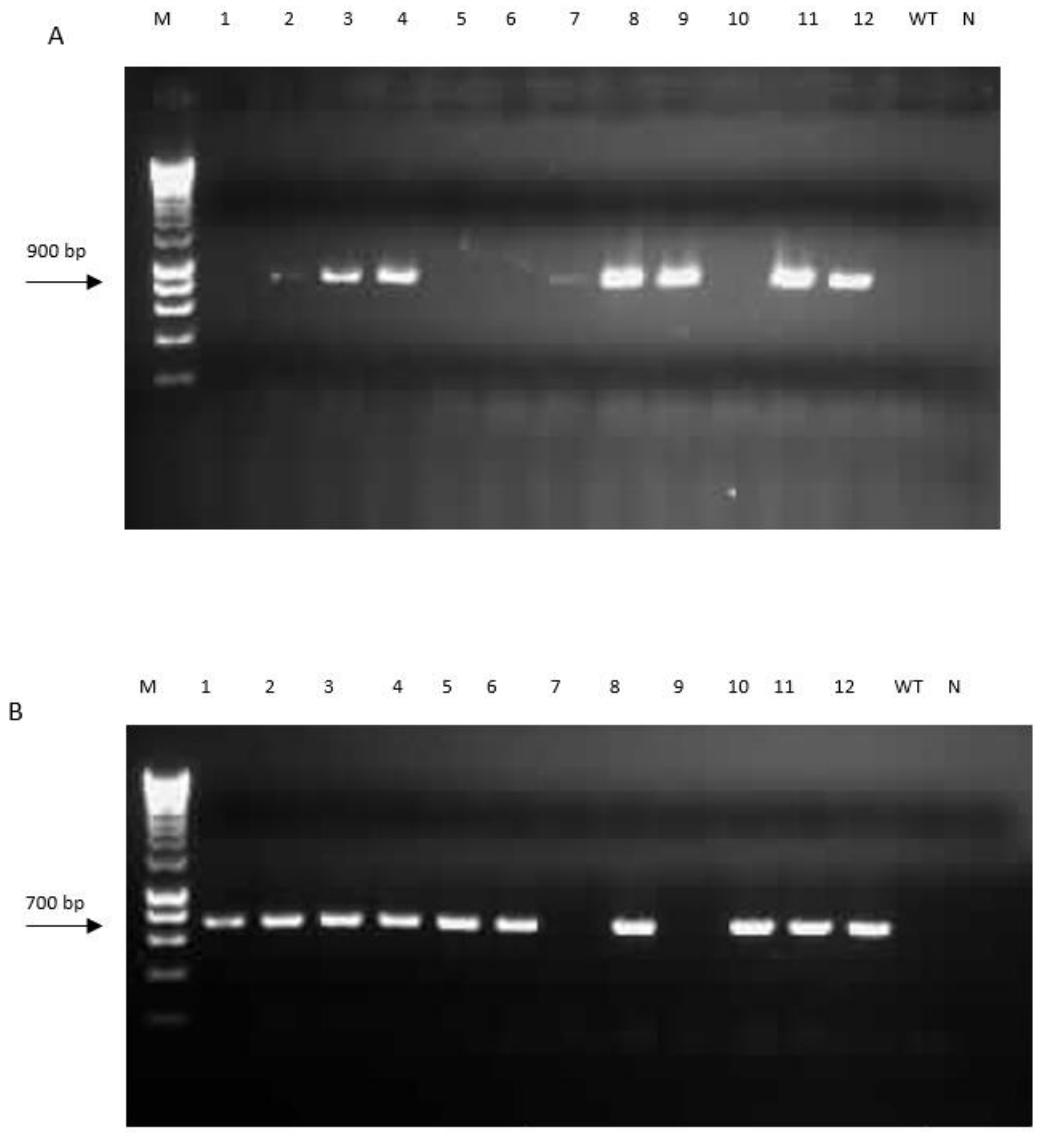

Figure 4.20: Screening F1 progenies of MTBΔSAM crossed with MTB mutant GK_332G03 line. (A) Genotyping PCR to confirm the heterozygous plants for MTB (GK_332G03) T-DNA insertion. (B) PCR to check the presence of 35S: MTBΔSAM stop construct in plants. Lines 2, 3, 4, 8, 11 and 12 represent 6 heterozygous individual F1 plants and contain MTBΔSAM construct at the same time.

From Figure 4.20, lines (2, 3, 4, 8, 11 and 12) were found to be positive for both PCR products. Lines 4 and 12 from F1 were selfed to generate F2 plants. Sixteen plants from each line 4 and 12 of F2 progeny were also confirmed by PCR using the same primer pairs mentioned earlier to distinguish heterozygous plants for MTB T-DNA insertion *(*GK_332G03), and to confirm the presence of the MTBΔSAM construct Figures (4.21, 4.22 and 4.23).

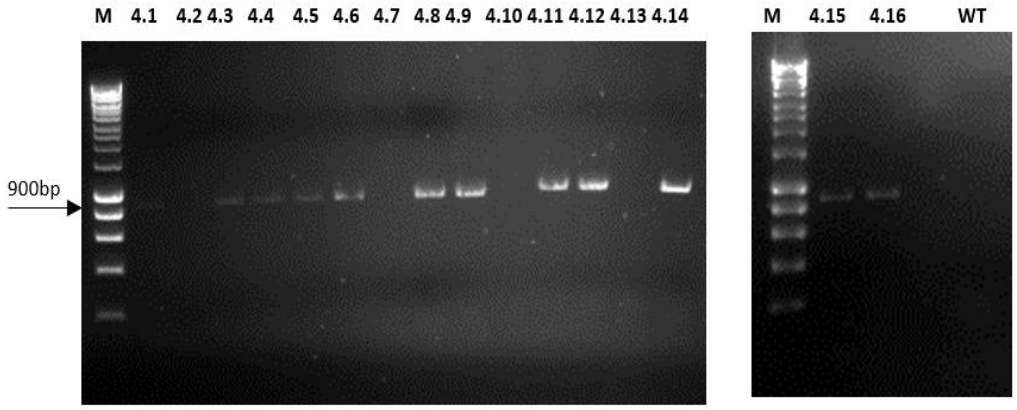

Figure 4.21: Screening F2 progenies (Line 4) of MTBΔSAM crossed with MTB (GK_332G03) line to confirm the presence of MTB (GK_332G03) T-DNA insertion by using MTB-GK-FW+GK.TDNA primers. Lines 4.1, 4.3, 4.4, 4.5, 4.6, 4.8, 4.9, 4.11, 4.12, 4.14, 4.15, 4.16 were heterozygous plants for MTB (GK_332G03) T-DNA insertion.

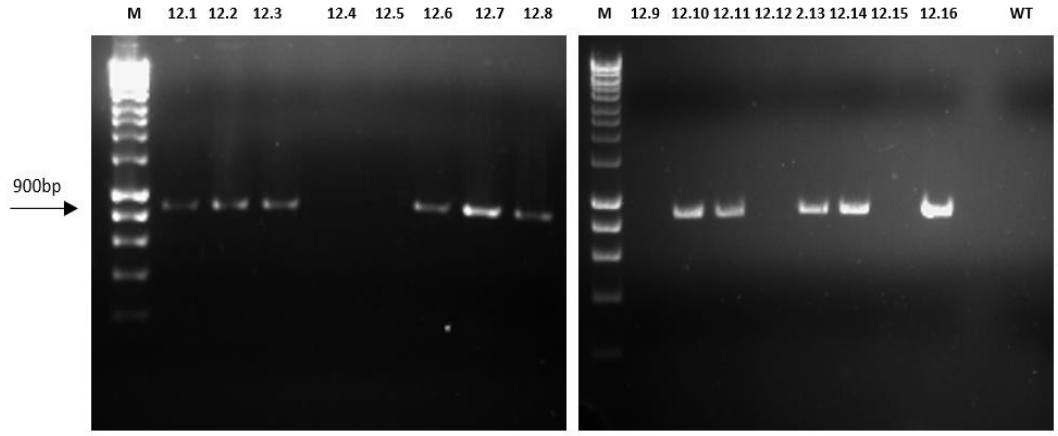

Figure 4.22: Screening F2 progenies (Line 12) of MTBΔSAM crossed with MTB (GK_332G03) line to confirm the presence of MTB (GK_332G03) T-DNA insertion by using MTB-GK-FW+GK.TDNA primers. Lines 12.1, 12.2, 12.3, 12.6, 12.7, 12.8, 12.10, 12.11, 12.13, 12.14, 12.16 were heterozygous plants for MTB (GK_332G03) T-DNA insertion.

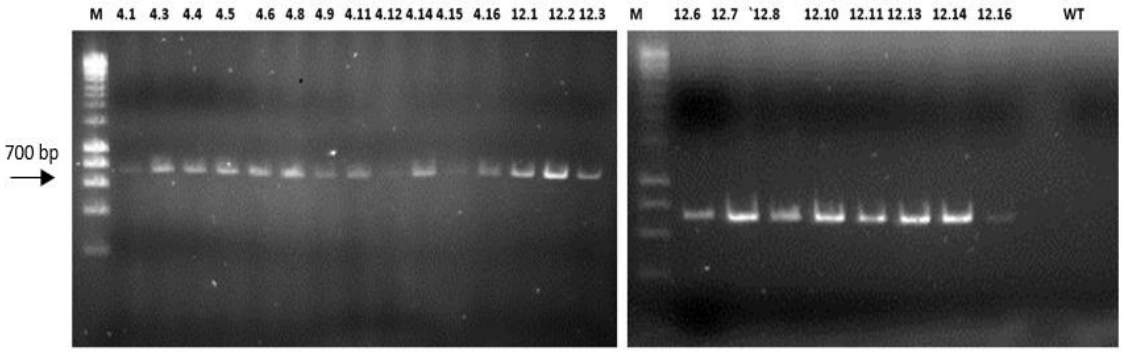

Figure 4.23: PCR analysis of F2 progenies (Lines 4 and 12) of MTBΔSAM crossed with MTB (GK_332G03) line to confirm the presence of MTBΔSAM construct in heterozygous plants by using MTB.FW2+GFPrev primers.

The phenotype of the F2 crossed plants are similar to WT and no plants homozygous for MTB T-DNA insertion *(*GK_332G03) were obtained in the F2 generation (23 plants from two lines). This was confirmed by the presence of a WT band of 1011 bp following PCR amplification for all F2 lines by using the forward and reverse primers in MTB introns (to prevent the appearance of MTBΔSAM construct derived bands) (Figure 4.24).

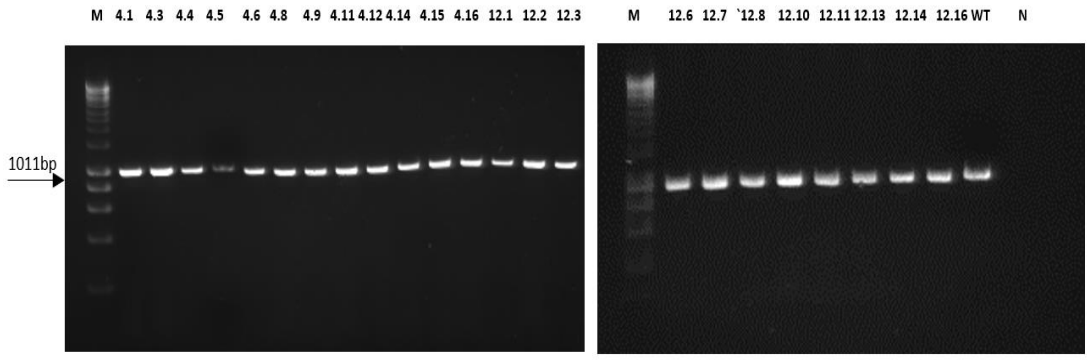

Figure 4.24: PCR amplification for F2 progenies of MTBΔSAM crossed with MTB (GK_332G03) line by using intron primers MTB-GK-FW + MTB-GK- REV to check for homozygous plants for (GK_332G03). WT=wild type Arabidopsis, N: negative control using water as a template.

This indicates that the MTBΔSAM was not able to complement the MTB-GK line. In this case, the control construct containing MTBcDNA (WT) instead of MTBΔSAM was transformed to WT and MTB T-DNA insertion *(*GK_332G03), to show if we can complement it. The transformed seeds were collected and due to time constraints, we could not finish this experiment during PhD thesis period.

4.5 Discussion

The fact that mRNA m^{6}A methyltransferase complex in animals is a multi-protein complex was known for a long time prior to the identification of any of the components. There are two putative catalytic subunits involved in the m^{6}A writer complex METTL3 and METTL14 (Liu et al., 2014). Previous studies have illustrated that METTL3 and METTL14 physically interact with each other and form a stable heterodimer core complex that produces specific m^{6}A marks on RNA (Liu et al., 2014). However, the specific roles of these two components in the MTase complex remains to be clarified. Both METTL3 and METTL14 polypeptides contain methyltransferase domains (Bujnicki et al., 2002). Knockdown of cellular *METTL3* and *METTL14* led to cell death in human HeLa cells and decreased the m^{6}A level in polyadenylated RNA (Bokar 2005; Liu et al., 2014). Compared to METTL3, METTL14 showed a stronger decrease in the m^{6}A level (Liu et al., 2014). Moreover, methyltransferase activity with METTL14 showed much higher activity *in vitro* (Liu et al., 2014). These results propose that METTL14 may play a more important role than METTL3 in m^{6}A modification. In contrast, three recent reports studied the crystal structures of the METTL3–METTL14 heterodimer, and they found that SAM was observed in only METTL3 and not in METTL14 suggesting that METTL3 is the sole catalytic subunit in the heterodimeric complex, while METTL14 may support and activate METTL3′s catalytic function (Wang X et al., 2016; Wang P et al., 2016; Śledź and Jinek, 2016).

The characterization of mRNA m^{6}A methyltransferase complex in *Arabidopsis* was initiated by the identification of MTA (a homolog of human mRNA m^{6}A methyltransferase). While *Arabidopsis* MTA has been studied in some detail, MTB characterization has been rather minimal. MTB is the homolog of human mRNA m^{6}A

methyltransferase METTL14, and as in human, it has been identified to be a part of the m^{6}A writer complex by tandem affinity purification (TAP) (Růžička et al., 2017) but its role in m^{6}A methylation remain to be clarified.

The results presented in this chapter detail the generation and analysis of MTB and MTA lines with expressing cDNAs encoding proteins with mutated SAM binding domains. Previous unpublished data indicated that for *MTA* this could give rise to a dominant negative phenotype. Plants homozygous for MTBΔSAM were selected and compared with similar MTAΔSAM plants. These mutations were generated in the SAM domain (DPPW) of an MTB peptide sequence by replacing Aspartic acid to Alanine (GAC → GCC) and Tryptophan to Glycine (TGG → GGG) by oligonucleotide-directed mutagenesis. The DPPW (Asp–Pro–Pro–Trp) is an active site that contains catalytic residues essential for methyltransfer and the SAM-binding motif (Bujnicki et al.,2002; Bokar et al.,1997).

Northern blot analysis was used to confirm the over-expression of both the *MTB* and the *MTA* mutant. The transcript levels in both of the MTBΔSAM and MTAΔSAM were higher than the non-mutated endogenous genes, but only those plants expressing the MTAΔSAM construct gave rise to a dominant negative phenotype with reduced m^{6}A. These MTAΔSAM over-expressing plants showed delayed development, reduced apical dominance and crinkled leaves, whereas *MTB* mutants more closely resembled WT. In addition, the m^{6}A to A ratio in the MTA dominant negative transgenic plants was less than the ratio in the wild-type *Arabidopsis* by more than 70 % (Fray's group unpublished). The m^{6}A measurement for MTBΔSAM expressing lines was not performed due to time constraints. Furthermore, the MTBΔSAM transgenic line was crossed with MTB G.K line to generate MTBΔSAM in the knockout mutant background. If the SAM binding site is dispensable for MTB

function, this might give rise to lines in which the GK insertion mutation could be complemented. This might be the case if MTB performed a structural function and its presence was required for the assembly of the writer complex, even if its SAM binding function were dispensable. However, no homozygous lines for MTB-GK T-DNA plant were obtained in the F2 generation, indicating that the MTBΔSAM did not complement the MTB-GK line. Thus, the control construct containing the MTBcDNA (WT) instead of MTBΔSAM was transformed to WT and MTB G.K line to show if this construct can complement the Gabi Kat line that's mean the reason of no complementation and no phenotype for MTBΔSAM because it does need this SAM domain for MTB.

The findings in this chapter are consistent with published studies in mammals which have shown that a mutation in the catalytic site of METTL3 led to an abolition of methyltransferase activity of the complex, whereas no effect was observed by mutating the putative catalytic site of METTL14 (Wang X et al., 2016; Wang P et al., 2016; Śledź and Jinek, 2016). They also showed the SAM domain in the catalytic cavity of METTL3 but not in METTL14 suggesting a catalytic role of METTL3 in the complex, whereas METTL14 supports METTL3 and contributes to RNA binding. Furthermore, two CCCH-type zinc fingers essential for catalytic activity of the full-length complex have been identified in METTL3 but not in METTL14 (Iyer et al. 2015). In addition, a recent study uncovered the direct role for METTL3 in promoting translation and they showed that METTL3 but not interact with other writer components observed in cytoplasmic fractions and links to ribosomes and its reduction impacts polysome profiles, leading to reduced target mRNA translation (Lin et al., 2016). In addition, they demonstrated that the METTL3 enhances translation independently of its methyltransferase activity, or the presence of other m^{6}A writer

complex and m^{6}A reader proteins (Lin et al., 2016). Moreover, METTL3 interacts in an RNA-independent manner with translation initiation factors and the *METTL3* knockdown lead to prevent the recruitment of eIF3 to cap-binding proteins CBP80- and eIF4E (Lin et al., 2016). Collectively these findings could explain why the MTAΔSAM construct does give a phenotype while no phenotype was observed with MTBΔSAM.

CHAPTER 5 : INVESTIGATION OF THE INTERACTION BETWEEN MTB AND PRMT4A AND PRMT4B USING YEAST-TWO-HYBRID.

5.1 Introduction

5.1.1 Arginine methylation

Arginine methylation is a widespread post-translation modification that acts as a transcription regulator and plays important roles in pre-mRNA splicing, DNA damage signalling, mRNA translation, and cell fate decisions (Auclair and Richard, 2013; Yang and Bedford, 2012; Goolam et al., 2016; Blanc and Richard, 2017). Arginine methylation can also have a significant impact on the subcellular localization of proteins and RNA (Fisk and Laurie ,2011). Arginine N-methyltransferase (PRMT) enzymes are responsible for the transferring of the methyl group from S-adenosylmethionine (AdoMet) to a guanidino nitrogen of Arginine (Bedford and Clark, 2009). Three main types of methylated arginine were identified in mammals, and their structures (MMA, ADMA, and SDMA) are shown in Figure 5.1 (Blanc and Richard, 2017). All PRMTs produce monomethylarginine (MMA) residues in which a single methyl group is positioned on one of the arginine terminal nitrogen atoms and produce either residues of asymmetric dimethylarginine (ADMA) or symmetric dimethylarginine (SDMA). The different PRMTs that carry out these reactions are referred to as Type I, Type II or Type III respectively. In Type I (ADMA) both methyl groups are placed on the same nitrogen atom of the guanidino group of arginine, PRMTs of this type include PRMT1, PRMT2, PRMT3, PRMT4, PRMT6, and PRMT8, whereas Type II (SDMA) generate one methyl group on each of the two-

terminal N atoms of arginine. PRMTs of this type include PRMT5 and PRMT9 (Lee and Stallcup, 2009; Raposo and Piller, 2018). Type III is represented by PRMT7 enzyme which only catalyzes MMA formation (Zurita-Lopez et al.,2012).

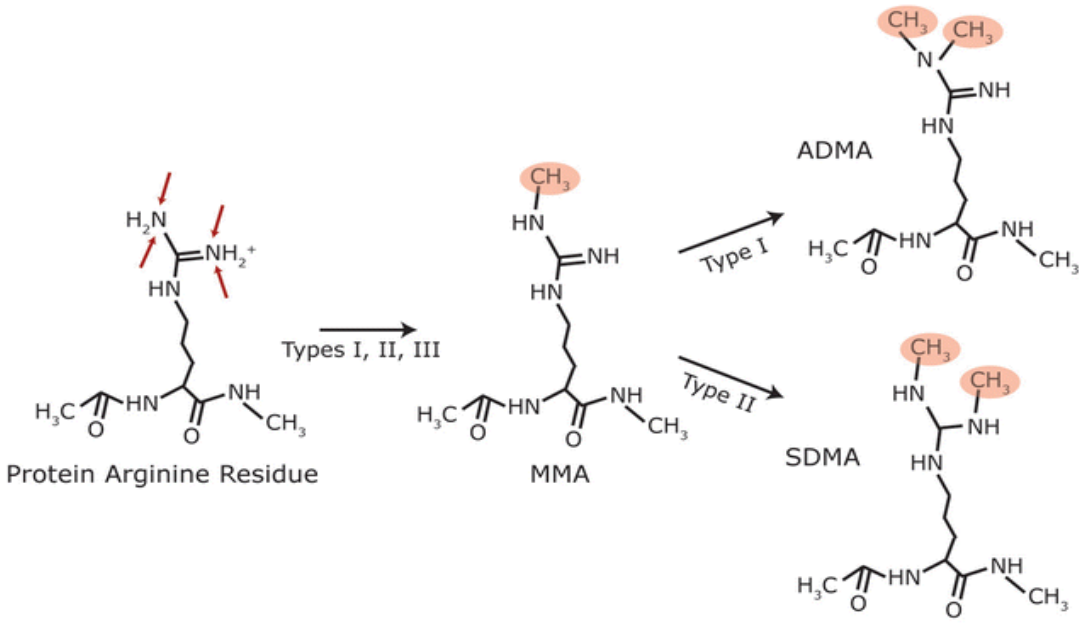

Figure 5.1: Types of Arginine methylation proteins in mammals. PRMTs are categorized as Type I, Type II or TypeIII, based on the methyl group position on the nitrogen atoms of the guanidine group of methylated arginine. Red arrows show known sites of methylation in mammalian cells; red circles show methyl groups (Raposo and Piller, 2018).

Among Type I PRMTs, PRMT4 or coactivator-associated arginine methyltransferase 1 (CARM1) have been well characterized. It has been reported that CARM1 methylates histone H3 at Arg-2, -17, and -26 in animals (Schurter et al., 2001) and plants (Niu et al., 2008). Besides histone H3, CARM1 methylates non-histone substrates involved in biological processes such as transcription, mRNA translation, cell signalling, pre-mRNA splicing and protein stability (Auclair and Richard, 2013; Yang and Bedford, 2012). Moreover, it has been identified as a secondary transcriptional coactivator of the p160 family members (Chen et al., 1999).

Nine PRMTs are present in the *Arabidopsis thaliana* genome (Niu et al., 2007). AtPRMT4a and AtPRMT4b, a pair of Arginine methyltransferases in *Arabidopsis* are homologs of mammalian CARM1/PRMT4, catalysing asymmetric dimethylation on Arginine (Arg) (Niu et al., 2008). Plants simultaneously homozygous for mutations in both AtPRMT4a and AtPRMT4b showed alterations in flowering time regulation (delayed flowering) through effects on FLOWERING LOCUS C (FLC) expression (Niu et al., 2008). However, the single mutants alone did not show this phenotype, indicating that both AtPRMT4a and AtPRMT4b act redundantly for proper flowering time regulation through the FLC-dependent pathway (Niu et al., 2008).

In a previous study, the PRMT4a and PRMT4b were found to interact with MTB methylase in Y2H assay (Fray group unpublished), and from proteomics data, 4 methylated arginine sites were found in MTB (Simpson group unpublished). In addition, we know that the FLC mRNA is strongly methylated (Fray's group unpublished) Figure 5.2.

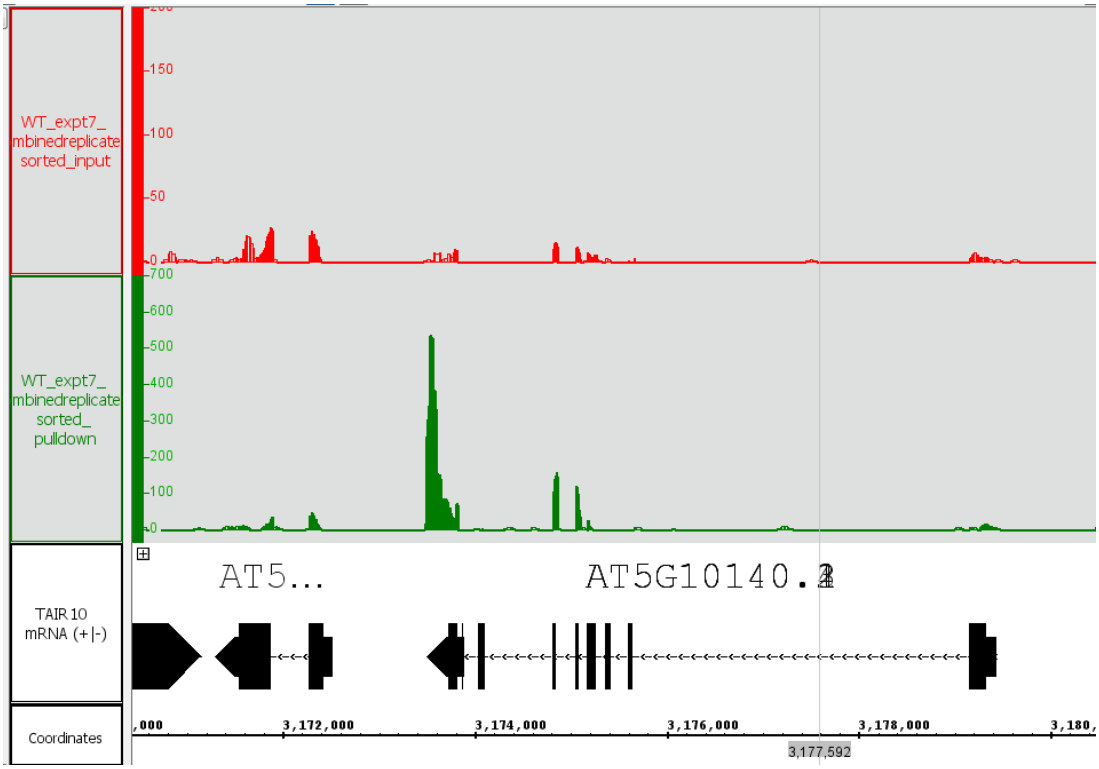

Figure 5.2: MeRIP-Seq, anti-m^{6}A antibody precipitated, fragmented mRNA sample (green), fragmented mRNA sample (input for the Immunoprecipitation) red. After alignment to TAIR10, peak calling was done using MACS2 software (Fray group unpublished). A strong methylation peak is present in the 3' region of the FLC gene AT5G10140.

In the current study, the interaction using PRMT4a.cDNA and PRMT4b.cDNA with the B methylase with and without the 4 sites of methylated Arginine in the bait and prey vectors were investigated via Yeast Two Hybrid. If the PRMT4a and PRMT4b are interacting because the MTB is the target, it would be expected that converting the 4 arginine targets to lysine might stop this interaction in Y2H. Further mutant crosses with, and m^{6}A measurements in, the *prmt4a/b* double mutant sought to investigate the importance of MTB arginine methylation in m^{6}A writing.

5.1.2 Yeast two-hybrid system

The Yeast two-hybrid system is one of the most powerful and commonly used methods for the identification of interactions between two proteins (Fields and Song 1989; Wan et al., 2006). When the two proteins of interest (fused to a split GAL4 transcription factor) interact within the yeast, a functional GAL4 transcription factor (TF) is reconstituted. This activates transcription of reporter genes, allowing the interaction to be detected. The transcription factor consists of a DNA-binding domain (DBD) and an activation domain (AD). Two separate hybrid proteins are constructed between the two proteins of interest. The first hybrid protein fused to the DBD is known as the "bait", and the second one fused to the AD known as the "prey". At the time of interaction between the bait (X) and the prey (Y) in the nucleus, the activation domain is brought alongside the DNA-binding domain and a functional TF is reconstituted. This reconstituted TF binds to upstream activator sequences (UAS), resulting in expression of the reporter genes (Figure 5.3). Gal4 is the most popular fusion used to provide the DBD and AD of the yeast TF. Positive interactions lead to a specific phenotype that can be detected by growth on a selective medium lacking the auxotrophic markers, such as Histidine or Uracil, or by a change in the colour of the yeast colonies using LacZ to screen yeast in a colorimetric assay. In this study, this technique was used to investigate the interaction between the methylase B and PRMT4A and PRMT4B.

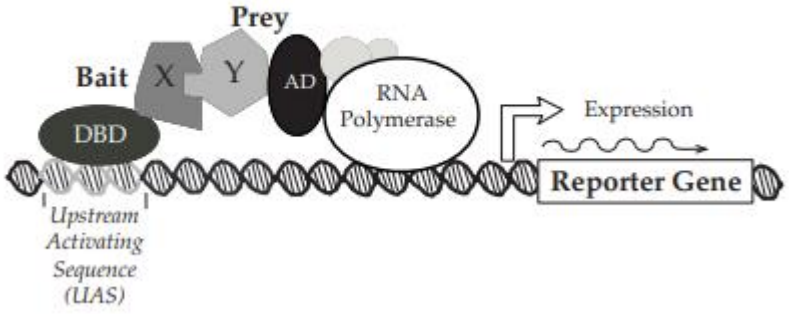

Figure 5.3: The classical system of yeast two-hybrid (ProQuestTM Two-Hybrid System with Gateway® Technology, Invitrogen). (X-Bait) fused to the DNA binding domain (DBD) and represent the protein of interest, while (Y-Prey) fused to the activation domain (AD) and represent the potential interacting protein. When the both fusion proteins Bait and Prey interacted together the functional transcription factor will be reconstituted. As a result, RNA polymerase II is further recruited, and transcription occurs.

5.2 The Aims of this chapter

5.2.1-Aims of generation MTB-lysine in which the four known sites of arginine methylation are replaced with lysine and testing this in a Yeast Two-Hybrid assay with PRMT4a and PRMT4b.

The aim is to test the interaction between both PRMT4a and PRMT4b with the B methylase with and without the 4 arginines that are methylation targets *in vivo*. This may indicate whether the reason that MTB interacts with PRMT4a and PRMT4b is because the MTB is a substrate for methylation.

5.2.2- Aims of the crossing between MTB-GFP and *prmt4a/b* double mutant.

1) If MTB is a substrate for methylation by PRMT4a/b, then the stability or subcellular localisation may change in the absence of arginine methylation.

2) Isolate MTB-GFP using the GFP tag and then test with an antibody against methyl arginine to i) confirm that MTB is arginine methylated in a WT background and ii) to demonstrate that this arginine methylation is lost in the *prmt4a/b* double mutant.

5.2.3- Generation and analyse CaMV 35S: MTB.Arg.mut construct.

This construct was transformed to mutant plants (MTB-GK) and to WT to study the phenotype and see 1) if complementation is possible with this construct and 2) if the complemented mutant has the same phenotype as the *prmt4a/b* double mutant (delayed flowering).

5.3 Methods

5.3.1 Complementary DNA (cDNA Synthesis).

Total RNA was prepared following the protocol described in section 2.19. First-strand cDNAs were synthesised following the manufacturer's protocol (SuperScript® II reverse transcriptase, Invitrogen™, Life Technologies). In a nuclease-free microcentrifuge tube, mix 1 µl of Oligo(dT), 5 µg total RNA, 1 µl dNTP (10 mM), and up to 12 µl by Sterile, distilled water. Subsequently, the mixture was placed at 65°C for 5 min and then quickly placed on ice. After brief centrifugation, 4 µl of 5X First-Strand Buffer, 2 µl 0.1 M DTT and 1 µL RNaseOUT™ (40 units/µL) were added. Afterwards, the tube was mixed gently and incubated at 42°C for 2 min. 1 µL (200 units) of SuperScript™ II RT was then added and mixed gently by pipetting up and down. The mixture was then incubated at 42°C for 50 min. In the last step the reaction was inactivated by heating at 70°C for 15 min and stored at -20°C to be used in other experiments.

5.3.2 Protein Experiments

5.3.2.1 Solution preparation

Lysis buffer: Mix 50 mM Tris-HCl (pH 8.0), 10 mM EDTA (pH 8.0), 1% [w/v] SDS, 1 mM phenylmethanesulfonyl fluoride (PMSF), 1% (v/v) Plant Protease Inhibitors (just before use).

Urea cracking buffer: Mix 8 M Urea, 40Mm Tris-HCL (PH 6.8), EDTA (PH 8.0) then incubate it at 90 °C for 5 min. Divide the buffer into 0.5 ml in Eppendorf tubes. For each tube (0.5 ml) add: 1.0% (v/v) B-meracapto-ethanol, 7.0 % (v/v) Plant Protease Inhibitors, 5.0 Mm PMSF.

IP dilution buffer: Mix 16.7 mM Tris-HCl (pH 8.0), 1.2 mM EDTA (pH 8.0), 167 mM NaCl, 1.1% (v/v) Triton X-100, 1% (v/v) Plant Protease Inhibitors (just before use). Store at 4°C.

Beads washing buffer: Mix 20 mM Tris-HCl (pH 8.0), 150 mM NaCl, 2 mM EDTA pH (8.0), 1% (v/v) Triton X-100, 0.1% (w/v) SDS, 1 mM PMSF (just before use). Store at 4°C.

1% (v/v) formaldehyde: Just before use, dilute from 37% (v/v) formaldehyde (Sigma-Aldrich) and using cold sterile water.

2 M glycine: In 1 L of sterile water, dissolve 150.14 g glycine powder, filter sterilization and store at 4°C.

5.3.2.2 Extraction of Protein

Two-week old *Arabidopsis* seedlings were harvested from ½ MS plates, then were ground into fine powder under liquid nitrogen. In each 1.5 ml Eppendorf tube, ~100 mg of powder and 400 µl of Lysis buffer was added and mixed by vortexing. Tubes were placed on ice for 15 min and were vortexed twice during this time. These were then spun down at 14,000 rpm for 5 min and the supernatants transferred into fresh tubes and used as protein samples. According to instructions for "Bio-Rad Protein Assay", the protein content was measured.

5.3.2.3 Protein extraction in 8M Urea

Two-week old *Arabidopsis* seedlings were harvested from ½ MS plates, then were ground into fine powder under liquid nitrogen. In each 1.5 ml Eppendorf tube, ~100 mg of powder and 300 µl of cracking buffer was added and mixed by vortexing. Tubes

were then incubated at 100 °C for 5 min. These were then centrifuged at 13,000 rpm for 1 min. 0.2 ml of the supernatants was transferred into fresh tubes and used as protein samples. Samples were frozen in liquid nitrogen and stored at – 80 °C.

5.3.2.4 Immunoprecipitation by GFP-Trap agarose beads (ChromoTek)

17 µl of GFP-Trap agarose beads (ChromoTek) were pre-washed 3-times with IP dilution buffer, then resuspended in 210 µl of IP dilution buffer. Afterwards, beads were divided into tubes containing diluted protein samples and then incubated for 5 h at 4°C with rotation. Tubes were centrifuged at 200 g for 3 min at 4°C. Subsequently, most of the supernatant was removed and about 1 ml was kept at the bottom of the tube. Beads were then resuspended and transferred to a 1.5 ml Eppendorf tube and washed 3 times with Beads washing buffer. Between washes, tubes were centrifuged at 400 g for 2 min at 4°C. After the last wash, the liquid was removed by using yellow or white tips and tubes containing beads were frozen in liquid nitrogen and stored at -80°C until use.

5.3.2.5 Lateral Root Induction with NPA and NAA.

In this inducible system, *Arabidopsis* seedlings were treated first with auxin transport inhibitor NPA and then with exogenous auxin NAA. These treatments have been used to avoid the first formative divisions and then to activate the whole pericycle (Himanen et al., 2002). After germination of *Arabidopsis* seedlings on ½ MS for 5 days, the seedlings were transferred to vertical square plates containing ½ MS and 10 µM NPA. Then on the third day, they were transferred to ½ MS containing 10 µM NAA. After that, GFP activity of treated seedlings was observed by confocal microscopy (Leica TCS SP5).

5.3.2.6 Formaldehyde Crosslinking

Arabidopsis seeds were germinated on petri dishes containing ½ MS. After two weeks the seedlings were harvested and washed 4 times with sterile cold water. Seedlings were then placed in a beaker containing 1% (v/v) formaldehyde inside a desiccator and the vacuum on for 15 min. The vacuum was then removed gently, and 2 M glycine solution was added to a final concentration of 0.125 M and mixed well then put it back inside the vacuum for another 5 min. The vacuum was then removed gently. Afterwards, crosslinked seedlings were washed 4 times with cold sterile water and then kept to dry. Seedlings were transferred into 50 ml Falcon tubes and were frozen in liquid nitrogen then stored at -80°C until use.

5.3.2.7 Western Blotting

5.3.2.7.1 Gel Electrophoresis

Protein sample was prepared by mixing: 35 µg of protein, up to 16 µl with sterile water and 4 µl of 5× Laemmli buffer (312.5 mM Tris-HCl pH 6.8; 50% (v/v) glycerol; 10% (w/v) SDS, 0.05% (w/v) bromophenol blue; and 25% (v/v) β-mercaptoethanol). The mixture was incubated at 95°C for 5 min and then loaded onto Bio-Rad Mini-PROTEAN® TGX™ Precast Gel (20) µl of each sample). In addition, 7 µl of Bio-Rad protein marker (Precision Plus Protein™ Dual Color Standards) was loaded. The gel was run in the electrophoresis buffer (25 mM Tris, 192 mM glycine, 0.1% (w/v) SDS) for approximately 60-70 min at 110 V.

5.3.2.7.2 Membrane Transfer

Before transferring, the gel was equilibrated by soaking in cold transfer buffer (25 mM Tris, 192 mM glycine and 20% (v/v) methanol, pH 8.3) for 30 min. Two fibre pads,

two pieces of filter paper and Amersham™ Protran® western blotting membrane (nitrocellulose, pore size: 0.2 μm) were also soaked in cold transfer buffer for 15-20 min before transferring. Membrane transfer was carried out according to instructions for "Mini Trans-Blot® Electrophoretic Transfer Cell" (Bio-Rad). The transfer cassette was assembled also according the manufacturer's instructions and run at 120 V for 1 h.

5.3.2.7.3 Blocking and Incubation with primary and secondary Antibodies

The following blocking and antibody incubation steps and solutions were prepared and carried out according to the protocol for "WesternBreeze® Chemiluminescent Western Blot Immunodetection" Kit.

Prepare Blocking Solution: for 20 ml total volume, mix 14 ml of distilled water, 4 ml of Blocker/Diluent (Part A) and 2 ml of Blocker/Diluent (Part B).

Prepare Primary Antibody Diluent: The primary antibody was diluted according to the manufacturer's instructions into 10 ml of Blocking solution.

Prepare Antibody Wash: for 160 ml total volume, mix 150 mL of distilled water with Antibody Wash Solution (16x) 10 ml.

In 10 ml of blocking solution the membrane was incubated for 1 h on a rotary shaker, then the blocking solution was removed. Subsequently, the membrane was rinsed twice with 20 ml of water for 5 minutes each time, then the water was removed. Next, the membrane was incubated with 10 ml of Primary Antibody Solution for 1 hour. Afterwards, the membrane was washed four times with 20 mL of prepared Antibody Wash for 5 minutes. The membrane was then incubated in 10 ml of Secondary Antibody Solution for 30 minutes, followed by four washes with 20 ml of prepared

Antibody Wash for 5 minutes. Then, the membrane was rinsed twice with 20 ml of water for 2 minutes.

GFP antibody is a mixture of two monoclonal antibodies from mouse IgG1 κ (Sigma-Aldrich) and an antibody to MonoMethyle-Arginine[mme-R] MultiMab^{TM} Rabbit mAb mix (Cell Signaling Technology) were used in this study.

5.3.2.7.4 Incubation with Chemiluminescent Substrate

The Chemiluminescent Substrate was prepared according to the manufacturer's Instructions for "WesternBreeze® Chemiluminescent Western Blot Immunodetection" Kit. The Chemiluminescent Substrate mixture was prepared by mixing 2.375 ml of Chemiluminescent Substrate with 0.125 ml of Chemiluminescent Substrate Enhancer to make total Volume 2.5 ml.

The membrane was placed on a sheet of transparency plastic and before the membrane dry, 2.5 ml of Chemiluminescent Substrate Solution was evenly applied onto the membrane without touching the surface. The reaction was developed for 5 minutes at room temperature then any extra substrate was removed using filter paper.

5.3.2.7.5 Detection

From the last step, the membrane was put between two pieces of transparency plastic and was then placed into a cassette. Afterwards, a film was put on the membrane and exposed for 1 min or longer in the dark room. The film was then developed in Carestream® Kodak® autoradiography GBX developer/replenisher (SigmaAldrich) and then fixed by Carestream® Kodak® autoradiography GBX fixer/replenisher (Sigma-Aldrich). The film was then scanned by using GS-800™ Calibrated Imaging Densitometer (Bio-Rad) in combination with Quantity One software.

5.3.3 Yeast two-hybrid assay

The yeast two-hybrid assay was performed following the manufacturer's protocol (ProQuest™ Two-Hybrid System with Gateway® Technology, Invitrogen). The yeast cell strain used in this experiment was MaV203 competent cells from (Invitrogen, UK).

5.3.3.1 Yeast Growth media and solution preparation.

YPAD medium and plates (500 ml): mix 5 g of Bacto-yeast extract, 10 g of Bacto-peptone, 10 g Dextrose and 50 mg of Adenine sulfate in 500 ml of distilled water then Autoclave. For 500 agar plates, add 20 g bacteriological-grade agar then autoclave at 121°C for 25 minutes. After cooling to 55°C, pour it into sterile Petri dishes and store plates at 4°C.

Synthetic complete (SC) drop-out media (1L): mix 6.7 g of Yeast nitrogen base without amino acids, 1.39-1.92 g of dropout mix, 20 g of Glucose in 1L of distilled water then Autoclave at 121°C for 25 minutes. For 1L agar plates, add 20 g of bacto agar (for plates) then Autoclave.

3-AT Plates: Follow the above SC-Leu-Trp-His medium recipe. Cool to approximately 65°C then add 3-AT in different concentration (10, 12.5, 15, and 20 mM).

10xTE: mix 100 mM Tris-HCl and 10 mM EDTA, adjust pH 7.5 then autoclave and store at room temperature.

10xLiAc: 1 M Lithium Acetate and filter sterilize.

1X LiAc/0.5X TE: for 100 total volume, mix 10 ml of 10xLiAc with 5 ml of 10xTE and 85 ml of sterile water, then filter sterilize.

1X LiAc/1X TE: mix 10 ml of 10xLiAc ,10 ml of 10xTE 80 ml of sterile water then filter sterilize.

1X LiAc/40% PEG3350/1X TE: mix 10 ml of 10xLiAc, 5 ml of 10xTE, 40 g PEG-3350, then make up to 100 ml by sterile water and filter sterilize.

Z buffer 1L: 16.1 g $Na_2HPO_4 \cdot 7H_2O$ (or 8.52 g anhydrous), 5.5 g $NaH_2PO_4 \cdot H_2O$ (or 4.8 g anhydrous), 0.75 g KCl, 0.246 g $MgSO_4 \cdot 7H_2O$ (or 0.12 g anhydrous) , up to 1000 ml by in sterile water. Adjust pH to 7.0 and filter sterilize.

5.3.3.2 Preparation of Competent Yeast Cells

A small amount of yeast competent cells (strain MaV203) were streaked on YPAD medium and incubated at 28ºC overnight. 10 ml of YPAD was inoculated with a fresh colony of MaV203 and incubated overnight at 28ºC with shaking. After that, the OD^{600} of overnight culture was determined and it should be $OD^{600} > 1.5$. The culture was then diluted to an OD_{600} of 0.4-0.8 by adding 100 ml of YPAD and incubated at 28ºC for an additional 2-4 hours. The cells were then collected by centrifugation at 2500 rpm for 10 min at RT. Afterwards, the pellet was resuspended in 40 ml sterile water, then centrifuged and the supernatant was removed. The pellet then was resuspended in 2 ml of 1X LiAc/0.5X TE and used for yeast transformation.

5.3.3.3 Transformation of Competent Yeast Cells

Each transformation mixture was prepared by mixing: 1 µg plasmid DNA (prey and bait), 100 µg denatured sheared salmon sperm DNA, 100 µl of the yeast suspension

from section 5.3.3.2, and 700 µl of 1X LiAc/40% PEG-3350/1X TE. The mixture was then inverted several times until homogenous, then incubated for 30 min at 28^0C with shaking. Then 88 µl of DMSO was added and mixed well by inversion, then heat shocked at 42^0C for 15 min. The mixture was then centrifuged at 3000 rpm and the supernatant was removed. The pellet was resuspended in 200 µl sterile water. 100 µl of this was plated on SC-L-T medium and then incubated at 28 °C for 2-4 days. Colonies were then used for further analysis.

5.3.3.4 Characterization of Yeast transformants

For each colony to be tested, different dilutions were made from master plates and plated on Sc-L-T-H with different concentrations of 3-Amino-1,2,4-triazole (3-AT), alongside the yeast control strains. Afterwards, the plates were incubated at 28 °C for 2-3days. Then the possible interactions between different baits and preys were tested according to the observed growth on 3-AT-HIS3 plates and compared to the controls.

5.3.3.5 X-gal Assay

Colonies to be tested were streaked on YPAD medium at 28 °C overnight. The next day, two round filter papers were placed in 15-cm petri dish and Saturated with 3ml X-gal solution (100 µl X-gal in DMF, 60 µl 2-mercaptoethanol and 10 ml Z buffer). The membrane was placed on the top of the colonies for a few minutes. Then the membrane with colonies was removed from the YPAD plate and frozen in liquid nitrogen for 45 seconds. The frozen membrane was placed on top of the two soaked filter papers colonies side up. The plate was then covered and incubated at 37°C overnight. The detection of positive interaction was made by the appearance of the blue colour and comparing to the controls.

5.4 Results

5.4.1 Synthesis and generation of MTB-Lysine construct by replacing the 4 methylated arginine in MTB with lysine and preparation of entry vectors of MTB splice variants 1.

Proteomics data showed 4 methylated arginine sites were found in MTB (Simpson group unpublished), and it was of interest in this study to determine if we could replace these four methylated arginine sites with lysine then study the effect and interaction between MTB with and without the 4 methylated Arginine sites and PRMT4a and PRMT4b (Figures 5.4 and 5.5).

Verified sites of arginine methylation in Arabidopsis MTB-METTL14

MKKKQEESSLEKLSTWYQDGEQDGGDRSEKRRMSLKASDFESSSRSGGSKSKEDNKSVVDVEHQDRDSKR
ERDGRERTHGSSSDSSKRKRWDEAGGLVNDGDHKSSKLSDSRHDSGGERVSVSNEHGESRRDLKSDRSLK
TSSRDEKSKSRGVKDDDRGSPLKKTSGKDGSEVVREVGRSNRSKTPDADYEKEKYSRKDERSRGRDDGWS
DRDRDQEGLKDNWKRRHSSSGDKDQKDGDLLYDRGREREFPRQGRERSEGERSHGRLGGRKDGNRGEAVK
ALSSGGVSNENYDVIEIQTKPHDYVRGESGPNFARMTESGQQPPKKPSNNEEEWAHNQEGRQRSETFGFG
SYGEDSRDEAGEASSDYSGAKARNQRGSTPGRTNFVQTPNRGYQTPQGTRGNRPLRGGKGRPAGGRENQQ
GAIPMPIMGSPFANLGMPPPSPIHSLTPGMSPIPGTSVTPVFMPPFAPTLIWPGARGVDGNMLPVPPVLS
PLPPGPSGPRFPSIGTPPNPNMFFTPPGSDRGGPPNFPGSNISGQMGRGMPSDKTSGGWVPPRGGGPPGK
APSRGEQNDYSQNFVDTGMRPQNFIRELELTNVEDYPKLRELIQKKDEIVSNSASAPMYLKGDLHEVELS
PELFGTKFDVILVDPPWEEYVHRAPGVSDSMEYWTFEDIINLKIEAIADTPSFLFLWVGDGVGLEQGRQC
LKKWGFRRCEDICWVKTNKSNAAPTLRHDSRTVFQRSKEHCLMGIKGTVRRSTDGHIIHANIDTDVIIAE
EPPYGSTQKPEDMYRIIEHFALGRRRLELFGEDHNIRAGWLTVGKGLSSSNFEPQAYVRNFADKEGKVWL
GGGGRNPPPDAPHLVVTTPDIESLRPKSPMKNQQQQSYPSSLASANSSNRRTTGNSPQANPNVVVLHQEA
SGSNFSVPTTPHWVPPTAPAAAGPPPMDSFRVPEGGNNTRPPDDKSFDMYGFN

Figure 5.4: Mass-spec data indicated that methylation is present at positions: 580, 586, 538 and 553 of MTB.

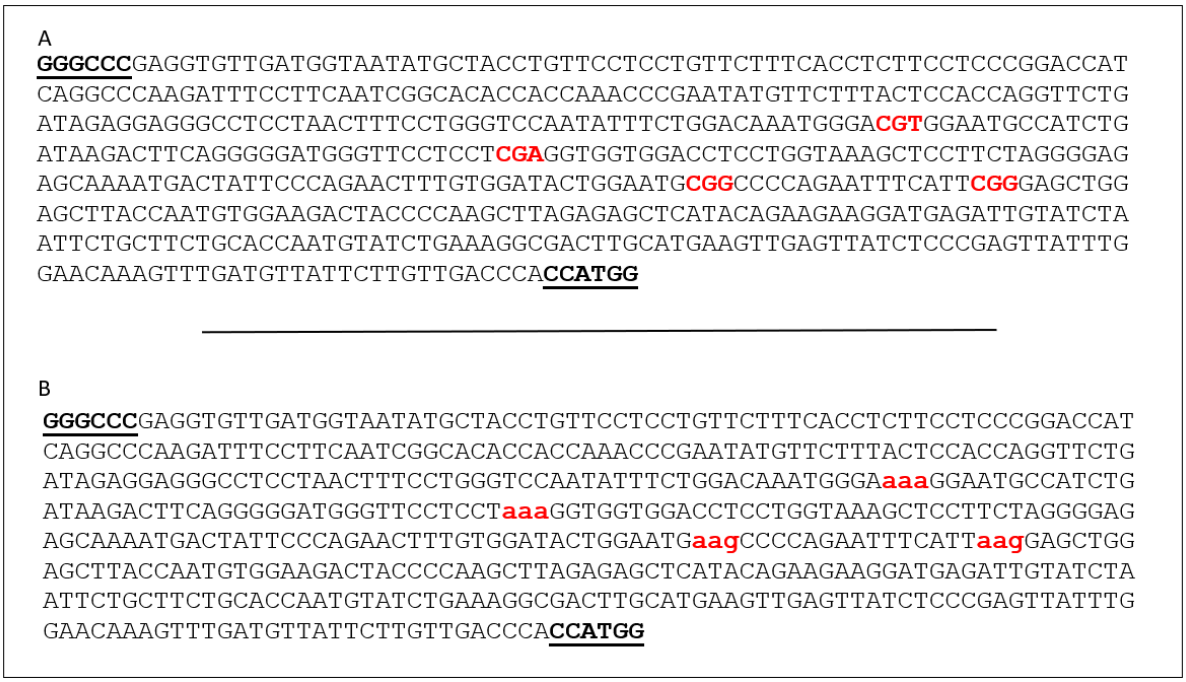

Figure 5.5: Synthesis of MTB-Lysine sequence. A: original MTB sequence with the 4 methylated arginine codons indicated by red colour. B: Synthesized MTB sequence by (Synbio Technologies company) to replace the 4 methylated arginine with Lysine, which indicated by red colour. GGGCCC=ApaI and CCATGG= NcoI Restriction enzymes.

These four sites of methylated arginine were replaced with lysine via a simple ApaI – NcoI digest and replacement by a synthetic DNA sequence (Synbio Technologies Company). Thereafter, the synthesized product with Lysine and the original sequence of MTB with Arginine using (PCR8:MTBcDNA.WT) plasmid were both doubly digested with ApaI and NcoI restriction enzymes, this produced three fragments of 3610 bp (a) belonging to MTB and PCR8 vector, 1526 bp (b) and 511 bp (c) for MTBcDNA.WT and two fragments at 2578 bp (d) and 511 (e) bp for MTB-Lys. Fragment (c) was replaced with fragment (e) to generate (MTBcDNA.Arg.mutant) entry vector. To achieve this, the desired fragments a, b and e were separately gel-purified (Figure 5.6). The purified fragments (a) and (e) were then ligated with T4 DNA ligase and transformed into *E. coli DH5α* cells. Colonies obtained after overnight

incubation were all confirmed by colony PCR using (MTBLysFor.new+ MTBLysRev.new) primers (Figure 5.7). Subsequently, one of the positive colonies containing fragments (a) and (e) was selected for plasmid preparation, confirmed by sequencing and then ligated with fragment (b) (treated with CIAP) to produce the entry vector named (PCR8;MTB.Arg.mut) with mutated arginine sites.

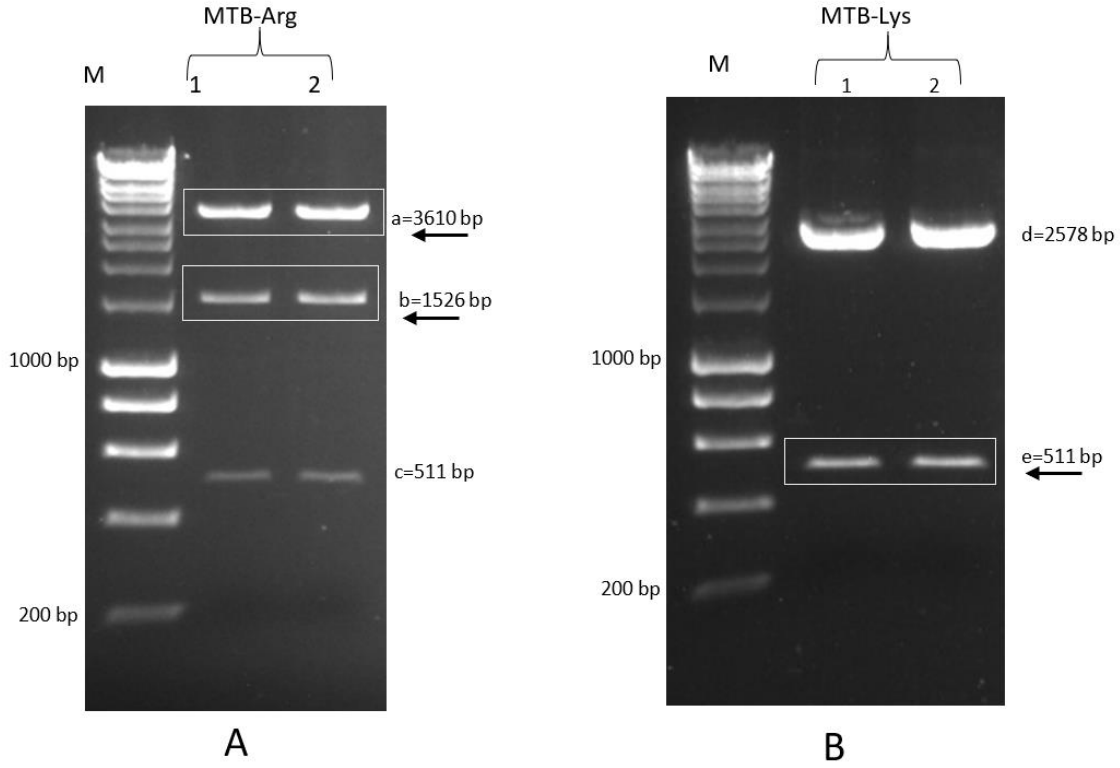

Figure 5.6: Restriction digestion of two plasmids of MTB with and without 4 methylated Arginine sites with ApaI and NcoI Restriction enzymes. A: plasmid of original sequence of MTBcDNA, Lane 1 and 2 used plasmid (PCR8:MTBcDNA.WT) as a template. The expected bands on 1% (w/v) agarose gels are (a)= 3610 bp, (b)= 1526 bp and (c)= 511 bp. B: Digestion of the new synthetic MTB with Lysine instead of Arginine (named MTB-Lys) by ApaI and NcoI. The expected bands are (d) = 2578 bp and (e) = 511 bp. The desired fragments were indicated by arrows. M=HyperLadder 1Kb (Bioline) was used as a marker.

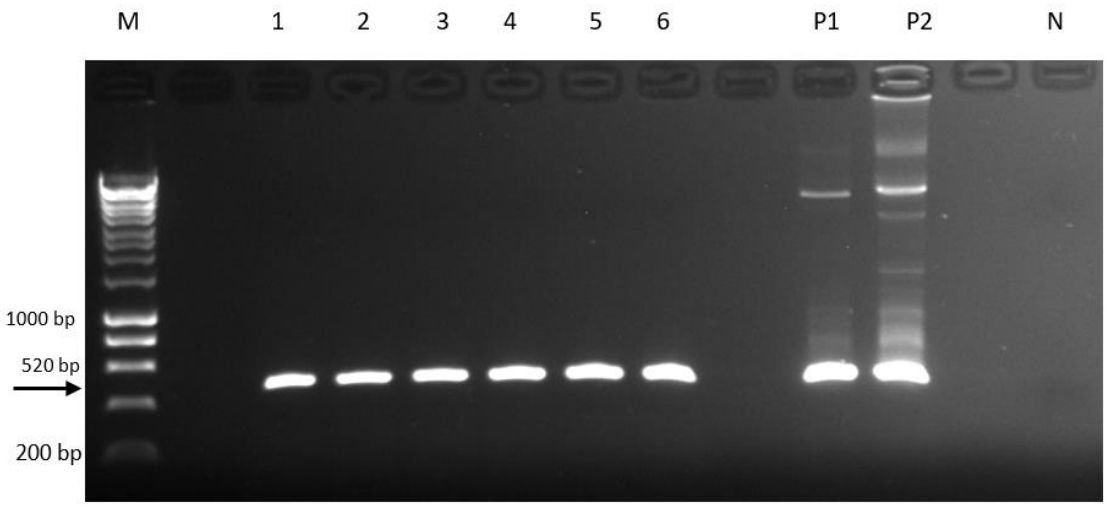

Figure 5.7: Colony PCR for *E. coli DH5α* transformed with a ligation mixture of fragments (a and e) using primers (MTBLysFor.new+ MTBLysRev.new). Lanes 1–6, colonies tested; P1, first positive control using PCR8:MTBcDNA.WT as a template; P2, second positive control using MTB-Lys as a template. N, negative control using water as a template. Arrow indicate to the expected size of the bands at 520bp. PCR product were run on 1 %(w/v) agarose gel, and HyperLadder 1Kb (Bioline) was used as a marker.

Subsequently, the ligation mixture containing all three desired fragments were transformed into *E. coli DH5α* cells. Colonies were then screened by PCR to confirm the ligation using the primers (MTBatgstart+ MTBnostop) (Figure 5.8).

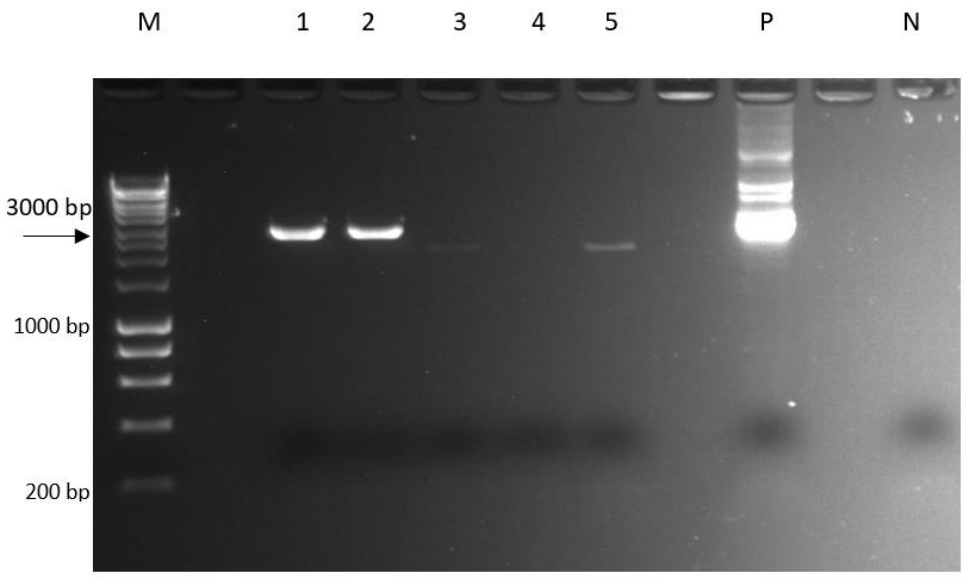

Figure 5.8: Colony PCR for *E. coli DH5α* transformed with a ligation mixture of fragments (ae+b) to produce the PCR8:MTB.Arg.mut construct using primers MTBatgstart+ MTBnostop. Lanes 1–5, colonies tested; P, positive control using MTBcDAN as a template. N, negative control using water as a template. Arrow indicates the expected size of the bands at 3000 bp. PCR product were run on 1 % (w/v) agarose gel, and HyperLadder 1Kb (Bioline) was used as a marker.

One of the positive colonies was chosen for plasmid preparation and was also verified by sequencing. The two entry vectors of MTB full length PCR8:MTB.Arg.mut.var1 and PCR8:MTBcDNA-WT.var1 were further used in the cloning to generate bait and prey constructs for Yeast-two Hybrid.

5.4.2 Preparation of both MTB splice variant entry vectors

Two splice variants of MTB have been reported. Variant 1 is the full-length correctly spliced form of MTB and the variant 2 lacks exons 5 and 6 of MTB (Figure 5.9).

Figure 5.9: Schematic diagram showing the MTB splice variant. Variant 1 is full-length correctly spliced form of MTB represented by AT4G09980.1. Variant 2 lacks exons 5 and 6 of MTB and represented by AT4G09980.2. Dark and light grey boxes represent exons and the 5′ or 3′ untranslated region, respectively. https://bar.utoronto.ca/eplant/.

A detailed description of the splice variant, the mRNAs and the predicted amino acid sequence encoded is shown in Appendix III. The splice variant results in the inclusion of a stop codon which would produce a protein lacking the last xx amino acids of the carboxy terminus. However, the SAM binding domain and all of the common METTL3/14 motifs identified by Bujinski et al (2002) are present in the truncated version.

Both splice variants of MTB were used to study the interaction between MTB and Arginine methylation in Y2H. MTB variant 1 entry vector (PCR8:MTBcDNA-WT.var1) was prepared in a previous study (Fray group), and the mutant version of (PCR8:MTB.Arg.mut.var1) was previously prepared (section 5.4.1). The MTB variant 2 entry vectors were generated by amplifying PCR8:MTBcDNA.WT and PCR8:MTBcDNA.Arg.Mut plasmids using the MTB.start + w.MTBsplice.rev primers. The reverse primer was designed to produce a PCR product of MTB lacking of exons 5 and 6 of MTB (Figure 5.10). The bands were excised from the gel and purified. The purified products were then cloned into pCR™8/GW/TOPO® entry vector then transformed to *E.coli* Top 10 cells. The obtained colonies were verified by PCR using MTB.start and w.MTBsplice.rev primers (Figure 5.11). Subsequently, one

positive colony for both PCR8:MTBcDNA.WT.var2 and PCR8:MTBcDNA.Arg.mut.var2 were chosen for plasmid extraction and confirmed by DNA sequencing. These two entry vectors of MTB variant 2 were further used in the cloning to generate bait and prey constructs.

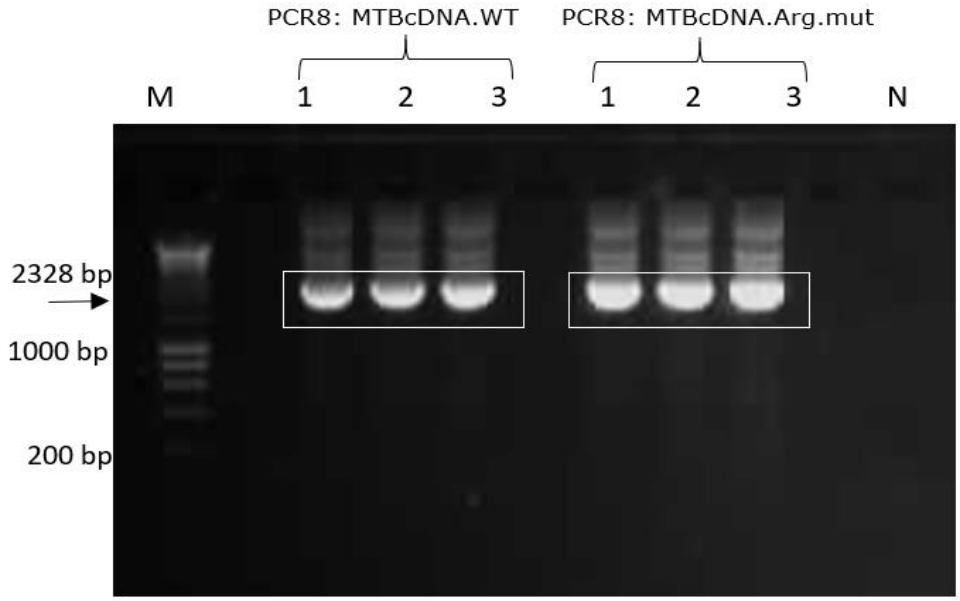

Figure 5.10: PCR amplification to generate MTB variant 2 lacking of exons 5 and 6 using MTB.start + w.MTBsplice.rev primers, and PCR8: MTBcDNA.WT and PCR8:MTBcDNA.Argmut plasmids as templates. N, negative control using water as a template. Arrow indicates the expected size of the bands at 2328 bp. PCR products were run on 1 % (w/v) agarose gel, and HyperLadder 1Kb (Bioline) was used as a marker.

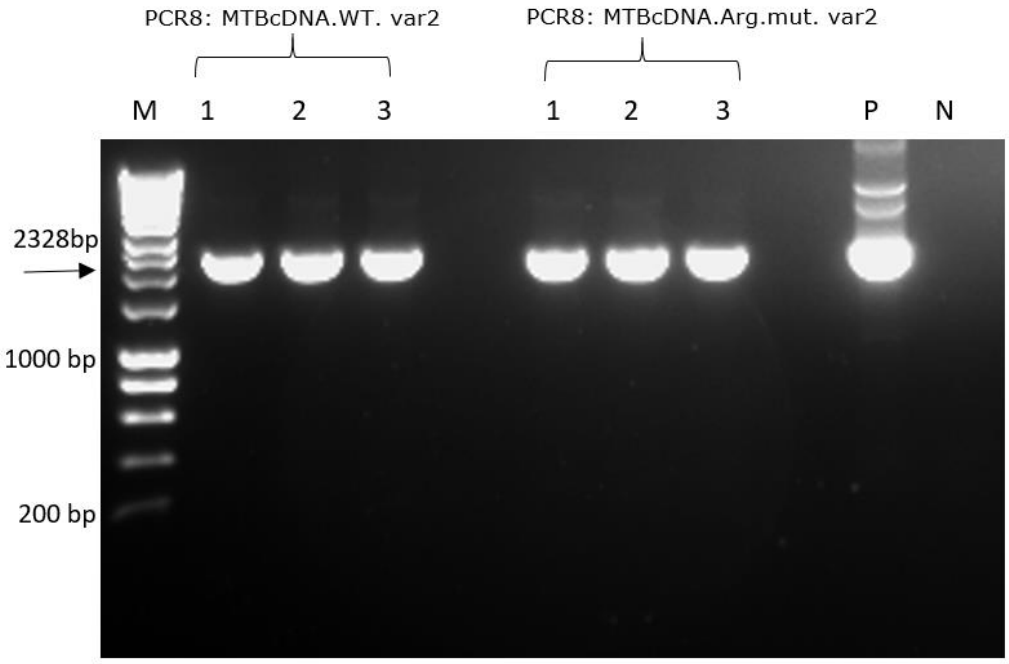

Figure 5.11: Colony PCR for *E. coli* TOP10 cells transformed with PCR8: MTBcDNA.WT.var2 and PCR8:MTBcDNA.Argmut.var2 using MTB.start and w.MTBsplice.rev primers. P, positive control using (PCR8: MTBcDAN) as a template. N, negative control using water as a template. Arrow indicates the expected size of the bands at 2328bp. PCR product were run on 1 % (w/v) agarose gel, and HyperLadder 1Kb (Bioline) was used as a marker.

5.4.3 Preparation of PCR8: PRMT4a cDNA and PCR8: PRMT4b cDNA entry vectors.

Total RNAs were isolated from *Arabidopsis* WT as described in section 2.19 then were reverse transcribed as described in section 5.3.1. The following primer pairs (prmt4aFw-y2h+prmt4aRev-y2h) for *AtPRMT4a* cDNA and *(*prmt4bFw-y2h+prmt4bRev-y2h) for *AtPRMT4b* cDNA and RT products were used to perform PCR (Figure 5.12). PCR products were purified and subsequently cloned into pCR™8/GW/TOPO® entry vector and then transformed into *E. coli* Top 10 competent cells. Colonies obtained after overnight incubation were all confirmed by colony PCR (Figure 5.13) and DNA sequencing, resulting in PCR8: PRMT4a cDNA and PCR8: PRMT4b cDNA entry vectors which were used later for Y2H.

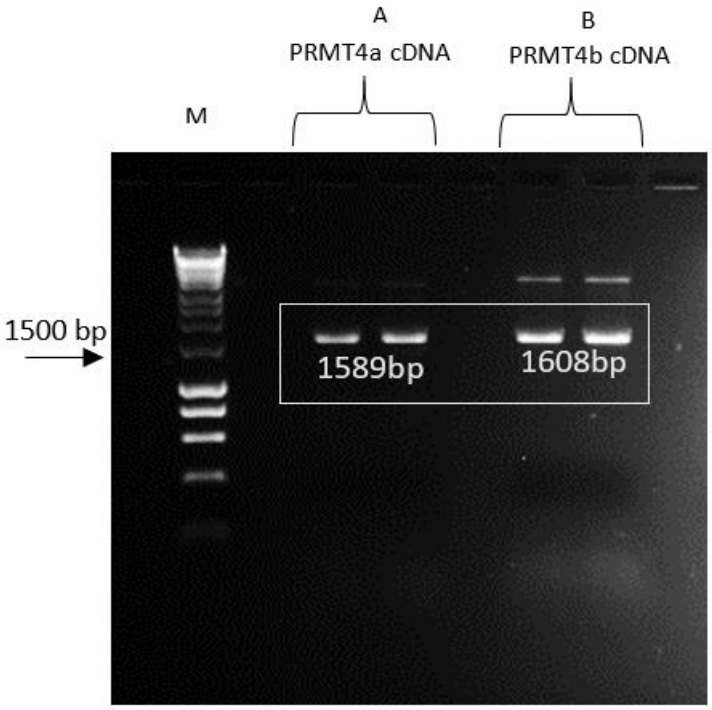

Figure 5.12: RT-PCR for PRMT4a and PRMT4b using *Arabidopsis* WT. A: PCR amplification of PRMT4a.cDNA used prmt4aFw-y2h+prmt4aRev-y2h. B: PCR amplification of PRMT4b.cDNA used prmt4bFw-y2h+ prmt4bRevy2h. The expected size of the bands were 1589bp and 1608bp respectively. PCR product were run on a 1 %(w/v) agarose gel, and HyperLadder 1Kb (Bioline) was used as a marker.

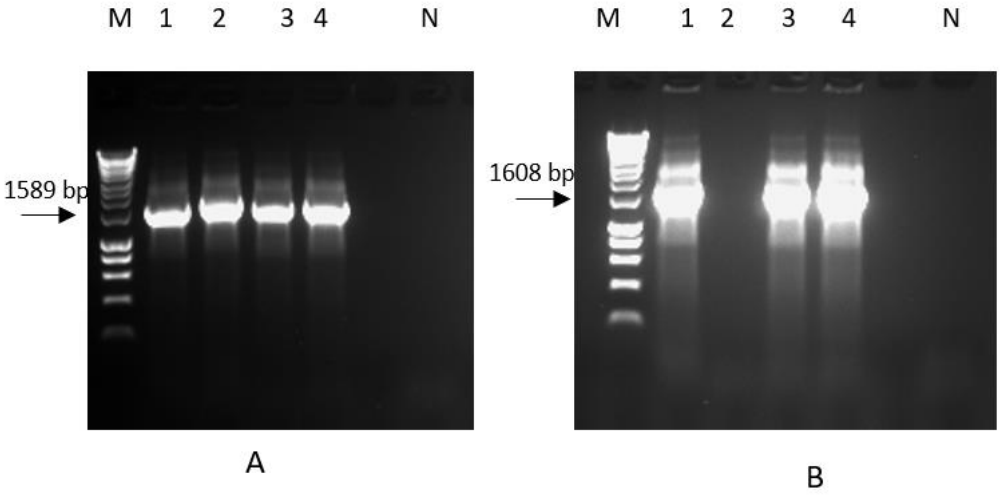

Figure 5.13: Colony PCR for *E. coli* TOP10 transformed with a ligation mixture of PCR8:PRMT4a cDNA using primers prmt4aFw-y2h+ prmt4aRev-y2h. Lanes 1–4, colonies tested. B: Colony PCR for *E. coli* Top 10 transformed with a ligation mixture of PCR8:PRMT4b cDNA using primers prmt4bFw-y2h+ prmt4bRev-y2h. Lanes 1–4, colonies tested. N, negative control using water as a Template. Arrows indicate the expected size of the bands at 1589bp and 1608bp respectively. PCR product were run on 1 %(w/v) agarose gel, and HyperLadder 1Kb (Bioline) was used as a marker.

5.4.4 Preparation of Bait and Prey constructs by LR Gateway cloning.

All entry vectors prepared in this chapter were cloned into both destination vectors pDEST32 (binding domain) as a bait and pDEST22 (activation domain) as a prey by using Gateway-based technology as described in section (2.13.1). All ligation mixtures were then transformed in to *E.coli* Top 10 cells , and then confirmed as positive colonies by PCR and sequencing. All colony PCR figures and construct maps are illustrated in Supplementary Data 5.6.1. Constructs generated in this chapter are summarised in Table 5.1.

Table 5.1: The summary of bait and prey constructs generated in this chapter.

Construct name	Construct description
pDEST 32: MTBcDNA-WTvar1	The entry vector of (PCR8-MTBcDNAvar1-WT) cloned into pDEST 32 Bait vector via LR Gateway cloning.
pDEST 32: MTBcDNA-WTvar2	The entry vector of (PCR8-MTBcDNAvar2-WT) cloned into pDEST 32 Bait vector via LR Gateway cloning.
pDEST 22: MTBcDNA-WTvar1	The entry vector of (PCR8-MTBcDNAvar1-WT) cloned into pDEST 22 Prey vector via LR Gateway cloning.
pDEST 22: MTBcDNA-WTvar2	The entry vector of (PCR8-MTBcDNAvar2-WT) cloned into pDEST 22 Prey vector via LR Gateway cloning.
pDEST 32: MTBcDNA-Arg.mut.var1	The entry vector of (PCR8-MTBcDNAvar1-Arg.mut) cloned into pDEST 32 Bait vector via LR Gateway cloning.
pDEST 32: MTBcDNA-Arg.mut.var2	The entry vector of (PCR8-MTBcDNAvar2-Arg-mut) cloned into pDEST 32 Bait vector via LR Gateway cloning.
pDEST 22: MTBcDNA-Arg.mut.var1	The entry vector of (PCR8-MTBcDNAvar1-Arg-mut) cloned into pDEST 22 Prey vector via LR Gateway cloning.
pDEST 22: MTBcDNA-Arg.mut.var2	The entry vector of (PCR8-MTBcDNAvar2-Arg-mut) cloned into pDEST 22 Prey vector via LR Gateway cloning.
pDEST 32: PRMT4a.cDNA	The entry vector of (PCR8-PRMT4a.cDNA) cloned into pDEST 32 Bait vector via LR Gateway cloning
pDEST 32: PRMT4b.cDNA	The entry vector of (PCR8-PRMT4b.cDNA) cloned into pDEST 32 Bait vector via LR Gateway cloning.
pDEST 22: PRMT4a.cDNA	The entry vector of (PCR8-PRMT4a.cDNA) cloned into pDEST 22 prey vector via LR Gateway cloning.
pDEST 22: PRMT4b.cDNA	The entry vector of (PCR8-PRMT4b.cDNA) cloned into pDEST 22 Prey vector via LR Gateway cloning.

5.4.5 Yeast two-hybrid analysis.

To investigate protein interactions between MTB and two Arginine methylation proteins (PRMT4a and PRMT4b), several pairwise interactions were examined by

using the yeast two-hybrid system (Y2H). All baits and preys to be tested are shown in Tables 5.2 and 5.3. These constructs were transformed into yeast cells MaV203 alongside the yeast control strains according to manufacturer's instructions (ProQuest™ Two-Hybrid System, Invitrogen). Protocols detailed in sections 5.3.3.2-5.3.3.5 of this Chapter. The yeast was first plated onto SC–Trp–Leu plates and then streaked on new plates of SC–Trp–Leu–His supplemented with four different concentrations of 3-Amino-1,2,4-Triazol (3AT) (10, 12.5, 15, and 20 mM) to balance basal expression of the *HIS3* reporter, and then incubated at 28 °C for three days to further validate positive interaction between the tested proteins. The constructs of the MTB gene as a full-length cDNA (splice variant 1) and a short one (variant 2) with and without 4 methylated Arginine sites were used. The Y2H results in Figures 5.14-5.15 showed that there is a weak interaction between both variants of MTB.WT with the two PRMT proteins, and this weak interaction is not capable of activating the URA3 and lacZ reporters. We also found that MTB.Arg.mut.var1 but not MTB.Arg.mut.var2 has also weak interaction with PRMT4a and PRMT4b. The interactions between MTB with PRMT4a and PRMT4b are summarised in Table 5.4.

Table 5.2: Baits and Preys to be tested using MTB splice variant 1 with PRMT4a and PRMT4b (9-16) alongside the yeast control strains 1-6 .17 were kindly provided by (Růžička et al.,2017) and used as positive interaction control.

LEU2 Plasmid	TRP1 Plasmid	Interaction
1-pEXP™32/Krev1	pEXP™22/RalGDS-wt	Strong positive interaction control
2-pEXP™32/Krev1	pEXP™22/RalGDS-m1	Weak positive interaction control
3-pEXP™32/Krev1	pEXP™22/RalGDS-m2	Negative interaction control
4-pDEST™32	pDEST™22	Test of self-activation
5-pDEST 32: MTBcDNA-WTvar1	pDEST 22 empty	Negative activation control; baseline
6-pDEST 32: MTBcDNA-Arg.mut.var1	pDEST 22 empty	Negative activation control; baseline
9-pDEST 32: MTBcDNA-WT.var1	pDEST 22: PRMT4a.cDNA	Baits and Preys to be tested
10-pDEST 32: MTBcDNA-WT.var1	pDEST 22: PRMT4b.cDNA	
11-pDEST 32: PRMT4a.cDNA	pDEST 22: MTBcDNA-WT.var1	
12-pDEST 32: PRMT4b.cDNA	pDEST 22: MTBcDNA-WT.var1	
13-pDEST 32: MTBcDNA-Arg.mut.var1	pDEST 22: PRMT4a.cDNA	
14-pDEST 32: MTBcDNA-Arg.mut.var1	pDEST 22: PRMT4b.cDNA	
15-pDEST 32: PRMT4a.cDNA	pDEST 22: MTBcDNA-Arg.mut.var1	
16-pDEST 32: PRMT4b.cDNA	pDEST 22: MTBcDNA-Arg.mut.var1	
17-MTB.32	MTB.22	Positive interaction control Růžička *et al.*,2017)

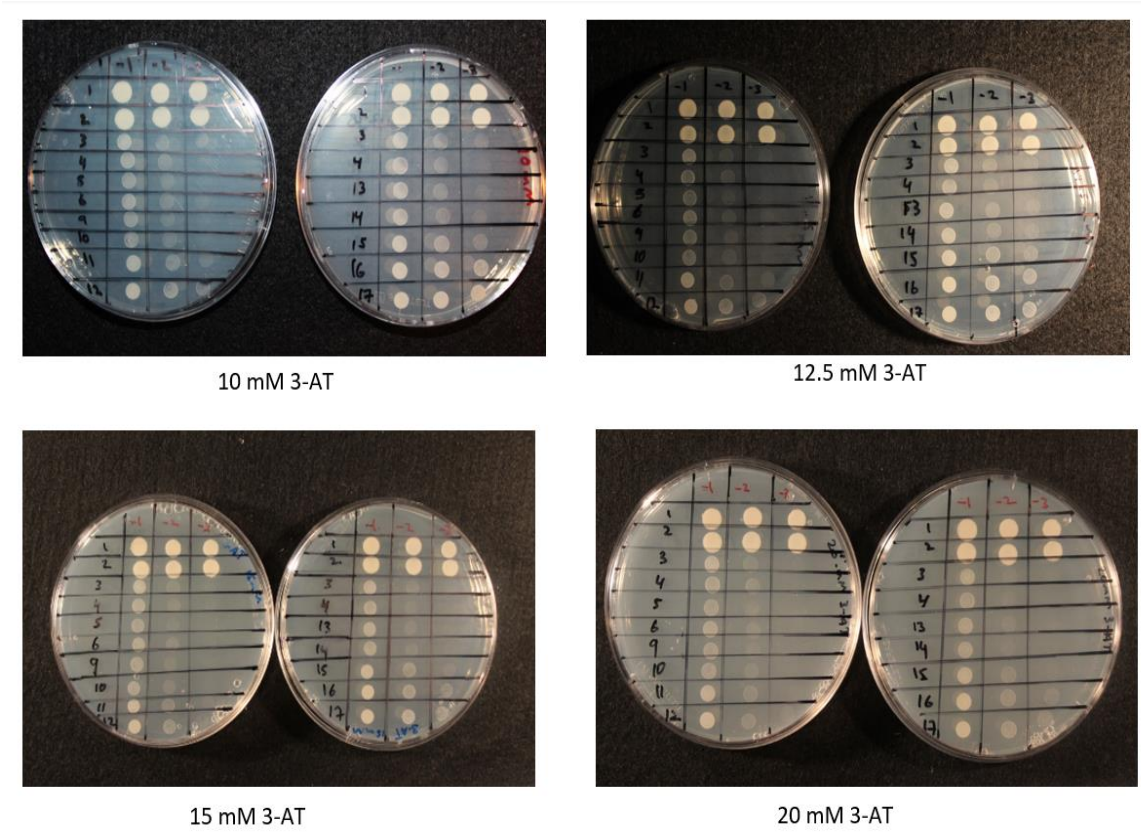

Figure 5.14: The Y2H result of MTB variant 1 in both cases (WT and mutant) with PRMT4a and PRMT4b. 1-6 the yeast control strains. 9-16 Baits and Preys to be tested using MTB splice variant 1 with PRMT4a and PRMT4b. 17 used as positive interaction control (Růžička et al.,2017). All tested partners are listed in Table 5.2. Selected medium is SC–Trp–Leu–His supplemented with four different concentration of 3-AT (10, 12.5, 15, and 20 mM).

Table 5.3: Baits and Preys to be tested using MTB splice variant 2 with PRMT4a and PRMT4b (5-12) alongside the yeast control strains 1-4 (Invitrogen).13-14 were kindly provided by (Růžička et al.,2017)and used as positive interaction controls.

LEU2 Plasmid	TRP1 Plasmid	Interaction
1-pEXP™32/Krev1	pEXP™22/RalGDS-wt	Strong positive interaction control
2-pEXP™32/Krev1	pEXP™22/RalGDS-m1	Weak positive interaction control
3-pEXP™32/Krev1	pEXP™22/RalGDS-m2	Negative interaction control
4-pDEST™32	pDEST™22	Test of self-activation
5-pDEST 32: MTBcDNA-WTvar2	pDEST 22: PRMT4a.cDNA	Baits and Preys to be tested
6-pDEST 32: MTBcDNA-WTvar2	pDEST 22: PRMT4b.cDNA	
7-pDEST 32: PRMT4a.cDNA	pDEST 22: MTBcDNA-WTvar2	
8-pDEST 32: PRMT4b.cDNA	pDEST 22: MTBcDNA-WTvar2	
9-pDEST 32: MTBcDNA-Arg.mut.var2	pDEST 22: PRMT4a.cDNA	
10-pDEST 32: MTBcDNA-Arg.mut.var2	pDEST 22: PRMT4b.cDNA	
11-pDEST 32: PRMT4a.cDNA	pDEST 22: MTBcDNA-Arg.mut.var2	
12-pDEST 32: PRMT4b.cDNA	pDEST 22: MTBcDNA-Arg.mut.var2	
13- MTB.32	HAKAI.22	Positive interaction control (Růžička *et al.*,2017)
14-MTB.32	MTB.22	Positive interaction control Růžička *et al.*,2017)

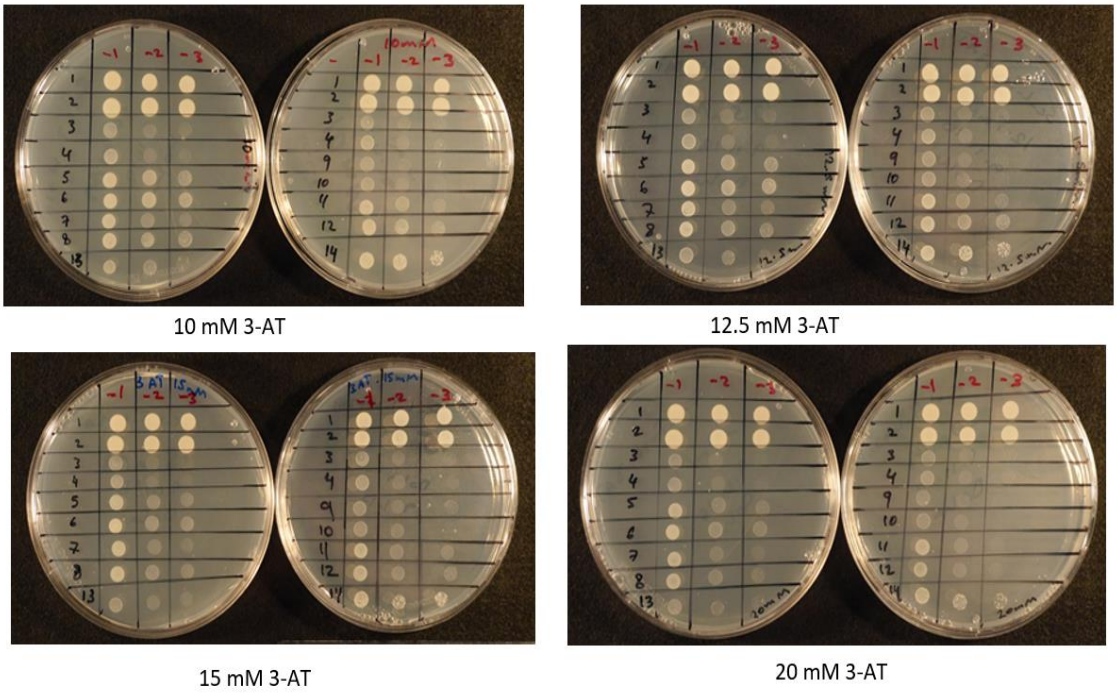

Figure 5.15: The Y2H result of MTB variant 2 in both cases (WT and mutant) with PRMT4a and PRMT4b. 1-4 the yeast control strains (Invitrogen).5-12 Baits and Preys to be tested using MTB splice variant 2 with PRMT4a and PRMT4b. 13-14 used as positive interaction controls (Růžička et al.,2017). All tested partners were listed in Table 5.3. Selected medium is SC–Trp–Leu–His supplemented with four different concentration of 3AT (10, 12.5, 15, and 20 mM).

Table 5.4: The summary of all interactions between MTB with PRMT4a and PRMT4b. (-) No interaction. (+) weak interaction. The grey areas indicated to not tested plasmids.

Prey pDEST 22 / Bait pDEST 32	MTB-WTvar1.22	MTB-WTvar2.22	MTB-Arg.mut.var1.22	MTB-Arg.mut.var2.22	PRMT4a.22	PRMT4b.22
MTB-WTvar1.32					-	-
MTB-WTvar2.32					+	+
MTB-Arg.mut.var1.32					+	+
MTB-Arg.mut.var2.32					-	-
PRMT4a.32	+	+	+	-		
PRMT4b.32	+	+	+	-		

5.4.6 TLC Detection of m^{6}A in *prmt4a/b* double mutant.

Three biological replicates of m^{6}A measurement via two-dimensional TLC analysis using seedlings from 2-week old double mutants *prmt4a/b* and WT revealed that there were no significant differences of m^{6}A levels between WT and *prmt4a/b* double mutant (Figures 5.16 and 5.17).

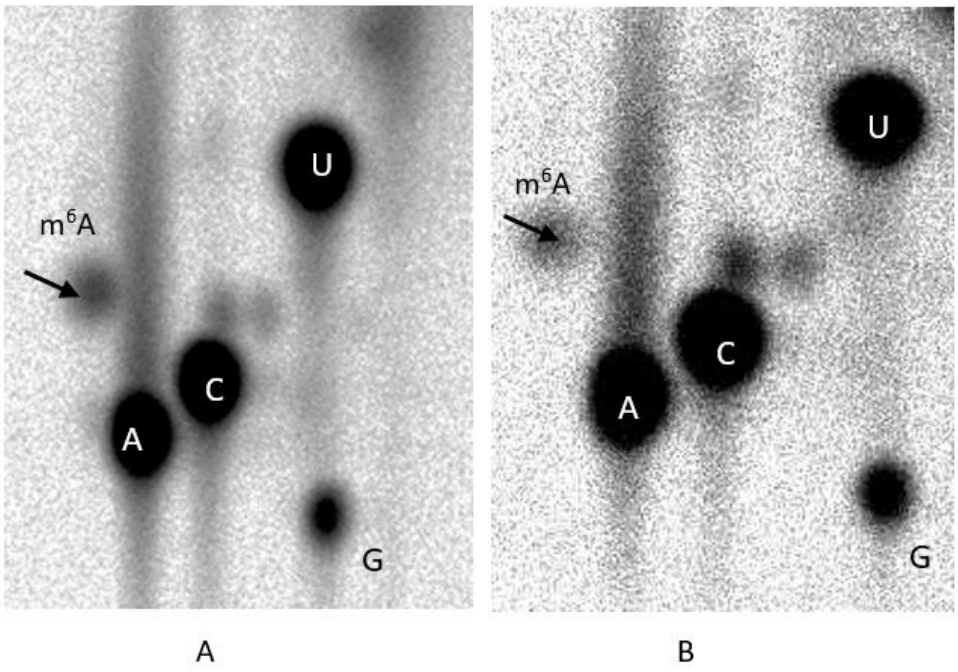

Figure 5.16: Two-dimensional TLC analysis of m^{6}A level. (A) WT. (B) *prmt4a/b* double mutant. Arrows indicated to m^{6}A spots.

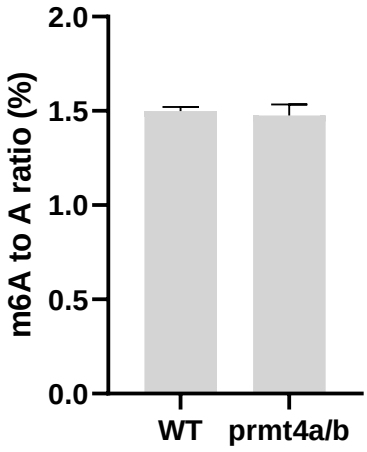

Figure 5.17: m^{6}A Levels of *prmt4a/b* double mutant checked by the TLC method. Level of m^{6}A in double mutant is similar to WT. Bars represent SD of three biological replicates.

5.4.7 Crossing MTB-GFP with the *prmt4a/b* double mutant and genotyping analysis

Based on the proteomics results, we hypothesized that the 4 sites of Arg methylation in MTB might influence its localization. Hence, we crossed MTB-GFP with *prmt4a/b* double mutant to check: 1) If MTB is a substrate for methylation by PRMT4a/b, and then if the stability or subcellular localisation may change in the absence of arginine methylation. 2) MTB-GFP (should be possible) to isolate using the GFP tag and this can then be checked with an antibody against methyl arginine to i) confirm that MTB is arginine methylated in a WT background and ii) to demonstrate that this arginine methylation is lost in the *prmt4a/b* double mutant. The *prmt4a/b* double mutant were constructed by crossing between the simple mutants *atprmt4a-2* (SALK_033423), *atprmt4b-1* (SALK_097442) and were kindly provided by (Simpson group). The locations of T-DNA insertion lines and primer pairs used for genotyping analysis are shown in (Figure 5.18). In the F1 generation, the presence of the MTB-GFP construct was verified by PCR using the primers MTB.FW.1 + GFP REV (Figure 5.19) , while progenies heterozygous for double mutant *atprmt4a* (SALK_033423) and *atprmt4b* (SALK_097442), T-DNA insertions were confirmed by two genotyping PCRs for each insertion to identify double mutant plants for *prmt4a/b* (Figures 5-20, 5.21).

A

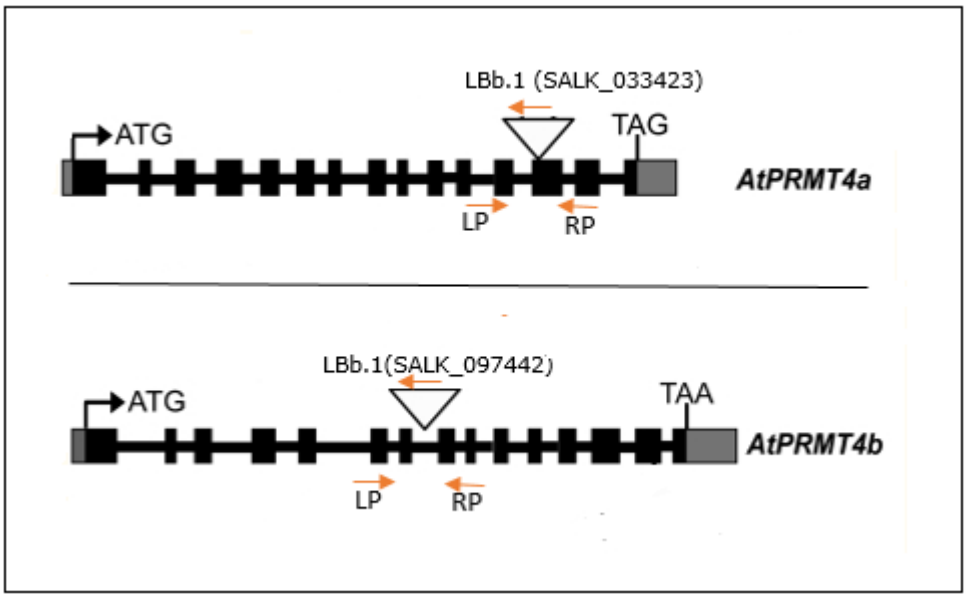

B

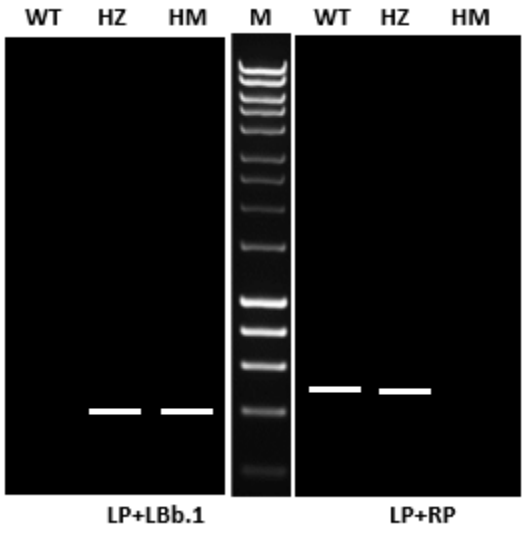

Figure 5.18: (A) Schematic diagram showing the positions of T-DNA insertions in AtPRMT4a and AtPRMT4b genes, arrows indicate primers that used (adapted from Niu et al., 2008). (B) Amplification products example expected for presence/absence of the insertions. (LP) represent left primer on the prmt4a or prmt4b, (RP) represent right primer on the prmt4a or prmt4b. (LBb.1) is the left border for T-DNA insertions atprmt4a (SALK_033423) and atprmt4b (SALK_097442). WT= wild type. HZ = Heterozygous. HM = Homozygous. M = HyperLadder 1Kb (Bioline).

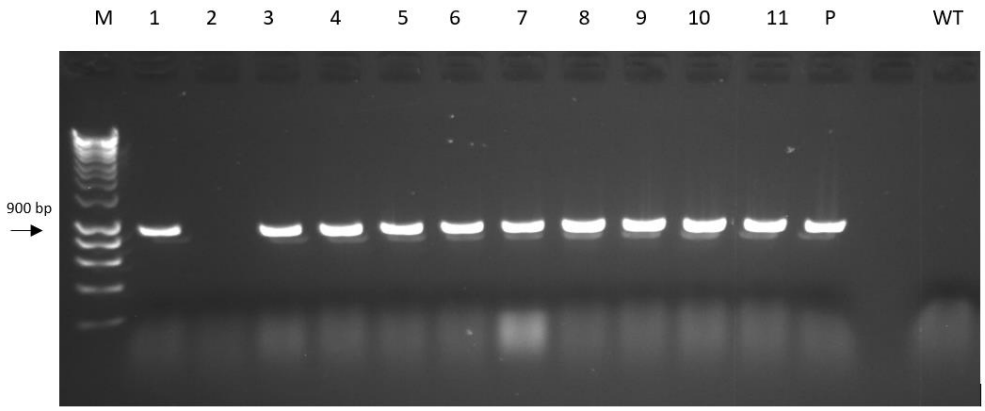

Figure 5.19: PCR to check the presence of MTB-GFP in F1 progenies of MTB-GFP crossed with *prmt4a/b* double mutant. All lines showed positive bands at the expected size except line 2. P=positive control using confirmed positive plant for MTBΔSAM as a template. WT= wild type DNA using as negative control.

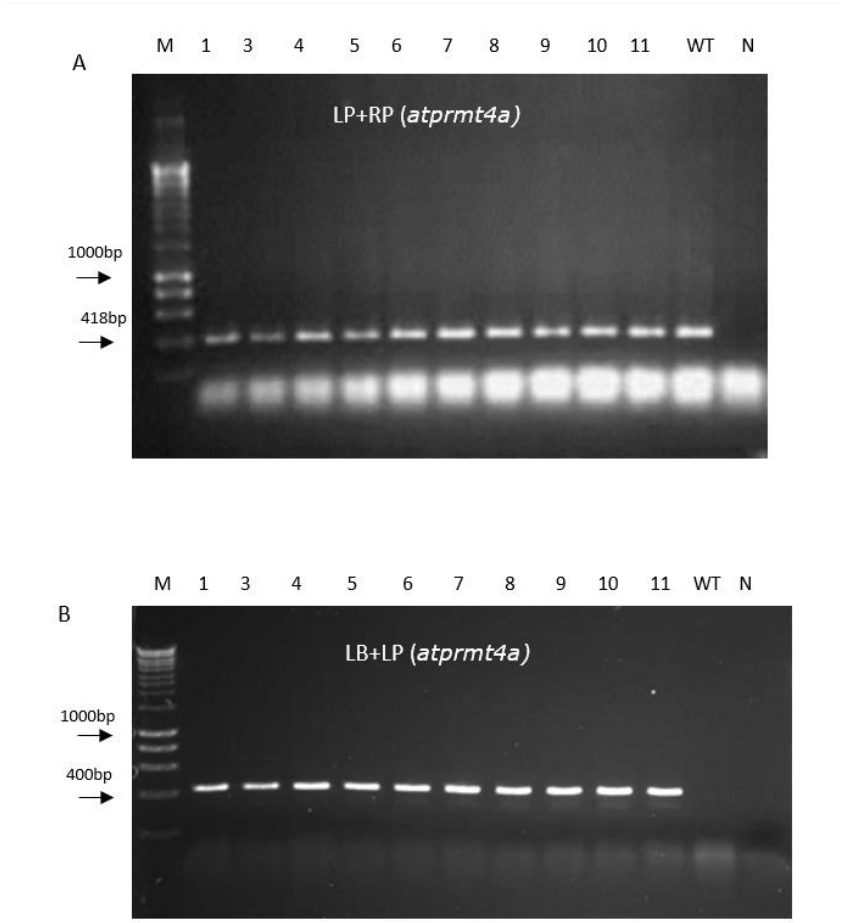

Figure 5.20: Genotyping PCRs to confirm the presence of atprmt4a (SALK_033423) T-DNA insertion in F1 progenies of MTB-GFP crossed with *prmt4a/b* line. (A) PCR1 using RP+LP (PRMT4a.2-fwd+PRMT4a.2-rev) primers to confirm WT band. (B) PCR2 using LBb.1+LP (LBb.1+PRMT4a.2 fwd) primers to distinguish heterozygous lines. WT = wild type. N= negative control using water as a template. Lines 1, 3, 4, 5, 6, 7, 8, 9, 10 and 11 represent 10 individual F1heterozygous plants.

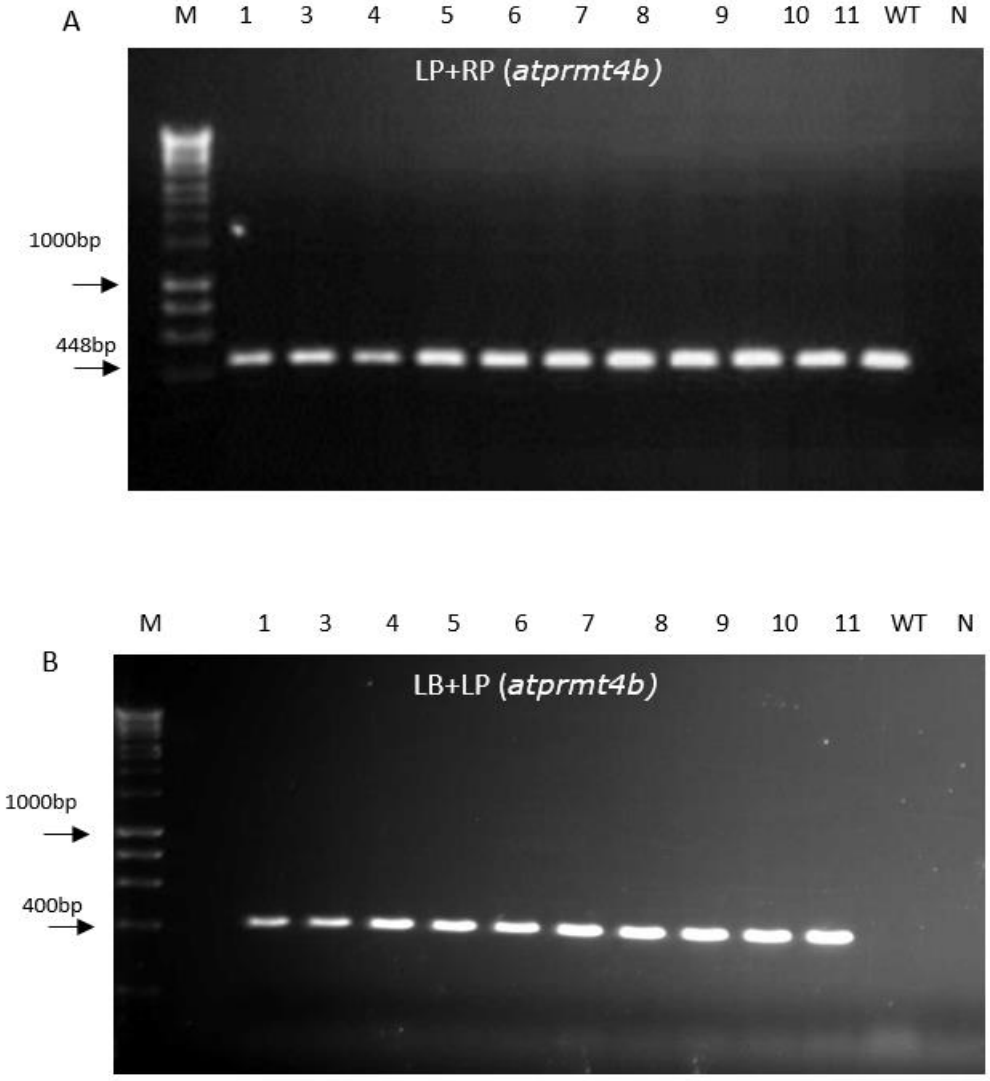

Figure 5.21: Genotyping PCRs to confirm the presence of atprmt4b (SALK_097442) T-DNA insertion in F1 progenies of MTB-GFP crossed with *prmt4a/b* line. (A) PCR1 using RP+LP (PRMT4b.1-fwd+PRMT4b.1-rev) primers to confirm WT band. (B) PCR2 using LBb.1+LP (LBb.1+PRMT4b.1 fwd) primers. WT = wild type. N= negative control using water as a template. Lines 1, 3, 4, 5, 6, 7, 8, 9, 10 and 11 represent 10 individual F1heterozygous plants.

The seeds from F1 were harvested, then planted on ½ MS to generate F2. Sixty-four plants that showed GFP under the Stereo Fluorescence Microscope (Leica) were transferred to compost and allowed to germinate. Among 64 plants of F2 progenies which were checked by PCR using the previous primers used in F1 for double mutants and MTB-FW2+ GFP-REV primers to confirm the presence of MTB-GFP, only one

line (18) showed double mutant for *prmt4a/b* and contained MTB-GFP construct at the same time (Figures 5.22 – 5.26).

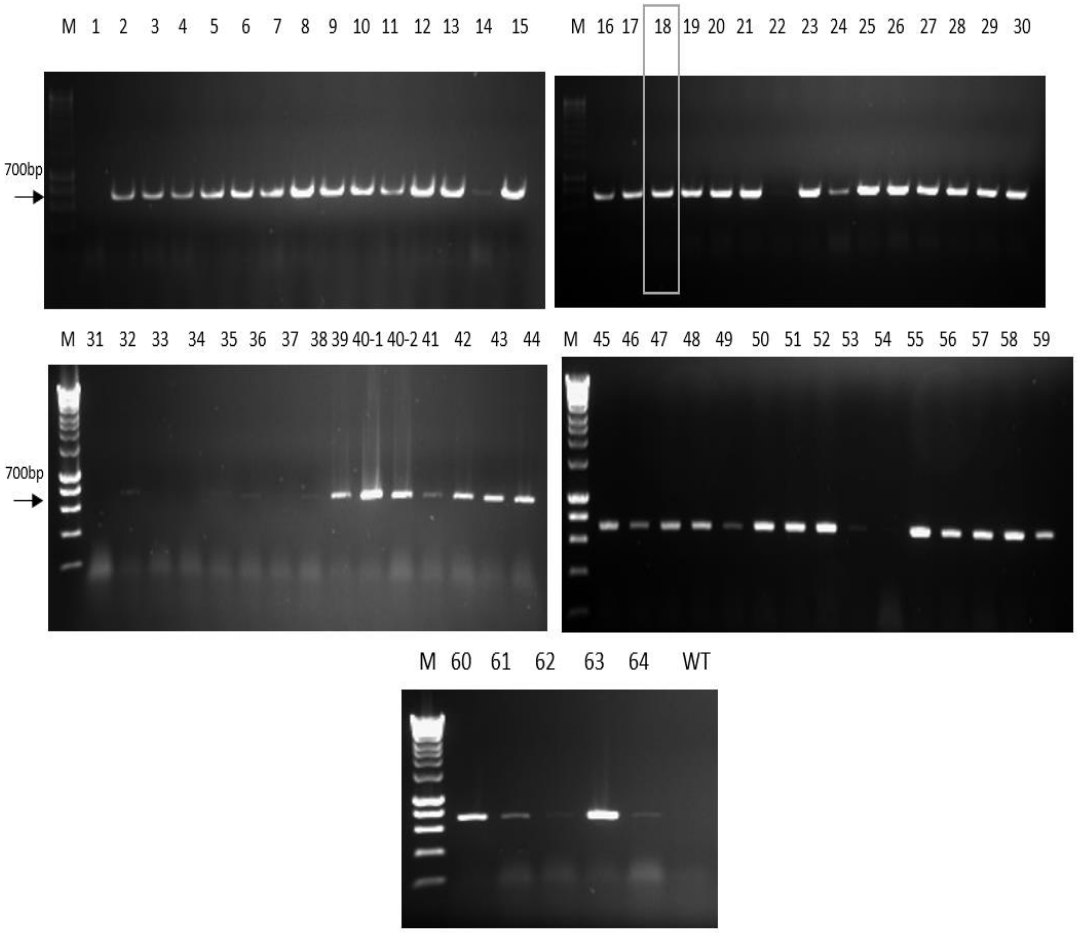

Figure 5.22: PCR to check the presence of MTB-GFP in F2 progenies of MTB-GFP crossed with *prmt4a/b* double mutant line. Grey box indicates to line 18.

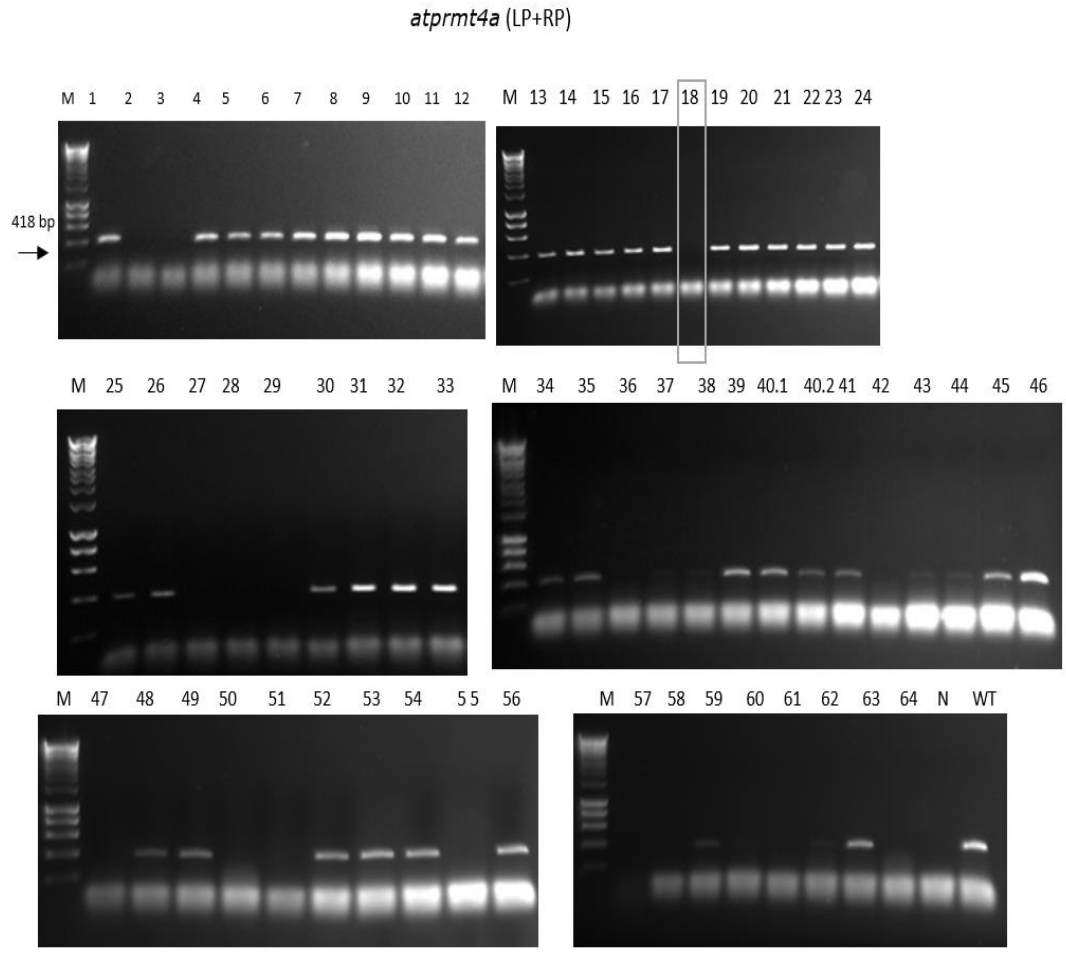

Figure 5.23: Genotyping PCR to check the presence/absence of the atprmt4a (SALK_033423) T-DNA insertion in F2 progenies of MTB-GFP crossed with *prmt4a/b* double mutant line using RP+LP (PRMT4A.2-FWD+PRMT4A.2-REV) primers. Grey box indicates to line 18.

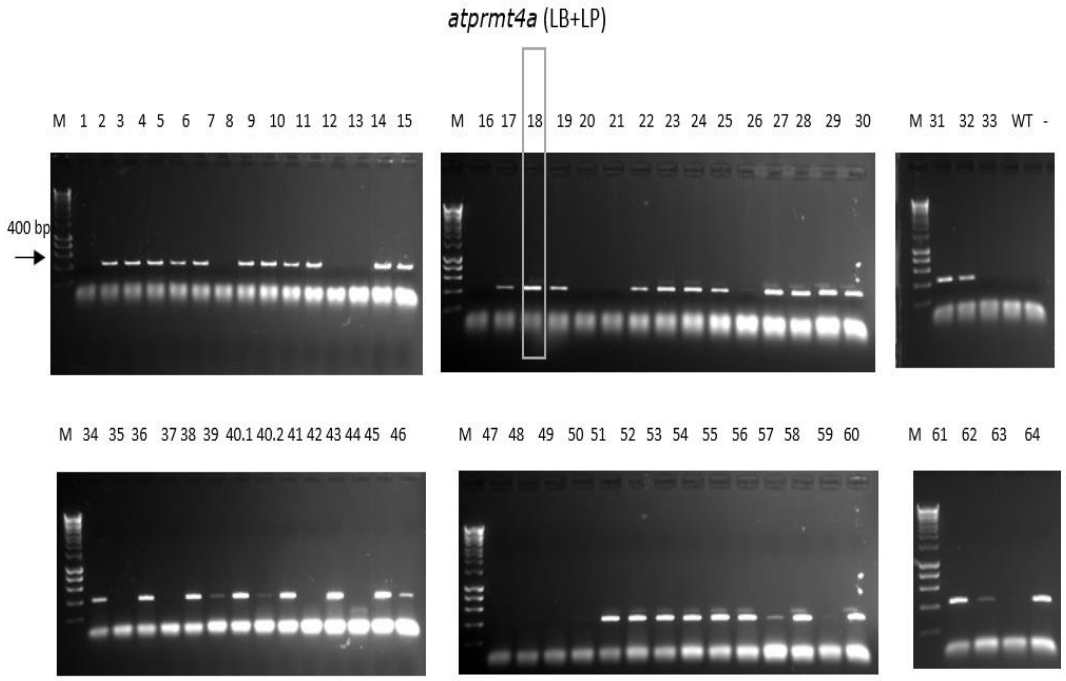

Figure 5.24: Genotyping PCR to check the presence/absence of the atprmt4a (SALK_033423) T-DNA insertion in F2 progenies of MTB-GFP crossed with *prmt4a/b* double mutant line using LBb.1+LP (LBb.1+PRMT4a.2- fwd) primers. Grey box indicates to line 18.

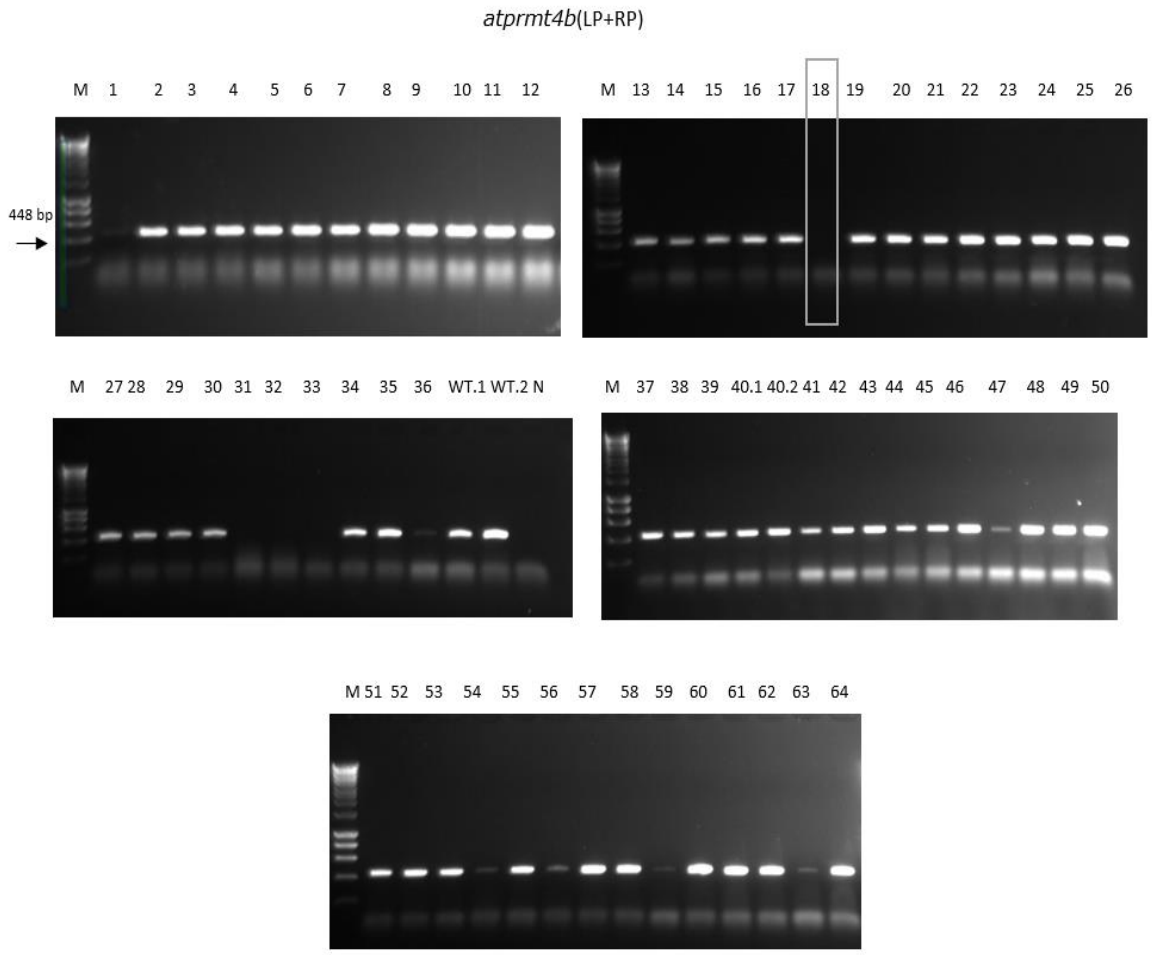

Figure 5.25: Genotyping PCR to check the presence/absence of the atprmt4b (SALK_097442) T-DNA insertion in F2 progenies of MTB-GFP crossed with *prmt4a/b* double mutant line using RP+LP (PRMT4b.1-fwd+PRMT4b.1-rev) primers. Grey box indicates to line 18.

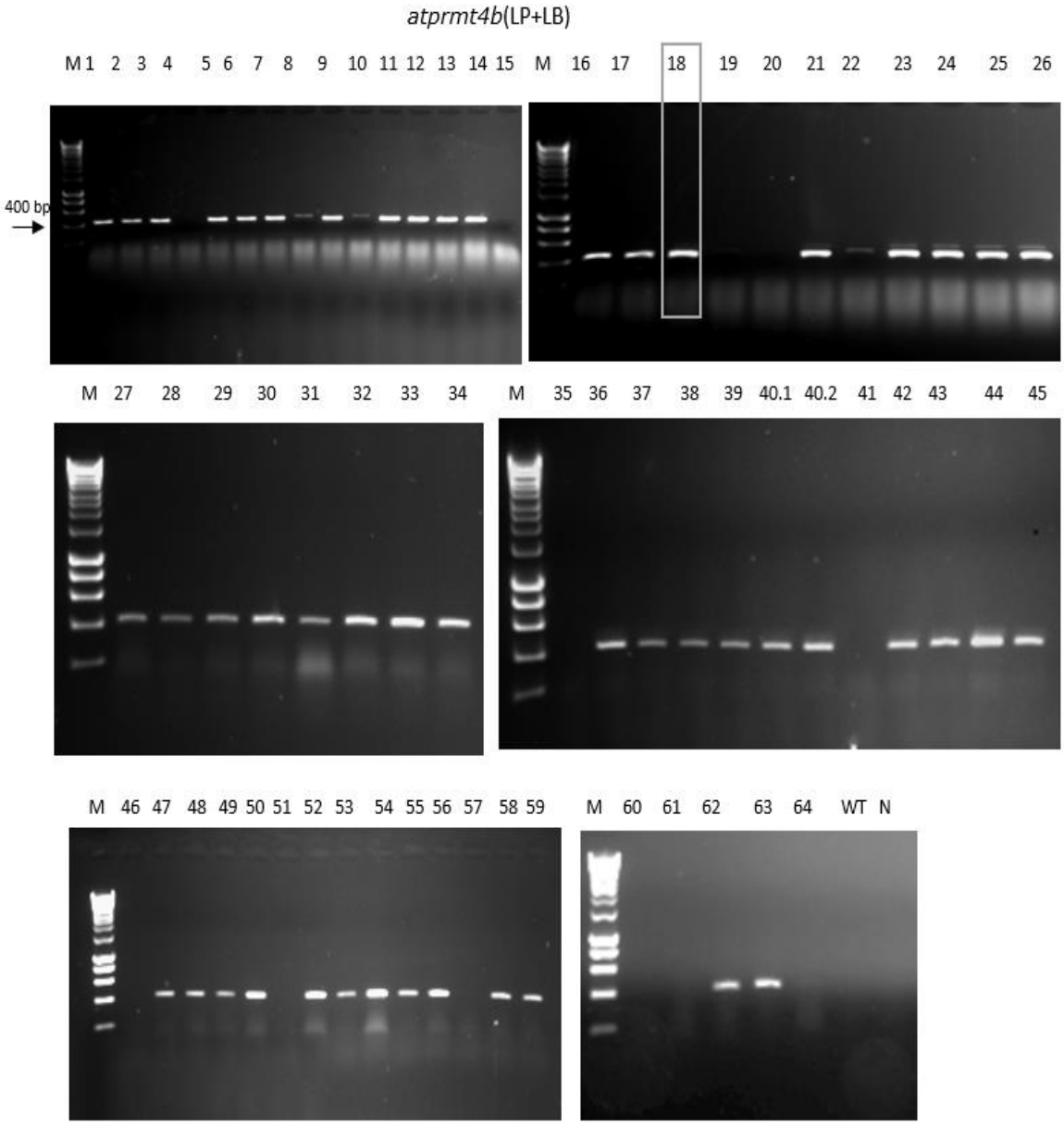

Figure 5.26: Genotyping PCR to check the presence/absence of the atprmt4b (SALK_097442) T-DNA insertion in F2 progenies of MTB-GFP crossed with *prmt4a/b* double mutant line using LBb.1+LP (LBb.1+PRMT4b-fwd) primers. Grey box indicates to line 18.

5.4.8 Localisation of GFP-tagged proteins in MTB-GFP and line 18.

Confocal microscopy analysis of 5-d old seedlings of MTB-GFP and line 18 (MTB-GFP x *prmt4 a/b*) showed that there is no difference between them and they were primarily expressed in the nuclei of cells in the primary root tip (Figure 5.27)

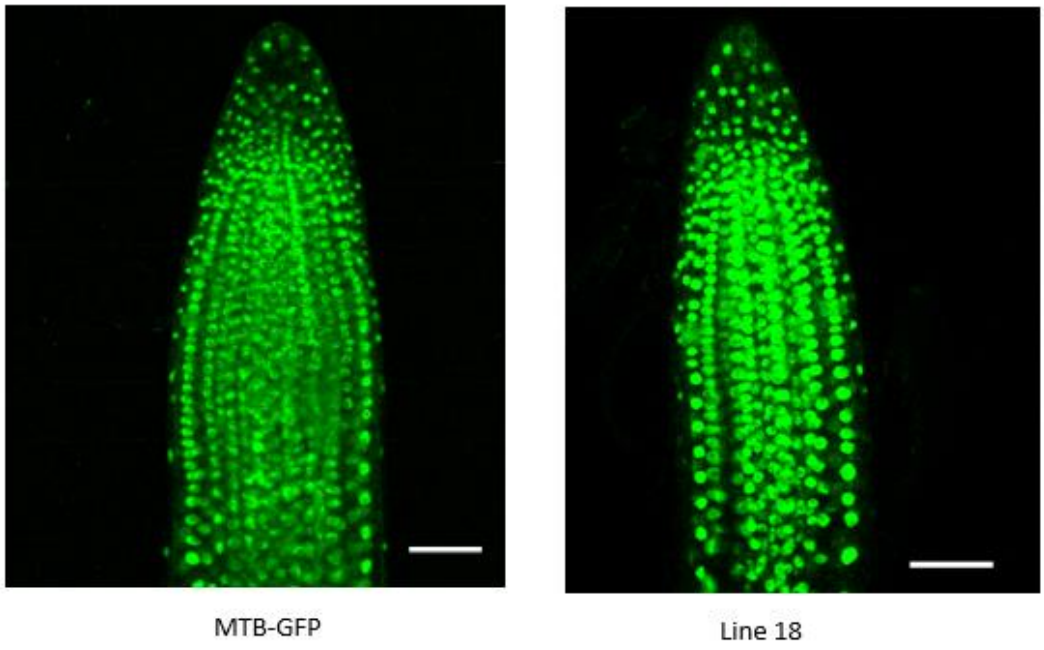

Figure 5.27: Confocal microscopy analysis showed GFP localisations of MTB-GFP and line 18. Scale bar = 50 µm

5.4.9 Western Blot analysis

Several attempts of Western blot have been made in order to confirm that MTB is arginine methylated in WT and to demonstrate that this arginine methylation is lost in the *prmt4a/b* double mutant. We assumed that it should be possible to isolate the MTB-GFP by antibody/GFP-Trap and that this could then be subjected to western blotting using an anti-ADMA antibody.

5.4.9.1 Immunoprecipitation via GFP-trap agarose beads

The proteins from WT, MTB-GFP and line 18 were extracted as described in section 5.3.2.2 followed by using GFP-Trap agarose beads (ChromoTek) to pull-down these GFP-fusion proteins detailed in section 5.3.2.4. These pull-down proteins were analysed by Western blotting with anti-GFP first and the line 18 checked with anti-methyl arginine antibody. In the western blot technique, a mixture of proteins is separated through gel electrophoresis based on the proteins molecular weight. The proteins are then transferred to a membrane to produce a band for each protein. Then, the membrane is incubated with protein-specific antibodies then with a labelled secondary antibody. Using these antibodies, no bands were observed. Thus, the western blot was repeated by using the previous antibody directed against GFP, but without using GFP-Trap, also MTA-GFP protein was used as control to check the specificity of the GFP antibody. In addition, line 18 was checked by western blot using anti-methyl arginine. Similar to previous results, the GFP antibody also did not detect the MTB-GFP, which should be at 133 KD, while a clear band was observed at the correct size for MTA-GFP at 103 KD (Figure 5.28). Moreover, unspecific bands were obtained by using anti-methyl arginine, which are probably due to the other methylases which may be modifying the histones.

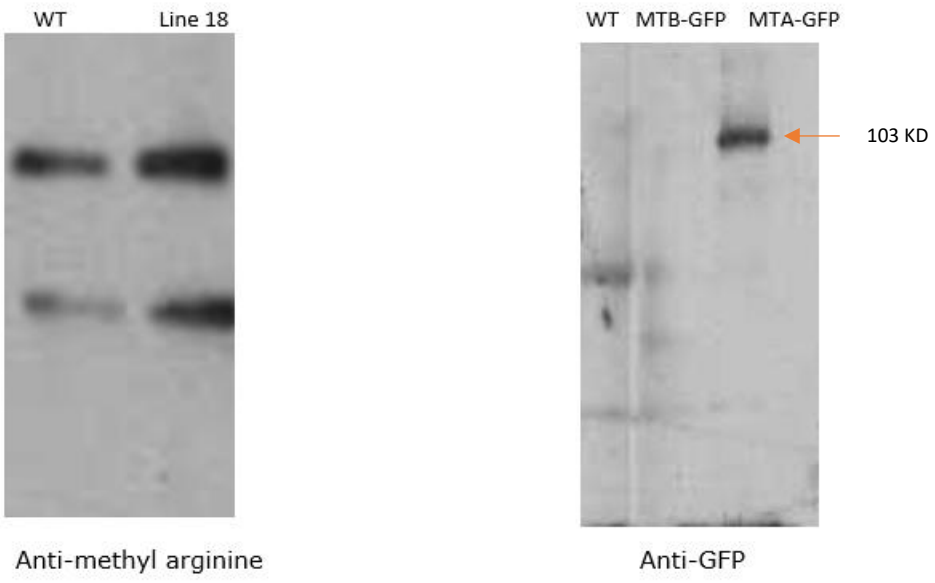

Figure 5.28: Western blotting to check GFP-tagged protein level for two-week-old *Arabidopsis* seedlings using antibodies against GFP and methyl arginine. By using Anti-GFP, no band of MTB-GFP was observed, which should be at 133 KD, while a clear band was observed at the correct size for MTA-GFP at 103 KD (right panel). Unspecific bands were obtained by using anti-methyl arginine, which are probably due to the other methylases which may be modifying the histones (left panel)..

5.4.9.2 Western blot after Lateral Root Induction by Auxin treatments

Because the MTB-GFP protein was not detected by western blot, we treated the roots with NPA and NAA as detailed in section 5.3.2.5. This system allows us to collect root samples enriched with MTB-GFP by growing quick, synchronous and extensive lateral roots (MTB is particularly abundant in such tissues). After treatment with NPA and NAA, LRs were clearly seen along the whole primary root of WT on the 5th day of NAA treatment. In addition, GFP expression analysis of MTB-GFP and line 18 treated with NPA and NAA showed that MTB-GFP was strongly expressed during the whole LR induction process, primarily in root tips, and showed no difference between them (Figures 5.29-5.31).

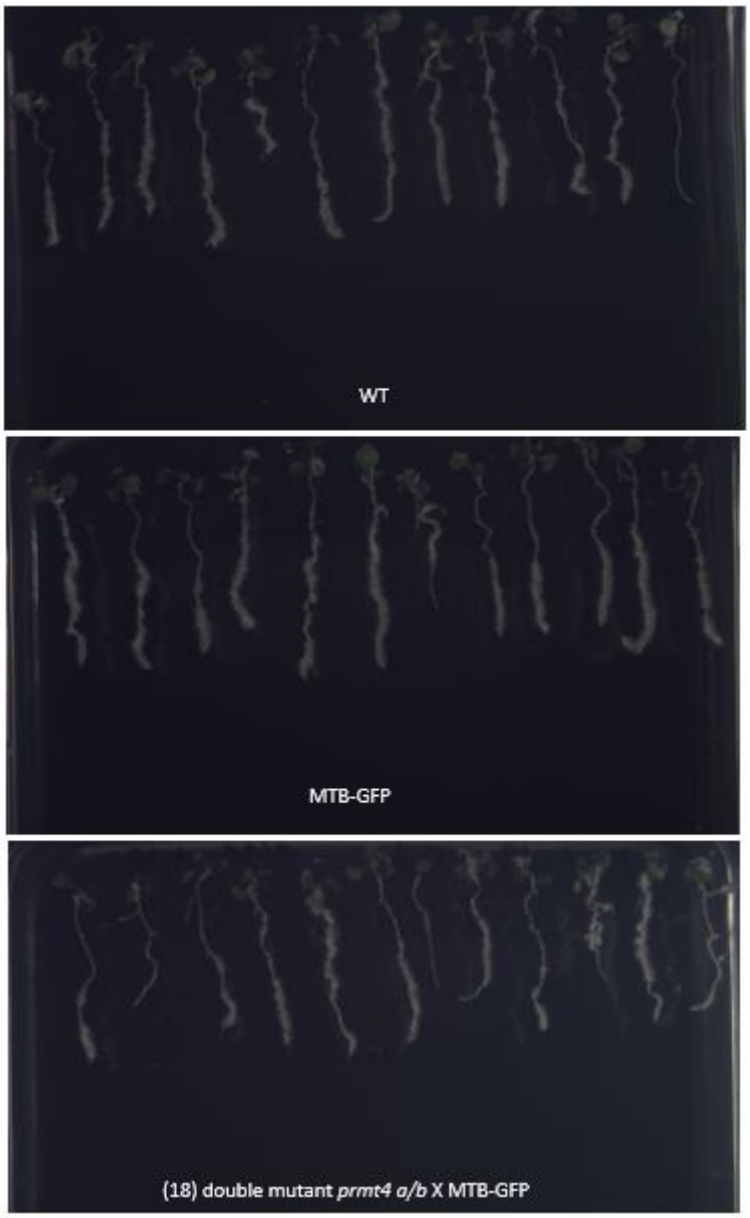

Figure 5.29: Roots after treatment with NPA and then transferred onto 1/2 MS with NAA for 5 days.

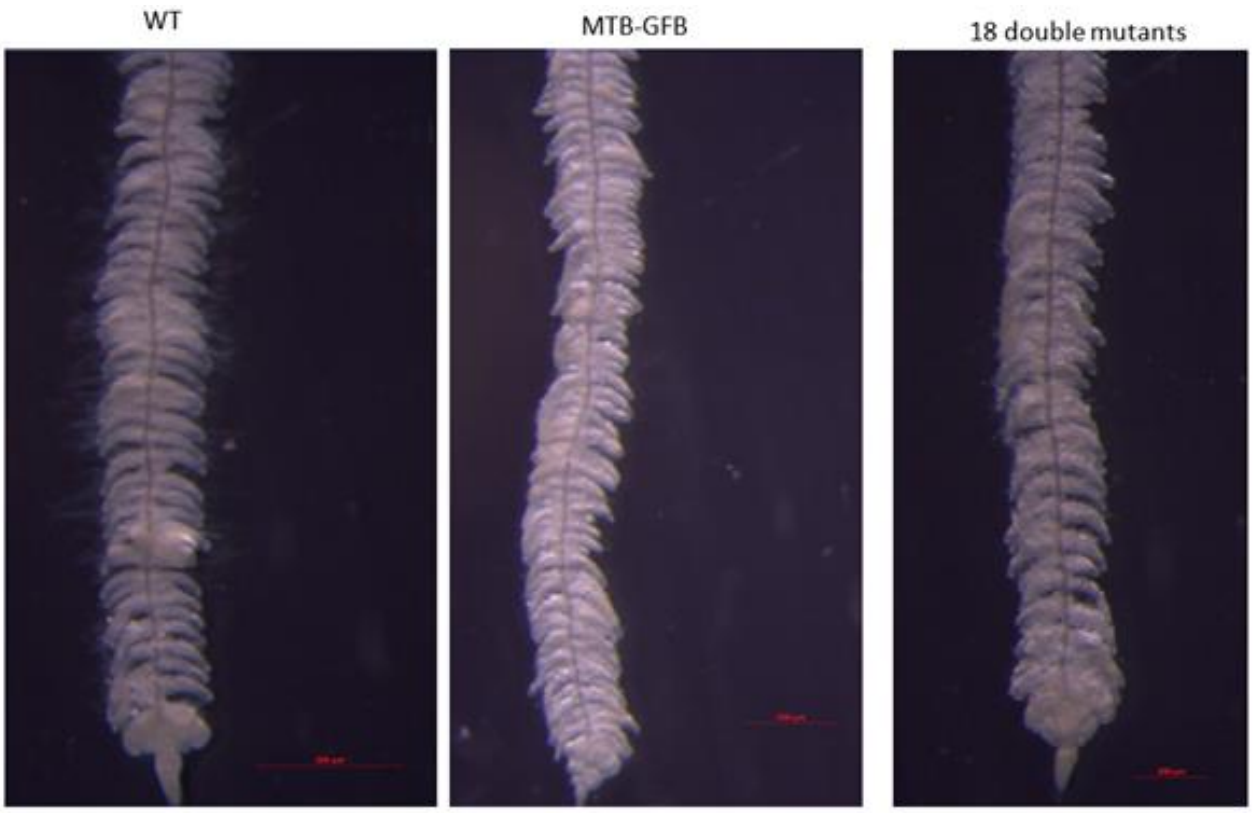

Figure 5.30: **Roots under the Stereo Dissecting Microscope after treatment with NPA and then transferred onto 1/2 MS with NAA for 5 days. Scale bar = 500 µm.**

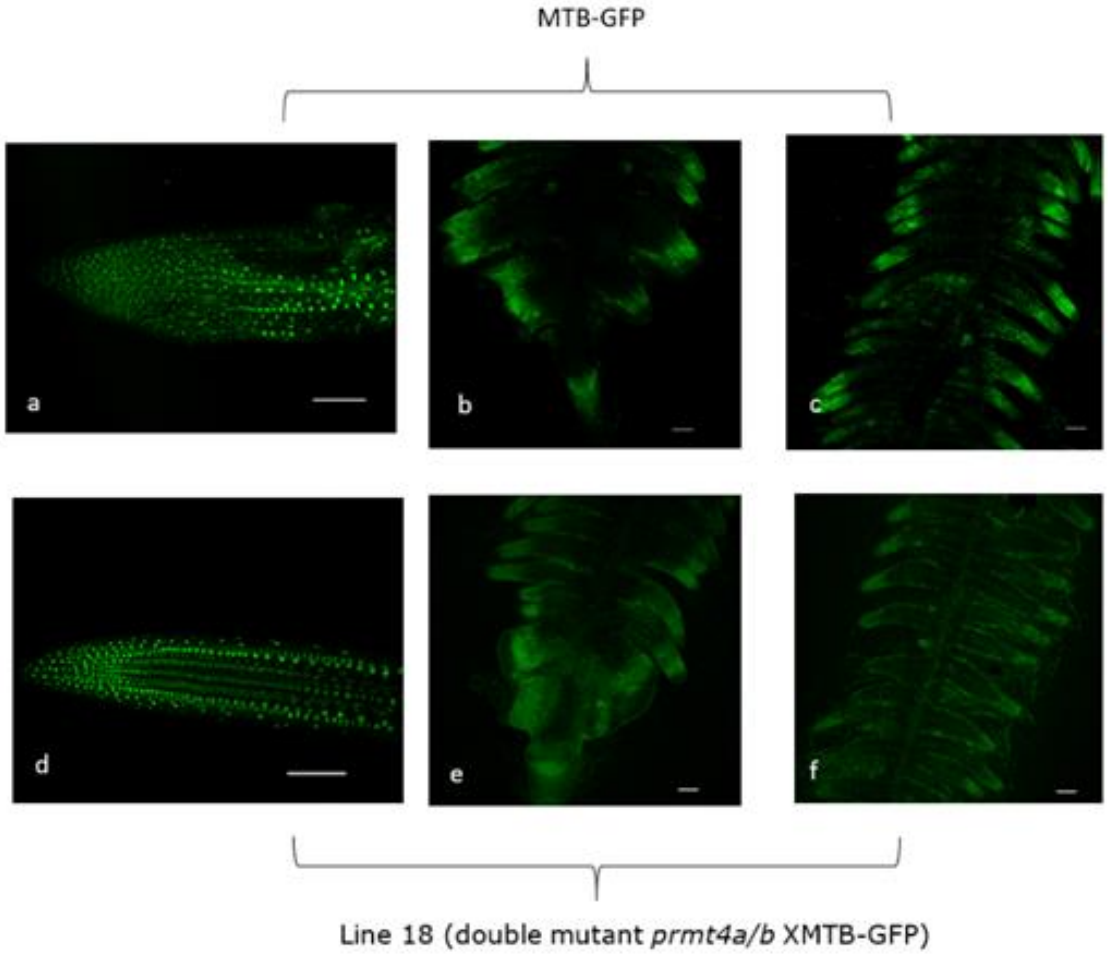

Figure 5.31: MTB-GFP and line 18 double mutant *prmt4a/b* X MTB-GFP roots under the confocal microscope after treatment with NPA and NAA. (a & d) The primary root tip without treatments. (b & e) The primary root tip induced by NAA for 5 d. (c & f) The elongation zone of the primary root induced by NAA for 5 d. Scale bar = 100µm.

The proteins then were extracted from treated roots as detailed in section 5.3.2.2 and used in western blot only with anti-GFP antibody. As shown in (Figure 5.32) the MTB-GFP protein also failed to be recognized by the antibody, or the MTB-GFP protein was absent.

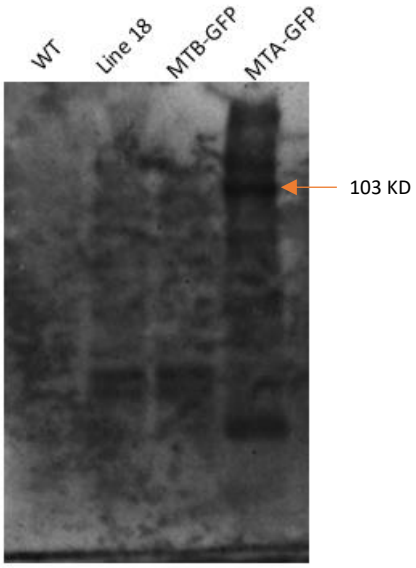

Figure 5.32: Western blotting to check GFP-tagged protein level for two-week-old *Arabidopsis* roots after treatment with NPA and NAA.

5.4.9.3 Western blot after Formaldehyde Crosslinking

Another attempt to detect the MTB-GFP by western blot was performed after using formaldehyde for crosslinking as described in section 5.3.2.6. This may help to stabilize the proteins, allowing them to be captured and analysed by western blot. As illustrated in Figure 5.33, only MTA-GFP bands were obtained by western blot.

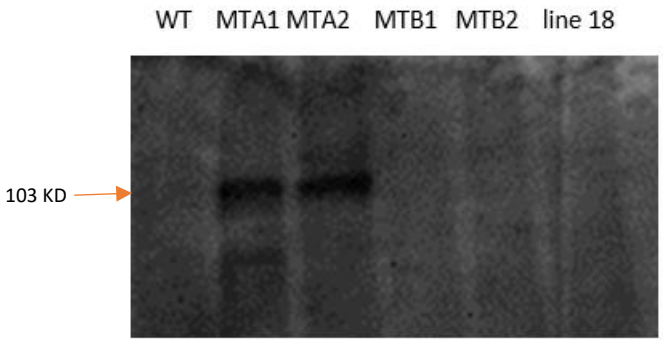

Figure 5.33: Western blotting to check GFP-tagged protein level for two-week-old *Arabidopsis* seedlings after Formaldehyde Crosslinking.

5.4.9.4 Western blot after protein preparation by Urea

As seen above and after several attempts to isolate the MTB -GFP, the detection of GFP was extremely difficult in this line. Thus, a different method for protein extraction by using 8M Urea as described in section 5.3.2.3 was tried. Urea can lead to disruption of the internal bonds in the proteins. This property can be used to improve the solubility of certain proteins. By using this method, the detection of MTB-GFP was successfully obtained (Figure 5.34).

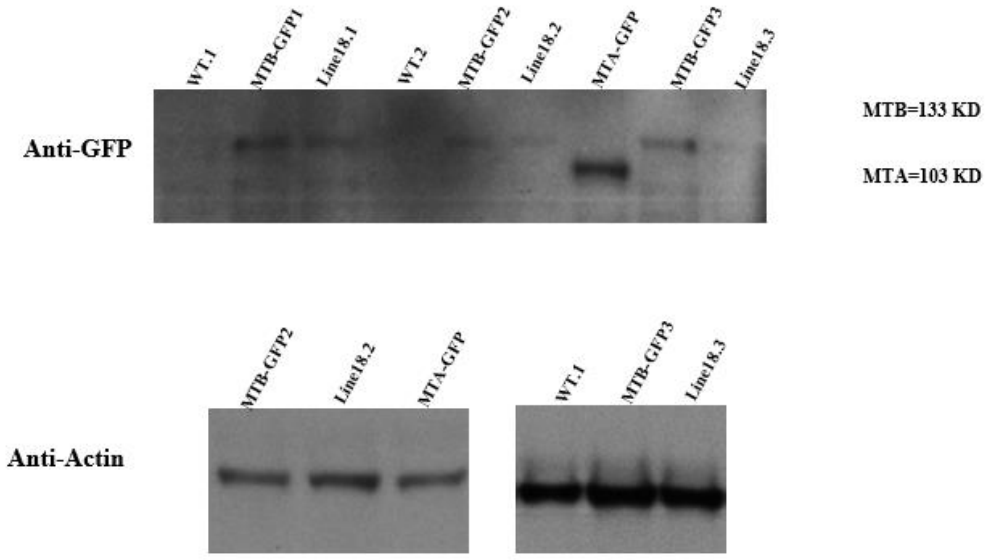

Figure 5.34:Western blotting to check GFP-tagged protein level for 17-day-old Arabidopsis seedlings for MTB.GFP and Line 18 (MTB-GFP X prmt4a/b double mutants).

5.4.10 Generation of CaMV 35S: MTB.Arg.mut construct and transfer to *MTB* mutant Plants

This construct was prepared using the entry vector (PCR8;MTB.Arg.mut) to transfer the MTB-Arg cassette into the plant binary destination vector pGKPGWG (contain CaMV35s promoter) via an LR clonase (Invitrogen) reaction as detailed in section 2.13.1. All cloning figures and maps are shown in the Supplementary Data 5.6.2. Subsequently, the construct was transformed to mutant plants MTB T-DNA insertion (GK_332G03) line and WT to study the phenotype and see: 1) if complementation is possible with this construct and 2) if the complemented mutant has the same phenotype for *prmt4a/b* double mutant (delayed flowering). The seeds were collected from dipped plants but due to time limitations, we could not finish this experiment during the PhD thesis period.

5.5 Discussion

Protein methylation is an important and widespread post-translational modification (PTM) which affects almost all basic cellular processes in eukaryotes by transferring a variable number of methyl groups to Lysine and Arginine residues within proteins. Lys and Arg can be methylated multiple times by adding one to three methyl groups in case of Lysine resulting in mono-, di- or tri-methyl lysine, and one to two methyl groups in case of Arginine resulting in mono- or di- methylarginine. Histone tails are greatly modified by methylation of lysine and arginine. These modifications are involved in chromatin remodelling and transcriptional regulation (Kouzarides 2007; Taverna et al., 2007). On histone H3, lysine methylation takes place at lysines 4, 9, 14, 27, 36 and 79 and occurs in lysines 20 and 59 on histone H4 (Lee et al., 2005; Zhang et al., 2002). Each residue can receive from one to three methyl groups to form mono-, di-, and trimethylated Lys (Paik et al., 2007). Histone H3 trimethylation at Lys36 (H3K36me3) is known to be enriched at the 3′-end of genes and interacts with RNA pol II, contributing to transcription elongation (Mas et al., 2011). Interestingly, a recent study has been shown that in the proximity of H3K36me3 peaks, the m^6A modifications are enriched, while when the cellular H3K36me3 is depleted, the m^6A modifications are decreased significantly (Huang et al., 2019). Furthermore, they found a positive association of histone methyltransferase SET domain containing 2 (SETD2) with m^6A metheltransferase genes (METTL3, METTL14 and WTAP) in mRNA expression. SETD2 is responsible for conversion of H3K36me2 to H3K36me3 (Sun et al.,2005). They clearly showed that the H3K36me3 is directly recognized and read by METTL14, an essential component of the m^6A methyltransferase complex and (a mammalian homologue of MTB), which assists the m^6A methyltransferase complex in binding to relative RNA polymerase II (Figure 5.35). Specifically, it binds

to the elongating form of Pol II (phosphorylated at Ser2) thus facilitating transferring the m^6A methyltransferase complex to actively transcribed nascent RNAs to allow the m^6A methyltransferase complex to methylate adjacent nascent RNAs during transcription elongation (Huang et al., 2019).

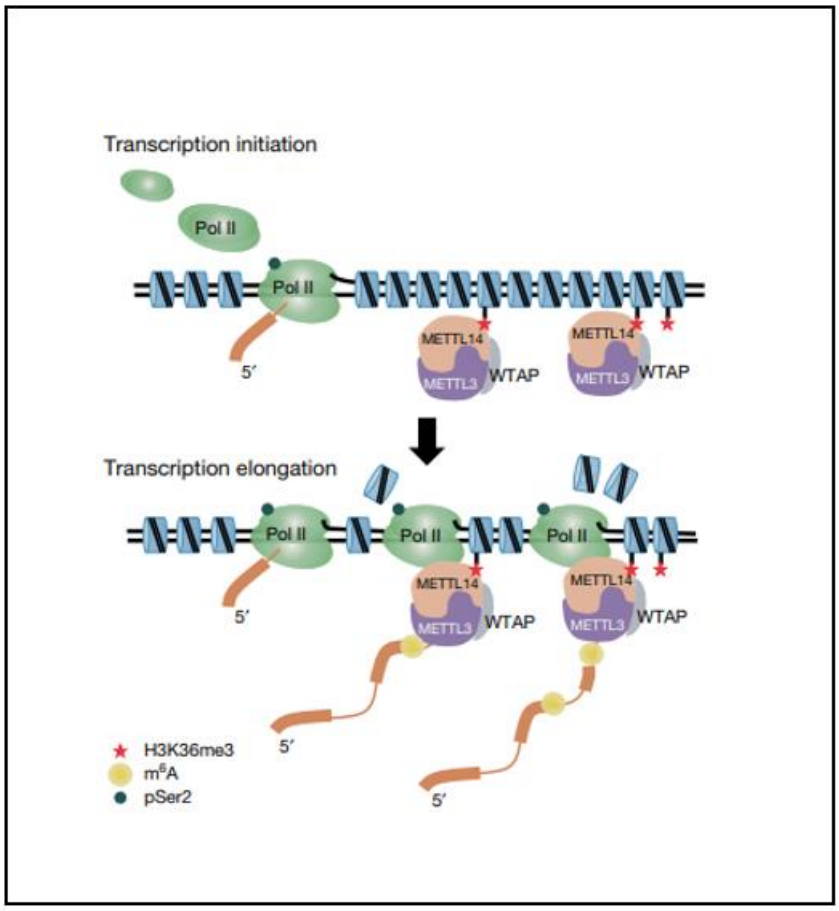

Figure 5.35: Proposed model to clarify the mechanism of guided m^6A methylation co-transcriptionally by H3K36me3 (Huang et al., 2019).

Methylation of arginine is a prevalent post-translational modification being involved in variety of cellular processes in eukaryotic organisms. A family of enzymes known as protein arginine methyltransferases (PRMTs) catalysed this modification. PRMTs are categorized as Type I, Type II, or Type III based on the methyl group place on the

nitrogen atoms of the guanidine group of methylated arginine (Bachand 2007; Hernando et al.,2015). To date, nine encoding PRMTs genes have been reported in humans, *Drosophila* and *Arabidopsis thaliana*, eight PRMTs genes in *Oryza sativa* and four in *Saccharomyces cerevisiae*. *(*Hernando et al.,2015*).* Earlier studies have connected symmetric R methylation with transcriptional repression, whereas asymmetric R methylation is linked to transcriptional activation. However, there are no global studies that support this conclusion (Hernando et al., 2015).

In the *Arabidopsis thaliana* genome there are nine of PRMTs, seven of them type I arginine methyltransferases (PRMT1a, PRMT1b, PRMT3, PRMT4a, PRMT4b, PRMT6 and PRMT10), and (PRMT5) represent type II enzyme (Hernando et al., 2015; Ahmad and Cao, 2012). PRMT5 is the most studied PRMT in plants, and plays a role in flowering time, circadian rhythms, photomorphogenic development and on pre-mRNA splicing of a sub-set of genes (Hong et al.,2010; Deng et al .,2010; Hernando et al.,2015).

AtPRMT4a and AtPRMT4b, a pair of Arginine methyltransferases in *Arabidopsis* are homologs of mammalian CARM1/PRMT4 and correspond to type I PRMTs (Niu et al.,2008). PRMT4a together with PRMT4b, are also playing a key role in the regulation of flowering time in *Arabidopsis thaliana*, via its influence on FLC expression (Niu et al., 2007; Niu et al., 2008). FLC is a MADS box transcription factor that represses flowering, and its expression increased in all *prmt5*, *prmt10* mutants and the *prmt4a/b* double mutant, leading to delayed flowering in these mutant plants (Niu et al.,2007; Niu et al.,2008; Hernando et al., 2015). Furthermore, RNA-seq analysis revealed that most of PRMT5 and PRMT4 have similar molecular functions to regulate gene expression at transcriptional and post-transcriptional levels (Hernando

et al., 2015). In the *prmt4a/b* double mutants, the level of asymmetric dimethylation on histone H3 Arg-17 is reduced globally, while in the same double mutant the mRNA level of FLC was increased (Niu et al.,2008). In the current study, the m^6A level do not seem to be altered in the *prmt4a/b* double mutants compared to WT.

Previous research has indicated an interaction between PRMT4a and PRMT4b and MTB in Y2H assay (Fray group unpublished). In addition, proteomics data showed 4 methylated arginine sites in MTB (Simpson group, unpublished). Furthermore, it was found that the FLC mRNA is strongly methylated (Fray group, unpublished). Based on these data, in this study we have investigated the interaction between MTB and arginine methylation. To gain insights into this interaction we tested several pairwise interactions between MTB with and without the 4 sites of methylated Arginine and two arginine methylation proteins using the yeast two-hybrid system (Y2H). The *MTB* mutant version was synthesised by (Synbio Technologies Company) by replacing the four sites of Arginine methylation in MTB to Lysine. If the PRMT4a and PRMT4b are interacting because the MTB is the target, it might be expected that converting the 4 arginine targets to lysine should stop this interaction in Y2H. Two splice variants of MTB have been reported. Variant 1 is full length correctly spliced form of MTB and the second splice variant lacks complete exons 5 and 6 of MTB. Both splice variants of MTB were used to study the interaction between MTB and Arginine methylation. As predicted, we observed weak positive interactions of MTB in both splice variants in the presence of the 4 sites of methylated Arginine with PRMT4a and PRMT4b as evidenced by the appearance of yeast growth in 3-AT-HIS3 plates. This weak interaction still occurred in the absence of 4 sites of methylated Arginine only in MTB

variant 1 but not in variant 2, which suggests that this interaction might be due to another methylated Arginine site that was not detected by proteomics analysis.

Protein arginine methylation can affect transcription by a range of molecular mechanisms. The effects can probably lead to either positive or negative impacts on the interaction of the methylated proteins with other molecules for instance: proteins, DNA, or RNA. However, these altered intermolecular interactions can influence the subcellular localization of proteins, on protein or RNA stability, or on the enzymatic activity of proteins (Lee and Stallcup, 2009). In the current study, according to the proteomics results of 4 methylated arginine sites in the MTB, we hypothesized that the sites of Arginine methylation in MTB might affect its localization. Thus, the MTB-GFP line was confirmed by PCR then was crossed with *prmt4a/b* double mutant to check: 1) If MTB is a substrate for methylation by PRMT4a/b, and then the stability or subcellular localisation may change in the absence of arginine methylation. 2) MTB-GFP (should be possible) to isolate using the GFP tag and this can then be checked with an antibody against methyl arginine to i) confirm that MTB is arginine methylated in a WT background and ii) to demonstrate that this arginine methylation is lost in the *prmt4a/b* double mutant. Among 64 plants of F2 progenies, only line 18 has double mutant for *prmt4a/b* and contained MTB-GFP construct at the same time. Several attempts have been made to see the expression of MTB by using the anti-GFP and checking the protein of the line 18 using anti-methyl arginine antibodies. Despite these attempts, which include immunoprecipitation via GFP-trap, Lateral Root Induction by Auxin treatment, and Formaldehyde crosslinking, and the MTB-GFP showed positive results in PCR and confocal microscopy, no expression of MTB was detected by using anti-GFP in any of these attempts. This might be due to its folding which might hide the epitope that the antibody can recognize (although this is unlikely

under the denaturing PAGE conditions used for western analysis) or perhaps the MTB protein is unstable and easily broken down. In addition, unspecific bands were obtained by using anti-methyl arginine for line 18 which are probably due to the other methylases which may be modifying the histones. Therefore, a different method for protein extraction by using 8M Urea was tried. Urea can lead to disruption of the internal bonds in the proteins. This property can be used to improve the solubility of certain proteins. By using this method, the detection of MTB-GFP was successfully obtained.

As mentioned above, PRMT4a together with PRMT4b, are involved in the regulation of flowering time in *Arabidopsis thaliana* through effects on FLC expression, and in this study to investigate the phenotype of *MTB* without Arginine sites, a new construct lacking 4 Arginine sites in MTB was generated and used for plant transformation of both the MTB T-DNA insertion (GK_332G03) line and WT. This will allow us to study the phenotype and see: 1) if complementation is possible with this construct and 2) if the complemented mutant has the same phenotype as the *prmt4a/b* double mutant (delayed flowering). In this chapter, we aimed to get insights into the interaction between MTB and arginine methylation, which may provide a foundation to build the relationships of enzymes/substrates and RNA methylation with arginine methylation. Unfortunately, data required for confirm if the MTB is a substrate for arginine methylation was incomplete, likely due to the MTB stability, expression or folding.

5.6 Supplementary Data

5.6.1 Supplementary Figures of Bait and Prey constructs.

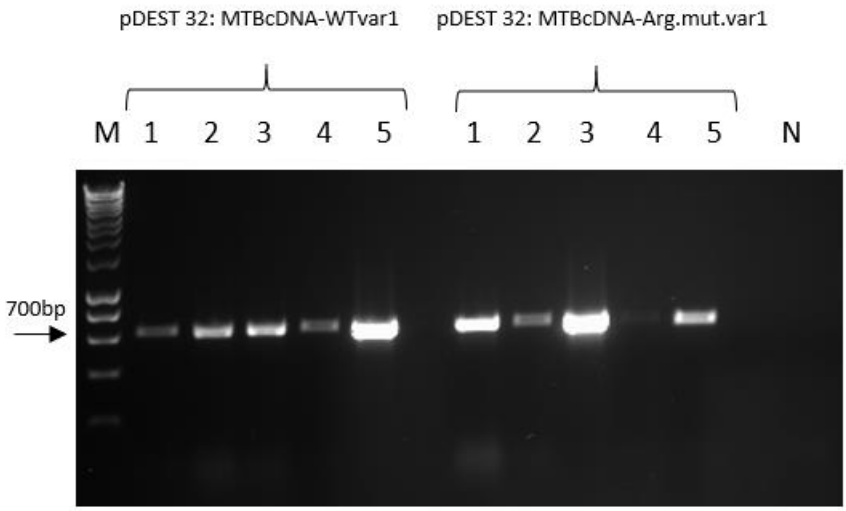

Figure 5.36: Colony PCR for *E. coli DH5α* transformed with a ligation mixture of pDEST32:MTBcDNA-WTvar1 and pDEST32:MTBcDNA-Arg.mut.var1 using primers MTBLys.Fw+ MTBLys.Rev. N, negative control using water as a Template. Arrow indicate to the expected size of the bands at 700bp. PCR product were run on 1 % (w/v) agarose gel, and HyperLadder 1Kb (Bioline) was used as a marker.

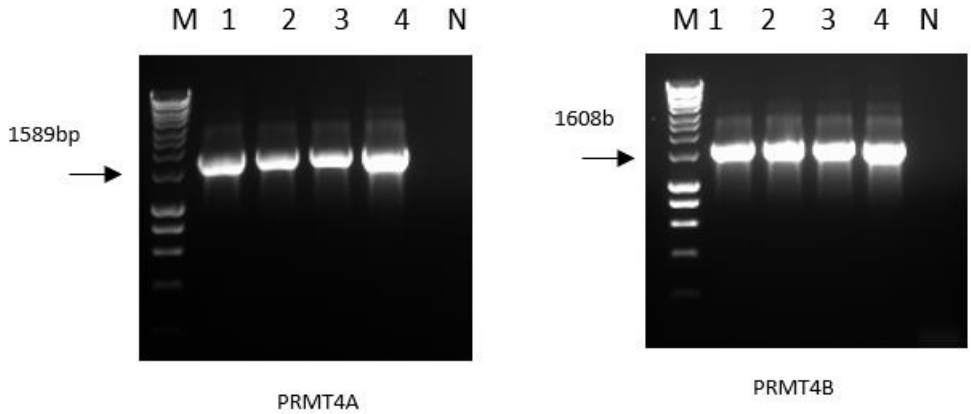

Figure 5.37: Colony PCR for *E. coli DH5α* transformed with a ligation mixture of (pDEST22:PRMT4AcDNA) using primers prmt4aFw+ prmt4aRev and pDEST22: PRMT4BcDNA using primers prmt4bFw+ prmt4bRev N, negative control using water as a Template. Arrows indicate to the expected size of the bands at at 1589bp and 1608bp respectively. PCR product were run on 1 % (w/v) agarose gel, and HyperLadder 1Kb (Bioline) was used as a marker.

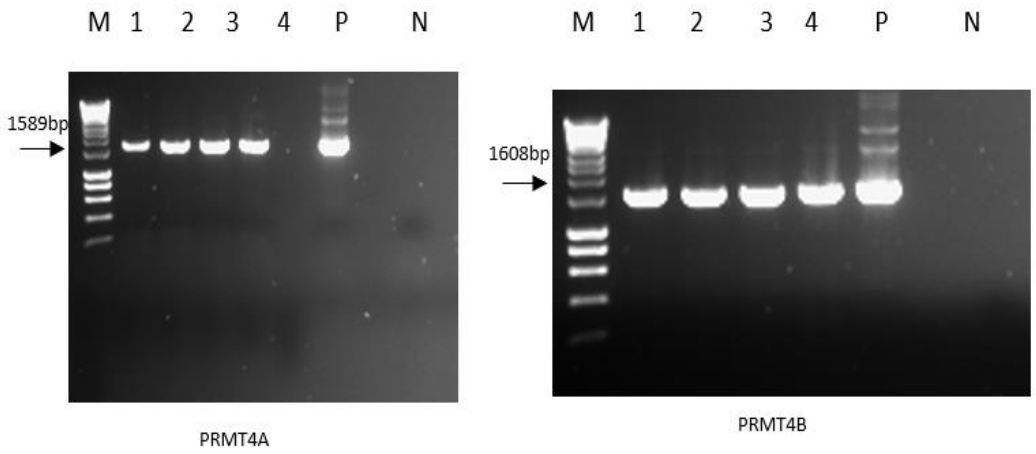

Figure 5.38: Colony PCR for *E. coli DH5α* transformed with a ligation mixture of pDEST32:PRMT4AcDNA using primers prmt4aFw-y2h + prmt4aRev-y2h and pDEST32:PRMT4BcDNA using primers prmt4bFw-y2h+ prmt4bRev-y2h. P, positive control using PCR8: PRMT4AcDNA and PCR8: PRMT4BcDNA as templates. N, negative control using water as a Template. Arrows indicate to the expected size of the bands at at 1589bp and 1608bp respectively. PCR product were run on 1 % (w/v) agarose gel, and HyperLadder 1Kb (Bioline) was used as a marker.

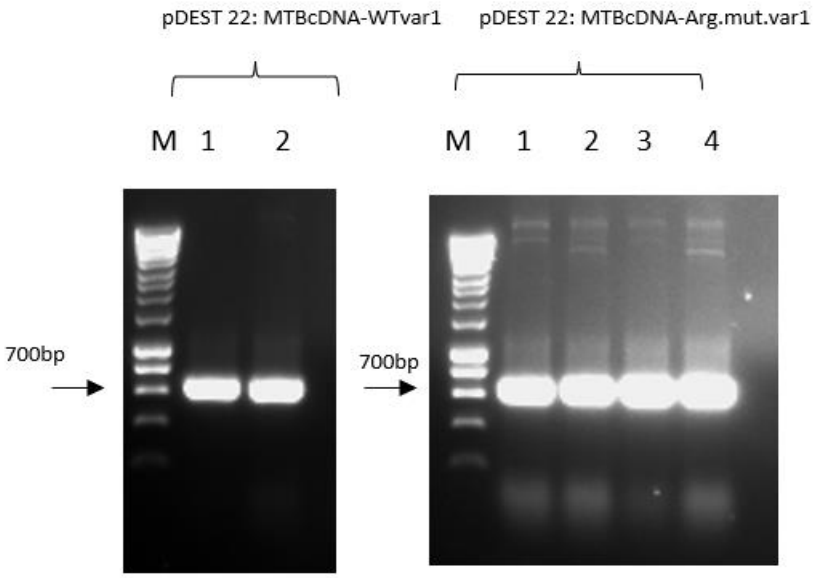

Figure 5.39: Colony PCR for *E. coli DH5α* transformed with a ligation mixture of pDEST 22: MTBcDNA-WTvar1 and pDEST 22: MTBcDNA-Arg.mut.var1 using primers MTBLys.Fw+ MTBLys.Rev. Arrow indicate to the expected size of the bands at 700bp. PCR product were run on 1 % (w/v) agarose gel, and HyperLadder 1Kb (Bioline) was used as a marker.

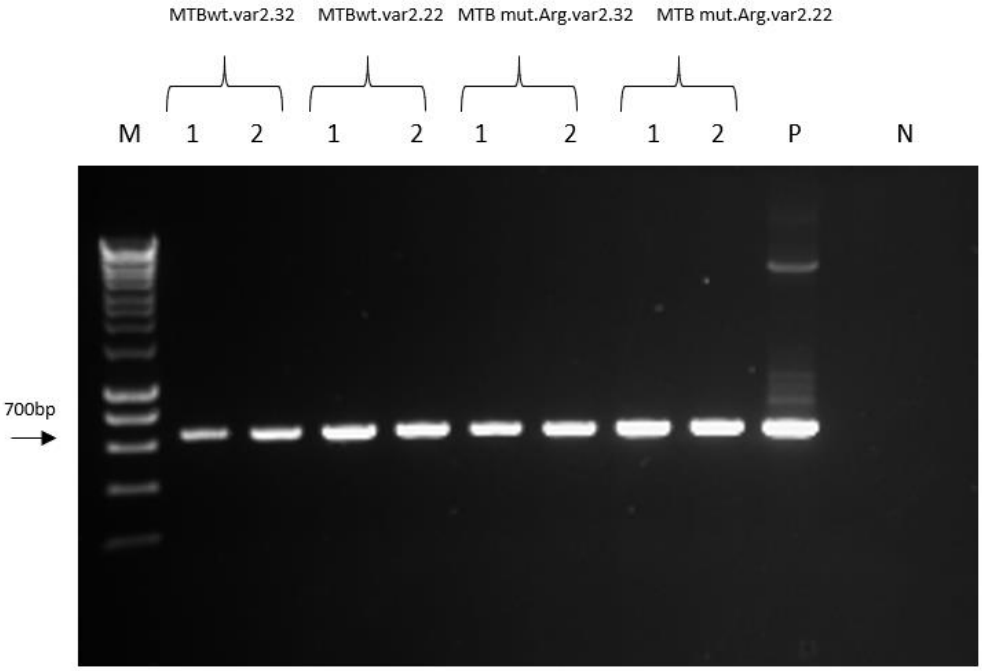

Figure 5.40: Colony PCR for *E. coli DH5α* transformed with a ligation mixture of pDEST 32: MTBcDNA-WTvar2, pDEST 22: MTBcDNA-WTvar2, pDEST 32: MTBcDNA-Arg.mut.var2 and pDEST 22: MTBcDNA-Arg.mut.var2 using primers MTBLys.Fw+ MTBLys.Rev. Arrow indicate to the expected size of the bands at 700 bp. PCR product were run on 1 % (w/v) agarose gel, and HyperLadder 1Kb (Bioline) was used as a marker.

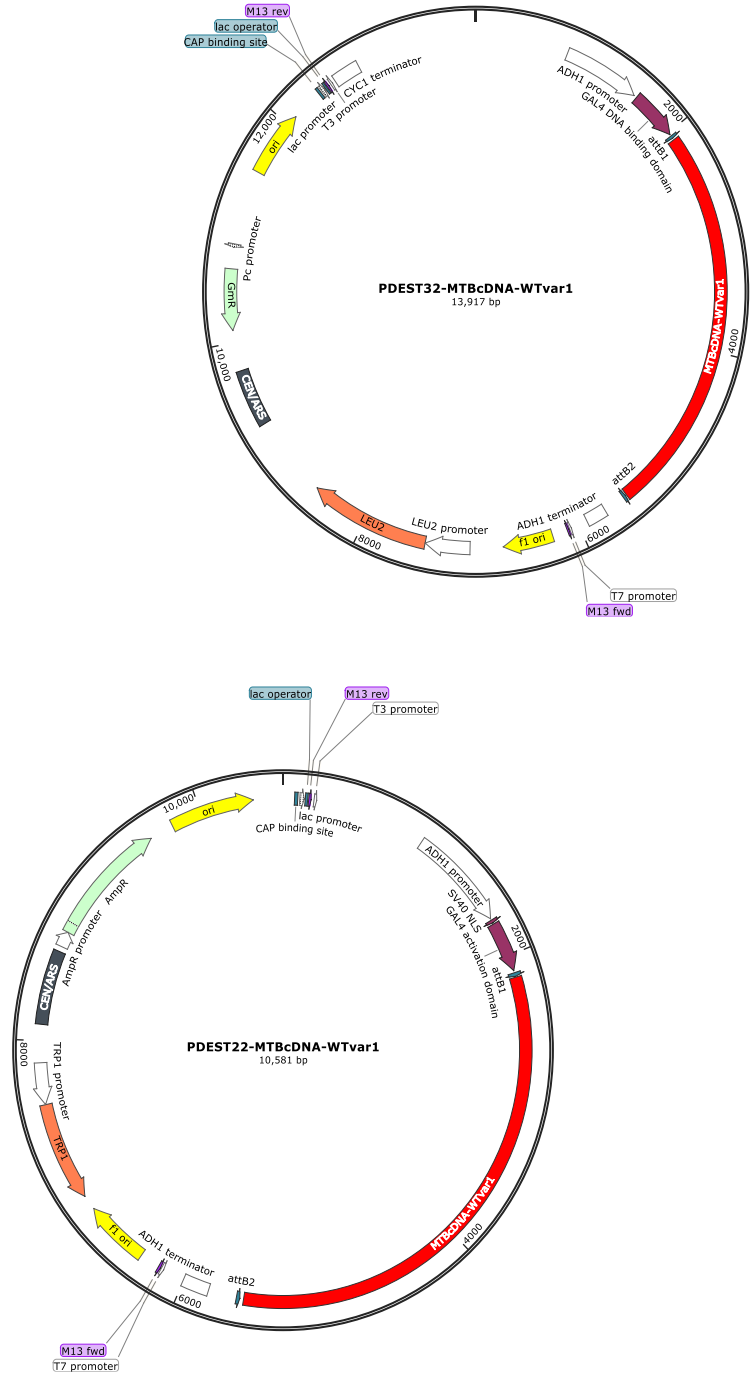

Figure 5.41: Plasmids maps of (pDEST 32: MTBcDNA-WTvar1) and (pDEST 22: MTBcDNA-WTvar1). Snap gene software generated the schematic diagrams. GmR is Gentamycin resistance gene for pDEST 32. AmpR is Ampicillin resistance gene for pDEST 22.

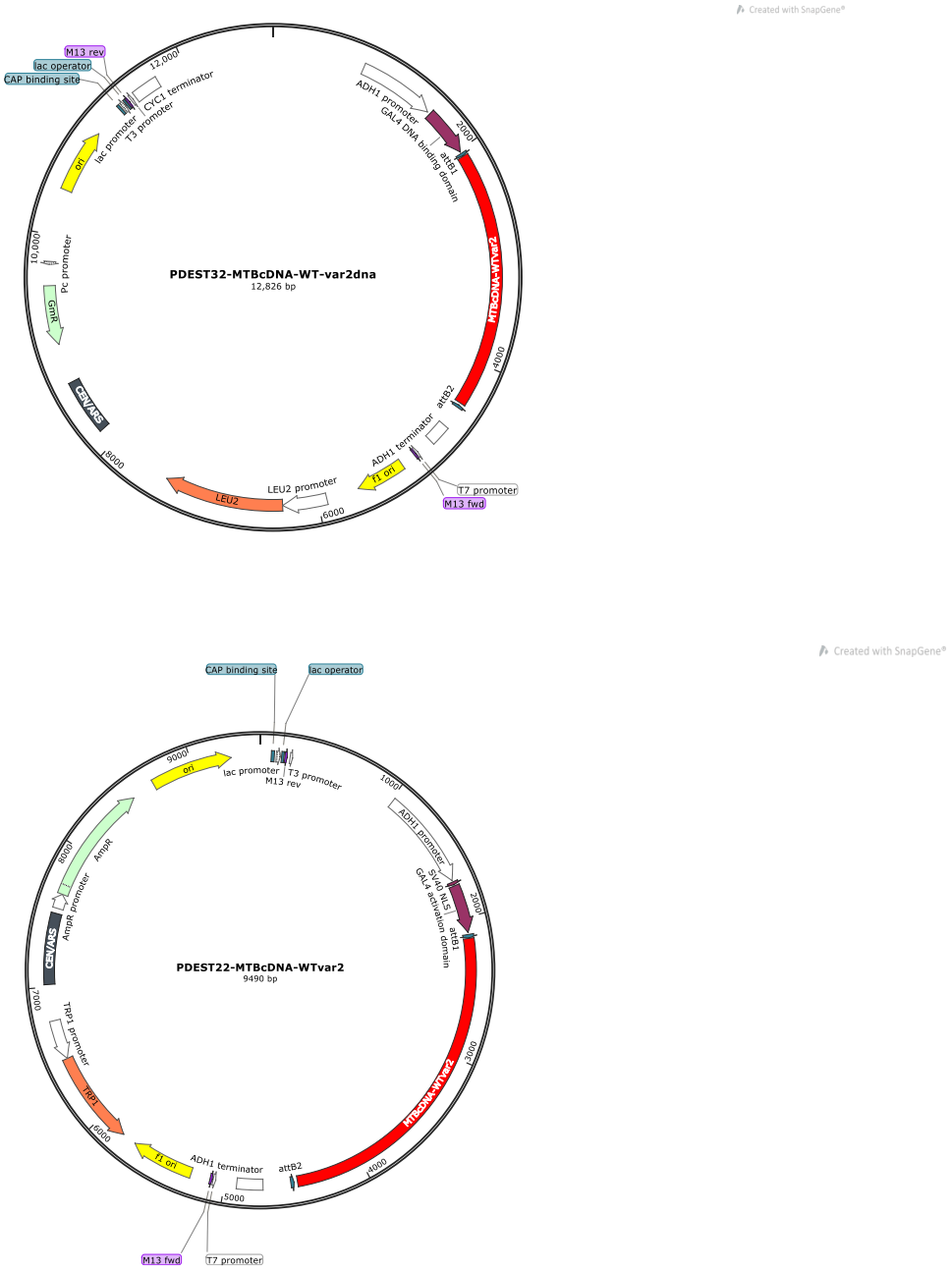

Figure 5.42: Plasmids maps of (pDEST 32: MTBcDNA-WTvar2) and (pDEST 22: MTBcDNA-WTvar2). Snap gene software generated the schematic diagrams. GmR is Gentamycin resistance gene for pDEST 32. AmpR is Ampicillin resistance gene for pDEST 22.

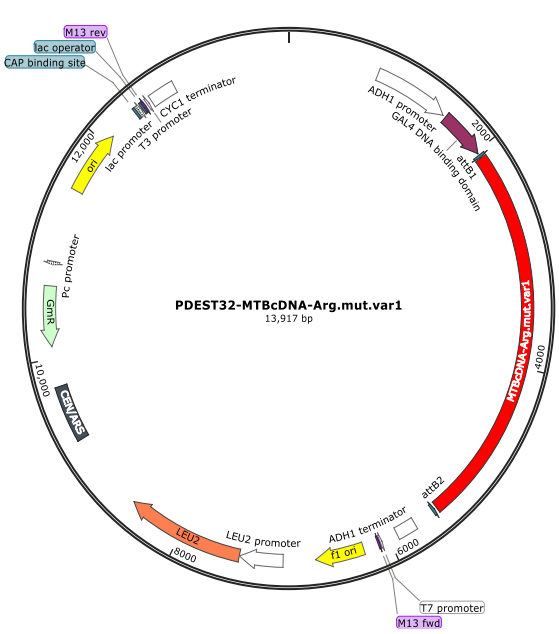

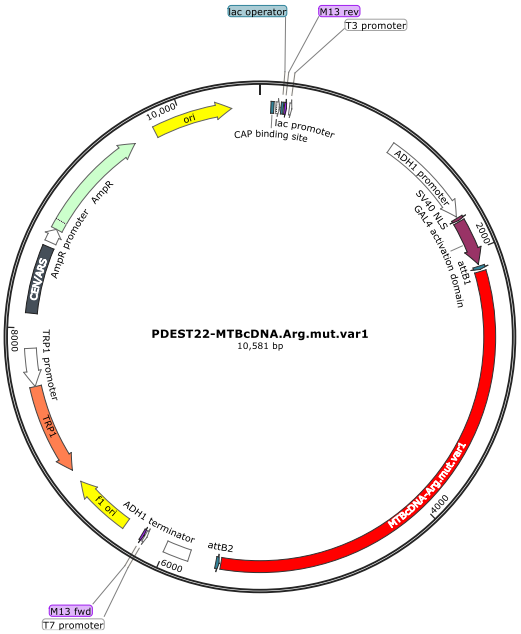

Figure 5.43: Plasmids maps of (pDEST 32: MTBcDNA-Arg.mut.var1) and (pDEST 22: MTBcDNA-Arg.mut.var1). Snap gene software generated the schematic diagrams. GmR is Gentamycin resistance gene for pDEST 32 and AmpR is Ampicillin resistance gene for pDEST 22.

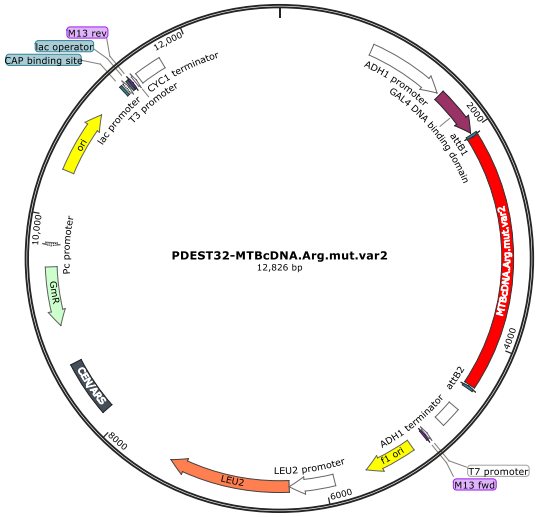

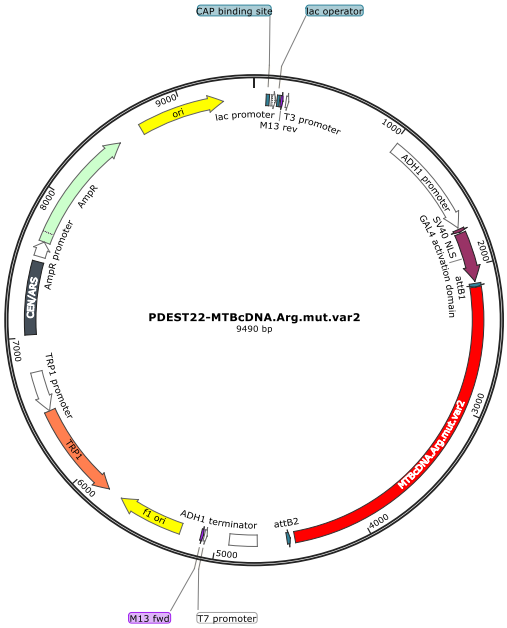

Figure 5.44: Plasmids maps of (pDEST 32: MTBcDNA-Arg.mut.var2) and (pDEST 22: MTBcDNA-Arg.mut.var2). Snap gene software generated the schematic diagrams. GmR is Gentamycin resistance gene for pDEST 32 and AmpR is Ampicillin resistance gene for pDEST 22.

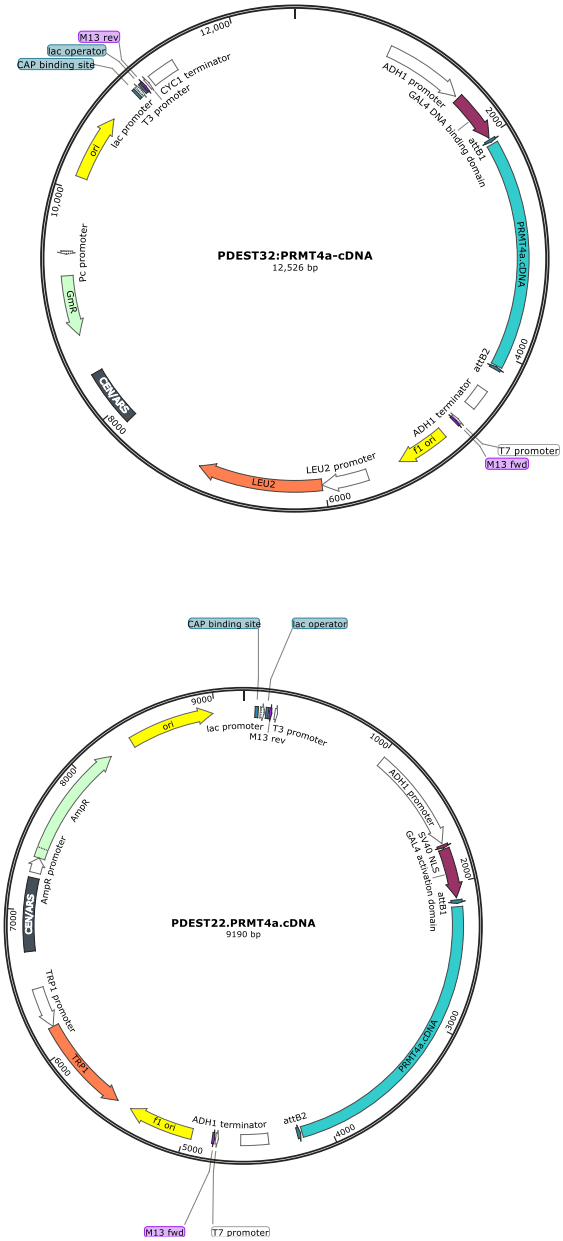

Figure 5.45: Plasmids maps of (pDEST 32: PRMT4a.cDNA) and (pDEST 22: PRMT4a.cDNA). Snap gene software generated the schematic diagrams. GmR is Gentamycin resistance gene for pDEST 32 and AmpR is Ampicillin resistance gene for pDEST 22.

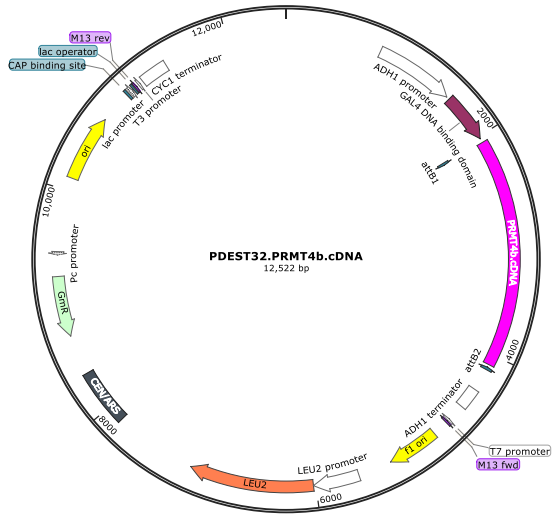

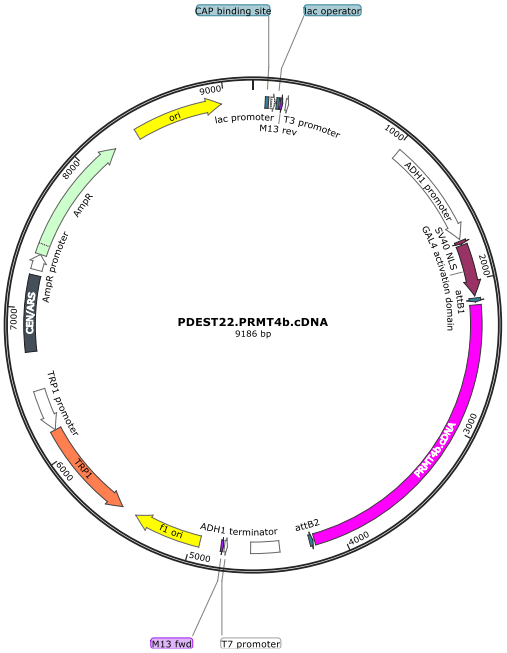

Figure 5.46: Plasmids maps of (pDEST 32: PRMT4b.cDNA) and (pDEST 22: PRMT4b.cDNA). Snap gene software generated the schematic diagrams. GmR is Gentamycin resistance gene for pDEST 32 and AmpR is Ampicillin resistance gene for pDEST 22.

5.6.2 Supplementary Figures for Generation of (CaMv35S:MTBcDNA.WT) and (CaMv35S:MTB.arg.mut) constructs

These two constructs were generated by cloned the entry vectors of PCR8;MTBcDNA.WT and PCR8;MTB.Arg.mut into the plant binary vector pGKPGWG contain CaMV35s promoter via an LR clonase (Invitrogen) reaction. All ligation mixtures were then transformed to *E.coli DH5α* competent cell, and then confirmed the positive colonies by PCR and sequencing Figure 5.47 .

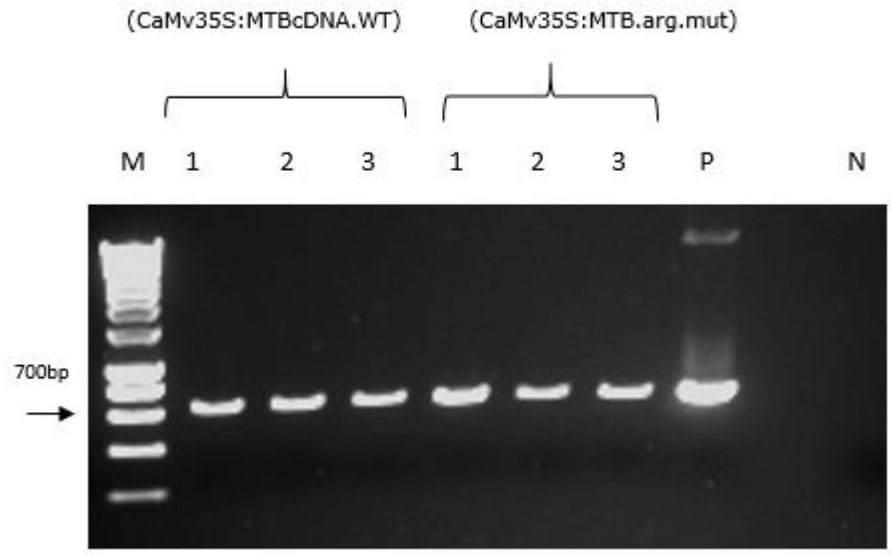

Figure 5.47: Colony PCR for *E.coli* DH5α transformed with a ligation mixture of CaMv35S:MTBcDNA.WT and CaMv35S:MTB.arg.mut using primers MTBLys.Fw+ MTBLys.Rev. P, positive control using PCR8: MTBcDAN as a template. N, negative control using water as a template Arrow indicate to the expected size of the bands at 700bp. PCR product were run on 1 % (w/v) agarose gel, and HyperLadder 1Kb (Bioline) was used as a marker.

The two constructs were then transferred to the *Agrobacterium* strain C58 by an electroporation and then confirmed by colony PCR Figure 5.48.

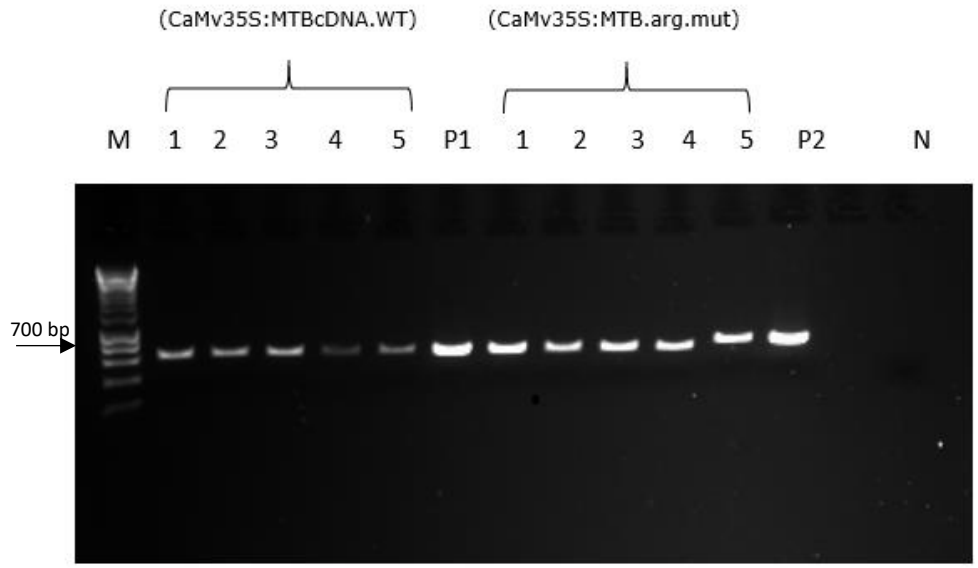

Figure 5.48: Colony PCR of *Agrobacterium* strain C58 transformed with CaMv35S:MTBcDNA.WT and CaMv35S:MTB.arg.mut using primers MTBLys.Fw+MTBLys.Rev. P1: positive control using CaMv35S:MTBcDNA.WT as a template and P2: positive control using CaMv35S:MTB.arg.mut as a template. N: negative control using water as a template. PCR products were resolved on a 1% (w/v) agarose gel using HyperLadder 1-kb (Bioline) as a marker.

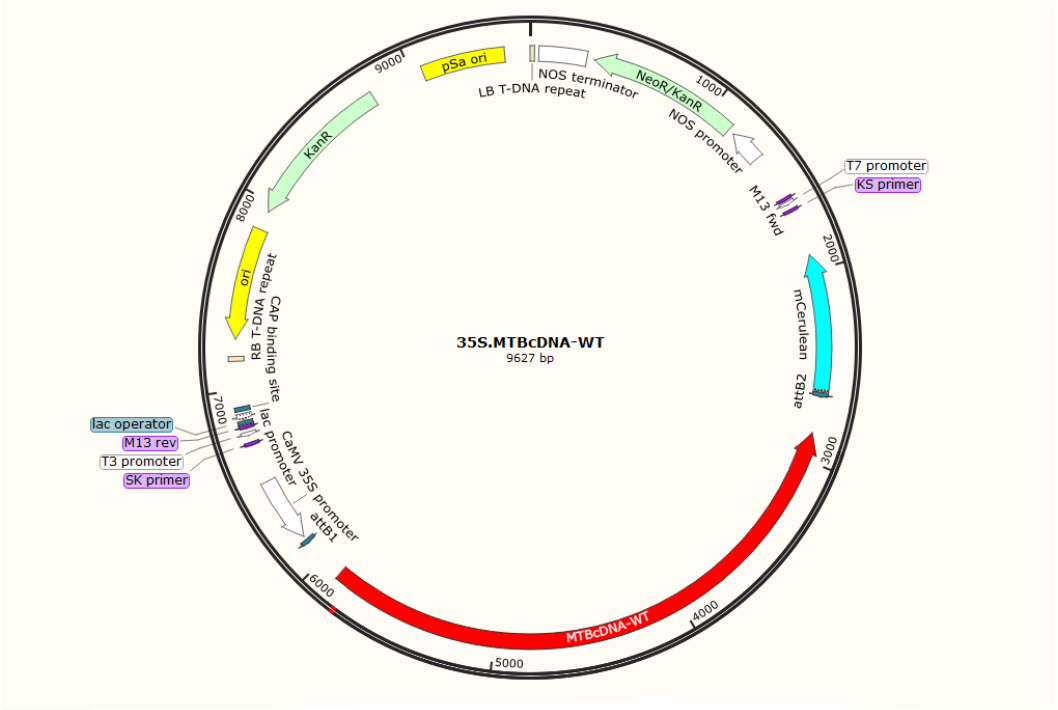

Figure 5.49: Plasmids maps of (CaMV 35S:MTBcDNA-WT) . Snap gene software generated the schematic diagrams. KanR is Kanamycin resistance gene

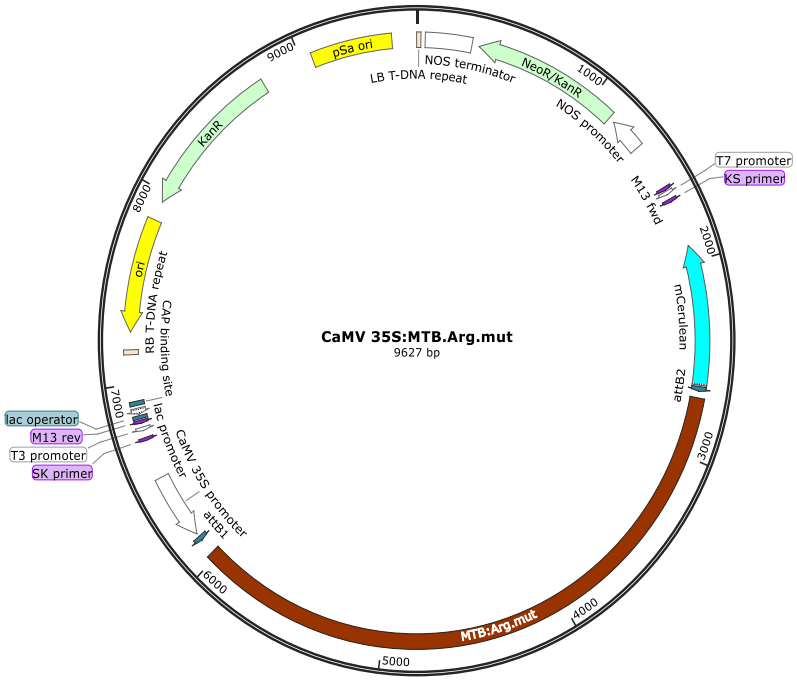

Figure 5.50: Plasmids maps of (CaMV 35S:MTB.Arg.mut) . Snap gene software generated the schematic diagrams. KanR is Kanamycin resistance gene.

CHAPTER 6 : SUMMARY AND CONCLUSION

6.1 Summary

It is emerging that the modification of m^6A plays a vital biological role in plants, yeast, flies, and mammals. It can influence developmental processes, cell differentiation, circadian clock regulation, control of cell fate and the initiation of meiosis in yeast and it has a critical role in embryo development and normal growth in plants (Fustin et al., 2013; Agarwala et al., 2012; Zhong et al., 2008; Bodi et al., 2012). Despite the biological importance of this modification, the mechanisms for regulating gene expression by m^6A have yet to be fully clarified. The conversion of A to m^6A is carried out by the mRNA (N^6-adenosine)-methyltransferase (MTase) "writer" complex, which are well conserved between plants and animals. The core set of mRNA m^6A writer proteins in *Arabidopsis thaliana* includes MTA (METTL3), MTB (METTL14), FIP37 (WTAP), VIRILIZER (VIRMA) and the E3 ubiquitin ligase HAKAI (Zhong et al., 2008; Bodi et al., 2012; Růžička et al., 2017). The MTB gene (encoded by At4g09980) is a member of the B subfamily of MT-A70 methylases, and is closely related to MTA (Bujnicki et al., 2002). In addition, it is a homolog of METTL14 and KAR4 in animals and yeast respectively. The expression of MTB occurs throughout plant development, thus its role probably involves many aspects of plant cell life or in essential pathway(s) for plant cell viability. In the present study, we aimed to elucidate the role and regulation of MTB (At4g09980) in mRNA methylation in *Arabidopsis* through mutant characterization, complementation and promoter studies.

6.1.1 The role of MTB in *Arabidopsis* development and the importance of the SAM binding domain in MTB.

Gene knockout is one of the most useful methods that can be used to understand the role of a specific gene. There are many ways to perform targeted mutagenesis in a specific gene. One of them is the insertion of foreign DNA into the specific gene of interest. In *Arabidopsis*, the most common method of insertional mutagenesis involves *Agrobacterium* T-DNA insertion which acts to disrupt or reduce the expression of the gene of interest. Null mutations generated by T-DNA insertions in m^6A writer proteins (*MTA*, *MTB*, *FIP37* and *VIR*, but not *HAKAI*) lead to embryo-lethal phenotypes and arrest at the globular stage (Zhong et al., 2008; Bodi, et al.,2012; Tzafrir et al., 2004; Vespa et al., 2004; Růžička et al., 2017). Hypomorphic mutants of *fip37* and *vir* have been obtained in which only small amounts of the correctly spliced transcripts are produced and m^6A levels are much reduced. Knockdown lines of *MTA* have been generated in which the SALK insertion knockout was partially rescued by expressing an MTA cDNA under the control of an embryo-specific ABI3 promoter. The ABI3 promoter has a very low level of activity in vegetative tissues post germination and as a result m^6A levels are reduced by~90%, resulting in developmental defects including leaf crinkling, shorter inflorescence, and reduced apical dominance (Bodi et al., 2012). In addition, RNA interference methods (RNAi) of *MTB* have been attempted, but these achieved only modest knockdown and showed delayed development of *Arabidopsis* (Růžička et al., 2017).

In this study, different approaches were adopted in order to establish stable lines with reduced MTB expression to allow investigations into the functional role of MTB during *Arabidopsis* development. Firstly, we identified two heterozygous T-DNA insertion mutants of *MTB*, (SALK-056904) and (GK-332G03) in the third exon and

fourth intron respectively. Both failed to produce viable homozygous seeds after self-pollination and could only be isolated as heterozygous, the homozygous knockout in *MTB* resulted in embryo lethality, young seeds were white rather than green and became brown and shrivelled at maturity. We have rescued this embryo lethality phenotype by employing the previously successful technique applied to rescue of the *MTA* embryo lethal phenotype (Bodi et al., 2012), in order to study the effects of reduced *MTB* in *Arabidopsis*. We crossed the *MTB* T-DNA insertion (SALK-056904) line with a plant harbouring MTB under the control of the ABI3 promoter. Homozygous plants with stunted growth, serrated leaves and very short flower stems were recovered after self-pollination. These homozygous *MTB* mutant plants demonstrate similar developmental defects but are more severe than previously published *MTA*, *FIP37* and *VIR* mutant plants (Bodi et al., 2012; Růžička et al., 2017).

Levels of MTA or MTB protein from transgene constructs will depend upon transcription rate, mRNA half-life, translation rate and protein half-life. Notably, the homozygous plants of *MTB* died before flowering and still have to be maintained as heterozygotes, whereas the ABI3-MTA previously allowed sufficient complementation to allow growth to set seed. This is probably due to the mRNA half-life, the half-life of MTA has been reported to be 1.98 h whereas the half-life of MTB is 3.5-fold lower (0.6 h) (Narsai et al., 2007). This is very low compared to the average of mRNA half-life in *Arabidopsis* which is 3.8 h (Narsai et al., 2007). In addition, a previous study showed that approximately 100 of unstable transcripts in *Arabidopsis thaliana* were described as being quickly degraded with half-lives of < 60 min (Gutierraz et al., 2002). According to the list created by Narsai et al., (2007), MTB (At4g09980) was defined as fast-decaying transcripts.

We found that levels of m^6A were reduced by more than 80% in the *MTB* hypomorphic lines, demonstrating that MTB is indispensable for writing WT levels of m^6A RNA methylation in *Arabidopsis*. Interestingly, we also observed significant alteration in trichome branching consistent with previous results of increasing trichome branching in *Arabidopsis* for reduced *MTA* methylation, overexpression of *FIP37* and knock out of the m^6A YTH reader protein *ECT2* (Bodi et al., 2012; Vespa et al., 2004;Wei et al., 2018).Together, these data are consistent with previous studies on MTA (Zhong et al., 2008; Bodi et al., 2012) and suggest that MTB is also required for embryogenesis, development and normal growth patterns in plants, apical dominance, and involved in regulating trichome morphology.

Catalytically inactive versions of proteins can sometimes be more informative than complete gene knockouts. Knockout of *MTA*, *MTB*, *FIP37* or *VIR* is embryo lethal, presumably because m^6A writing is abolished. However, the writer complex is large, and it is possible that the lethality seen when one these proteins is lost is due to loss of a structural role which prevents the complex from properly assembling, rather than to loss of a specific (enzymatic) function of the protein itself. In a further approach to investigate the function of the MTB protein, versions of *MTB* in which the S-adenosylmethionine (SAM) binding domain has been mutated were generated for use in overexpression and complementation studies. Both MTA and MTB contain motifs characteristic of S-adenosylmethionine (SAM) (methyl donor) binding domains. At the core of this SAM binding domain are the four amino acids DPPW (Bujnicki et al.,2002; Bokar et al.,1997). A similar approach for *MTA* previously generated a dominant methylation mutant in which the DPPW SAM binding site had been mutated. When constitutively expressed in a wild type background, this transgene gave rise to *Arabidopsis* plants similar in appearance to the low m^6A ABI3MTA lines

(Fray group unpublished). We hypothesise that overexpression of the non-SAM binding (catalytically inactive) MTA competes with native MTA for binding to other writer complex members and so titrates out the functional writer complex. The plant MTB peptide harbours a similar DPPW (predicted SAM binding) domain, so the objective was to create a mutant *MTB* protein lacking this domain, for introduction into wild-type and *MTB* knockout *Arabidopsis* plants. The Northern blotting data clearly confirmed the overexpression of both MTBΔSAM and MTAΔSAM, but only those plant expressing the MTAΔSAM construct gave rise to a dominant negative phenotype with reduced m^6A. These MTAΔSAM overexpressing plants showed delayed development, reduced apical dominance and crinkled leaves, whereas *MTB* mutants more closely resembled WT. These findings are in consistent with a previous reports in mammals which studied the crystal structures of METTL3-METTL14 complex and showed that a mutation in the catalytic site of *METTL3* led to an abolition of methyltransferase activity of the complex, whereas no effect was observed by mutating the putative catalytic site of *METTL14* indicating a catalytic role of METTL3 in the complex, whereas METTL14 support METTL3 and contributes to RNA binding (Wang X et al., 2016; Wang P et al., 2016b; Śledź and Jinek, 2016; Huang and Yin, 2018). In addition, they demonstrated that the SAM domain is in the catalytic cavity of METTL3 but not in METTL14 (Wang P et al. 2016). Another explanation for why the MTAΔSAM construct gives a phenotype, but the MTBΔSAM does not, could come from a recent study which reported that in mammalian cells METTL3 (but not the other writer components) is observed in cytoplasmic fractions and promotes translation in the cytoplasm, independently of its methyltransferase activity, m^6A writer proteins, and m^6A reader proteins (Lin et al., 2016). Furthermore, two CCCH-

type zinc fingers important for catalytic activity of the full-length complex have been identified in METTL3, but not in METTL14 (Iyer et al. 2015;Huang et al., 2018)

To validate this hypothesis in this study and to check if the SAM binding site is dispensable for MTB function, the MTBΔSAM transgenic line was crossed with MTB-GK T-DNA insertion line to generate MTBΔSAM in the knockout mutant background. This might give rise to lines in which the GK insertion mutation could be complemented. This might be the case if MTB performed a structural function and its presence was required for the assembly of the writer complex, even if its SAM binding function were dispensable. So far, and after testing 23 plants, no homozygous lines for MTB-GK T-DNA insertion was obtained in the F2 generation, indicating that the MTBΔSAM did not complement the MTB-GK line. As a control an additional non mutated construct containing MTBcDNA (WT) instead of MTBΔSAM was generated and transformed to WT and MTB-GK line to confirm that this construct can complement Gabi Kat line - meaning that the reason of no complementation and no phenotype for MTBΔSAM is because it does need this SAM domain for MTB. The seeds were collected from dipped plants but due to time limitations, we could not finish this experiment during the PhD thesis period.

6.1.2 Investigating if m^6A writing is regulated by arginine methylation of MTB

In a previous study, two arginine methylases were identified as putative MTB-interacting proteins in a yeast two hybrid screen. Furthermore, in collaboration with the Simpson lab in Dundee, mass spectrometry of native m^6A writer proteins identified four methyl arginine sites in MTB. The Yeast-two hybrid assay was repeated and extended to confirm this interaction by using PRMT4a and PRMT4b with both splice variants of MTB in the bait and prey vectors. Additionally, to investigate the functional relevance of the modified Arginine residues of MTB, we mutated the 4 identified

Arginine sites in MTB to Lysine and used it in Y2H. If the PRMT4a and PRMT4b are interacting because the MTB is one of their target substrates, it would be expected that converting the 4 arginine targets to lysine should stop this interaction in Y2H. As expected, we observed weak interactions between MTB in both splice variants in the presence of the 4 sites of methylated Arginine with PRMT4a and PRMT4b and this weak interaction still occurred in the absence of 4 sites of methylated Arginine only in MTB variant 1 but not in variant 2.This suggests that this interaction in the case of the short MTB splice variant is due to the presence of the Arg target residues, however, the interaction with the longer MTB form (both with and without the four modified Arg) might be due to additional methylated Arginine site(s) that were not detected by Proteomics analysis.

Arginine methylation is involved in a diversity of cellular processes including signal transduction, transcriptional regulation and DNA repair (Bedford and Clarke, 2009). In addition, specific protein-protein interactions have also been shown to be regulated by Arginine methylation. Arginine methylation in the Sam68-proline-rich domains, for instance, controls Sam68 nuclear localization and reduces its interaction with SH3 domain binding partners but not with WW domain proteins (Bedford et al.,2000; Côté et al., 2003). Arginine methylation can also have a significant effect on the subcellular localization of proteins and RNA. A previous study has demonstrated that the methylation of three arginines located in the SR protein SF2/ASF control its subcellular localization, and mutations that block methylation as an SF2/ASF by converting all three arginines into alanines results in increased cytoplasmic accumulation of SF2/ASF (Sinha et al.,2010). The resulting reduction in nuclear SF2/ASF levels prohibits it from modulating alternative splicing of target genes, leads

to increase stimulation of translation and abolishes the enhancement of nonsense-mediated mRNA decay (Sinha et al.,2010).

In this study, according to the proteomics results of 4 methylated arginine sites in the MTB, we hypothesized that the sites of Arginine methylation in MTB might affect its localization, stability or interaction with writer complex partners. Thus, to check if MTB is a substrate for methylation by PRMT4a/b, and then the stability or subcellular localisation may change in the absence of arginine methylation, we crossed the MTB-GFP line with *prmt4a/b* double mutant. Furthermore, we assumed the MTB-GFP (should be possible) to isolate using the GFP tag and this can then be checked with an antibody against methyl arginine to confirm that MTB is arginine methylated in a WT background and to demonstrate that this arginine methylation is lost in the *prmt4a/b* double mutant. We could not detect MTB-GFP in western blot, despite positive results in PCR and confocal microscopy. This is probably due to protein folding or stability. Therefore, a different method for protein extraction by using 8M Urea was tried. Urea can lead to disruption of the internal bonds in the proteins. This property can be used to improve the solubility of certain proteins. By using this method, the detection of MTB-GFP was successfully obtained. In addition, a new construct with the four known methylated Arginine sites in MTB replaced with Lysine and this construct transformed to MTB-GK line to check if complementation is possible with this construct and if the complemented mutant has the same phenotype as a *prmt4a/b* double mutant (delayed flowering) but we could not finish this experiment during the PhD thesis. However, our results in this study could provide a foundation to build the relationships between RNA methylation and arginine methylation in plants and other organisms.

6.2 Conclusion and Future work.

6.2.1 Conclusion

The current study aimed to elucidate the role of MTB (a member of m^6A methyltransferase (MTase) complex in *Arabidopsis*). Key findings are summarised as follows.

- The embryo lethality phenotype of MTB can be rescued by crossing the transgene plants that contain *MTB* T-DNA insertion (SALK-056904) with plants containing and MTB transgene under the control of a seed-specific promoter. The homozygous plants obtained using this approach show phenotypes similar to but more severe developmental defects than either *MTA*, *FIP37* or *Virilizer* knockdowns.
- The m^6A level in *MTB* hypomorphic lines was decreased by approximately more than 80% compared with that in WT.
- Significant alterations in trichome branching was observed in *MTB* hypomorphic lines with 64.84 % of four or more branched trichomes compared to 17.69% in WT.
- A mutant *MTB* line (MTBΔSAM) was generated and characterised then compared with previous similar MTAΔSAM. The northern blotting analyses confirmed the overexpression of both MTBΔSAM and MTAΔSAM, but only those plant expressing the MTAΔSAM construct gave rise to a dominant negative phenotype with reduced m^6A whereas *MTB* mutants more closely resembled WT.
- The MTBΔSAM did not complement MTB-GK line.
- A construct of MTB-lysine in which the four known sites of arginine methylation are replaced with lysine was generated and used in Y2H.

- Both MTB splice variants showed weak interaction with PRMT4a and PRMT4b via Y2H and this weak interaction still occurred in the absence of 4 sites of methylated Arginine only in MTB variant 1 but not in variant 2.

In conclusion, MTB is a member of m^6A methyltransferase (MTase) complex in *Arabidopsis* and is required for embryogenesis, development and normal growth patterns in plants, apical dominance, involved in regulating trichome morphology and is necessary for full m^6A mRNA methylation. In addition, the SAM binding site may be dispensable for MTB function. However, this hypothesis needs further investigations. Moreover, we confirmed the weak interaction between MTB and PRMT4a and PRMT4b via Yeast two-hybrid analysis, but the confirmation if the MTB is substrate for arginine methylation or not needs more investigations. Our findings provide information that may increase our knowledge of the m^6A writer complex and could pave the way to start studying the interaction between RNA methylation and Arginine methylation in plants and other organisms.

6.2.2 Future work

Due to time constraints, we could not finish all planned experiments during the PhD thesis period. It would be interesting to check if the two prepared constructs CaMv35S:MTBcDNA.WT and CaMv35S:MTB.arg.mut can complement the MTB-GK line and determine the phenotype in *Arabidopsis* and also look at methylation in *FLC* transcript in *prmt4a/b* and Arg deficient complementing lines. In addition, if I have more time, I will also check the level of m^6A in MTBΔSAM through TLC analysis. Moreover, we also can complement the MTB mutant using the MTB-GFP construct.

Analysis of gene expression of ABI3::MTB by qRT-PCR can be used to check the expression level of MTB hypomorphic lines. For global analysis of gene expression, full RNASeq could be carried out to see what genes are altered in expression. This could be then compared with MeRIPSeq data from seedlings at a similar age to see if there is a correlation between altered transcript levels and methylation status, this would help determine whether transcripts which are normally methylated are reduced in abundance.

BIBLIOGRAPHY

Agarwala, S., Blitzblau, H., Hochwagen, A. and Fink, G. (2012). RNA Methylation by the MIS Complex Regulates a Cell Fate Decision in Yeast. *PLoS Genetics*, 8(6), p.e1002732.

Aguilo, F., Zhang, F., Sancho, A., Fidalgo, M., Di Cecilia, S., Vashisht, A., Lee, D., Chen, C., Rengasamy, M., Andino, B., Jahouh, F., Roman, A., Krig, S., Wang, R., Zhang, W., Wohlschlegel, J., Wang, J. and Walsh, M. (2015). Coordination of m 6 A mRNA Methylation and Gene Transcription by ZFP217 Regulates Pluripotency and Reprogramming. *Cell Stem Cell*, 17(6), pp.689-704.

Ahmad, A. and Cao, X. (2012). Plant PRMTs Broaden the Scope of Arginine Methylation. *Journal of Genetics and Genomics*, 39(5), pp.195-208.

Alarcón, C., Goodarzi, H., Lee, H., Liu, X., Tavazoie, S. and Tavazoie, S. (2015). HNRNPA2B1 Is a Mediator of m6A-Dependent Nuclear RNA Processing Events. *Cell*, 162(6), pp.1299-1308.

Arribas-Hernández, L., Bressendorff, S., Hansen, M., Poulsen, C., Erdmann, S. and Brodersen, P. (2018). An m6A-YTH Module Controls Developmental Timing and Morphogenesis in Arabidopsis. *The Plant Cell*, 30(5), pp.952-967.

Auclair, Y. and Richard, S. (2013). The role of arginine methylation in the DNA damage response. *DNA Repair*, 12(7), pp.459-465.

Bachand, F. (2007). Protein Arginine Methyltransferases: from Unicellular Eukaryotes to Humans. *Eukaryotic Cell*, 6(6), pp.889-898.

Batista, P., Molinie, B., Wang, J., Qu, K., Zhang, J., Li, L., Bouley, D., Lujan, E., Haddad, B., Daneshvar, K., Carter, A., Flynn, R., Zhou, C., Lim, K., Dedon, P., Wernig, M., Mullen, A., Xing, Y., Giallourakis, C. and Chang, H. (2014). m6A RNA Modification Controls Cell Fate Transition in Mammalian Embryonic Stem Cells. *Cell Stem Cell*, 15(6), pp.707-719.

Bedford, M. and Clarke, S. (2009). Protein Arginine Methylation in Mammals: Who, What, and Why. *Molecular Cell*, 33(1), pp.1-13.

Bedford, M., Frankel, A., Yaffe, M., Clarke, S., Leder, P. and Richard, S. (2000). Arginine Methylation Inhibits the Binding of Proline-rich Ligands to Src Homology 3, but Not WW, Domains. *Journal of Biological Chemistry*, 275(21), pp.16030-16036.

Bhat, S., Bielewicz, D., Jarmolowski, A. and Szweykowska-Kulinska, Z. (2018). N6-methyladenosine (m6A): Revisiting the Old with Focus on New, an Arabidopsis thaliana Centered Review. *Genes*, 9(12), p.596.

Blanc, R. and Richard, S. (2017). Arginine Methylation: The Coming of Age. *Molecular Cell*, 65(1), pp.8-24.

Boccaletto, P., Machnicka, M., Purta, E., Piątkowski, P., Bagiński, B., Wirecki, T., de Crécy-Lagard, V., Ross, R., Limbach, P., Kotter, A., Helm, M. and Bujnicki, J. (2017). MODOMICS: a database of RNA modification pathways. 2017 update. *Nucleic Acids Research*, 46(D1), pp.D303-D307.

Bodi, Z. and Fray, R. (2017). Detection and Quantification of N 6-Methyladenosine in Messenger RNA by TLC. In: A. Lusser, ed., *RNA Methylation - 2017*. New York: Humana Press, pp.79-87.

Bodi, Z., Button, J., Grierson, D. and Fray, R. (2010). Yeast targets for mRNA methylation. *Nucleic Acids Research*, 38(16), pp.5327-5335.

Bodi, Z., Zhong, S., Mehra, S., Song, J., Graham, N., Li, H., May, S. and Fray, R. (2012). Adenosine Methylation in Arabidopsis mRNA is Associated with the 3′ End and Reduced Levels Cause Developmental Defects. *Frontiers in Plant Science*, 3.

Boissel, S., Reish, O., Proulx, K., Kawagoe-Takaki, H., Sedgwick, B., Yeo, G., Meyre, D., Golzio, C., Molinari, F., Kadhom, N., Etchevers, H., Saudek, V., Farooqi, I., Froguel, P., Lindahl, T., O'Rahilly, S., Munnich, A. and Colleaux, L. (2009). Loss-of-Function Mutation in the Dioxygenase-Encoding FTO Gene Causes Severe Growth Retardation and Multiple Malformations. *The American Journal of Human Genetics*, 85(1), pp.106-111.

Bokar, J. (2005). The biosynthesis and functional roles of methylated nucleosides in eukaryotic mRNA. In: H. Grosjean, ed., *Fine-Tuning of RNA Functions by Modification and Editing*, 1st ed. Berlin: Springer, pp.141-177.

Bokar, J., Rath-Shambaugh, M., Ludwiczak, R., Narayan, P. and Rottman, F. (1994). Characterization and partial purification of mRNA N6-adenosine methyltransferase from HeLa cell nuclei. Internal mRNA methylation requires a multisubunit complex. *Journal of Biological Chemistry*, [online] 269(26), pp.17697-17704. Available at: http://www.jbc.org/content/269/26/17697.short [Accessed 29 Dec. 2015].

Bokar, J., Shambaugh, M., Polayes, D., Matera, A. and Rottman, F. (1997). Purification and cDNA cloning of the AdoMet-binding subunit of the human mRNA (N6-adenosine)-methyltransferase. *RNA*, [online] 3(11), pp.1233-1247. Available at: http://rnajournal.cshlp.org/content/3/11/1233.short [Accessed 29 Dec. 2015].

Bringmann, P. and Lührmann, R. (1987). Antibodies specific for N 6-methyladenosine react with intact snRNPs U2 and U4/U6. *FEBS Letters*, 213(2), pp.309-315.

Bujnicki, J., Feder, M., Radlinska, M. and Blumenthal, R. (2002). Structure Prediction and Phylogenetic Analysis of a Functionally Diverse Family of Proteins Homologous to the MT-A70 Subunit of the Human mRNA:m6A Methyltransferase. *Journal of Molecular Evolution*, 55(4), pp.431-444.

Camper, S., Albers, R., Coward, J. and Rottman, F. (1984). Effect of undermethylation on mRNA cytoplasmic appearance and half-life. *Molecular and Cellular Biology*, 4(3), pp.538-543.

Cantara, W., Crain, P., Rozenski, J., McCloskey, J., Harris, K., Zhang, X., Vendeix, F., Fabris, D. and Agris, P. (2010). The RNA modification database, RNAMDB: 2011 update. *Nucleic Acids Research*, 39(Database), pp.D195-D201.

Carroll, S., Narayan, P. and Rottman, F. (1990). N6-methyladenosine residues in an intron-specific region of prolactin pre-mRNA. *Molecular and Cellular Biology*, 10(9), pp.4456-4465.

Casalegno-Garduño, R., Schmitt, A., Wang, X., Xu, X. and Schmitt, M. (2010). Wilms' Tumor 1 as a Novel Target for Immunotherapy of Leukemia. *Transplantation Proceedings*, 42(8), pp.3309-3311.

Chen, D., Ma, H., Hong, H., Koh, S., Huang, S., Schurter, B., Aswad, D. and Stallcup, M. (1999). Regulation of Transcription by a Protein Methyltransferase. *Science*, 284(5423), pp.2174-2177.

Chen, K., Lu, Z., Wang, X., Fu, Y., Luo, G., Liu, N., Han, D., Dominissini, D., Dai, Q., Pan, T. and He, C. (2015). High-ResolutionN6-Methyladenosine (m6A) Map Using Photo-Crosslinking-Assisted m6A Sequencing. *Angewandte Chemie International Edition*, 54(5), pp.1587-1590.

Chen, T., Hao, Y., Zhang, Y., Li, M., Wang, M., Han, W., Wu, Y., Lv, Y., Hao, J., Wang, L., Li, A., Yang, Y., Jin, K., Zhao, X., Li, Y., Ping, X., Lai, W., Wu, L., Jiang, G., Wang, H., Sang, L., Wang, X., Yang, Y. and Zhou, Q. (2015). m6A RNA Methylation Is Regulated by MicroRNAs and Promotes Reprogramming to Pluripotency. *Cell Stem Cell*, 16(3), p.338.

Cho, S., Kim, S., Kim, J. and Kim, J. (2013). Targeted genome engineering in human cells with the Cas9 RNA-guided endonuclease. *Nature Biotechnology*, 31(3), pp.230-232.

Church, C., Lee, S., Bagg, E., McTaggart, J., Deacon, R., Gerken, T., Lee, A., Moir, L., Mecinović, J., Quwailid, M., Schofield, C., Ashcroft, F. and Cox, R. (2009). A Mouse Model for the Metabolic Effects of the Human Fat Mass and Obesity Associated FTO Gene. *PLoS Genetics*, 5(8), p.e1000599.

Church, C., Moir, L., McMurray, F., Girard, C., Banks, G., Teboul, L., Wells, S., Brüning, J., Nolan, P., Ashcroft, F. and Cox, R. (2010). Overexpression of Fto leads to increased food intake and results in obesity. *Nature Genetics*, 42(12), pp.1086-1092.

Clancy, M., Shambaugh, M., Timpte, C. and Bokar, J. (2002). Induction of sporulation in Saccharomyces cerevisiae leads to the formation of N6-methyladenosine in mRNA: a potential mechanism for the activity of the IME4 gene. *Nucleic Acids Research*, 30(20), pp.4509-4518.

Cohn, W. (1960). Pseudouridine, a carbon-carbon linked ribonucleoside in ribonucleic acids: isolation, structure, and chemical characteristics. *J. Biol. Chem.*, 235, pp.1488-1498.

Côté, J., Boisvert, F., Boulanger, M., Bedford, M. and Richard, S. (2003). Sam68 RNA Binding Protein Is an In Vivo Substrate for Protein Arginine N-Methyltransferase 1. *Molecular Biology of the Cell*, 14(1), pp.274-287.

Cui, Q., Shi, H., Ye, P., Li, L., Qu, Q., Sun, G., Sun, G., Lu, Z., Huang, Y., Yang, C., Riggs, A., He, C. and Shi, Y. (2017). m 6 A RNA Methylation Regulates the Self-Renewal and Tumorigenesis of Glioblastoma Stem Cells. *Cell Reports*, 18(11), pp.2622-2634.

Delatte, B., Wang, F., Ngoc, L., Collignon, E., Bonvin, E., Deplus, R., Calonne, E., Hassabi, B., Putmans, P., Awe, S., Wetzel, C., Kreher, J., Soin, R., Creppe, C., Limbach, P., Gueydan, C., Kruys, V., Brehm, A., Minakhina, S., Defrance, M., Steward Fuks F, R. and Fuks, F. (2016). RNA biochemistry. Transcriptome-wide distribution and function of RNA hydroxymethylcytosine. *Science*, 351, pp.282-285.

Deng, X., Gu, L., Liu, C., Lu, T., Lu, F., Lu, Z., Cui, P., Pei, Y., Wang, B., Hu, S. and Cao, X. (2010). Arginine methylation mediated by the Arabidopsis homolog of PRMT5 is essential for proper pre-mRNA splicing. *Proceedings of the National Academy of Sciences*, 107(44), pp.19114-19119.

Despres, B., Delseny, M. and Devic, M. (2001). Partial complementation of embryo defective mutations: a general strategy to elucidate gene function. *The Plant Journal*, 27(2), pp.149-159.

Desrosiers, R., Friderici, K. and Rottman, F. (1974). Identification of Methylated Nucleosides in Messenger RNA from Novikoff Hepatoma Cells. *Proceedings of the National Academy of Sciences*, 71(10), pp.3971-3975.

Deveau, H., Garneau, J. and Moineau, S. (2010). CRISPR/Cas System and Its Role in Phage-Bacteria Interactions. *Annual Review of Microbiology*, 64(1), pp.475-493.

Dominissini, D., Moshitch-Moshkovitz, S., Schwartz, S., Salmon-Divon, M., Ungar, L., Osenberg, S., Cesarkas, K., Jacob-Hirsch, J., Amariglio, N., Kupiec, M., Sorek, R. and Rechavi, G. (2012). Topology of the human and mouse m6A RNA methylomes revealed by m6A-seq. *Nature*, 485(7397), pp.201-206.

Dominissini, D., Nachtergaele, S., Moshitch-Moshkovitz, S., Peer, E., Kol, N., Ben-Haim, M., Dai, Q., Di Segni, A., Salmon-Divon, M., Clark, W., Zheng, G., Pan, T., Solomon, O., Eyal, E., Hershkovitz, V., Han, D., Doré, L., Amariglio, N., Rechavi, G. and He, C. (2016). The dynamic N1-methyladenosine methylome in eukaryotic messenger RNA. *Nature*, 530(7591), pp.441-446.

Du, H., Zhao, Y., He, J., Zhang, Y., Xi, H., Liu, M., Ma, J. and Wu, L. (2016). YTHDF2 destabilizes m6A-containing RNA through direct recruitment of the CCR4–NOT deadenylase complex. *Nature Communications*, 7(1).

Du, T., Rao, S., Wu, L., Ye, N., Liu, Z., Hu, H., Xiu, J., Shen, Y. and Xu, Q. (2015). An association study of the m6A genes with major depressive disorder in Chinese Han population. *Journal of Affective Disorders*, 183, pp.279-286.

Duan, H., Wei, L., Zhang, C., Wang, Y., Chen, L., Lu, Z., Chen, P., He, C. and Jia, G. (2017). ALKBH10B Is an RNA N6-Methyladenosine Demethylase Affecting Arabidopsis Floral Transition. *The Plant Cell*, 29(12), pp.2995-3011.

Dubin, D. and Taylor, R. (1975). The methylation state of poly A-containing-messenger RNA from cultured hamster cells. *Nucleic Acids Research*, 2(10), pp.1653-1668.

Edwards, K., Johnstone, C. and Thompson, C. (1991). A simple and rapid method for the preparation of plant genomic DNA for PCR analysis. *Nucleic Acids Research*, 19(6), pp.1349-1349.

Engler, C., Gruetzner, R., Kandzia, R. and Marillonnet, S. (2009). Golden Gate Shuffling: A One-Pot DNA Shuffling Method Based on Type IIs Restriction Enzymes. *PLoS ONE*, 4(5), p.e5553.

Fields, S. and Song, O. (1989). A novel genetic system to detect protein–protein interactions. *Nature*, 340(6230), pp.245-246.

Finkel, D. and Groner, Y. (1983). Methylations of adenosine residues (m6A) in pre-mRNA are important for formation of late simian virus 40 mRNAs. *Virology*, 131(2), pp.409-425.

Fischer, J., Koch, L., Emmerling, C., Vierkotten, J., Peters, T., Brüning, J. and Rüther, U. (2009). Inactivation of the Fto gene protects from obesity. *Nature*, 458(7240), pp.894-898.

Fisk, J. and Read, L. (2011). Protein Arginine Methylation in Parasitic Protozoa. *Eukaryotic Cell*, 10(8), pp.1013-1022.

Fray, R. and Simpson, G. (2015). The Arabidopsis epitranscriptome. *Current Opinion in Plant Biology*, 27, pp.17-21.

Frayling, T., Timpson, N., Weedon, M., Zeggini, E., Freathy, R., Lindgren, C., Perry, J., Elliott, K., Lango, H., Rayner, N., Shields, B., Harries, L., Barrett, J., Ellard, S., Groves, C., Knight, B., Patch, A., Ness, A., Ebrahim, S., Lawlor, D., Ring, S., Ben-Shlomo, Y., Jarvelin, M., Sovio, U., Bennett, A., Melzer, D., Ferrucci, L., Loos, R., Barroso, I., Wareham, N., Karpe, F., Owen, K., Cardon, L., Walker, M., Hitman, G., Palmer, C., Doney, A., Morris, A., Smith, G., Hattersley, A. and McCarthy, M. (2007). A common variant in the FTO gene is associated with body mass index and predisposes to childhood and adult obesity. *Science*, 316, pp.889–894.

Fu, Y., Dominissini, D., Rechavi, G. and He, C. (2014). Gene expression regulation mediated through reversible m6A RNA methylation. *Nat Rev Genet*, 15(5), pp.293-306.

Fustin, J., Doi, M., Yamaguchi, Y., Hida, H., Nishimura, S., Yoshida, M., Isagawa, T., Morioka, M., Kakeya, H., Manabe, I. and Okamura, H. (2013). RNA-Methylation-Dependent RNA Processing Controls the Speed of the Circadian Clock. *Cell*, 155(4), pp.793-806.

Gao, X., Shin, Y., Li, M., Wang, F., Tong, Q. and Zhang, P. (2010). The Fat Mass and Obesity Associated Gene FTO Functions in the Brain to Regulate Postnatal Growth in Mice. *PLoS ONE*, 5(11), p.e14005.

Gasiunas, G., Barrangou, R., Horvath, P. and Siksnys, V. (2012). Cas9-crRNA ribonucleoprotein complex mediates specific DNA cleavage for adaptive immunity in bacteria. *Proceedings of the National Academy of Sciences*, 109(39), pp.E2579-E2586.

Geula, S., Moshitch-Moshkovitz, S., Dominissini, D., Mansour, A., Kol, N., Salmon-Divon, M., Hershkovitz, V., Peer, E., Mor, N., Manor, Y., Ben-Haim, M., Eyal, E., Yunger, S., Pinto, Y., Jaitin, D., Viukov, S., Rais, Y., Krupalnik, V., Chomsky, E., Zerbib, M., Maza, I., Rechavi, Y., Massarwa, R., Hanna, S., Amit, I., Levanon, E., Amariglio, N., Stern-Ginossar, N., Novershtern, N., Rechavi, G. and Hanna, J. (2015). m6A mRNA methylation facilitates resolution of naïve pluripotency toward differentiation. *Science*, 347(6225), pp.1002-1006.

Goolam, M., Scialdone, A., Graham, S., Macaulay, I., Jedrusik, A., Hupalowska, A., Voet, T., Marioni, J. and Zernicka-Goetz, M. (2016). Heterogeneity in Oct4 and Sox2 Targets Biases Cell Fate in 4-Cell Mouse Embryos. *Cell*, 165(1), pp.61-74.

Gray, K., Yates, B., Seal, R., Wright, M. and Bruford, E. (2015). Genenames.org: the HGNC resources in 2015. *Nucleic Acids Research*, 43(D1), pp.D1079-D1085.

Grosjean, H. (2005). *Fine-Tuning of RNA Functions by Modification and Editing. Topics in Current Genetics, Volume 12*. Springer.

Guruswamy, S., Swamy, M., Choi, C., Steele, V. and Rao, C. (2008). S-adenosylL-methionine inhibits azoxymethane-induced colonic aberrant crypt foci in F344 rats and suppresses human colon cancer Caco-2 cell growth in 3D culture. *International Journal of Cancer*, 122(1), pp.25-30.

Gutierrez, R., Ewing, R., Cherry, J. and Green, P. (2002). Identification of unstable transcripts in Arabidopsis by cDNA microarray analysis: Rapid decay is associated with a group of touch- and specific clock-controlled genes. *Proceedings of the National Academy of Sciences*, 99(17), pp.11513-11518.

Harigaya, Y., Tanaka, H., Yamanaka, S., Tanaka, K., Watanabe, Y., Tsutsumi, C., Chikashige, Y., Hiraoka, Y., Yamashita, A. and Yamamoto, M. (2006). Selective elimination of messenger RNA prevents an incidence of untimely meiosis. *Nature*, 442(7098), pp.45-50.

HAUGLAND, R. and CLINE, M. (1980). Post-transcriptional Modifications of Oat Coleoptile Ribonucleic Acids. 5'-Terminal Capping and Methylation of Internal Nucleosides in Poly(A)-Rich RNA. *Eur J Biochem*, 104(1), pp.271-277.

Haussmann, I., Bodi, Z., Sanchez-Moran, E., Mongan, N., Archer, N., Fray, R. and Soller, M. (2016). m6A potentiates Sxl alternative pre-mRNA splicing for robust Drosophila sex determination. *Nature*, 540(7632), pp.301-304.

He, C. (2010). Grand Challenge Commentary: RNA epigenetics?. *Nature Chemical Biology*, 6(12), pp.863-865.

Hernando, C., Sanchez, S., Mancini, E. and Yanovsky, M. (2015). Genome wide comparative analysis of the effects of PRMT5 and PRMT4/CARM1 arginine methyltransferases on the Arabidopsis thaliana transcriptome. *BMC Genomics*, 16(1).

Herskowitz, I. (1987). Functional inactivation of genes by dominant negative mutations. *Nature*, 329(6136), pp.219-222.

Hess, M., Hess, S., Meyer, K., Verhagen, L., Koch, L., Brönneke, H., Dietrich, M., Jordan, S., Saletore, Y., Elemento, O., Belgardt, B., Franz, T., Horvath, T., Rüther, U., Jaffrey, S., Kloppenburg, P. and Brüning, J. (2013). The fat mass and obesity associated gene (Fto) regulates activity of the dopaminergic midbrain circuitry. *Nature Neuroscience*, 16(8), pp.1042-1048.

Himanen, K., Boucheron, E., Vanneste, S., de Almeida Engler, J., Inzé, D. and Beeckman, T. (2002). Auxin-Mediated Cell Cycle Activation during Early Lateral Root Initiation. *The Plant Cell*, 14(10), pp.2339-2351.

Hong, S., Song, H., Lutz, K., Kerstetter, R., Michael, T. and McClung, C. (2010). Type II protein arginine methyltransferase 5 (PRMT5) is required for circadian period determination in

Arabidopsis thaliana. *Proceedings of the National Academy of Sciences*, 107(49), pp.21211-21216.

Hongay, C. and Orr-Weaver, T. (2011). Drosophila Inducer of MEiosis 4 (IME4) is required for Notch signaling during oogenesis. *Proceedings of the National Academy of Sciences*, 108(36), pp.14855-14860.

Horiuchi, K., Kawamura, T., Iwanari, H., Ohashi, R., Naito, M., Kodama, T. and Hamakubo, T. (2013). Identification of Wilms' Tumor 1-associating Protein Complex and Its Role in Alternative Splicing and the Cell Cycle. *Journal of Biological Chemistry*, 288(46), pp.33292-33302.

Hsu, P., Zhu, Y., Ma, H., Guo, Y., Shi, X., Liu, Y., Qi, M., Lu, Z., Shi, H., Wang, J., Cheng, Y., Luo, G., Dai, Q., Liu, M., Guo, X., Sha, J., Shen, B. and He, C. (2017). Ythdc2 is an N6-methyladenosine binding protein that regulates mammalian spermatogenesis. *Cell Research*, 27(9), pp.1115-1127.

Huang, H., Weng, H., Zhou, K., Wu, T., Zhao, B., Sun, M., Chen, Z., Deng, X., Xiao, G., Auer, F., Klemm, L., Wu, H., Zuo, Z., Qin, X., Dong, Y., Zhou, Y., Qin, H., Tao, S., Du, J., Liu, J., Lu, Z., Yin, H., Mesquita, A., Yuan, C., Hu, Y., Sun, W., Su, R., Dong, L., Shen, C., Li, C., Qing, Y., Jiang, X., Wu, X., Sun, M., Guan, J., Qu, L., Wei, M., Müschen, M., Huang, G., He, C., Yang, J. and Chen, J. (2019). Histone H3 trimethylation at lysine 36 guides m6A RNA modification co-transcriptionally. *Nature*, 567(7748), pp.414-419.

Huang, J. and Yin, P. (2018). Structural Insights into N 6 -methyladenosine (m 6 A) Modification in the Transcriptome. *Genomics, Proteomics & Bioinformatics*, 16(2), pp.85-98.

Huang, J., Dong, X., Gong, Z., Qin, L., Yang, S., Zhu, Y., Wang, X., Zhang, D., Zou, T., Yin, P. and Tang, C. (2018). Solution structure of the RNA recognition domain of METTL3-METTL14 N6-methyladenosine methyltransferase. *Protein & Cell*, 10(4), pp.272-284.

Hülskamp, M., Miséra, S. and Jürgens, G. (1994). Genetic dissection of trichome cell development in Arabidopsis. *Cell*, 76(3), pp.555-566.

Hunt, A. (2014). The Arabidopsis polyadenylation factor subunit CPSF30 as conceptual link between mRNA polyadenylation and cellular signaling. *Current Opinion in Plant Biology*, 21, pp.128-132.

Ito, T., Chiba, T., Ozawa, R., Yoshida, M., Hattori, M. and Sakaki, Y. (2001). A comprehensive two-hybrid analysis to explore the yeast protein interactome. *Proceedings of the National Academy of Sciences*, 98(8), pp.4569-4574.

Iwanami, Y. and Brown, G. (1968). Methylated bases of ribosomal ribonucleic acid from HeLa cells. *Archives of Biochemistry and Biophysics*, 126(1), pp.8-15.

Iyer, L., Zhang, D. and Aravind, L. (2015). Adenine methylation in eukaryotes: Apprehending the complex evolutionary history and functional potential of an epigenetic modification. *BioEssays*, 38(1), pp.27-40.

Jia, G., Fu, Y. and He, C. (2013). Reversible RNA adenosine methylation in biological regulation. *Trends in Genetics*, 29(2), pp.108-115.

Jia, G., Fu, Y., Zhao, X., Dai, Q., Zheng, G., Yang, Y., Yi, C., Lindahl, T., Pan, T., Yang, Y. and He, C. (2011). N6-Methyladenosine in nuclear RNA is a major substrate of the obesity-associated FTO. *Nature Chemical Biology*, 7(12), pp.885-887.

Jinek, M., Chylinski, K., Fonfara, I., Hauer, M., Doudna, J. and Charpentier, E. (2012). A Programmable Dual-RNA-Guided DNA Endonuclease in Adaptive Bacterial Immunity. *Science*, 337(6096), pp.816-821.

Kahaka, G. (2010). *Analysis of a Putative RNA Methylase Family Member in Arabidopsis Thaliana*. PhD Thesis. The University of Nottingham.

Kan, L., Grozhik, A., Vedanayagam, J., Patil, D., Pang, N., Lim, K., Huang, Y., Joseph, B., Lin, C., Despic, V., Guo, J., Yan, D., Kondo, S., Deng, W., Dedon, P., Jaffrey, S. and Lai, E. (2017). The m6A pathway facilitates sex determination in Drosophila. *Nature Communications*, 8(1).

Kane, S. and Beemon, K. (1985). Precise localization of m6A in Rous sarcoma virus RNA reveals clustering of methylation sites: implications for RNA processing. *Molecular and Cellular Biology*, 5(9), pp.2298-2306.

Kane, S. and Beemon, K. (1987). Inhibition of methylation at two internal N6-methyladenosine sites caused by GAC to GAU mutations. *Journal of Biological Chemistry*, [online] 262(7), pp.3422-3427. Available at: http://www.jbc.org/content/262/7/3422.short [Accessed 3 Jan. 2016].

Ke, S., Alemu, E., Mertens, C., Gantman, E., Fak, J., Mele, A., Haripal, B., Zucker-Scharff, I., Moore, M., Park, C., Vågbø, C., Kusśnierczyk, A., Klungland, A., Darnell, J. and Darnell, R. (2015). A majority of m6A residues are in the last exons, allowing the potential for 3′ UTR regulation. *Genes & Development*, 29(19), pp.2037-2053.

Keith, G. (1995). Mobilities of modified ribonucleotides on two-dimensional cellulose thin-layer chromatography. *Biochimie*, 77(1-2), pp.142-144.

Keith, J., Ensinger, M. and Mose, B. (1978). HeLa cell RNA (2'-O-methyladenosine-N6-)-methyltransferase specific for the capped 5'-end of messenger RNA. *J. Biol. Chem.*, 253, pp.5033–5039.

Kennedy, T. and Lane, B. (1979). Wheat embryo ribonucleates. XIII. Methyl-substituted nucleoside constituents and 5′-terminal dinucleotide sequences in bulk poly(A)-rich RNA from imbibing wheat embryos. *Canadian Journal of Biochemistry*, 57(6), pp.927-931.

Knuckles, P., Lence, T., Haussmann, I., Jacob, D., Kreim, N., Carl, S., Masiello, I., Hares, T., Villaseñor, R., Hess, D., Andrade-Navarro, M., Biggiogera, M., Helm, M., Soller, M., Bühler, M. and Roignant, J. (2018). Zc3h13/Flacc is required for adenosine methylation by bridging the mRNA-binding factor Rbm15/Spenito to the m6A machinery component Wtap/Fl(2)d. *Genes & Development*, 32(5-6), pp.415-429.

Kouzarides, T. (2007). Chromatin Modifications and Their Function. *Cell*, 128(4), pp.693-705.

Krug, R., Morgan, M. and Shatkin, A. (1976). Influenza viral mRNA contains internal N6-methyladenosine and 5'-terminal 7-methylguanosine in cap structures. *Journal of Virology*, [online] 20(1), pp.45-53. Available at: http://jvi.asm.org/content/20/1/45.short [Accessed 29 Dec. 2015].

Lahav, R., Gammie, A., Tavazoie, S. and Rose, M. (2007). Role of Transcription Factor Kar4 in Regulating Downstream Events in the Saccharomyces cerevisiae Pheromone Response Pathway. *Molecular and Cellular Biology*, 27(3), pp.818-829.

Lee, D., Teyssier, C., Strahl, B. and Stallcup, M. (2005). Role of Protein Methylation in Regulation of Transcription. *Endocrine Reviews*, 26(2), pp.147-170.

Lee, Y. and Stallcup, M. (2009). Minireview: Protein Arginine Methylation of Nonhistone Proteins in Transcriptional Regulation. *Molecular Endocrinology*, 23(4), pp.425-433.

Lence, T., Akhtar, J., Bayer, M., Schmid, K., Spindler, L., Ho, C., Kreim, N., Andrade-Navarro, M., Poeck, B., Helm, M. and Roignant, J. (2016). m6A modulates neuronal functions and sex determination in Drosophila. *Nature*, 540(7632), pp.242-247.

Lesbirel, S., Viphakone, N., Parker, M., Parker, J., Heath, C., Sudbery, I. and Wilson, S. (2018). The m6A-methylase complex recruits TREX and regulates mRNA export. *Scientific Reports*, 8(1).

Levis, R. and Penman, S. (1978). 5′-Terminal structures of poly(A)+ cytoplasmic messenger RNA and of poly(A)+ and poly(A)− heterogeneous nuclear RNA of cells of the dipteran Drosophila melanogaster. *Journal of Molecular Biology*, 120(4), pp.487-515.

Li, D., Zhang, H., Hong, Y., Huang, L., Li, X., Zhang, Y., Ouyang, Z. and Song, F. (2014). Genome-Wide Identification, Biochemical Characterization, and Expression Analyses of the YTH Domain-Containing RNA-Binding Protein Family in Arabidopsis and Rice. *Plant Molecular Biology Reporter*, 32(6), pp.1169-1186.

Li, L., Zang, L., Zhang, F., Chen, J., Shen, H., Shu, L., Liang, F., Feng, C., Chen, D., Tao, H., Xu, T., Li, Z., Kang, Y., Wu, H., Tang, L., Zhang, P., Jin, P., Shu, Q. and Li, X. (2017). Fat mass and obesity-associated (FTO) protein regulates adult neurogenesis. *Human Molecular Genetics*, 26(13), pp.2398-2411.

Li, M., Zhao, X., Wang, W., Shi, H., Pan, Q., Lu, Z., Perez, S., Suganthan, R., He, C., Bjørås, M. and Klungland, A. (2018). Ythdf2-mediated m6A mRNA clearance modulates neural development in mice. *Genome Biology*, 19(1).

Li, X., Xiong, X. and Yi, C. (2017). Erratum: Epitranscriptome sequencing technologies: decoding RNA modifications. *Nature Methods*, 14(3), pp.323-323.

Li, X., Zhu, P., Ma, S., Song, J., Bai, J., Sun, F. and Yi, C. (2015). Chemical pulldown reveals dynamic pseudouridylation of the mammalian transcriptome. *Nature Chemical Biology*, 11(8), pp.592-597.

Li, Y., Wang, X., Li, C., Hu, S., Yu, J. and Song, S. (2014). Transcriptome-wide N6-methyladenosine profiling of rice callus and leaf reveals the presence of tissue-specific competitors involved in selective mRNA modification. *RNA Biology*, 11(9), pp.1180-1188.

Liang, Z., Geng, Y. and Gu, X. (2018). Adenine Methylation: New Epigenetic Marker of DNA and mRNA. *Molecular Plant*, 11(10), pp.1219-1221.

Liao, S., Sun, H. and Xu, C. (2018). YTH Domain: A Family of N 6 -methyladenosine (m 6 A) Readers. *Genomics, Proteomics & Bioinformatics*, 16(2), pp.99-107.

Lin, S., Choe, J., Du, P., Triboulet, R. and Gregory, R. (2016). The m 6 A Methyltransferase METTL3 Promotes Translation in Human Cancer Cells. *Molecular Cell*, 62(3), pp.335-345.

Linder, B., Grozhik, A., Olarerin-George, A., Meydan, C., Mason, C. and Jaffrey, S. (2015). Single-nucleotide-resolution mapping of m6A and m6Am throughout the transcriptome. *Nature Methods*, 12(8), pp.767-772.

Linnebacher, M., Wienck, A., Boeck, I. and Klar, E. (2010). Identification of an MSI-H Tumor-Specific Cytotoxic T Cell Epitope Generated by the (−1) Frame ofU79260(FTO). *Journal of Biomedicine and Biotechnology*, 2010, pp.1-6.

Little, N., Hastie, N. and Davies, R. (2000). Identification of WTAP, a novel Wilms' tumour 1-associating protein. *Human Molecular Genetics*, 9(15), pp.2231-2239.

Liu, J. and Jia, G. (2014). Methylation Modifications in Eukaryotic Messenger RNA. *Journal of Genetics and Genomics*, 41(1), pp.21-33.

Liu, J., Yue, Y., Han, D., Wang, X., Fu, Y., Zhang, L., Jia, G., Yu, M., Lu, Z., Deng, X., Dai, Q., Chen, W. and He, C. (2013). A METTL3–METTL14 complex mediates mammalian nuclear RNA N6-adenosine methylation. *Nature Chemical Biology*, 10(2), pp.93-95.

Liu, N., Parisien, M., Dai, Q., Zheng, G., He, C. and Pan, T. (2013). Probing N6-methyladenosine RNA modification status at single nucleotide resolution in mRNA and long noncoding RNA. *RNA*, 19(12), pp.1848-1856.

Loos, R. and Yeo, G. (2013). The bigger picture of FTO—the first GWAS-identified obesity gene. *Nature Reviews Endocrinology*, 10(1), pp.51-61.

Lu, S., Ramani, K., Ou, X., Lin, M., Yu, V., Ko, K., Park, R., Bottiglieri, T., Tsukamoto, H., Kanel, G., French, S., Mato, J., Moats, R. and Grant, E. (2009). S-adenosylmethionine in the chemoprevention and treatment of hepatocellular carcinoma in a rat model. *Hepatology*, 50(2), pp.462-471.

Luo, G., MacQueen, A., Zheng, G., Duan, H., Dore, L., Lu, Z., Liu, J., Chen, K., Jia, G., Bergelson, J. and He, C. (2014). Unique features of the m6A methylome in Arabidopsis thaliana. *Nature Communications*, 5(1).

Luo, J., Liu, H., Luan, S., He, C. and Li, Z. (2018). Aberrant Regulation of mRNA m6A Modification in Cancer Development. *International Journal of Molecular Sciences*, 19(9), p.2515.

Machnicka, M., Milanowska, K., Osman Oglou, O., Purta, E., Kurkowska, M., Olchowik, A., Januszewski, W., Kalinowski, S., Dunin-Horkawicz, S., Rother, K., Helm, M., Bujnicki, J. and Grosjean, H. (2013). MODOMICS: a database of RNA modification pathways—2013 update. *Nucleic Acids Research*, 41(D1), pp.D262-D267.

Maity, A. and Das, B. (2015). N 6-methyladenosine modification in mRNA : machinery, function and implications for health and diseases. *The FEBS Journal*, 283(9), pp.1607-1630.

Martínez-Pérez, M., Aparicio, F., López-Gresa, M., Bellés, J., Sánchez-Navarro, J. and Pallás, V. (2017). Arabidopsism6A demethylase activity modulates viral infection of a plant virus and the m6A abundance in its genomic RNAs. *Proceedings of the National Academy of Sciences*, 114(40), pp.10755-10760.

Mas, J., Noël, E. and Ober, E. (2011). Chromatin Modification in Zebrafish Development. In: H. DETRICH, M. Westerfield and L. Zon, ed., *The zebrafish: genetics, genomics and informatics*. London: Elsevier, pp.401-428.

Matsuoka, S., Ballif, B., Smogorzewska, A., McDonald, E., Hurov, K., Luo, J., Bakalarski, C., Zhao, Z., Solimini, N., Lerenthal, Y., Shiloh, Y., Gygi, S. and Elledge, S. (2007). ATM and ATR Substrate Analysis Reveals Extensive Protein Networks Responsive to DNA Damage. *Science*, 316(5828), pp.1160-1166.

Mauer, J., Luo, X., Blanjoie, A., Jiao, X., Grozhik, A., Patil, D., Linder, B., Pickering, B., Vasseur, J., Chen, Q., Gross, S., Elemento, O., Debart, F., Kiledjian, M. and Jaffrey, S. (2016). Reversible methylation of m6Am in the 5′ cap controls mRNA stability. *Nature*, 541(7637), pp.371-375.

McBride, A. and Silver, P. (2001). State of the Arg;Protein Methylation at Arginine Comes of Age. *Cell*, 106(1), pp.5-8.

McMurray, F., Church, C., Larder, R., Nicholson, G., Wells, S., Teboul, L., Tung, Y., Rimmington, D., Bosch, F., Jimenez, V., Yeo, G., O'Rahilly, S., Ashcroft, F., Coll, A. and Cox, R. (2013). Adult Onset Global Loss of the Fto Gene Alters Body Composition and Metabolism in the Mouse. *PLoS Genetics*, 9(1), p.e1003166.

Meyer, K., Patil, D., Zhou, J., Zinoviev, A., Skabkin, M., Elemento, O., Pestova, T., Qian, S. and Jaffrey, S. (2015). 5′ UTR m6A Promotes Cap-Independent Translation. *Cell*, 163(4), pp.999-1010.

Meyer, K., Saletore, Y., Zumbo, P., Elemento, O., Mason, C. and Jaffrey, S. (2012). Comprehensive Analysis of mRNA Methylation Reveals Enrichment in 3′ UTRs and near Stop Codons. *Cell*, 149(7), pp.1635-1646.

Mielecki, D., Zugaj, D., Muszewska, A., Piwowarski, J., Chojnacka, A., Mielecki, M., Nieminuszczy, J., Grynberg, M. and Grzesiuk, E. (2012). Novel AlkB Dioxygenases—Alternative Models for In Silico and In Vivo Studies. *PLoS ONE*, 7(1), p.e30588.

Molinie, B., Wang, J., Lim, K., Hillebrand, R., Lu, Z., Van Wittenberghe, N., Howard, B., Daneshvar, K., Mullen, A., Dedon, P., Xing, Y. and Giallourakis, C. (2016). m6A-LAIC-seq reveals the census and complexity of the m6A epitranscriptome. *Nature Methods*, 13(8), pp.692-698.

Nachtergaele, S. and He, C. (2017). The emerging biology of RNA post-transcriptional modifications. *RNA Biology*, 14(2), pp.156-163.

Narsai, R., Howell, K., Millar, A., O'Toole, N., Small, I. and Whelan, J. (2007). Genome-Wide Analysis of mRNA Decay Rates and Their Determinants in Arabidopsis thaliana. *The Plant Cell*, 19(11), pp.3418-3436.

Nichols, J. (1979). 'Cap' structures in maize poly(A)-containing RNA. *Biochimica et Biophysica Acta (BBA) - Nucleic Acids and Protein Synthesis*, 563(2), pp.490-495.

Niessen, M., Schneiter, R. and Nothiger, R. (2001). Molecular identification of virilizer, a gene required for the expression of the sex-determining gene Sex-lethal in Drosophila melanogaster. *Genetics*, 157, pp.679–688.

Nishikura, K. (2010). Functions and Regulation of RNA Editing by ADAR Deaminases. *Annual Review of Biochemistry*, 79(1), pp.321-349.

Niu, L., Lu, F., Pei, Y., Liu, C. and Cao, X. (2007). Regulation of flowering time by the protein arginine methyltransferase AtPRMT10. *EMBO reports*, 8(12), pp.1190-1195.

Niu, L., Zhang, Y., Pei, Y., Liu, C. and Cao, X. (2008). Redundant Requirement for a Pair of PROTEIN ARGININE METHYLTRANSFERASE4 Homologs for the Proper Regulation of Arabidopsis Flowering Time. *Plant Physiology*, 148(1), pp.490-503.

Noack, F. and Calegari, F. (2018). Epitranscriptomics: A New Regulatory Mechanism of Brain Development and Function. *Frontiers in Neuroscience*, 12.

Ok, S., Jeong, H., Bae, J., Shin, J., Luan, S. and Kim, K. (2005). Novel CIPK1-Associated Proteins in Arabidopsis Contain an Evolutionarily Conserved C-Terminal Region That Mediates Nuclear Localization. *Plant Physiology*, 139(1), pp.138-150.

Paik, W., Paik, D. and Kim, S. (2007). Historical review: the field of protein methylation. *Trends in Biochemical Sciences*, 32(3), pp.146-152.

Pakneshan, P., Szyf, M., Farias-Eisner, R. and Rabbani, S. (2004). Reversal of the Hypomethylation Status of Urokinase (uPA) Promoter Blocks Breast Cancer Growth and Metastasis. *Journal of Biological Chemistry*, 279(30), pp.31735-31744.

Pascale, R., Simile, M., De Miglio, M. and Feo, F. (2002). Chemoprevention of hepatocarcinogenesis. *Alcohol*, 27(3), pp.193-198.

Patil, D., Chen, C., Pickering, B., Chow, A., Jackson, C., Guttman, M. and Jaffrey, S. (2016). m6A RNA methylation promotes XIST-mediated transcriptional repression. *Nature*, 537(7620), pp.369-373.

Pei, Y., Niu, L., Lu, F., Liu, C., Zhai, J., Kong, X. and Cao, X. (2007). Mutations in the Type II Protein Arginine Methyltransferase AtPRMT5 Result in Pleiotropic Developmental Defects in Arabidopsis. *Plant Physiology*, 144(4), pp.1913-1923.

Penalva, L., Ruiz, M., Ortega, A., Granadino, B., Vicente, L., Segarra, C., Valcárcel, J. and Sánchez, L. (2000). The Drosophila fl(2)d gene, required for female-specific splicing of Sxl and tra pre-mRNAs, encodes a novel nuclear protein with a HQ-rich domain. *Genetics 155*, 155, pp.129-139.

Perry, R., Kelley, D., Friderici, K. and Rottman, F. (1975). The methylated constituents of L cell messenger RNA: Evidence for an unusual cluster at the 5′ terminus. *Cell*, 4(4), pp.387-394.

Ping, X., Sun, B., Wang, L., Xiao, W., Yang, X., Wang, W., Adhikari, S., Shi, Y., Lv, Y., Chen, Y., Zhao, X., Li, A., Yang, Y., Dahal, U., Lou, X., Liu, X., Huang, J., Yuan, W., Zhu, X., Cheng, T., Zhao, Y., Wang, X., Danielsen, J., Liu, F. and Yang, Y. (2014). Mammalian WTAP is a regulatory subunit of the RNA N6-methyladenosine methyltransferase. *Cell Research*, 24(2), pp.177-189.

Porteus, M. (2003). Chimeric Nucleases Stimulate Gene Targeting in Human Cells. *Science*, 300(5620), pp.763-763.

Ramani, K., Yang, H., Kuhlenkamp, J., Tomasi, L., Tsukamoto, H., Mato, J. and Lu, S. (2009). Changes in the expression of methionine adenosyltransferase genes and S-adenosylmethionine homeostasis during hepatic stellate cell activation. *Hepatology*, p.NA-NA.

Raposo, A. and Piller, S. (2018). Protein arginine methylation: an emerging regulator of the cell cycle. *Cell Division*, 13(1).

ROHDE, A., VAN MONTAGU, M. and BOERJAN, W. (1999). The ABSCISIC ACID-INSENSITIVE 3 (ABI3) gene is expressed during vegetative quiescence processes in Arabidopsis. *Plant, Cell and Environment*, 22(3), pp.261-270.

Roost, C., Lynch, S., Batista, P., Qu, K., Chang, H. and Kool, E. (2015). Structure and Thermodynamics of N6-Methyladenosine in RNA: A Spring-Loaded Base Modification. *Journal of the American Chemical Society*, 137(5), pp.2107-2115.

Rottman, F., Shatkin, A. and Perry, R. (1974). Sequences containing methylated nucleotides at the 5′ termini of messenger RNAs: Possible implications for processing. *Cell*, 3(3), pp.197-199.

Roundtree, I., Evans, M., Pan, T. and He, C. (2017). Dynamic RNA Modifications in Gene Expression Regulation. *Cell*, 169(7), pp.1187-1200.

Růžička, K., Zhang, M., Campilho, A., Bodi, Z., Kashif, M., Saleh, M., Eeckhout, D., El-Showk, S., Li, H., Zhong, S., De Jaeger, G., Mongan, N., Hejátko, J., Helariutta, Y. and Fray, R. (2017). Identification of factors required for m6A mRNA methylation in Arabidopsis reveals a role for the conserved E3 ubiquitin ligase HAKAI. *New Phytologist*, 215(1), pp.157-172.

Saletore, Y., Meyer, K., Korlach, J., Vilfan, I., Jaffrey, S. and Mason, C. (2012). The birth of the Epitranscriptome: deciphering the function of RNA modifications. *Genome Biology*, 13(10), p.175.

Saneyoshi, M., Harada, F. and Nishimura, S. (1969). Isolation and characterization of N6-methyladenosine from Escherichia coli valine transfer RNA. *Biochimica et Biophysica Acta (BBA) - Nucleic Acids and Protein Synthesis*, 190(2), pp.264-273.

Sanjana, N., Cong, L., Zhou, Y., Cunniff, M., Feng, G. and Zhang, F. (2012). A transcription activator-like effector toolbox for genome engineering. *Nature Protocols*, 7(1), pp.171-192.

Scavetta, R. (2000). Structure of RsrI methyltransferase, a member of the N6-adenine beta class of DNA methyltransferases. *Nucleic Acids Research*, 28(20), pp.3950-3961.

Schibler, U. and Perry, R. (1977). The 5′-termini of heterogeneous nuclear RNA: a comparison among molecules of different sizes and ages. *Nucleic Acids Research*, 4(12), pp.4133-4150.

Schibler, U., Kelley, D. and Perry, R. (1977). Comparison of methylated sequences in messenger RNA and heterogeneous nuclear RNA from mouse L cells. *Journal of Molecular Biology*, 115(4), pp.695-714.

Schmitt, M., Brown, T. and Trumpower, B. (1990). A rapid and simple method for preparation of RNA fromSaccharomyces cerevisiae. *Nucleic Acids Research*, 18(10), pp.3091-3092.

Schurter, B., Koh, S., Chen, D., Bunick, G., Harp, J., Hanson, B., Henschen-Edman, A., Mackay, D., Stallcup, M. and Aswad, D. (2001). Methylation of Histone H3 by Coactivator-Associated Arginine Methyltransferase 1†. *Biochemistry*, 40(19), pp.5747-5756.

Schütt, C. and Nöthiger, R. (2000). Structure, function and evolution of sex-determining systems in Dipteran insects. *Development*, 127, pp.667-677.

Schwartz, S., Agarwala, S., Mumbach, M., Jovanovic, M., Mertins, P., Shishkin, A., Tabach, Y., Mikkelsen, T., Satija, R., Ruvkun, G., Carr, S., Lander, E., Fink, G. and Regev, A. (2013). High-Resolution Mapping Reveals a Conserved, Widespread, Dynamic mRNA Methylation Program in Yeast Meiosis. *Cell*, 155(6), pp.1409-1421.

Schwartz, S., Mumbach, M., Jovanovic, M., Wang, T., Maciag, K., Bushkin, G., Mertins, P., Ter-Ovanesyan, D., Habib, N., Cacchiarelli, D., Sanjana, N., Freinkman, E., Pacold, M., Satija, R., Mikkelsen, T., Hacohen, N., Zhang, F., Carr, S., Lander, E. and Regev, A. (2014). Perturbation of m6A Writers Reveals Two Distinct Classes of mRNA Methylation at Internal and 5′ Sites. *Cell Reports*, 8(1), pp.284-296.

Shah, J. and Clancy, M. (1992). IME4, a gene that mediates MAT and nutritional control of meiosis in Saccharomyces cerevisiae. *Molecular and Cellular Biology*, 12(3), pp.1078-1086.

Shen, L., Liang, Z. and Yu, H. (2016). N6-Methyladenosine RNA Modification Regulates Shoot Stem Cell Fate in Arabidopsis. *Mechanisms of Development*, 145, p.S171.

Sinha, R., Allemand, E., Zhang, Z., Karni, R., Myers, M. and Krainer, A. (2010). Arginine Methylation Controls the Subcellular Localization and Functions of the Oncoprotein Splicing Factor SF2/ASF. *Molecular and Cellular Biology*, 30(11), pp.2762-2774.

Śledź, P. and Jinek, M. (2016). Structural insights into the molecular mechanism of the m6A writer complex. *eLife*, 5.

Squires, J., Patel, H., Nousch, M., Sibbritt, T., Humphreys, D., Parker, B., Suter, C. and Preiss, T. (2012). Widespread occurrence of 5-methylcytosine in human coding and non-coding RNA. *Nucleic Acids Research*, 40(11), pp.5023-5033.

Stoltzfus, C. and Dane, R. (1982). Accumulation of Spliced Avian Retrovirus mRNA Is Inhibited in S-Adenosylmethionine-Depleted Chicken Embryo Fibroblasts. *Journal of Virology*, [online] 42(3), pp.918-931. Available at: http://jvi.asm.org/content/42/3/918.short [Accessed 3 Jan. 2016].

Strahl, B. and Allis, C. (2000). The language of covalent histone modifications. *Nature*, 403(6765), pp.41-45.

Strahl, B., Grant, P., Briggs, S., Sun, Z., Bone, J., Caldwell, J., Mollah, S., Cook, R., Shabanowitz, J., Hunt, D. and Allis, C. (2002). Set2 Is a Nucleosomal Histone H3-Selective Methyltransferase That Mediates Transcriptional Repression. *Molecular and Cellular Biology*, 22(5), pp.1298-1306.

Sun, X., Wei, J., Wu, X., Hu, M., Wang, L., Wang, H., Zhang, Q., Chen, S., Huang, Q. and Chen, Z. (2005). Identification and Characterization of a Novel Human Histone H3 Lysine 36-specific Methyltransferase. *Journal of Biological Chemistry*, 280(42), pp.35261-35271.

Suzuki, M. and Bird, A. (2008). DNA methylation landscapes: provocative insights from epigenomics. *Nature Reviews Genetics*, 9(6), pp.465-476.

Tang, Y., Chen, K., Wu, X., Wei, Z., Zhang, S., Song, B., Zhang, S., Huang, Y. and Meng, J. (2019). DRUM: Inference of Disease-Associated m6A RNA Methylation Sites From a Multi-Layer Heterogeneous Network. *Frontiers in Genetics*, 10.

Taverna, S., Li, H., Ruthenburg, A., Allis, C. and Patel, D. (2007). How chromatin-binding modules interpret histone modifications: lessons from professional pocket pickers. *Nature Structural & Molecular Biology*, 14(11), pp.1025-1040.

Tzafrir, I., Pena-Muralla, R., Dickerman, A., Berg, M., Rogers, R., Hutchens, S., Sweeney, T., McElver, J., Aux, G., Patton, D. and Meinke, D. (2004). Identification of Genes Required for Embryo Development in Arabidopsis. *Plant Physiology*, 135(3), pp.1206-1220.

Vespa, L., Vachon, G., Berger, F., Perazza, D., Faure, J. and Herzog, M. (2004). The Immunophilin-Interacting Protein AtFIP37 from Arabidopsis Is Essential for Plant Development and Is Involved in Trichome Endoreduplication. *Plant Physiology*, 134(4), pp.1283-1292.

Wan, B., Shi, Y. and Huo, K. (2006). An improved yeast two-hybrid approach for detection of interacting proteins. *Frontiers of Biology in China*, 1(2), pp.120-126.

Wang, P., Doxtader, K. and Nam, Y. (2016). Structural Basis for Cooperative Function of Mettl3 and Mettl14 Methyltransferases. *Molecular Cell*, 63(2), pp.306-317.

Wang, X., Feng, J., Xue, Y., Guan, Z., Zhang, D., Liu, Z., Gong, Z., Wang, Q., Huang, J., Tang, C., Zou, T. and Yin, P. (2016). Structural basis of N6-adenosine methylation by the METTL3–METTL14 complex. *Nature*, 534(7608), pp.575-578.

Wang, X., Lu, Z., Gomez, A., Hon, G., Yue, Y., Han, D., Fu, Y., Parisien, M., Dai, Q., Jia, G., Ren, B., Pan, T. and He, C. (2014). N6-methyladenosine-dependent regulation of messenger RNA stability. *Nature*, 505(7481), pp.117-120.

Wang, X., Zhao, B., Roundtree, I., Lu, Z., Han, D., Ma, H., Weng, X., Chen, K., Shi, H. and He, C. (2015). N6-methyladenosine Modulates Messenger RNA Translation Efficiency. *Cell*, 161(6), pp.1388-1399.

Wang, Y. and Zhao, J. (2016). Update: Mechanisms Underlying N 6 -Methyladenosine Modification of Eukaryotic mRNA. *Trends in Genetics*, 32(12), pp.763-773.

Wang, Y., Li, Y., Toth, J., Petroski, M., Zhang, Z. and Zhao, J. (2014). N6-methyladenosine modification destabilizes developmental regulators in embryonic stem cells. *Nature Cell Biology*, 16(2), pp.191-198.

Wei, C. and Moss, B. (1977). Nucleotide sequences at the N6-methyladenosine sites of HeLa cell messenger ribonucleic acid. *Biochemistry*, 16(8), pp.1672-1676.

Wei, C., Gershowitz, A. and Moss, B. (1975). Methylated nucleotides block 5′ terminus of HeLa cell messenger RNA. *Cell*, 4(4), pp.379-386.

Wei, C., Gershowitz, A. and Moss, B. (1976). 5'-Terminal and internal methylated nucleotide sequences in HeLa cell mRNA. *Biochemistry*, 15(2), pp.397-401.

Wei, L., Song, P., Wang, Y., Lu, Z., Tang, Q., Yu, Q., Xiao, Y., Zhang, X., Duan, H. and Jia, G. (2018). The m6A Reader ECT2 Controls Trichome Morphology by Affecting mRNA Stability in Arabidopsis. *The Plant Cell*, 30(5), pp.968-985.

Wen, J., Lv, R., Ma, H., Shen, H., He, C., Wang, J., Jiao, F., Liu, H., Yang, P., Tan, L., Lan, F., Shi, Y., He, C., Shi, Y. and Diao, J. (2018). Zc3h13 Regulates Nuclear RNA m6A Methylation and Mouse Embryonic Stem Cell Self-Renewal. *Molecular Cell*, 69(6), pp.1028-1038.e6.

Whetstine, J., Nottke, A., Lan, F., Huarte, M., Smolikov, S., Chen, Z., Spooner, E., Li, E., Zhang, G., Colaiacovo, M. and Shi, Y. (2006). Reversal of Histone Lysine Trimethylation by the JMJD2 Family of Histone Demethylases. *Cell*, 125(3), pp.467-481.

Wickramasinghe, V. and Laskey, R. (2015). Control of mammalian gene expression by selective mRNA export. *Nature Reviews Molecular Cell Biology*, 16(7), pp.431-442.

Wood, A., Lo, T., Zeitler, B., Pickle, C., Ralston, E., Lee, A., Amora, R., Miller, J., Leung, E., Meng, X., Zhang, L., Rebar, E., Gregory, P., Urnov, F. and Meyer, B. (2011). Targeted Genome Editing Across Species Using ZFNs and TALENs. *Science*, 333(6040), pp.307-307.

Wulff, B., Sakurai, M. and Nishikura, K. (2010). Elucidating the inosinome: global approaches to adenosine-to-inosine RNA editing. *Nature Reviews Genetics*, 12(2), pp.81-85.

Xiao, W., Adhikari, S., Dahal, U., Chen, Y., Hao, Y., Sun, B., Sun, H., Li, A., Ping, X., Lai, W., Wang, X., Ma, H., Huang, C., Yang, Y., Huang, N., Jiang, G., Wang, H., Zhou, Q., Wang, X., Zhao, Y. and Yang, Y. (2016). Nuclear m 6 A Reader YTHDC1 Regulates mRNA Splicing. *Molecular Cell*, 61(4), pp.507-519.

Xu, C., Wang, X., Liu, K., Roundtree, I., Tempel, W., Li, Y., Lu, Z., He, C. and Min, J. (2014). Structural basis for selective binding of m6A RNA by the YTHDC1 YTH domain. *Nature Chemical Biology*, 10(11), pp.927-929.

Yang, X., Yang, Y., Sun, B., Chen, Y., Xu, J., Lai, W., Li, A., Wang, X., Bhattarai, D., Xiao, W., Sun, H., Zhu, Q., Ma, H., Adhikari, S., Sun, M., Hao, Y., Zhang, B., Huang, C., Huang, N., Jiang, G., Zhao, Y., Wang, H., Sun, Y. and Yang, Y. (2017). 5-methylcytosine promotes mRNA export — NSUN2 as the methyltransferase and ALYREF as an m5C reader. *Cell Research*, 27(5), pp.606-625.

Yang, Y. and Bedford, M. (2012). Protein arginine methyltransferases and cancer. *Nature Reviews Cancer*, 13(1), pp.37-50.

Yang, Y., Hsu, P., Chen, Y. and Yang, Y. (2018). Dynamic transcriptomic m6A decoration: writers, erasers, readers and functions in RNA metabolism. *Cell Research*, 28(6), pp.616-624.

Yang, Y., Sun, B., Xiao, W., Yang, X., Sun, H., Zhao, Y. and Yang, Y. (2015). Dynamic m 6 A modification and its emerging regulatory role in mRNA splicing. *Science Bulletin*, 60(1), pp.21-32.

Yi, C. and Pan, T. (2011). Cellular Dynamics of RNA Modification. *Accounts of Chemical Research*, 44(12), pp.1380-1388.

Yoon, K., Ringeling, F., Vissers, C., Jacob, F., Pokrass, M., Jimenez-Cyrus, D., Su, Y., Kim, N., Zhu, Y., Zheng, L., Kim, S., Wang, X., Doré, L., Jin, P., Regot, S., Zhuang, X., Canzar, S., He, C., Ming, G. and Song, H. (2018). Temporal Control of Mammalian Cortical Neurogenesis by m(6)A Methylation. *Cell.*, 171, pp.877–889.

Zhang, C., Fu, J. and Zhou, Y. (2019). A Review in Research Progress Concerning m6A Methylation and Immunoregulation. *Frontiers in Immunology*, 10.

Zhang, K., Tang, H., Huang, L., Blankenship, J., Jones, P., Xiang, F., Yau, P. and Burlingame, A. (2002). Identification of Acetylation and Methylation Sites of Histone H3 from Chicken Erythrocytes by High-Accuracy Matrix-Assisted Laser Desorption Ionization–Time-of-Flight, Matrix-Assisted Laser Desorption Ionization–Postsource Decay, and Nanoelectrospray Ionization Tandem Mass Spectrometry. *Analytical Biochemistry*, 306(2), pp.259-269.

Zhao, B. and He, C. (2015). Fate by RNA methylation: m6A steers stem cell pluripotency. *Genome Biology*, 16(1), p.43.

Zhao, B., Roundtree, I. and He, C. (2017). Post-transcriptional gene regulation by mRNA modifications. *Nature Reviews Molecular Cell Biology*, 18(1), pp.31-42.

Zhao, X., Yang, Y., Sun, B., Shi, Y., Yang, X., Xiao, W., Hao, Y., Ping, X., Chen, Y., Wang, W., Jin, K., Wang, X., Huang, C., Fu, Y., Ge, X., Song, S., Jeong, H., Yanagisawa, H., Niu, Y., Jia,

G., Wu, W., Tong, W., Okamoto, A., He, C., Danielsen, J., Wang, X. and Yang, Y. (2014). FTO-dependent demethylation of N6-methyladenosine regulates mRNA splicing and is required for adipogenesis. *Cell Research*, 24(12), pp.1403-1419.

Zheng, G., Dahl, J., Niu, Y., Fedorcsak, P., Huang, C., Li, C., Vågbø, C., Shi, Y., Wang, W., Song, S., Lu, Z., Bosmans, R., Dai, Q., Hao, Y., Yang, X., Zhao, W., Tong, W., Wang, X., Bogdan, F., Furu, K., Fu, Y., Jia, G., Zhao, X., Liu, J., Krokan, H., Klungland, A., Yang, Y. and He, C. (2013). ALKBH5 Is a Mammalian RNA Demethylase that Impacts RNA Metabolism and Mouse Fertility. *Molecular Cell*, 49(1), pp.18-29.

Zhong, S., Li, H., Bodi, Z., Button, J., Vespa, L., Herzog, M. and Fray, R. (2008). MTA Is an Arabidopsis Messenger RNA Adenosine Methylase and Interacts with a Homolog of a Sex-Specific Splicing Factor. *THE PLANT CELL ONLINE*, 20(5), pp.1278-1288.

Zhou, J., Wan, J., Gao, X., Zhang, X., Jaffrey, S. and Qian, S. (2015). Dynamic m6A mRNA methylation directs translational control of heat shock response. *Nature*, 526(7574), pp.591-594.

Zurita-Lopez, C., Sandberg, T., Kelly, R. and Clarke, S. (2012). Human Protein Arginine Methyltransferase 7 (PRMT7) Is a Type III Enzyme Forming ω-NG-Monomethylated Arginine Residues. *Journal of Biological Chemistry*, 287(11), pp.7859-7870.

APPENDICES

Appendix I

Primers used in this study and their sequences. These primers were designed from the sequences of genes.

Primer name	Sequence (5′ to 3′)
LB-SALK	CAGAAATGGATAAATAGCCTTGCTTCC
Intron 1	GGACCTTGTGGGTAAAGTTAC
Intron 3	GCTCCTATACAAAGAGAAACC
MTBatgstart	AAATGAAGAAGAAACAAGAAGAG
MTBnoStop	ATTAAAGCCGTACATGTCAA
B-sequence-FW	CGTTCCAAGGAGCACTGCTTG
MTB-GK-FW	GGACCTTGTGGGTAAAGTTACC
MTB-GK-Rev	GTGGATAACCCAAGACTAATCC
MTBForKoz	aaaCaATGAAGAAGAAACAAGAAGAGAG
MTBmutBamRev	ggaTCCCcgGGTGGGgCAACAAGAATAACATCAAAC
MTBmutFor	CCACCcgGGGAGGAATATGTCCATAGAG
MTBnoStopBam	ggatccATTAAAGCCGTACATGTCAAAAC
MTBstopBam	ggatccTCAATTAAAGCCGTACATGTC
MTB-FW2	GCTTATGTGAGGAACTTCGCAGAC
GFP-rev	GAAGTCGTGCTGCTTCATGTGG
MTBnor-fw	GCTTATGTGAGGAACTTCGCAGAC
MTBnor-rev	TAATACGACTCACTATAGGATTAAAGCCGTACATGTCAAAAC
A6fwd1	AACTGTGACATCCGTTCTTTTC
T7A6revNEW1	TAATACGACTCACTATAGGTGGTGGCTGGACATCTATTT

MTB-FW1(MI)	GCATTTTGCACTTGGTCGCC
GK-TDNA	ATATAACGCTGCGGACATCTACATTTT
MTB-GK-FW	GGACCTTGTGGGTAAAGTTACC
MTB-GK-REV	GTGGATAACCCAGACTAATCC
SALK.homo.rev	CTATTAGAATGTGGGGTGGGTG
MTB.start	ATGAAGAAGAAGAAACAAGAAGAGAGT
w.MTBsplicerev	CTAACCATAAGGAGGCTCTTCAGC
prmt4aFw-y2h	ATGGAGATTCCTTCTCTGA
prmt4aRev-y2h	CTAGAGCTGAGCGTTTTGCG
prmt4bFw-y2h	ATGGAGGTATCTTCTGTGA
prmt4bRev-y2h	TTAGAGCTGGGCACTTGGGT
MTBLysFW	CACCCAGTCCCATTCATTCT
MTBLysREV	CACCAGGAGCTCTATGGACA
PRMT4a.2fwd	CGTCCCTGTTTAGTGAATGGCA
PRMT4a.2rev-new	CCAGTGATCTCTTGCCCTGCC
PRMT4b.1fwd	TGCCAAACATGTGTATGCGGT
PRMT4b.1rev-new	CTCGTTGACCAATAAGGTGCc
LBb.1. SALK	GCGTGGACCGCTTGCTGCAACT
MTBLYS.FWNEW	CCCGAGGTGTTGATGGTAAT
MTBLYS.REVNEW	TGCAAGTCGCCTTTCAGATA

Appendix II

Growth media

½ MS medium (400 ml)

0.88 g Murashige Skooge salts

4 g sucrose

Adjust PH to 5.7

4 g Agar

Autoclave at 121 °C for 30min

LB Agar 500 ml

5 g tryptone

2.5 g yeast extract

2.5 g NaCl

3 g agar

sterile distilled water: Up to 500

Autoclave at 121 °C for 30min

Luria Broth (LB)

10 g tryptone

5 g yeast extract

10 g NaCl

Adjust PH to 7.0 with NaOH

sterile distilled water : Up to 1L

Autoclave at 121 °C for 30 min

Buffers

NEBNext RNA binding buffer

1M LiCl

40mM Tris HCL (pH 7.5)

2mM EDTA

0.1% Triton-X-100 or NP4O

NEBNext wash buffer

150mM LiCl

20mM Tris HCL (pH 7.5)

1mM EDTA

0.01% Triton-X-100 or NP40

Autoclave the buffers then add the NP40.

Appendix III

Appendix discussing splice variant

cacttcgccgtgttctctctctctctcacaaactcactcatcttctccgacccaacattttccgatct
tcttcgctctaatttcatttctaaactcaaatttttcatctgtaatctcgaaacgattttggaattga
aaatccaaactctattgtggatgttttaagtaacgaaactcagttatagaaaatcgaacccgaattga
tcgtggtaatgtcgaaaccctaatttcgtgggtttagggttttgtagcacagttttcgcaaaaaATGA
AGAAGAAACAAGAAGAGAGTTCGTTGGAGAAGCTAAGTACTTGGTATCAAGATGGAGAGCAAGACGGT
GGAGATAGAAGTGAGAAGAGAAGAATGAGTCTTAAAGCATCAGACTTTGAGAGTAGTTCTCGAAGTGG
TGGAAGTAAAAGCAAAGAAGATAATAAGTCTGTTGTTGATGTTGAGCATCAAGATCGTGATTCCAAGA
GAGAAAGAGATGGGAGAGAACGAACACATGGATCTTCTTCTGATTCGAGTAAGAGGAAGAGATGGGAT
GAAGCAGGTGGTCTTGTTAATGATGGTGATCATAAAAGTAGTAAGCTTTCTGATTCTAGACATGATAG
TGGTGGAGAAAGAGTTAGTGTTAGTAATGAACATGGTGAGAGTAGGAGAGATTTGAAGTCTGATAGGA
GTTTGAAGACTAGTAGTAGAGATGAGAAGAGTAAGAGTCGTGGTGTGAAAGATGATGATAGAGGTAGT
CCTTTGAAGAAAACTAGTGGTAAGGATGGTTCTGAGGTAGTTAGAGAAGTGGGTCGATCTAATAGGTC
GAAAACACCGGATGCGGATTATGAGAAGGAGAAGTATAGTCGAAAAGATGAGAGGTCTAGAGGTAGGG
ATGATGGGTGGTCTGATAGGGATAGAGATCAAGAAGGTTTGAAGGATAATTGGAAGAGAAGGCATTCT
AGTAGTGGTGATAAAGATCAGAAAGATGGGGACTTGCTTTATGATCGTGGTAGGGAACGGGAATTTCC
TAGGCAAGGACGTGAAAGGAGTGAAGGAGAGAGGTCTCATGGTCGTTTGGGTGGGAGGAAAGATGGAA
ACAGGGGGGAAGCTGTTAAAGCTTTGTCCAGTGGTGGCGTTTCAAATGAGAATTATGATGTGATTGAG
ATACAAACCAAGCCACATGATTATGTCAGGGGAGAATCAGGACCCAACTTTGCTCGTATGACTGAATC
TGGTCAGCAACCTCCTAAAAAACCTAGTAATAATGAGGAAGAGTGGGCTCACAACCAGGAAGGTAGAC
AGAGAAGTGAAACTTTTGGTTTTGGGTCTTATGGGGAAGATTCGAGAGATGAAGCTGGTGAAGCCAGT
TCTGATTACTCAGGGGCTAAAGCAAGAAACCAGAGAGGTTCAACACCTGGTAGAACTAATTTTGTGCA
AACCCCTAATCGTGGTTATCAGACTCCACAAGGCACTAGAGGGAACAGACCCTTAAGGGGTGGGAAAG
GAAGACCTGCCGGTGGCAGAGAAAACCAACAAGGTGCCATTCCAATGCCTATCATGGGGTCACCATTT
GCAAACCTTGGAATGCCACCACCCAGTCCCATTCATTCTCTTACTCCTGGCATGTCGCCAATTCCGGG
CACTTCTGTCACCCCTGTCTTCATGCCTCCATTTGCCCCAACTCTTATATGGCCTGGGGCCCGAGGTG
TTGATGGTAATATGCTACCTGTTCCTCCTGTTCTTTCACCTCTTCCTCCCGGACCATCAGGCCCAAGA
TTTCCTTCAATCGGCACACCACCAAACCCGAATATGTTCTTTACTCCACCAGGTTCTGATAGAGGAGG
GCCTCCTAACTTTCCTGGGTCCAATATTTCTGGACAAATGGGACGTGGAATGCCATCTGATAAGACTT
CAGGGGGATGGGTTCCTCCTCGAGGTGGTGGACCTCCTGGTAAAGCTCCTTCTAGGGGAGAGCAAAAT
GACTATTCCCAGAACTTTGTGGATACTGGAATGCGGCCCCAGAATTTCATTCGGGAGCTGGAGCTTAC
CAATGTGGAAGACTACCCCAAGCTTAGAGAGCTCATACAGAAGAAGGATGAGATTGTATCTAATTCTG
CTTCTGCACCAATGTATCTGAAAGGCGACTTGCATGAAGTTGAGTTATCTCCCGAGTTATTTGGAACA
AAGTTTGATGTTATTCTTGTTGACCCA**CCATGG**GAGGAATATGTCCATAGAGCTCCTGGTGTTTCTGA
TAGTATGGAGTATTGGACATTTGAGGACATTATCAATCTCAAGATTGAGgtgactatcctctacactc
ttcaattactcataggattttagggtacatgcattcgctcgttggtatacttcaattgctctttgctt
agcaatagatctaatagcggggtagcatatatcatctgtcatctgagtattatctagatgaagtagtg
gtactcaacatatagtaatttaacttgtgtgtaggaccttgtgggtaaagttacctagatgacgtagt
ggtactcaacatatagatatagtaacttaacttgtctgtaaatcttgtgggtacggtttcctagatga
tgtagctggtacgaaacatatagtattttaacttgtgtgtagaccttgtaggtaaggttgtttgccat
cattgttatttataacaaaagtgaattcttccatgtatatgtagGCAATAGCTGACACTCCATCCTTC
CTCTTCCTCTGGGTTGGTGATGGTGTTGGGCTTGAGCAAGGGCGCCAATGCCTGAAAAAGgtacagga
tccaaaccaaatcgcatttcctttattgttttggatttgtttctcttgacagtatgtacttaatctgt
atttattttgtttgggtttgacagTGGGGTTTCAGAAGGTGTGAAGACATTTGCTGGGTGAAAACCAA
CAAAAGTAATGCAGCACCAACATTGCGACATGATTCTCGTACTGTGTTTCAGCG*SALK*TTCCAAGg
tccagtatggtctgccattgccttctcttttgttttccgtgttgcatatcttttgcttaatcttttgt
attggtttctctttgtatagGAGCACTGCTTGATGGGGATAAAGGGTACTGTTCGACGTAGCACTGAT
GGCCATATAATCCATGCTAACATCGACACTGACGTAATTATTGCTGAAGAGCCTCCTTATGgttagta
aaatgtgtgttcctgatagactgataaaatcgagagtgtcttgcttgtcatatcatgttccttctctc
tgttctgcttccagcatcctgtttcttttaaagtgagcatgctagtacatcagcaatcaattgtgtat

aaataggatcgttgcttaatgtgattaaggtatcgagtgtttttgtatttggtactagtgttgggagg
caaggttttgggttctcgaaaacaaagacctatgtttcttttggctctcggttatggtacacgtgatt
agtttgctggattagtcttgggttatccacactgtaagctggttcattgagaaatacattagattctg
tggttgattttagcattgccatgtctaaaatattagtgaatttgtatcctcctattattgcaagctgg
tttgcttaactgcatttctttacgttgcaaaactccagGTTCGACTCAGAAGCCTGAAGATATGTATA
GGATAATAGAGCATTTTGCACTTGGTCGCCGGAGGCTTGAGCTTTTCGGTGAAGACCACAATATTCGA
GCTGGCTGGCTTACTGTTGGAAAAGGCCTTTCGTCCTCAAACTTTGAGCCACAGgtaagatctcatgt
tcgctctgtagacatctatccacctcctgtttatatgagctttagacctatgcaaggagcttctttga
ctgtttgatctgttttggatattgtgtgctttagGCTTATGTGAGGAACTTCGCAGACAAGGAGGGTA
AAGTGTGGCTAGGAGGAGGAGGAAGAAATCCACCTCCAGACGCACCGCATCTTGTTGTGACTACTCCC
GATATAGAATCGCTGCGGCCCAAATCACCAATGAAGAATCAGCAACAACAATCGTATCCATCGTCTCT
AGCTTCTGCAAATTCCTCAAACCGAAGAACCACAGGAAACTCACCACAAGCAAATCCTAATGTTGTTG
TCTTACATCAAGAGGCTTCTGGATCTAACTTCTCTGTTCCTACCACCCCGCATTGGGTGCCACCAACG
GCACCAGCTGCCGCAGGGCCACCTCCAATGGACAGCTTTAGAGTACCTGAAGGTGGCAACAACACAAG
ACCACCTGACGACAAGAGTTTTGACATGTACGGCTTTAATTGAgcctctcccaaaattgcagagtttc
cagaaccgtttctattgaatggatattttacccctttgctttgagaaactctgctgcgcacggttttg
gttctctttttgtaattctgttcatttttttcacttccgtagagccaatactttatattcatttcatta
tcaatcaagctttacctaataatcccaatttgctccatacaatgtgatgtatccaaatcaaatcgca
tttaaccaccctttatattcacaattacaaagtcttatatggtaaatgcatgcagtgtcccagtaatc
accaaacaaaaagtccttagagactctggagtagccatgatttgctcaagaactacttgtaggagcct
taaggagaccagag

ATGAAGAAGAAACAAGAAGAGAGTTCGTTGGAGAAGCTAAGTACTTGGTATCAAGATGGAGAGCAAGA
CGGTGGAGATAGAAGTGAGAAGAGAAGAATGAGTCTTAAAGCATCAGACTTTGAGAGTAGTTCTCGAA
GTGGTGGAAGTAAAAGCAAAGAAGATAATAAGTCTGTTGTTGATGTTGAGCATCAAGATCGTGATTCC
AAGAGAGAAAGAGATGGGAGAGAACGAACACATGGATCTTCTTCTGATTCGAGTAAGAGGAAGAGATG
GGATGAAGCAGGTGGTCTTGTTAATGATGGTGATCATAAAAGTAGTAAGCTTTCTGATTCTAGACATG
ATAGTGGTGGAGAAAGAGTTAGTGTTAGTAATGAACATGGTGAGAGTAGGAGAGATTTGAAGTCTGAT
AGGAGTTTGAAGACTAGTAGTAGAGATGAGAAGAGTAAGAGTCGTGGTGTGAAAGATGATGATAGAGG
TAGTCCTTTGAAGAAAACTAGTGGTAAGGATGGTTCTGAGGTAGTTAGAGAAGTGGGTCGATCTAATA
GGTCGAAAACACCGGATGCGGATTATGAGAAGGAGAAGTATAGTCGAAAAGATGAGAGGTCTAGAGGT
AGGGATGATGGGTGGTCTGATAGGGATAGAGATCAAGAAGGTTTGAAGGATAATTGGAAGAGAAGGCA
TTCTAGTAGTGGTGATAAAGATCAGAAAGATGGGGACTTGCTTTATGATCGTGGTAGGGAACGGGAAT
TTCCTAGGCAAGGACGTGAAAGGAGTGAAGGAGAGAGGTCTCATGGTCGTTTGGGTGGGAGGAAAGAT
GGAAACAGGGGGGAAGCTGTTAAAGCTTTGTCCAGTGGTGGCGTTTCAAATGAGAATTATGATGTGAT
TGAGATACAAACCAAGCCACATGATTATGTCAGGGGAGAATCAGGACCCAACTTTGCTCGTATGACTG
AATCTGGTCAGCAACCTCCTAAAAAACCTAGTAATAATGAGGAAGAGTGGGCTCACAACCAGGAAGGT
AGACAGAGAAGTGAAACTTTTGGTTTTGGGTCTTATGGGGAAGATTCGAGAGATGAAGCTGGTGAAGC
CAGTTCTGATTACTCAGGGGCTAAAGCAAGAAACCAGAGAGGTTCAACACCTGGTAGAACTAATTTTG
TGCAAACCCCTAATCGTGGTTATCAGACTCCACAAGGCACTAGAGGGAACAGACCCTTAAGGGGTGGG
AAAGGAAGACCTGCCGGTGGCAGAGAAAACCAACAAGGTGCCATTCCAATGCCTATCATGGGGTCACC
ATTTGCAAACCTTGGAATGCCACCACCCAGTCCCATTCATTCTCTTACTCCTGGCATGTCGCCAATTC
CGGGCACTTCTGTCACCCCTGTCTTCATGCCTCCATTTGCCCCAACTCTTATATGGCCTGGGGCCCGA
GGTGTTGATGGTAATATGCTACCTGTTCCTCCTGTTCTTTCACCTCTTCCTCCCGGACCATCAGGCCC
AAGATTTCCTTCAATCGGCACACCACCAAACCCGAATATGTTCTTTACTCCACCAGGTTCTGATAGAG
GAGGGCCTCCTAACTTTCCTGGGTCCAATATTTCTGGACAAATGGGACGTGGAATGCCATCTGATAAG
ACTTCAGGGGGATGGGTTCCTCCTCGAGGTGGTGGACCTCCTGGTAAAGCTCCTTCTAGGGGAGAGCA
AAATGACTATTCCCAGAACTTTGTGGATACTGGAATGCGGCCCCAGAATTTCATTCGGGAGCTGGAGC
TTACCAATGTGGAAGACTACCCCAAGCTTAGAGAGCTCATACAGAAGAAGGATGAGATTGTATCTAAT
TCTGCTTCTGCACCAATGTATCTGAAAGGCGACTTGCATGAAGTTGAGTTATCTCCCGAGTTATTTGG
AACAAAGTTTGATGTTATTCTTGTTGACCCA**CCATGG**GAGGAATATGTCCATAGAGCTCCTGGTGTTT
CTGATAGTATGGAGTATTGGACATTTGAGGACATTATCAATCTCAAGATTGAGGCAATAGCTGACACT

CCATCCTTCCTCTTCCTCTGGGTTGGTGATGGTGTTGGGCTTGAGCAAGGGCGCCAATGCCTGAAAAA
GTGGGGTTTCAGAAGGTGTGAAGACATTTGCTGGGTGAAAACCAACAAAAGTAATGCAGCACCAACAT
TGCGACATGATTCTCGTACTGTGTTTCAGCGTTCCAAGGAGCACTGCTTGATGGGGATAAAGGGTACT
GTTCGACGTAGCACTGATGGCCATATAATCCATGCTAACATCGACACTGACGTAATTATTGCTGAAGA
GCCTCCTTATGgttagtaaaatGTTCGACTCAGAAGCCTGAAGATATGTATAGGATAATAGAGCATTT
TGCACTTGGTCGCCGGAGGCTTGAGCTTTTCGGTGAAGACCACAATATTCGAGCTGGCTGGCTTACTG
TTGGAAAAGGCCTTTCGTCCTCAAACTTTGAGCCACAGGCTTATGTGAGGAACTTCGCAGACAAGGAG
GGTAAAGTGTGGCTAGGAGGAGGAGGAAGAAATCCACCTCCAGACGCACCGCATCTTGTTGTGACTAC
TCCCGATATAGAATCGCTGCGGCCCAAATCACCAATGAAGAATCAGCAACAACAATCGTATCCATCGT
CTCTAGCTTCTGCAAATTCCTCAAACCGAAGAACCACAGGAAACTCACCACAAGCAAATCCTAATGTT
GTTGTCTTACATCAAGAGGCTTCTGGATCTAACTTCTCTGTTCCTACCACCCCGCATTGGGTGCCACC
AACGGCACCAGCTGCCGCAGGGCCACCTCCAATGGACAGCTTTAGAGTACCTGAAGGTGGCAACAACA
CAAGACCACCTGACGACAAGAGTTTTGACATGTACGGCTTTAATTGA

MKKKQEESSLEKLSTWYQDGEQDGGDRSEKRRMSLKASDFESSSRSGGSKSKEDNKSVVDVEHQDRDSKRERDG
RERTHGSSSDSSKRKRWDEAGGLVNDGDHKSSKLSDSRHDSGGERVSVSNEHGESRRDLKSDRSLKTSSRDEKSKS
RGVKDDDRGSPLKKTSGKDGSEVVREVGRSNRSKTPDADYEKEKYSRKDERSRGRDDGWSDRDRDQEGLKDNW
KRRHSSSGDKDQKDGDLLYDRGREREFPRQGRERSEGERSHGRLGGRKDGNRGEAVKALSSGGVSNENYDVIEIQ
TKPHDYVRGESGPNFARMTESGQQPPKKPSNNEEEWAHNQEGRQRSETFGFGSYGEDSRDEAGEASSDYSGAK
ARNQRGSTPGRTNFVQTPNRGYQTPQGTRGNRPLRGGKGRPAGGRENQQGAIPMPIMGSPFANLGMPPPSPI
HSLTPGMSPIPGTSVTPVFMPPFAPTLIWPGARGVDGNMLPVPPVLSPLPPGPSGPRFPSIGTPPNPNMFFTPPGS
DRGGPPNFPGSNISGQMGRGMPSDKTSGGWVPPRGGGPPGKAPSRGEQNDYSQNFVDTGMRPQNFIRELELT
NVEDYPKLRELIQKKDEIVSNSASAPMYLKGDLHEVELSPELFGTKFDVILVDPPWEEYVHRAPGVSDSMEYWTFE
DIINLKIEAIADTPSFLFLWVGDGVGLEQGRQCLKKWGFRRCEDICWVKTNKSNAAPTLRHDSRTVFQRSKEHCLM
GIKGTVRRSTDGHIIHANIDTDVIIAEEPPYGAT

ATGAAGAAGAAACAAGAAGAGAGTTCGTTGGAGAAGCTAAGTACTTGGTATCAAGATGGAGAGCAAGA
CGGTGGAGATAGAAGTGAGAAGAGAAGAATGAGTCTTAAAGCATCAGACTTTGAGAGTAGTTCTCGAA
GTGGTGGAAGTAAAAGCAAAGAAGATAATAAGTCTGTTGTTGATGTTGAGCATCAAGATCGTGATTCC
AAGAGAGAAAGAGATGGGAGAGAACGAACACATGGATCTTCTTCTGATTCGAGTAAGAGGAAGAGATG
GGATGAAGCAGGTGGTCTTGTTAATGATGGTGATCATAAAAGTAGTAAGCTTTCTGATTCTAGACATG
ATAGTGGTGGAGAAAGAGTTAGTGTTAGTAATGAACATGGTGAGAGTAGGAGAGATTTGAAGTCTGAT
AGGAGTTTGAAGACTAGTAGTAGAGATGAGAAGAGTAAGAGTCGTGGTGTGAAAGATGATGATAGAGG
TAGTCCTTTGAAGAAAACTAGTGGTAAGGATGGTTCTGAGGTAGTTAGAGAAGTGGGTCGATCTAATA
GGTCGAAAACACCGGATGCGGATTATGAGAAGGAGAAGTATAGTCGAAAAGATGAGAGGTCTAGAGGT
AGGGATGATGGGTGGTCTGATAGGGATAGAGATCAAGAAGGTTTGAAGGATAATTGGAAGAGAAGGCA
TTCTAGTAGTGGTGATAAAGATCAGAAAGATGGGGACTTGCTTTATGATCGTGGTAGGGAACGGGAAT
TTCCTAGGCAAGGACGTGAAAGGAGTGAAGGAGAGAGGTCTCATGGTCGTTTGGGTGGGAGGAAAGAT
GGAAACAGGGGGGAAGCTGTTAAAGCTTTGTCCAGTGGTGGCGTTTCAAATGAGAATTATGATGTGAT
TGAGATACAAACCAAGCCACATGATTATGTCAGGGGAGAATCAGGACCCAACTTTGCTCGTATGACTG
AATCTGGTCAGCAACCTCCTAAAAAACCTAGTAATAATGAGGAAGAGTGGGCTCACAACCAGGAAGGT
AGACAGAGAAGTGAAACTTTTGGTTTTGGGTCTTATGGGGAAGATTCGAGAGATGAAGCTGGTGAAGC
CAGTTCTGATTACTCAGGGGCTAAAGCAAGAAACCAGAGAGGTTCAACACCTGGTAGAACTAATTTTG
TGCAAACCCCTAATCGTGGTTATCAGACTCCACAAGGCACTAGAGGGAACAGACCCTTAAGGGGTGGG
AAAGGAAGACCTGCCGGTGGCAGAGAAAACCAACAAGGTGCCATTCCAATGCCTATCATGGGGTCACC
ATTTGCAAACCTTGGAATGCCACCACCCAGTCCCATTCATTCTCTTACTCCTGGCATGTCGCCAATTC
CGGGCACTTCTGTCACCCCTGTCTTCATGCCTCCATTTGCCCCAACTCTTATATGGCCTGGGGCCCGA
GGTGTTGATGGTAATATGCTACCTGTTCCTCCTGTTCTTTCACCTCTTCCTCCCGGACCATCAGGCCC

AAGATTTCCTTCAATCGGCACACCACCAAACCCGAATATGTTCTTTACTCCACCAGGTTCTGATAGAG
GAGGGCCTCCTAACTTTCCTGGGTCCAATATTTCTGGACAAATGGGACGTGGAATGCCATCTGATAAG
ACTTCAGGGGGATGGGTTCCTCCTCGAGGTGGTGGACCTCCTGGTAAAGCTCCTTCTAGGGGAGAGCA
AAATGACTATTCCCAGAACTTTGTGGATACTGGAATGCGGCCCCAGAATTTCATTCGGGAGCTGGAGC
TTACCAATGTGGAAGACTACCCCAAGCTTAGAGAGCTCATACAGAAGAAGGATGAGATTGTATCTAAT
TCTGCTTCTGCACCAATGTATCTGAAAGGCGACTTGCATGAAGTTGAGTTATCTCCCGAGTTATTTGG
AACAAAGTTTGATGTTATTCTTGTTGACCCA**CCATGG**GAGGAATATGTCCATAGAGCTCCTGGTGTTT
CTGATAGTATGGAGTATTGGACATTTGAGGACATTATCAATCTCAAGATTGAGGCAATAGCTGACACT
CCATCCTTCCTCTTCCTCTGGGTTGGTGATGGTGTTGGGCTTGAGCAAGGGCGCCAATGCCTGAAAAA
GTGGGGTTTCAGAAGGTGTGAAGACATTTGCTGGGTGAAAACCAACAAAAGTAATGCAGCACCAACAT
TGCGACATGATTCTCGTACTGTGTTTCAGCGTTCCAAGGAGCACTGCTTGATGGGGATAAAGGGTACT
GTTCGACGTAGCACTGATGGCCATATAATCCATGCTAACATCGACACTGACGTAATTATTGCTGAAGA
GCCTCCTTATGGTTCGACTCAGAAGCCTGAAGATATGTATAGGATAATAGAGCATTTTGCACTTGGTC
GCCGGAGGCTTGAGCTTTTCGGTGAAGACCACAATATTCGAGCTGGCTGGCTTACTGTTGGAAAAGGC
CTTTCGTCCTCAAACTTTGAGCCACAGGCTTATGTGAGGAACTTCGCAGACAAGGAGGGTAAAGTGTG
GCTAGGAGGAGGAGGAAGAAATCCACCTCCAGACGCACCGCATCTTGTTGTGACTACTCCCGATATAG
AATCGCTGCGGCCCAAATCACCAATGAAGAATCAGCAACAACAATCGTATCCATCGTCTCTAGCTTCT
GCAAATTCCTCAAACCGAAGAACCACAGGAAACTCACCACAAGCAAATCCTAATGTTGTTGTCTTACA
TCAAGAGGCTTCTGGATCTAACTTCTCTGTTCCTACCACCCCGCATTGGGTGCCACCAACGGCACCAG
CTGCCGCAGGGCCACCTCCAATGGACAGCTTTAGAGTACCTGAAGGTGGCAACAACACAAGACCACCT
GACGACAAGAGTTTTGACATGTACGGCTTTAATTGA

MKKKQEESSLEKLSTWYQDGEQDGGDRSEKRRMSLKASDFESSSRSGGSKSKEDNKSVVDVEHQDRDS
KRERDGRERTHGSSSDSSKRKRWDEAGGLVNDGDHKSSKLSDSRHDSGGERVSVSNEHGESRRDLKSD
RSLKTSSRDEKSKSRGVKDDDRGSPLKKTSGKDGSEVVREVGRSNRSKTPDADYEKEKYSRKDERSRG
RDDGWSDRDRDQEGLKDNWKRRHSSSGDKDQKDGDLLYDRGREREFPRQGRERSEGERSHGRLGGRKD
GNRGEAVKALSSGGVSNENYDVIEIQTKPHDYVRGESGPNFARMTESGQQPPKKPSNNEEEWAHNQEG
RQRSETFGFGSYGEDSRDEAGEASSDYSGAKARNQRGSTPGRTNFVQTPNRGYQTPQGTRGNRPLRGG
KGRPAGGRENQQGAIPMPIMGSPFANLGMPPPSPIHSLTPGMSPIPGTSVTPVFMPPFAPTLIWPGAR
GVDGNMLPVPPVLSPLPPGPSGPRFPSIGTPPNPNMFFTPPGSDRGGPPNFPGSNISGQMGRGMPSDK
TSGGWVPPRGGGPPGKAPSRGEQNDYSQNFVDTGMRPQNFIRELELTNVEDYPKLRELIQKKDEIVSN
SASAPMYLKGDLHEVELSPELFGTKFDVILVDPPWEEYVHRAPGVSDSMEYWTFEDIINLKIEAIADT
PSFLFLWVGDGVGLEQGRQCLKKWGFRRCEDICWVKTNKSNAAPTLRHDSRTVFQRSKEHCLMGIKGT
VRRSTDGHIIHANIDTDVIIAEEPPYGSTQKPEDMYRIIEHFALGRRRLELFGEDHNIRAGWLTVGKG
LSSSNFEPQAYVRNFADKEGKVWLGGGGRNPPPDAPHLVVTTPDIESLRPKSPMKNQQQQSYPSSLAS
ANSSNRRTTGNSPQANPNVVVLHQEASGSNFSVPTTPHWVPPTAPAAAGPPPMDSFRVPEGGNNTRPP
DDKSFDMYGFN